ulm university universität

uulm

Fakultät für Mathematik und Wirtschaftswissenschaften

Institut für Numerische Mathematik

Dissertation

On Fundamental Concepts for Model Reduction in Multiscale Combustion Models

Slow Invariant Manifold and Inertial Manifold Computation

zur Erlangung des Doktorgrades Dr. rer. nat.
der Fakultät für Mathematik und Wirtschaftswissenschaften
der Universität Ulm

vorgelegt von
Jonas Unger
aus Backnang

Dezember 2015

Abstract

Simulation of chemically reacting flows modeled by dissipative dynamical systems with spectral gaps requires an immense expenditure of time despite the continual advancement of digital computing power. In order to decrease this effort to an acceptable level, model reduction methods aim at a low-dimensional approximation of the underlying model equations. In this context, it is observed that solution trajectories bundle near invariant manifolds of successively lower dimension during time evolution which is caused by the spectral gaps generating multiple time scales. There are two different types of model reduction methods: (i) methods that use spatially homogeneous manifolds as low-dimensional approximation of the chemical reaction and then account for reaction–transport coupling and (ii) methods that identify low-dimensional approximations in terms of manifolds based on the full reaction–transport model. The focus of this work is on a discussion of fundamental and unifying geometric and analytic issues of various approaches to trajectory-based numerical approximation techniques of those spatially homogeneous manifolds that are in practical use for model reduction in chemical kinetics. In this context, two basic concepts are pointed out reducing various model reduction approaches to a common denominator. Both of them are related in a variational boundary value problem viewpoint. Furthermore, a fundamental study of the previously with respect to model reduction little researched unreduced nonlinear reaction–transport model is presented, wherefrom suggestions arise for both the insertion of the spatially homogeneous manifolds into the reaction–transport coupling (i) as well as the approximation of manifolds based on the reaction–transport system (ii).

Kurzzusammenfassung

Die Simulation chemisch reaktiver Strömungen modelliert durch dynamische Systeme mit spektralen Lücken erfordert trotz des ständigen Fortschritts von digitaler Rechenleistung einen enormen Zeitaufwand. Um diesen Aufwand auf ein akzeptables Maß zu reduzieren, streben Modellreduktionsmethoden nach einer niedrigdimensionalen Beschreibung der zugrunde liegenden Modellgleichungen. In diesem Zusammenhang wird beobachtet, dass Lösungstrajektorien im zeitlichen Verlauf auf invariante Mannigfaltigkeiten von sukzessiv niedrigenderer Dimension bündeln, was anhand der spektralen Lücken und den damit einhergehenden unterschiedlichen Zeitskalen zu begründen ist. Zwei Verfahren werden dargestellt: (i) Methoden, die räumlich homogene Mannigfaltigkeiten als niedrigdimensionale Approximation der chemischen Reaktion verwenden und sich anschließend um die Kopplung von Reaktion und Transport kümmern und (ii) Methoden, die ausgehend von vollen Reaktions–Transport Modellen niedrigdimensionale Beschreibungen in Form von Mannigfaltigkeiten identifizieren. Der Fokus dieser Arbeit liegt auf der Diskussion grundlegender und vereinigender geometrischer und analytischer Aspekte verschiedener Ansätze zur trajektorienbasierten numerischen Approximation solcher räumlich homogenen Mannigfaltigkeiten, die sich im praktischen Einsatz zur Modellreduktion in der chemischen Kinetik befinden. In diesem Zusammenhang werden zwei Konzepte herausgearbeitet, die einen gemeinsamen Nenner für verschiedene Modellreduktionsmethoden bilden. Diese werden in einer variationellen Randwertproblembetrachtung zusammengeführt. Darüberhinaus wird eine grundlegende Untersuchung des bis heute bezüglich Modellreduktion noch kaum erforschten nichtlinearen Reaktions–Transport Modells dargelegt, wodurch sich Anregungen sowohl für die Einbringung der räumlich homogenen Mannigfaltigkeiten in die Reaktions–Transport Kopplung als auch die Approximation von Mannigfaltigkeiten basierend auf dem Reaktions–Transport System ergeben.

Acknowledgments

Firstly, I would like to express my sincere gratitude to my advisor PROF. DR. DIRK LEBIEDZ for the continuous support of my PhD study and related research, for his patience, motivation, and immense knowledge. His guidance helped me in all the time of research and writing of this thesis. I could not have imagined having a better advisor and mentor for my PhD study.

Besides my advisor, I would like to thank my second assessor, PROF. DR. STEFAN FUNKEN, for his insightful comments and encouragement, but also for being trainer and training partner at the same time. I simply would not have finished an Ironman up to now without your support. I thank my colleagues at the Institute for Numerical Analysis and the Scientific Computing Centre Ulm for the stimulating discussions and for all the fun we have had during the last five years. You have made it a pleasure to be a member of this community. A special thanks goes to everyone who proofread this dissertation.

Last but not the least, I would like to thank my family for supporting me spiritually throughout writing this thesis and my life in general. I have always been assured that there is no problem on which I cannot seek their help and advice. A very special acknowledgment goes to my girlfriend STEFANIE ERMER, who loved and supported me during the whole time of my dissertation, and made me feel like anything was possible. I love you, STEFFI.

Contents

Contents

Introduction

Energy is a central component of our life. Approximately 90 percent of the energy generation and therefore the main energy source of today's world is ensured by combustion processes which are, roughly speaking, a high temperature chemical reaction between a fuel and an oxidizer (typically air), usually a complicated sequence of elementary reactions. If the participating chemical species are not located within a flow field anyway, the reactions themselves initiate a movement of those species. Therefore, combustion processes are the most important respresentatives of chemically reacting flows. Examples include combustion engines in cars, power plants, and firing, to name just a few (see Figure 0.1). Due to this high significance it

| (a) Combustion engine | (b) Power plant | (c) Firing |

Figure 0.1: Application examples for chemically reacting flows in form of combustion processes.

is hardly surprising that research of combustion processes is indispensable, not least because of economical and ecological needs. In this context, optimization or minimization of pollution call for the quantitative assessment of these processes. This is a hard challenge due to complexity caused by an interplay between convective and diffusive species transport and chemical reaction processes and large size (dimension): realistic combustion mechanisms include up to 1200 chemical species and 7000 reactions [Wal99]. A further challenge arises from the multiple time scales within the chemical reaction processes with time scales ranging from nanoseconds to seconds inducing high stiffness of the kinetic model equations. On the basis of these difficulties, simulation of combustion processes was not practicable about 50 years ago, partly because the fastest supercomputers worldwide performed at 'just' 10^6 FLOPS[1]. Today, this is still a highly time-consuming task despite continuing exponential growth of computer power (cf. Figure 0.2)

---

[1]FLOPS (floating-point operations per seconds) is a measure of computer performance.

and sophisticated mathematical algorithms for efficiently solving the underlying large systems of partial differential equations. This is also made evident by the fact, that simulation of com-
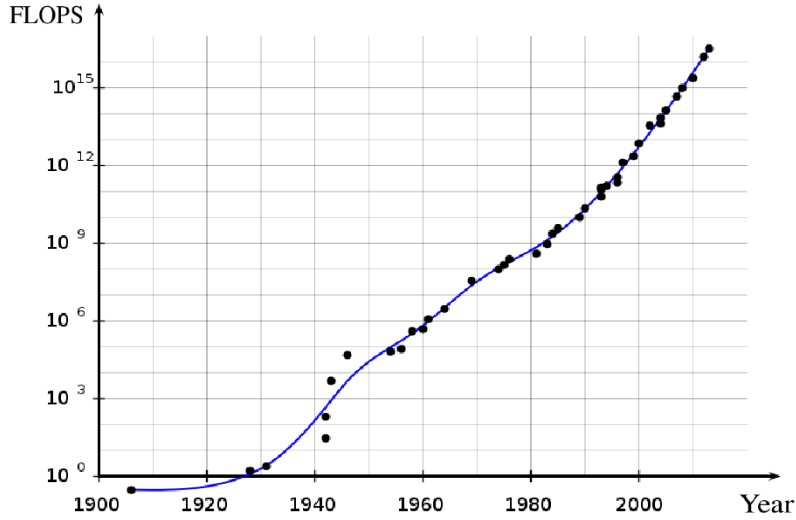
Figure 0.2: Chronological development of the worldwide fastest supercomputers.[2]

bustion processes is listed in the 'grand challenges' for future computer generations [War99].

To lower computational complexity in the simulation of chemical combustion processes, model reduction methods have to be applied aiming at a reduced description of the full model equations, obviously including the most important information, which is usually given by the long-term behavior and thus by the slow modes of the underlying combustion process. This approximation to the original model can then be evaluated with lower accuracy but in significantly less time allowing for a faster simulation and eventually a deeper insight into the underlying process. To illustrate an idealized reduced model, we consider the following example.

Example 0.0.1 (Plant growth model)**.** We consider a plant growth model (see [Vel09]) which is intended to predict the time evolution of the overall biomass of a plant. Here, the system that is supposed to be reduced is given by a potted plant (see Figure 0.3(a)) where non of the complex details are required with the exception of the growth rate r. As a consequence, a corresponding reduced system $\mathfrak{Z}_{\mathrm{red}}$ is given by a single parameter in this model: $\mathfrak{Z}_{\mathrm{red}} = \{r\}$. Obviously, a lot of information of the original system 'potted plant' is neglected in this reduction, but nevertheless the reduced system contains all information necessary to answer the question about the time evolution of the overall biomass.

There exists a large variety of model reduction methods for combustion processes with little or no conspicuous relation to each other. The first methods were published over one hundred years

---

[2]URL: `https://de.wikipedia.org/w/index.php?title=Supercomputer&oldid=146018665`

(a) Potted plant   (b) The same potted plant written as reduced model

Figure 0.3: Example for model reduction.

ago, while the large majority has been developed during the last 25 years as depicted in Figure 0.4. This is exactly where this dissertation comes into play. Namely, we focus on the search for broad common denominators and the discussion of fundamental and unifying geometric and analytic issues of various approaches that are in practical use for model reduction in combustion processes (a detailed description of those methods is found in Sections 2.1 and 2.2 of this work).

Two Ways to Obtain a Reduced Combustion Model

Until now, the usual procedure for obtaining a reduced combustion model has been to consider the chemical reaction processes solely as a first step, that is to say, without accounting for the transport processes in form of diffusion and/or convection. In this context, it is observed that solution trajectories of chemical reaction processes modeled by (spatially homogeneous) dissipative systems of ordinary differential equations bundle near invariant manifolds of successively lower dimension during time evolution. This is caused by the previously mentioned multiple time scales generating spectral gaps. Exactly this time scale separation of the model solution

1907 — Quasi–Steady–State Assumption (QSSA) [Bod07, Bod13, CU13] (see 2.1.1)

1913 — Partial Equilibrium Assumption (PEA) [MP13] (see 2.1.2)

1992 — Intrinsic Low Dimensional Manifold (ILDM) [MP92] (see 2.1.3)

1999 — Saddle Point Method (SPM) [DS99] (see 2.1.4)

2004 — Trajectory Based Optimization Approach (TBOA) [Leb04] (see 2.2)

2005 — Zero–Derivative Principle (ZDP) [GKK$^+$05, ZGK$^+$09] (see 2.1.6)

Invar. Constr. Equilibr. Edge Preimage Curves (ICE-PIC) [RPV$^+$06] (see 2.1.7)

2006 — Functional Equation Truncation (FET) [RT06, Rou12] (see 2.1.8)

2007 — Stretching–Based Diagnostics (SBD) [ACC$^+$07, ACG$^+$07] (see 2.1.9)

2008 — Flow Curvature Method (FCM) [GRC08] (see 2.1.10)

Figure 0.4: Timeline with representative model reduction methods for combustion processes arranged by year of first publication.

into fast and slow modes is the basis for most model reduction techniques, where the long time scale system dynamics is approximated via elimination of the fast relaxing modes by enslaving them to the slow ones. The outcome of this is in the ideal case an invariant manifold of slow motion (denoted as **slow invariant manifold (SIM)**) possessing the property of attracting system trajectories from arbitrary initial values. Many model reduction methods make use of a **species reconstruction** (cf. Section 1.3) for SIM computation which is provided by an implicitly defined function mapping a subset of the chemical species of the full model—denoted by **reaction progress variables (RPVs)**—onto the full species composition by determining a point on the SIM. This species reconstruction as well as the attraction of SIMs is schematically illustrated in Figure 0.5, where it can be seen that solution trajectories (black curves) emanating from different initial values (black crosses) relax onto a two-dimensional manifold (bounded red) before

approaching a one-dimensional one (red curve). Finally, the trajectories converge towards the zero-dimensional manifold: the chemical equilibrium. As a consequence, the dynamics of re-

(a) Attracting SIMs

(b) Species reconstruction
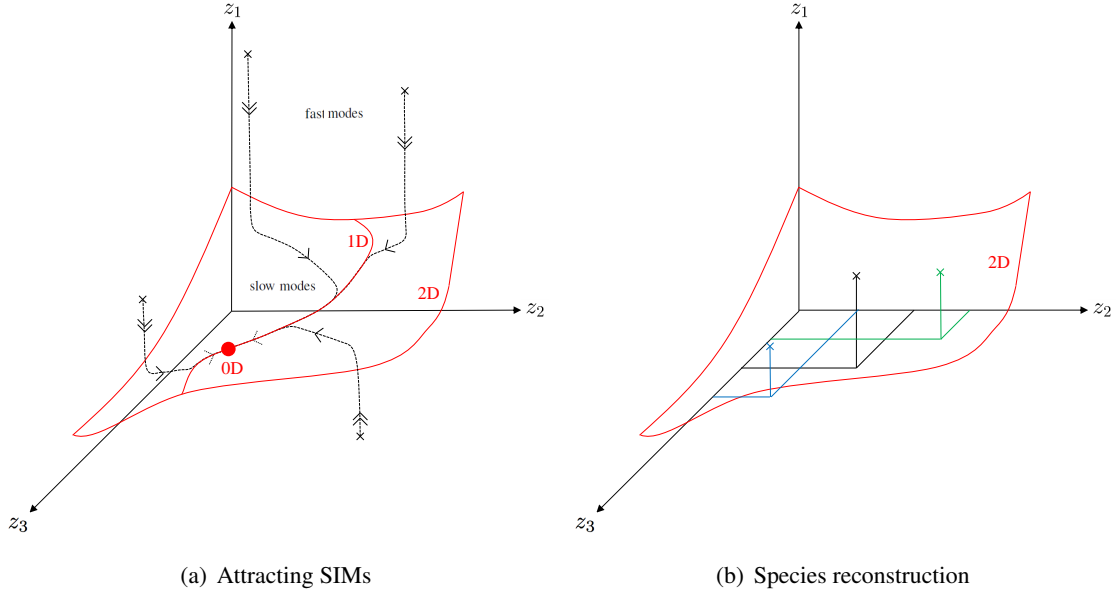
Figure 0.5: Schematic illustration of attracting SIMs and species reconstruction.

duced reaction models proceed along those SIMs.

However, regarding Figure 0.6, originating from a combustion model at the top left, the reduced reaction model at the bottom right is reached via SIM computation (1b), but not yet the desired reduced combustion model at the bottom left. For this purpose, a reintegration of the (spatially inhomogeneous) transport processes into the reduced reaction model is required (1c). Until about ten years ago, there was no appreciable publication concerning this issue. Up until
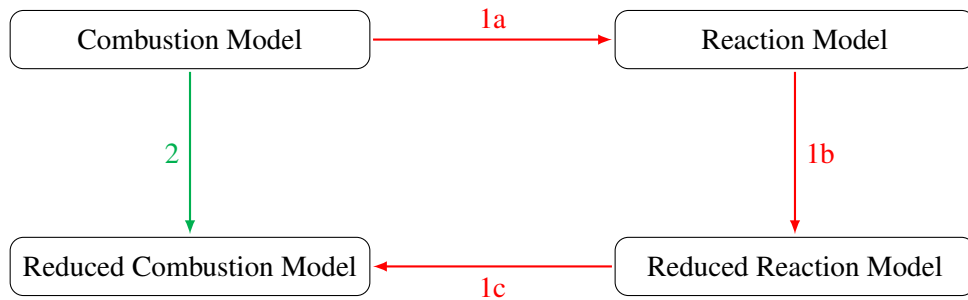
Figure 0.6: Schematic illustration of two possibilities for model reduction applied to a combustion model.

today, this problem is largely unexplored, although there are a few attempts trying to handle this problem with moderate success [TP02, RP06, RP07, RPV$^+$07]. The question if it is necessary

to take the red colored indirect route 1 or if there is a possibility to reduce the underlying combustion model directly (2), i.e. without considering the pure reaction process solely, is at least as unexplored [BM07b, MP13]. These issues are concerned with the approximation of so-called **inertial manifolds (IM)**. Chapter 3 of this work deals with some fundamental studies to this and furthermore, some basic ideas for IM computation are presented.

Two Fundamental Concepts for Model Reduction

As already mentioned, the focus of this dissertation is on the search for broad common denominators and the discussion of fundamental and unifying concepts of various model reduction methods in combustion processes. In this context, two fundamental concepts turned out—the **derivative–of–the–state–vector–concept** on the one hand and the **boundary–value–concept** on the other hand—underlying, combining, and collecting several methods (cf. Figure 0.4). Both concepts provide an exact identification of at least the reduced reaction model (i.e. without accounting for diffusive or convective terms (cf. Figure 0.6)). The first concept is based on the time derivative of the state vector (i.e. the vector containing the chemical species concentrations): with increasing derivative order the error associated with the computation of the reduced model decreases and finally vanishes in the limit, i.e. for an infinite derivative order. In contrast, the boundary–value–concept exploits an attraction property and can be formulated in form of a boundary value problem where the associated boundary conditions are specified at two values of the time variable t: t_* and $t_0(< t_*)$. For fixed t_*, the aforementioned error of the reduced model decreases with decreasing t_0 even exponentially. Thus, already small time intervals $|t_* - t_0|$ ensure an immense decrease of the inaccuracy. Here again, an exact identification is guaranteed for $t_0 = -\infty$. Based on these fundamental concepts, we succeeded to develop a novel model reduction method within this work making use of such basic concepts in condenced form. In comparison to other approaches, the advantage of the new approach lies in the fact that two independent parameters are provided that can be used as adjusting screws to improve the accuracy of the reduced model: the derivative order of the state vector as well as the time interval $|t_* - t_0|$ within the boundary value formulation. Accordingly, this approach can be seen as generalization or fusion of many previous ones allowing now for considerations how to efficiently decrease the numerical effort.

Outline

Chapter 1 provides a theoretical foundation of this work. It contains the definition of a dynamical system, whose formulation is derived based solely on the concept of a set. Dynamical systems can be classified, inter alia, into systems of partial differential equations and systems

of ordinary ones, which serve as mathematical models within this work. A special type of the latter are singularly perturbed systems which give rise to processes evolving on two different time scales and whose analysis is presented in Section 1.2. Based on this, existence of a specific manifold is stated in FENICHEL's invariant manifold theorem 1.2.2 serving as SIM whenever using models in singularly perturbed form. The general procedure of how to compute such a SIM already known as species reconstruction is presented in the subsequent Section (1.3). Since one important formulation of species reconstruction is in form of an optimization problem, the associated theory is discussed in Section 1.4.

Chapter 2 is concerned with the spatially homogeneous reaction model and the reduction of it, i.e. 1b in Figure 0.6. First, various methods for model reduction are presented and briefly described. Following the introduction of two simple test models (see 2.3), two important questions are discussed: how to estimate the accuracy of SIM approximation without knowing the location of this manifold (cf. 2.4) and the question concerning the number and the choice of the RPVs (cf. 2.5). This is followed by the presentation of the two previously mentioned fundamental concepts unifying the approaches presented in 2.1 and 2.2. These concepts are united in condensed form in a novel approach (see 2.6.4) where two adjusting screws can improve the accuracy of SIM approximation. Finally, one further idea concerning the search for an exact SIM computation is presented in 2.9 after considering the model reduction method presented in 2.2 from another viewpoint (see 2.8).

Spatially inhomogeneous systems, i.e. systems including diffusive and/or convective transport terms are discussed in Chapter 3. For this purpose, the modeling of diffusion and convection in one spatial dimension is demonstrated in 3.1. This is followed by a section discussing fundamental concepts about theory of partial differential equations (cf. 3.2), whereas the subsequent sections deal with the question how to obtain a reduced combustion model based on the reduced reaction model (1c) or by taking the direct route 2 (cf. Figure 0.6).

Subsequently, the dissertation is summarized. The main aspects and results are presented briefly in condenced form.

1 Analytical Basics

This chapter deals with fundamental aspects underlying the mathematical framework of this work, including:

- Theory of Dynamical Systems and Systems of Ordinary Differential Equations 1.1

- Theory of Singularly Perturbed Systems 1.2

- Species Reconstruction 1.3

- Theory of Optimization Problems 1.4

Given this introduction, the reader has the mathematical understanding to follow the subsequent chapters. First, it is shown that the formulation of the most central concept of this work—the concept of a dynamical system—requires only a small number of simple definitions. These arise directly from the concept of a set, one of the most important and most elementary concepts in mathematics in general. Building on this, classifications of a dynamical system are discussed placing greater emphasis on systems of ordinary differential equations and the question on existence and uniqueness of a solution. In Section 1.2 a special type of systems of ordinary differential equations is analyzed, namely those that involve two different time scales and are available in an explicit fast–slow form, called singularly perturbed systems. In this context, FENICHEL'S invariant manifold theorem is discussed, which asserts existence of a manifold that is used in the context of model reduction in a subsequent chapter and whose computation or the basic procedure of the computation, known as species reconstruction, is discussed in the following section. Especially, the formulation of an optimization problem plays an important role, which is why the theory of optimization problems is discussed in the last section of this chapter. Exactly for this species reconstruction approach in form of an optimization problem the existence of a solution is shown in Theorem 1.4.4, being of particular significance in the context of model reduction via manifold computation in this work. Within the whole chapter, different concepts are demonstrated by means of a simple example—a two-dimensional linear system of ordinary differential equations, introduced in Example 1.1.3.

1.1 Theory of Dynamical Systems and Systems of Ordinary Differential Equations

One of the most basic concepts in mathematics is the concept of a **set**. In his work *Beiträge zur Begründung der transfiniten Mengenlehre* [Can95], the founder of set theory, CANTOR, gave the following definition of a set:

> "A set is a gathering together into a whole of definite, distinct objects of our perception or of our thought—which are called elements of the set."

In general, a set is described as a well defined collection of objects—called **elements**. If X and Y are sets and every element of X is also an element of Y, then X is a **subset** of Y ($X \subset Y$). The **cartesian product** of two sets X and Y is the set of all ordered pairs (x, y), $x \in X$, $y \in Y$ and is denoted by $X \times Y$. A **function** $f\colon X \to Y$, $x \mapsto y$ from a set X to a set Y is a set f, which is a subset of the cartesian product $X \times Y$ subject to the following condition: every element of X is the first component of one and only one ordered pair in the subset. In other words, for every $x \in X$ there is exactly one element $y \in Y$ such that the ordered pair $(x, y) \in X \times Y$ is contained in the subset defining the function f. In this context, the elements of X are called arguments of f and the corresponding unique $y \in Y$ is called image of x under f denoted by $f(x)$. A set with one or more finitary operations defined on it is called **algebraic structure**. A special one is a **magma** $(X, *)$ consisting of a set X together with a binary operation $*$, which is a function $*\colon X \times X \to X$. Under the condition that this binary operation satisfies the associative property (for all $x_1, x_2, x_3 \in X$, the equation $(x_1 * x_2) * x_3 = x_1 * (x_2 * x_3)$ holds) and there exists an element $e \in X$, such that for all elements $x \in X$, the equation $e * x = x * e = x$ holds (identity element), the magma becomes a **monoid** $(X, *, e)$.

This mathematical framework suffices for the definition of a **dynamical system** (in the further course of this thesis certain terms are assumed to be known and cannot be derived and defined as detailed as done before).

Definition 1.1.1 (Dynamical System). A dynamical system is a triple (T, Z, φ) where T is a monoid, written additively[3], Z is a set, and φ is a function

$$\varphi\colon U \subset (T \times Z) \to Z \tag{1.1}$$

with

$$\varphi(0, z) = z \tag{1.2a}$$

$$\varphi(t_2, \varphi(t_1, z)) = \varphi(t_1 + t_2, z), \text{ for } t_1, t_2, t_1 + t_2 \in I(z) \tag{1.2b}$$

---

[3]For simplicity reasons the monoid $(T, +, 0)$ is denoted as T.

where $I(z) := \{t \in T \mid (t, z) \in U\}$. The function $\varphi(t, z)$ is called the **evolution function** of the dynamical system, which associates to every point of Z a unique image, depending on the **evolution parameter** t. The set Z is denoted as **phase space**, while the variable z represents an **initial state** of the system. If z is chosen constant, $\varphi_z(t) := \varphi(t, z)$ is the notation that defines the **flow** through z given by $\varphi_z \colon I(z) \to Z$ and whose graph is called **trajectory**.

The particular importance of a dynamical system comes to bear in its relation to everyday events. Time dependent processes, where the temporal evolution is not determined by the starting time, but by the initial state (such processes are called homogeneous in time), are mathematically modeled by dynamical systems, allowing a wide range of applications and insights into different scientific fields like physics (oscillating movement), biology (predator-prey relationship), and chemistry (combustion processes), to name only a few.

The dynamical systems (T, Z, φ) considered within the scope of this work are **dissipative** implying the possession of a bounded **absorbing** set $B_0 \subset Z$. A bounded set $B_0 \subset Z$ in turn is said to be absorbing for a dynamical system (T, Z, φ), if for any bounded set B in Z there exists $t_0 = t_0(B)$ such that $\varphi(t, B) \subset B_0$ for every $t \geq t_0$. Especially, if the phase space Z of a dissipative dynamical system (T, Z, φ) is a BANACH space $(Z, \|\cdot\|_Z)$, a ball of the form $\{z \in Z \colon \|z\|_Z \leq R\}$ can be taken as an absorbing set, where $R \in \mathbb{R}$ is referred to as **radius of dissipativity**.

The further classification of dynamical systems is done by specification of the triple (T, Z, φ), wherefore the definition of a manifold is required, which is given below.

A **topological space** $(X, \mathcal{T})$ is a set X together with a collection $\mathcal{T}$ of subsets of X, called **open sets** and satisfying the following axioms:

1. The empty set and X itself are open.

2. Any union of open sets is open.

3. The intersection of any finite number of open sets is open.

Underlying the previous definitions, the collection $\mathcal{T}$ of open sets is also called a **topology** on X. If the topology does not need an explicit name, then the topological space $(X, \mathcal{T})$ is denoted by X. Points x_1 and x_2 in a topological space X can be **separated by neighborhoods** if there exists a neighborhood U of x_1 and a neighborhood V of x_2 such that U and V are disjoint. If any two distinct points of X can be separated by neighborhoods, X is a **HAUSDORFF space**. A topological space X is **second-countable** if there exists some countable collection $\mathcal{U} = \{U_i\}_{i=1}^{\infty}$

of open subsets of X such that any open subset of X can be written as a union of elements of some subfamily of $\mathcal{U}$.

Definition 1.1.2 (Topological Manifold). A topological space M is called an n-dimensional **topological manifold** if

1. M is a HAUSDORFF space.

2. M is second-countable.

3. M is locally EUCLIDEAN, i.e. every point $x \in M$ has an open neighborhood $U \subset M$ that is homeomorphic to an open subset of $\mathbb{R}^m$.

In the remainder of this work a **manifold** will mean a topological manifold.

A dynamical system (T, M, φ_z) is called **real dynamical system** if T is an open interval in the real numbers $\mathbb{R}$, M a manifold locally diffeomorphic to a BANACH space, and φ_z a continuous function. Additionally, if the manifold M is locally diffeomorphic to $\mathbb{R}^m$, the dynamical system is **finite-dimensional**, if not, it is **infinite-dimensional**.

Example 1.1.3 (Finite-Dimensional Real Dynamical System). A finite-dimensional real dynamical system is given by $(\mathbb{R}, \mathbb{R}^2, \varphi_{z^0})$, where $\varphi_{z^0}(t) =: z(t) = (z_1(t), z_2(t))^\top$ is solution of

$$\mathrm{d}_t z_1(t) = \left(-1 - \frac{\gamma}{2}\right) z_1(t) + \frac{\gamma}{2} z_2(t) \tag{1.3a}$$

$$\mathrm{d}_t z_2(t) = \frac{\gamma}{2} z_1(t) + \left(-1 - \frac{\gamma}{2}\right) z_2(t) \tag{1.3b}$$

$$z_1(0) = z_1^0 \tag{1.3c}$$

$$z_2(0) = z_2^0 \tag{1.3d}$$

with $\gamma \in \mathbb{R}$, $\gamma > 0$, and $z^0 := (z_1^0, z_2^0)^\top$.[4]

Example 1.1.4 (Infinite-Dimensional Real Dynamical System). An infinite-dimensional real dynamical system is given by $(\mathbb{R}, \mathcal{B}, \varphi_{z^0})$, where $\mathcal{B}$ is an infinite-dimensional function space

---

[4]Notation: $\mathrm{d}_t := \frac{\mathrm{d}}{\mathrm{d}t}$, $\mathrm{d}_t^n := \frac{\mathrm{d}^n}{\mathrm{d}t^n}$

and $\varphi_{z^0}(t) =: z(t,x) = (z_1(t,x), z_2(t,x))^\top$ is solution of

$$\partial_t z_1(t,x) = \mathcal{D}_1 \partial_{xx}^2 z_1(t,x) + \left(-1 - \frac{\gamma}{2}\right) z_1(t,x) + \frac{\gamma}{2} z_2(t,x) \tag{1.4a}$$

$$\partial_t z_2(t,x) = \mathcal{D}_2 \partial_{xx}^2 z_2(t,x) + \frac{\gamma}{2} z_1(t,x) + \left(-1 - \frac{\gamma}{2}\right) z_2(t,x) \tag{1.4b}$$

$$z_1(0,x) = z_1^0(x) \tag{1.4c}$$

$$z_2(0,x) = z_2^0(x) \tag{1.4d}$$

$$z_1(t,0) = a_1 \tag{1.4e}$$

$$z_1(t,1) = b_1 \tag{1.4f}$$

$$z_2(t,0) = a_2 \tag{1.4g}$$

$$z_2(t,1) = b_2 \tag{1.4h}$$

with $\gamma, x, a_1, b_1, a_2, b_2, \mathcal{D}_1, \mathcal{D}_2 \in \mathbb{R}$ and $z^0 := \left(z_1^0(x), z_2^0(x)\right)^\top$.[5]

Equations (1.3a), (1.3b) and (1.4a), (1.4b) are **differential equations** which are mathematical equations that relate some function with its derivatives. There are two important kinds of differential equations: **ordinary differential equations (ODEs)** and **partial differential equations (PDEs)**. An ODE is a differential equation containing a function of one independent variable and its derivatives (cf. (1.3a), (1.3b)), whereas a PDE contains unknown multivariable functions and their partial derivatives (cf. (1.4a), (1.4b)). More precisely, a **system of ODEs of order** $n \in \mathbb{N}$ is given by

$$S(t, z, \mathrm{d}_t z, \mathrm{d}_t^2 z, \ldots, \mathrm{d}_t^n z) = 0 \tag{1.5}$$

where $S \colon \Omega \subset \left(\mathbb{R} \times (\mathbb{R}^m)^{n+1}\right) \to \mathbb{R}^m$, $m \in \mathbb{N}$ is a continuous vector-valued function of z and its derivatives and z is a vector whose elements are functions $z(\cdot) = (z_1(\cdot), z_2(\cdot), \ldots, z_m(\cdot))^\top$. For $m = 1$ it is just referred to as ODE of order n. If it is possible to solve the system of ODEs of order n for the highest occuring derivation and consequently is in the following form

$$\mathrm{d}_t^n z = S(t, z, \mathrm{d}_t z, \mathrm{d}_t^2 z, \ldots, \mathrm{d}_t^{n-1} z), \tag{1.6}$$

it is called **explicit**. Furthermore, an explicit system of ODEs of order n not depending explicitly on the independent variable (here t) is called **autonomous**. A further classification is linearity/nonlinearity: A system of ODEs of order n in form of (1.5) is **linear** if S can be written as a linear combination of the derivatives of z

$$\mathrm{d}_t^n z = \sum_{i=0}^{n-1} a_i(t) \mathrm{d}_t^i z + r(t) \tag{1.7}$$

---

[5]Notation: $\partial_t := \frac{\partial}{\partial t}$, $\partial_{xx}^2 := \frac{\partial^2}{\partial x^2}$

where $a_i(t)$ and $r(t)$ are continuous functions in t, otherwise it is called **nonlinear**. Additionally, if $r(t) \equiv 0$, the linear system of ODEs of order n is specified as **homogeneous**, if $r(t) \not\equiv 0$ it is referred to as **nonhomogeneous**. In summary, Equations (1.3a) and (1.3b) are a homogeneous, linear, autonomous, and explicit system of ODEs of order one. In the remainder of this work we restrict ourselves to explicit, autonomous systems of ODEs of order one (note that on the one hand any system of ODEs can be transformed into an autonomous one by adding $z_{m+1} := t$, $\mathrm{d}_t z_{m+1} = 1$ and on the other hand any system of ODEs of order greater than one can rewritten as one of order one).

As already indicated, a wide range of disciplines are concerned with systems of ODEs of various types. The subsequent three examples demonstrate exemplarily the importance of systems of ODEs in physics, biology, and chemistry, where processes are virtually modeled by these kinds of equations. Especially the third example shows the modeling of a chemical reaction process serving as a basis for the content of this work.

Example 1.1.5 (Mathematical Pendulum)**.** The mathematical pendulum is an idealized pendulum where on the one hand the cord on which the bob swings is massless, inextensible, and always remains taut and on the other hand the bob is believed to be a point mass with mass m_{G}. Furthermore, the motion occurs only in two dimensions and loses no energy to friction or air resistance. The whole arrangement takes place in an isolated system. By using the small-angle approximation $\sin(\phi) \approx \phi$, the motion of this pendulum is given by the following ODE of order two:

$$\mathrm{d}_t^2 \phi(t) + \frac{g}{\ell}\phi(t) = 0 \tag{1.8}$$

Here, g is acceleration due to gravity, ℓ is the length of the pendulum, and ϕ is the angular displacement.
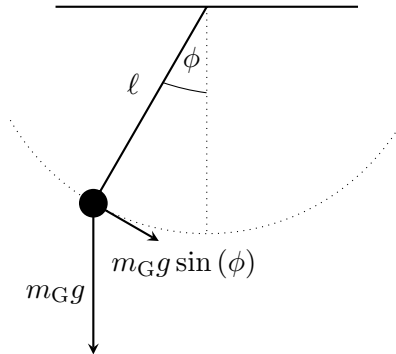
Figure 1.1: Schematic illustration of the mathematical pendulum.

Example 1.1.6 (SIR Model)**.** The SIR model [KM27], created by KERMACK and MCKENDRICK in 1927, describes the spread of an infectious disease taking also development of immunities into consideration. The model considers a fixed population $N = S(t) + I(t) + R(t)$ with three components:

$S(t)$ is used to represent the number of individuals not yet infected with the disease at time t (susceptibles).

$I(t)$ denotes the number of individuals who have been infected with the disease and are capable of spreading the disease to those in the susceptible category (infected).

$R(t)$ is the compartment used for those individuals who have been infected and then removed from the disease, either due to immunization or due to death (recovered).

The spread of the disease is formulated by KERMACK and MCKENDRICK by the following system of ODEs

$$\mathrm{d}_t S(t) = -cI(t)S(t) \tag{1.9a}$$

$$\mathrm{d}_t I(t) = iI(t)S(t) - wI(t) \tag{1.9b}$$

$$\mathrm{d}_t R(t) = wI(t) \tag{1.9c}$$

where c is the rate of disease and w the rate of recovery. Thus, this example demonstrates the application of ODEs in the biology, more precisely in epidemiology.

Figure 1.2: Schematic illustration of the SIR model by KERMACK and MCKENDRICK [KM27].

Example 1.1.7 (Chemical Reaction Kinetics)**.** The following example demonstrates the modeling of chemical reaction mechanisms by systems of ODEs. Assuming m_{spec} chemical species—denoted as $X_1, \ldots, X_{m_{\mathrm{spec}}}$—participating in a chemical reaction mechanism composed of m_{reac} reactions, this mechanism taking place in a closed system is given by

$$\sum_{s=1}^{m_{\mathrm{spec}}} \nu_{rs}^{(\mathrm{e})} X_s \underset{k_{r,-}}{\overset{k_{r,+}}{\rightleftharpoons}} \sum_{s=1}^{m_{\mathrm{spec}}} \nu_{rs}^{(\mathrm{p})} X_s, \quad r = 1, \ldots, m_{\mathrm{reac}}. \tag{1.10}$$

Here, $\nu_{rs}^{(\mathrm{e})}$ and $\nu_{rs}^{(\mathrm{p})}$ are stoichiometric coefficients of reactants and products in reaction r and $k_{r,+}$ and $k_{r,-}$ indicate the rate coefficients of an elementary reaction r. The concentration of a chemical species X_i is given by

$$z_i = \frac{n_i}{V} \tag{1.11}$$

with n_i being the amount of substance (number of particles) of that species and V being the volume. In the isochoric case (V being constant) the reaction kinetic equations are given by the following system of ODEs

$$\mathrm{d}_t z = \sum_{r=1}^{m_{\mathrm{reac}}} \nu_r W_r(z) \tag{1.12}$$

where ν_r is the vector $\nu_r = (\nu_{r1}^{(\mathrm{p})} - \nu_{r1}^{(\mathrm{e})}, \ldots, \nu_{rm_{\mathrm{spec}}}^{(\mathrm{p})} - \nu_{rm_{\mathrm{spec}}}^{(\mathrm{e})})^\top$ and $W_r(z)$ is the reaction rate function of reaction r defined by the mass action law

$$W_r(z) = W_{r,+}(z) - W_{r,-}(z) = k_{r,+} \prod_{s=1}^{m_{\mathrm{reac}}} z_s^{\nu_{rs}^{(\mathrm{e})}} - k_{r,-} \prod_{s=1}^{m_{\mathrm{spec}}} z_s^{\nu_{rs}^{(\mathrm{p})}}. \tag{1.13}$$

Thus, the rate coefficients $k_{r,+}$ and $k_{r,-}$ are the constants of the direct ($W_{r,+}(z)$) and of the inverse ($W_{r,-}(z)$) reaction rates of the rth elementary reaction and can be computed by the ARRHENIUS law given by

$$k_{r,\pm} = A_{r,\pm} T^{b_{r,\pm}} \exp\left(-\frac{E_{\mathrm{a},r,\pm}}{RT}\right). \tag{1.14}$$

Here $A_{r,\pm}$ and $b_{r,\pm}$ are constants, $E_{\mathrm{a},r,\pm}$ is the activation energy, R is the gas constant, and T denotes the temperature.

The **solution** of a system of ODEs $\mathrm{d}_t z = S(z)$ is a differentiable function $u : I \subset \mathbb{R} \to \mathbb{R}^m$ with $\mathrm{d}_t u = S(u)$, $t \in I$. The differential equation itself is not sufficient for existence and uniqueness of a solution. Therefore, additional information in form of **initial conditions** or **boundary conditions** is necessary. The former is a value of an evolving variable at some point in time designated as **initial time** ($t = t_0$). If a solution z of a system of ODEs additionally satisfies a given initial condition, the solution z is said to be a solution of an **initial value problem (IVP)**.

Definition 1.1.8 (Initial Value Problem (IVP))**.** An initial value problem is a differential equation

$$\mathrm{d}_t z = S(z) \tag{1.15}$$

with $S : \Omega \subset \mathbb{R}^m \to \mathbb{R}^m$, together with a point in the domain of S

$$z(t_0) = z^0 \in \Omega, \tag{1.16}$$

called the initial condition. The solution z of an IVP is also denoted by $z(\cdot; z^0)$.

Two important theorems regarding existence and uniqueness of solutions to IVPs are **PEANO existence theorem** [Pea86, Pea90] and **PICARD–LINDELÖF theorem** [Lin94]. The former guarantees the local existence of solutions to certain IVPs, but there is no statement regarding uniqueness. This is realized in the PICARD–LINDELÖF theorem where stronger conditions are required. A brief comparison of both theorems is given in Table 1.1.

Theorem 1.1.9 (PEANO Existence Theorem)**.** *Let Ω be an open subset of $\mathbb{R}^m$ with $S\colon \Omega \to \mathbb{R}^m$ a continuous function and $\mathrm{d}_t z = S(z)$ a system of ODEs defined on Ω, then every IVP*

$$\mathrm{d}_t z = S(z), \quad z(t_0) = z^0 \tag{1.17}$$

with $z^0 \in \Omega$ has a local solution

$$u\colon I \to \mathbb{R}^m \tag{1.18}$$

where I is a neighborhood of $t_0 \in \mathbb{R}$, such that $\mathrm{d}_t u = S(u)$ for all $t \in I$.

Proof. See e.g. [SB02]. $\qquad\qquad\square$

Definition 1.1.10 (LIPSCHITZ Continuity)**.** A function $S\colon \Omega \subset \mathbb{R}^m \to \mathbb{R}^m$, $m \in \mathbb{N}$ is called **LIPSCHITZ continous** if

$$\|S(\hat{z}) - S(\check{z})\| \leq L\,\|\hat{z} - \check{z}\|, \quad \hat{z}, \check{z} \in \Omega \tag{1.19}$$

holds with a so-called **LIPSCHITZ constant** $L > 0$.

Theorem 1.1.11 (PICARD–LINDELÖF Theorem)**.** *Consider the IVP*

$$\mathrm{d}_t z = S(z), \quad z(t_0) = z^0, \quad z \in \mathbb{R}^m. \tag{1.20}$$

Let $\Omega = \overline{B(z^0, R)}$ (the closed ball in $\mathbb{R}^m$ around z^0 with radius R) and $I = [t_0 - \varepsilon, t_0 + \varepsilon]$, where $S\colon \Omega \to \mathbb{R}^m$ is LIPSCHITZ continuous in z with LIPSCHITZ constant L and $|S(z)| \leq \beta$ for all $z \in \Omega$. Then, the IVP has a unique solution $z(\cdot\,; z^0) \in \mathcal{C}^0(I, \Omega)$ as long as the time interval is chosen with a satisfying $0 < \varepsilon < \min\left(\frac{1}{L}, \frac{R}{\beta}\right)$.

Proof. See e.g. [Wal00]. $\qquad\qquad\square$

Table 1.1: Comparison of the two main theorems relating to solutions of IVPs involving ODEs.

Theorem	Assumption	Conclusion
PEANO existence theorem	S continuous	local existence only
PICARD–LINDELÖF theorem	S LIPSCHITZ continuous	local existence and uniqueness

Example 1.1.12. The IVP (1.3) fulfills the requirements of Theorem 1.1.11, since $S(z) = Az$ with

$$A := \begin{pmatrix} -1 - \frac{\gamma}{2} & \frac{\gamma}{2} \\ \frac{\gamma}{2} & -1 - \frac{\gamma}{2} \end{pmatrix} \in \mathbb{R}^{2\times 2} \tag{1.21}$$

is linear in z and any linear function is LIPSCHITZ continous. Accordingly, there locally exists a unique solution $z(\cdot\,; z^0) \in \mathbb{R}^2$ of (1.3).

1. Analytical Basics

There are various types of stability for the solutions of differential equations describing dynamical systems. A solution to a system of ODEs or—more generally—an invariant set $M \subset \mathbb{R}^{m+1}$ (a set $M \subset \mathbb{R}^{m+1}$ is called **invariant** under the differential equation $\mathrm{d}_t z = S(z)$ if for any $z(t_0) = z^0 \in M$ there is $z(t; z^0) \in M$ for all t) is

- **LYAPUNOV stable** if for any given $\varepsilon > 0$ there exists a $\delta = \delta(\varepsilon) > 0$ such that $\rho\left(M, z(t; z^0)\right) < \varepsilon$ holds for any $z(t_0) = z^0$ that satisfies $\rho\left(M, z^0\right) < \delta$ for all $t > t_0$.[6]

- **attractive** if there exists a constant $\eta > 0$ such that $\lim_{t \to \infty} \rho\left(M, z(t; z^0)\right) = 0$ follows from $\rho\left(M, z^0\right) < \eta$.

- **asymptotically stable** if M is both, LYAPUNOV stable and attractive.

- **exponentially stable** if it is asymptotically stable and there exist $\alpha, \beta, \eta > 0$ such that if $\rho\left(M, z^0\right) < \eta$, then $\rho\left(M, z(t; z^0)\right) \leq \alpha \rho\left(M, z^0\right) e^{-\beta t}$ for all $t > t_0$.

In other words, LYAPUNOV stability means that solutions starting close to M will remain close to M, asymptotic stability means that solutions that start close enough not only remain close enough but also eventually converge to M, and exponentially stability means that solutions converge faster than or at least as fast as a particular known rate.

Stability properties of an equilibrium solution $z(t) = z^{\mathrm{eq}}$ of a system of ODEs (an equilibrium solution is a solution that does not change with time or, more precisely, the system of ODEs $\mathrm{d}_t z = S(z)$ has an equilibrium solution $z(t) = z^{\mathrm{eq}}$ if $S(z^{\mathrm{eq}}) = 0$ for all t) are determined by analyzing the JACOBIAN $J_S(z^{\mathrm{eq}}) := \left(\partial_{z_j} S_i(z^{\mathrm{eq}})\right)_{i,j=1,\dots,m}$ of the right-hand side $S(z)$, which is supposed to be continuously differentiable here: if all eigenvalues of $J_S(z^{\mathrm{eq}})$ have strictly negative real part then the equilibrium solution is asymptotically stable.

Furthermore, there is a result from [RS03] concerning existence of exponentially stable manifolds: an invariant manifold M of an autonomous system of ODEs is exponentially stable if and only if all components, transversal to M, of solutions of the linearized equations exponentially tend to zero. In addition to it, the work shows the existence of a function which characterizes points on exponentially stable manifolds.

In Figure 1.3 solutions of the linear IVP (1.3) with $\gamma = 10$ are illustrated in the two-dimensional phase space for different values of z^0 represented by the crosses. Accordingly, the trajectories represent the appropriate solutions $z(\cdot; z^0)$, while the red dot constitutes the asymptotically stable equilibrium $z^{\mathrm{eq}} = (0.0, 0.0)^\top$, since eigenvalues of the JACOBIAN $J_S(z^{\mathrm{eq}}) =$

---

[6] $\rho(M, \hat{z}) := \inf_{y \in M} \|y - \hat{z}\|, \ \hat{z} \in \mathbb{R}^m$

$\begin{pmatrix} -6.0 & 5.0 \\ 5.0 & -6.0 \end{pmatrix}$ arise as $\lambda_1 = -1$ and $\lambda_2 = -11$. The invariance property of trajectories is demonstrated by the green curve: for $z^0 = z(t_0) = (0.0, 6.0)^\top$ and $z^1 = z(t_1; z^0) \in z(\cdot; z^0)$, $t_1 > t_0$, represented by the green cross, there is $z(\cdot; z^1) \in z(\cdot; z^0)$ for all t. Futhermore, the red curve shows an exponentially stable manifold.
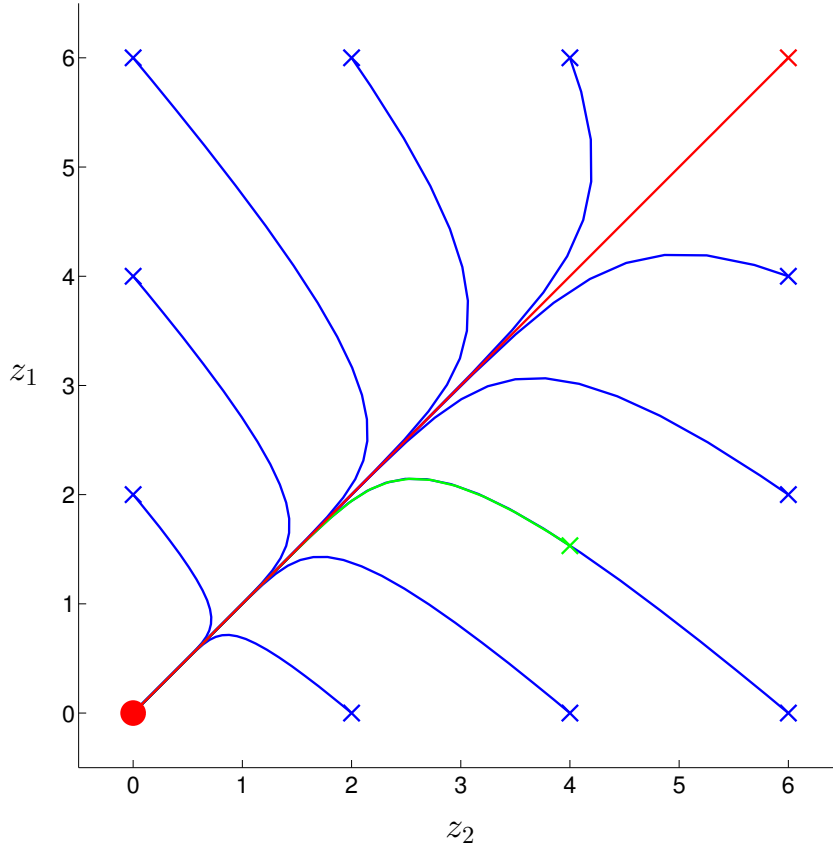
Figure 1.3: Phase space plot of the linear IVP (1.3) with $\gamma = 10$ for different values of z^0.

The unique solution to (1.3) (see Example 1.1.12) is given by

$$z_1(t) = \frac{z_1^0 + z_2^0}{2} e^{-t} + \frac{z_1^0 - z_2^0}{2} e^{(-1-\gamma)t} \tag{1.22a}$$

$$z_2(t) = \frac{z_1^0 + z_2^0}{2} e^{-t} - \frac{z_1^0 - z_2^0}{2} e^{(-1-\gamma)t} \tag{1.22b}$$

where a separation of time scales[7] is visible (depending on the parameter γ): the first term $\frac{z_1^0 + z_2^0}{2} e^{-t}$ represents the slow modes of the system and the second one $\frac{z_1^0 - z_2^0}{2} e^{(-1-\gamma)t}$ the fast modes. As can be seen, the fast mode terms vanish for $z_1^0 = z_2^0$ and thus, $z_1(t) \equiv z_2(t)$. As a consequence, the slow time scales of the system are associated with the exponentially stable

---

[7]Formally defined, a time scale is a closed subset of the real number line $\mathbb{R}$.

manifold $z_1 \equiv z_2$ (red curve in Figure 1.3).

Chemical reaction kinetics modeled by systems of ODEs as illustrated in Example 1.1.7 often show—under certain conditions—very similar features as the linear model discussed above: solution trajectories bundle near asymptotically stable manifolds of successively lower dimension during time evolution caused by spectral gaps generating multiple time scales. This time scale separation into fast and slow modes is the basis for most model and complexity reduction techniques, where the long time scale system dynamics is approximated via elimination of the fast relaxing modes by enslaving them to the slow ones. The outcome of this is in the ideal case an invariant manifold of slow motion, which is denoted as **slow invariant manifold (SIM)**. Existence results of such SIMs are analyzed in the theory of **singularly perturbed systems**.

1.2 Theory of Singularly Perturbed Systems

Systems of ODEs in form of (1.15) that involve processes evolving on two different time scales naturally give rise to systems of the form

$$\mathrm{d}_t z_\mathrm{f} = S_\mathrm{f}\left(z_\mathrm{f}, z_\mathrm{s}; \varepsilon\right) \tag{1.23a}$$

$$\mathrm{d}_t z_\mathrm{s} = \varepsilon S_\mathrm{s}\left(z_\mathrm{f}, z_\mathrm{s}; \varepsilon\right) \tag{1.23b}$$

called **singularly perturbed systems of ODEs**. Here, the functions $S_\mathrm{f} : \Omega \times I \to \mathbb{R}^{m_\mathrm{f}}$ and $S_\mathrm{s} : \Omega \times I \to \mathbb{R}^{m_\mathrm{s}}$ are assumed to be smooth with Ω being an open subset of $\mathbb{R}^{m_\mathrm{f}} \times \mathbb{R}^{m_\mathrm{s}}$ and $I \subset \mathbb{R}^+$. Furthermore, $z_\mathrm{f} \in \mathbb{R}^{m_\mathrm{f}}$ and $z_\mathrm{s} \in \mathbb{R}^{m_\mathrm{s}}$ with $m_\mathrm{f}, m_\mathrm{s} \in \mathbb{N}$ and $m_\mathrm{f} + m_\mathrm{s} = m$. The parameter $\varepsilon \in I$ is assumed to be small in the sense that $0 < \varepsilon \ll 1$ and measures the separation of time scales. The so-called **fast variables** z_f change at a rate of $\mathcal{O}(1)$, whereas the **slow variables** z_s evolve more slowly, at a rate $\mathcal{O}(\varepsilon)$. System (1.23) can be rewritten with a time transformation

$$\varepsilon \mathrm{d}_\tau z_\mathrm{f} = S_\mathrm{f}\left(z_\mathrm{f}, z_\mathrm{s}; \varepsilon\right) \tag{1.24a}$$

$$\mathrm{d}_\tau z_\mathrm{s} = S_\mathrm{s}\left(z_\mathrm{f}, z_\mathrm{s}; \varepsilon\right) \tag{1.24b}$$

where $\tau := \varepsilon t$ defines the **slow time** τ. Accordingly, systems (1.23) and (1.24) are referred to as **fast** and **slow systems**, respectively. Whenever $\varepsilon \neq 0$, fast and slow system are equivalent. Conversely, there is a discontinous limiting behavior as $\varepsilon \to 0$ determining the label 'singular': The fast system (1.23) turns into the **reduced fast system**

$$\mathrm{d}_t z_\mathrm{f} = S_\mathrm{f}\left(z_\mathrm{f}, z_\mathrm{s}; 0\right) \tag{1.25a}$$

$$\mathrm{d}_t z_\mathrm{s} = 0 \tag{1.25b}$$

when $\varepsilon = 0$, describing an m_f-dimensional system of ODEs with z_s as constant parameter, whereas the slow system (1.24) reduces to a differential–algebraic system—the **reduced slow system**

$$0 = S_f\left(z_f, z_s; 0\right) \tag{1.26a}$$

$$d_\tau z_s = S_s\left(z_f, z_s; 0\right), \tag{1.26b}$$

where the number of ODEs decreases from m to m_s. It is natural to attempt to solve z_f in terms of z_s from Equation (1.26a) and plug it into (1.26b), wherefore the **implicit function threorem** can be applied.

Theorem 1.2.1 (Implicit Function Theorem). *Let $S_f : \Omega \to \mathbb{R}^{m_f}$, $(z_f, z_s) \mapsto S_f\left(z_f, z_s\right)$ be a continuously differentiable function with Ω being an open subset of $\mathbb{R}^{m_f} \times \mathbb{R}^{m_s}$. Fix a point $(z_f^0, z_s^0) \in \Omega$ with $S_f(z_f^0, z_s^0) = 0$. If the matrix $\partial_{z_f} S_f\left(z_f^0, z_s^0\right)$ is invertible, then there exists an open set Ω_1 containing z_f^0, an open set Ω_2 containing z_s^0, and a unique continuously differentiable function $h^0 : \Omega_2 \to \Omega_1$ with $h^0(z_s^0) = z_f^0$ such that $S_f\left(h^0(z_s), z_s\right) = 0$ for all $z_s \in \Omega_2$.*

Proof. See e.g. [Heu04]. $\qquad\square$

Provided that all eigenvalues of $\partial_{z_f} S_f\left(z_f, z_s; 0\right)$ have negative real part, the implicit function theorem guarantees existence of a continuously differentiable function $h^0 : \Omega_2 \subset \mathbb{R}^{m_s} \to \mathbb{R}^{m_f}$ with $h^0(z_s) = z_f$ such that $S_f\left(h^0(z_s), z_s; 0\right) = 0$ for all $z_s \in \Omega_2$ represents a slow manifold defined by

$$\mathcal{M}^0 := \{(z_f, z_s) \mid z_f = h^0(z_s), \ z_s \in \Omega_2\} \subset \mathbb{R}^m. \tag{1.27}$$

As a consequence, the dynamics of the reduced slow system (1.26) are given by

$$d_\tau z_s = S_s\left(h^0\left(z_s\right), z_s; 0\right). \tag{1.28}$$

Beyond that, each point $\left(h^0(z_s), z_s\right) \in \mathcal{M}^0$ is an asymptotically stable equilibrium solution of Equation (1.25a) and thus, $\mathcal{M}^0$ is asymptotically stable.

By using $\varepsilon := \frac{1}{\gamma+1}$ and $z = R\tilde{z}$ with $R = \begin{pmatrix} \cos\frac{\pi}{4} & -\sin\frac{\pi}{4} \\ \sin\frac{\pi}{4} & \cos\frac{\pi}{4} \end{pmatrix}$, the linear model $d_\tau z = Az$ with A given by (1.21) becomes

$$d_\tau \tilde{z}_1 = -\tilde{z}_1 \tag{1.29a}$$

$$\varepsilon d_\tau \tilde{z}_2 = -\tilde{z}_2 \tag{1.29b}$$

comprising the slow system form (1.24) of a singularly perturbed system with $\tilde{z}_1$ representing the slow variable and $\tilde{z}_2$ the fast one. The corresponding reduced slow system

$$\mathrm{d}_\tau \tilde{z}_1 = -\tilde{z}_1 \tag{1.30a}$$

$$0 = -\tilde{z}_2 \tag{1.30b}$$

yields the $\tilde{z}_1$-axis being the slow manifold

$$\mathcal{M}^0 := \{(\tilde{z}_1, \tilde{z}_2) \mid \tilde{z}_2 = h^0(\tilde{z}_1) = 0\} \tag{1.31}$$

and by using again $z = R\tilde{z}$ the first bisectrix $z_2 \equiv z_1$.

FENICHEL's invariant manifold theorem (see e.g. [Jon95]) asserts existence and properties of a manifold $\mathcal{M}^\varepsilon$ for system (1.23) or (1.24) in case $\varepsilon > 0$ that is a perturbation of $\mathcal{M}^0$. For this result, the definition of a **locally invariant set** is necessary: a set U is called locally invariant under (1.23) if it has a neighborhood V such that no trajectory can leave U without also leaving V. Furthermore, we say that $\mathcal{M}^0$ is **normally hyperbolic** if the linearization of (1.25) at each point $(\hat{z}_\mathrm{f}, \hat{z}_\mathrm{s}) \in \hat{\mathcal{M}}^0$ has exactly m_s eigenvalues with zero real part, where $\hat{\mathcal{M}}^0$ is an m_s-dimensional manifold in $\{S_\mathrm{f}(z_\mathrm{f}, z_\mathrm{s}; 0) = 0\}$ containing $\mathcal{M}^0$ in its interior.

Theorem 1.2.2 (FENICHEL Invariant Manifold Theorem). *If $\mathcal{M}^0$ is a normally hyperbolic manifold then there exists, for $\varepsilon > 0$ sufficiently small,*

- *a manifold $\mathcal{M}^\varepsilon$ that is diffeomorphic to $\mathcal{M}^0$ and has **HAUSDORFF distance**[8] $\mathcal{O}(\varepsilon)$ (as $\varepsilon \to 0$) from $\mathcal{M}^0$.*

- *a function $h^\varepsilon(z_\mathrm{s}) = z_\mathrm{f}$ defined on a compact set $\mathcal{K} \subset \mathbb{R}^{m_\mathrm{s}}$ such that the graph*

$$\mathcal{M}^\varepsilon = \{(z_\mathrm{f}, z_\mathrm{s}) \mid z_\mathrm{f} = h^\varepsilon(z_\mathrm{s}),\ z_\mathrm{s} \in \mathcal{K}\} \subset \mathbb{R}^m \tag{1.32}$$

  is locally invariant under (1.23).

Proof. See [Fen72, Fen79]. □

Furthermore, the function h^ε admits an asymptotic perturbation expansion

$$h^\varepsilon(z_\mathrm{s}) = h^0(z_\mathrm{s}) + \varepsilon h^{(1)}(z_\mathrm{s}) + \varepsilon^2 h^{(2)}(z_\mathrm{s}) + \mathcal{O}(\varepsilon^3) \tag{1.33}$$

---

[8]The HAUSDORFF distance between two nonempty sets $V, W \subset \mathbb{R}^m$ is defined by

$$d_H(V, W) := \max\{\sup_{v \in V} \inf_{w \in W} \|v - w\|,\ \sup_{w \in W} \inf_{v \in V} \|v - w\|\}$$

.

as $\varepsilon \searrow 0$ where the coefficients $h^{(\ell)} : \mathcal{K} \to \mathbb{R}^{m_\mathrm{f}}$, $\ell \in \mathbb{N}$ are found successively from plugging $h^\varepsilon(z_\mathrm{s})$ into the **invariance equation**: an equation that holds, in particular, along trajectories on invariant manifolds

$$\varepsilon \cdot J_{h^\varepsilon}(z_\mathrm{s}) \cdot S_\mathrm{s}\left(h^\varepsilon(z_\mathrm{s}), z_\mathrm{s}; \varepsilon\right) = S_\mathrm{f}\left(h^\varepsilon(z_\mathrm{s}), z_\mathrm{s}; \varepsilon\right), \quad \forall z_\mathrm{s} \in \mathcal{K} \tag{1.34}$$

and follows immediately from the chain rule $\mathrm{d}_t z_\mathrm{f} = J_{h^\varepsilon}(z_\mathrm{s}) \cdot \mathrm{d}_t z_\mathrm{s}$ and Equations (1.23). Consequently, the dynamics of System (1.23) on $\mathcal{M}^\varepsilon$ are given by the reduced equation

$$\mathrm{d}_\tau z_\mathrm{s} = S_\mathrm{s}\left(h^\varepsilon(z_\mathrm{s}), z_\mathrm{s}; \varepsilon\right). \tag{1.35}$$

When applying this to the linear example (1.29) the perturbation expansion yields $h^\varepsilon \equiv h^0$ and thus, concerning $\mathrm{d}_\tau z = Az$, the first bisectrix coincides not only with $\mathcal{M}^0$, but also with $\mathcal{M}^\varepsilon$, which in general is not usual at all. Finally, the reduced equation (1.35) results as

$$\mathrm{d}_\tau z_1 = \left(-1 - \frac{\gamma}{2}\right) z_1 + \frac{\gamma}{2} h^\varepsilon(z_1) = -z_1. \tag{1.36}$$

Generally, chemical reation kinetic models with multiple time scales in form of a system of ODEs are not in singularly perturbed form as (1.23). Nevertheless, to guarantee existence of SIMs, the existence of a diffeomophism is assumed that transforms the general system of ODEs $\mathrm{d}_t z = S(z)$ into as singularly perturbed one (1.23). By doing this, a SIM is defined by (1.32) with h^ε given in (1.33) posessing the property of attracting system trajectories from arbitraty inital values. As mentioned before, SIMs play a significant role in the context of model reduction in chemical reaction kinetics, which is why the computation of $\mathcal{M}^\varepsilon$ and thus also h^ε is absolutely essential. However, it is not feasible to obtain an analytic expression for h^ε from the theory of singularly perturbed systems for realistic kinetic models, the consequence being that numerical computation approaches are required.

1.3 Species Reconstruction

In general chemical reaction kinetic models $\mathrm{d}_t z = S(z)$, where the diffeomorphism transforming the system of ODEs into a singularly perturbed one is not known (existence is assumed anyway), it is far from clear how to split the full composition state vector of the system $z = (z_i)_{i=1}^m$ into slow and fast variables. Therefore, most kinetic model reduction approaches define a subset of the state variables, the **reaction progress variables (RPVs)** z_j, $j \in \mathcal{I}_\mathrm{fixed}$, where $\mathcal{I}_\mathrm{fixed} \subset \{1, \dots, m\}$ is the index set for the RPVs that parameterize a SIM and whose

determination is a substantial challenge in the context of model reduction in chemically re-acting flows which will be partially discussed later. **Species reconstruction** is the process of fixing the RPVs at a given point in time $t = t_*$ and determining the free variables (non RPVs) $z_k(t_*)$, $k \notin \mathcal{I}_{\text{fixed}}$ from $z_j^{t_*} := z_j(t_*)$, $j \in \mathcal{I}_{\text{fixed}}$, which implicitly defines a species reconstruction function $h \in \mathcal{C}(\mathbb{R}^{\#\mathcal{I}_{\text{fixed}}}, \mathbb{R}^{m-\#\mathcal{I}_{\text{fixed}}})$ mapping the RPVs to the full species composition thus determining a point on a SIM. The resulting point $z(t_*)$ consisting of the RPVs $z_j^{t_*}$ and $h\left(z_j^{t_*}\right)$ is referred to as **point of interest (POI)**. In comparison to the singularly perturbed system of ODEs, the RPVs, in the ideal case, correspond to the slow variables, the species reconstruction function h to h^ε, and a SIM is the diffeomorphic manifestation of $\mathcal{M}^\varepsilon$. Accordingly, the reduced dynamics on a SIM is given by

$$\mathrm{d}_t z_j = S_j\left(z\right), \qquad\qquad j \in \mathcal{I}_{\text{fixed}} \tag{1.37a}$$

$$z_k = h\left(z_j\right), \qquad\qquad j \in \mathcal{I}_{\text{fixed}}, \ k \notin \mathcal{I}_{\text{fixed}} \tag{1.37b}$$

where the number of ODEs has reduced from m to $\#\mathcal{I}_{\text{fixed}}$.

Figure 1.4 illustrates species reconstruction applied to the Linear Model (1.3a), (1.3b), where $\mathcal{I}_{\text{fixed}} = \{2\}$ is chosen as index set for determining the RPV that parameterizes the SIM (red line). Fixing the PRV at time $t = t_*$ is done for three different values of $z_2^{t_*}$ ($z_2^{t_*} = 1.0$, $z_2^{t_*} = 3.0$, and $z_2^{t_*} = 5.0$), whereby the corresponding points in phase space are restricted to the respective black dashed lines. Then, the species reconstruction function h identifies the respective values of the non RPVs in a way that the resulting POIs $\left(z_2^{t_*}, h\left(z_2^{t_*}\right)\right)^\top$ represented by the black crosses identify the SIM exactly.

To sum up, trajectories of system of ODEs modeling chemical combustion processes with spectral gaps generating multiple time scales bundle on hierarchically ordered manifolds of successively lower dimension in phase space during time evolution. These asymptotically stable SIMs—representing the slow modes of the system and whose existence (cf. 1.2.2) is given by assuming a diffeomorphism transforming the kinetic model equations into a singularly perturbed form—are the basis for many model reduction approaches, where the identification of the slow modes of the system and thus, the computation of SIMs is realized via species reconstruction. A sketch of this situation is depicted in Figure 1.5, where a three-dimensional phase space—spanned by the dependent state variables—is restricted to a physically meaningful domain given by the positivity of the values of the state variables and several conservation relations (e.g. elemental mass in chemical kinetics). The edges of this polytope are visualized by the blue dashed lines, whereas the black lines show trajectories starting from different initial values represented by the black crosses and converging towards the chemical equilibrium depicted by the red dot. It can be observed, that trajectories first bundle onto a two-dimensional SIM (red bounded) dur-
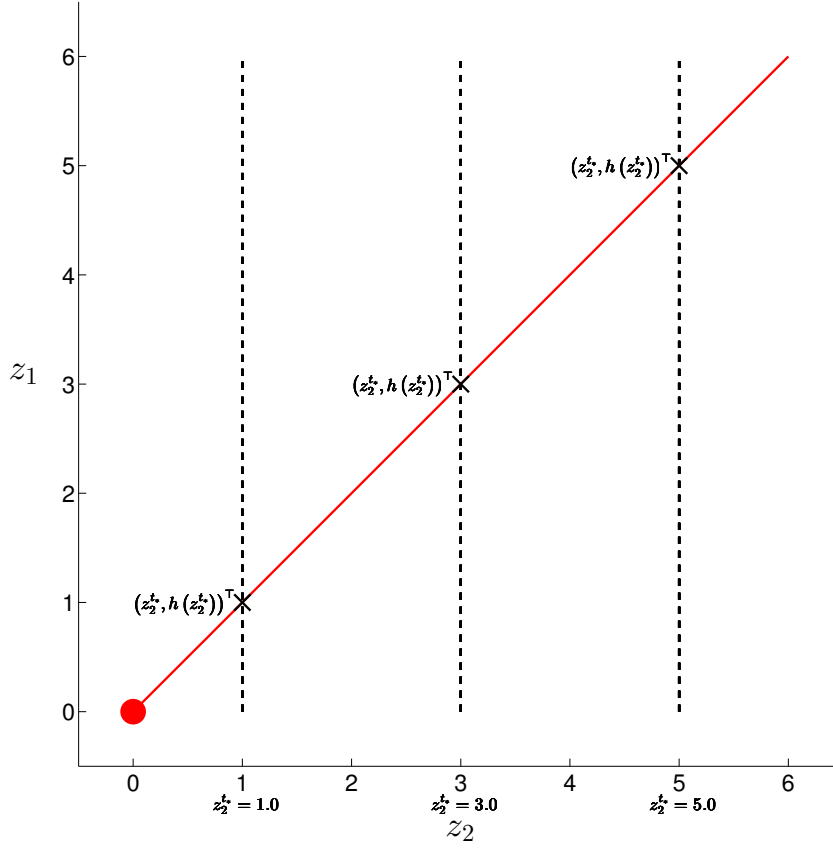
Figure 1.4: Illustration of species reconstruction applied to (1.3a), (1.3b) with three different values of $z_2^{t_*}$.

ing time evolution followed by a bundling onto a one-dimensional SIM before converging to equilibrium—also denoted as 'zero-dimensional manifold'. Since the temporal rate of change of the state vector converges to zero along the course of a trajectory through phase space, SIMs represent the slow modes of the kinetic model and thus it is desirable to find a constructive representation hereof. This representation is realized via species reconstruction, demonstrated in Figure 1.6. Here, Figure 1.6(a) represents a sketch of the identification of a two-dimensional SIM by using $\mathcal{I}_{\text{fixed}} = \{2, 3\}$ as index set for the selection of the RPVs, whereas in Figure 1.6(b), z_2 is determined as RPV w.l.o.g. for parameterizing the one-dimensional SIM. For several values of these RPVs ($\left(z_2^{t_*}, z_3^{t_*}\right)^\top$, $\left(z_2^{t_*}, z_3^{t_*}\right)^\top$, and $\left(z_2^{t_*}, z_3^{t_*}\right)^\top$ in Figure 1.6(a) and $z_2^{t_*}$, $z_2^{t_*}$, and $z_2^{t_*}$ in Figure 1.6(b)) the species reconstruction function h identifies the corresponding POIs on the SIMs.

Finding a functional $\Phi \in \mathcal{C}^\infty\left(\mathcal{C}^\infty\left(\mathbb{R}, \mathbb{R}^m\right), \mathbb{R}^p\right)$, $p \leq m$ with $\Phi(z) = 0$ that automatically eliminates the fast modes without knowing the analytical solution $z \in \mathcal{C}^\infty\left(\mathbb{R}, \mathbb{R}^m\right)$ of the underlying ODE model equations is the main challenge of trajectory–based model reduction
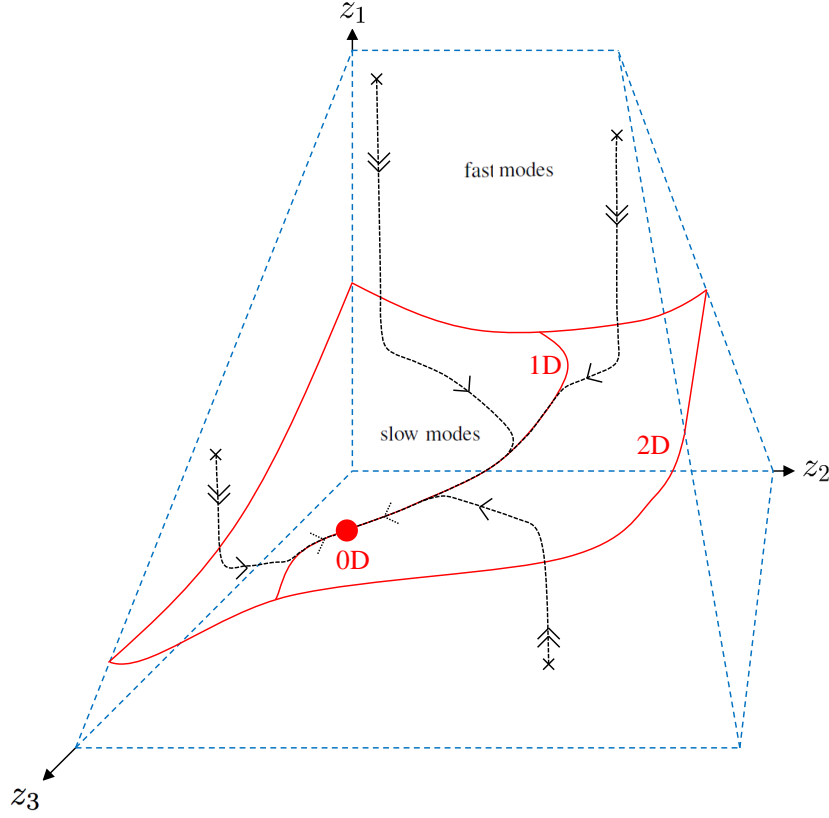
Figure 1.5: Sketch of a three-dimensional phase space of a chemical reaction kinetic model. Trajectories bundle near SIMs of successively lower dimension during time evolution caused by multiple time scales.

approaches. With the intention of finding the species reconstruction function h, the resulting general species reconstruction problem can be formulated as

$$\Phi(z) = 0 \tag{1.38a}$$

$$\mathrm{d}_t z(t) = S\left(z(t)\right) \tag{1.38b}$$

$$0 = g\left(z(t_*)\right) \tag{1.38c}$$

$$z_j(t_*) = z_j^{t_*}, \quad j \in \mathcal{I}_{\text{fixed}} \tag{1.38d}$$

$$0 \leq z(t_*), \tag{1.38e}$$

with (1.38b) describing the kinetic model equations and (1.38d) the fixing of the RPVs at time $t = t_*$. The function $g \in \mathcal{C}^\infty\left(\mathbb{R}^m, \mathbb{R}^b\right)$ in (1.38c) contains possible additional constraints (for instance chemical element mass conservation relations). Furthermore, the positivity of the state vector (1.38e) is required in real-life applications, which is mostly omitted in the further course of this work, since this work is restricted to toy examples where no negative values of the state vector occur. Alternatively, true to the motto
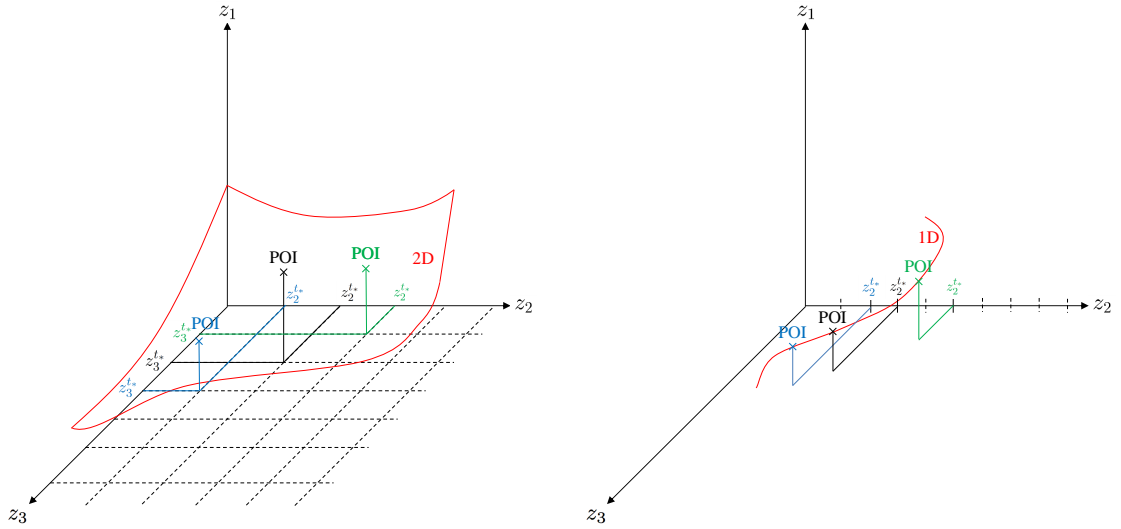
(a) Sketch of species reconstruction with two RPVs and thus a two-dimensional SIM is computed.

(b) Sketch of species reconstruction with one RPV and thus a one-dimensional SIM is computed.

Figure 1.6: Sketch of species reconstruction. For fixed values of the RPVs the species reconstruction function identifies POIs on SIMs.

"For since the fabric of the universe is most perfect and the work of a most wise Creator, nothing at all takes place in the universe in which some rule of maximum or minimum does not appear. "

famously uttered by L. EULER in 1744 [Eul44], the species reconstruction problem can be written—as suggested by LEBIEDZ in [Leb04]—in form of the following optimization problem

$$\min \quad \Phi(z) \tag{1.39a}$$

subject to

$$\mathrm{d}_t z(t) = S\left(z(t)\right) \tag{1.39b}$$

$$0 = g\left(z(t_*)\right) \tag{1.39c}$$

$$z_j(t_*) = z_j^{t_*}, \quad j \in \mathcal{I}_{\text{fixed}} \tag{1.39d}$$

$$0 \leq z(t_*) \tag{1.39e}$$

with $\Phi \in \mathcal{C}^\infty\left(\mathcal{C}^\infty\left(\mathbb{R}, \mathbb{R}^m\right), \mathbb{R}\right)$, wherefore a few basic concepts concerning theory of optimization problems have to be discussed.

1.4 Theory of Optimization Problems

As mentioned before, this work deals with model reduction in the context of chemical reaction kinetics where the reduced dynamics are identified via SIM computation, wherefore a species

1. Analytical Basics

reconstruction in form of an **Optimization Problem** (1.39) can be used. In short, an optimization problem is the problem of finding the best solution from all feasible ones. A general form of an optimization problem is

$$\min \quad \Phi(z) \tag{1.40a}$$

subject to

$$z \in \mathcal{S} \tag{1.40b}$$

where Z is a topological space, $\mathcal{S} \subset Z$ being the **feasible set**, and $\Phi : Z \to \mathbb{R}$ is a given function, denoted as **objective function**, to be minimized over the variable $z \in \mathcal{S}$. The optimization problems considered in this work are in form of a minimization problem. A maximization problem can be treated by negating the objective function.

Definition 1.4.1 (Basic Notions). Consider Optimization Problem (1.40).

(i) The vector $z \in Z$ is called **feasible** w.r.t. (1.40), if $z \in \mathcal{S}$.

(ii) The feasible vector $\bar{z}$ is called **strict** **global minimizer** w.r.t. (1.40) (cf. Figure 1.7), if

$$\Phi(\bar{z}) \overset{\leq}{_<} \Phi(z) \quad \forall z \in Z,\ z \neq \bar{z}. \tag{1.41}$$

(iii) The feasible vector $\bar{z}$ is called **strict** **local minimizer** w.r.t. (1.40) (cf. Figure 1.7), if there exists a neighborhood $U \subset Z$ with $\bar{z} \in U$, such that

$$\Phi(\bar{z}) \overset{\leq}{_<} \Phi(z) \quad \forall z \in Z \cap U,\ z \neq \bar{z}. \tag{1.42}$$

(iv) The optimal value w.r.t. (1.40) (cf. Figure 1.7) is defined by $v := \inf\{\Phi(z) \mid z \in \mathcal{S}\}$ if $\mathcal{S} \neq \emptyset$ and $v := \infty$ if $\mathcal{S} = \emptyset$.

Example 1.4.2 (Nonlinear Programming Problem in Standard Form). The Optimization Problem (1.40) appears often in the following **standard form**

$$\min \quad \Phi(z) \tag{1.43a}$$

subject to

$$g^{\mathrm{in}}(z) \leq 0 \tag{1.43b}$$
$$h^{\mathrm{eq}}(z) = 0 \tag{1.43c}$$

where the feasible set $\mathcal{S} \subset Z = \mathbb{R}^m$ from (1.40) is given by

$$\mathcal{S} = \{z \in \mathbb{R}^m \mid g^{\mathrm{in}}(z) \leq 0,\ h^{\mathrm{eq}}(z) = 0\}. \tag{1.44}$$

Here, $\Phi, g^{\mathrm{in}} : \mathcal{S} \to \mathbb{R}^{m_{\mathrm{in}}}$, and $h^{\mathrm{eq}} : \mathcal{S} \to \mathbb{R}^{m_{\mathrm{eq}}}$ are assumed to be twice continuously differentiable.
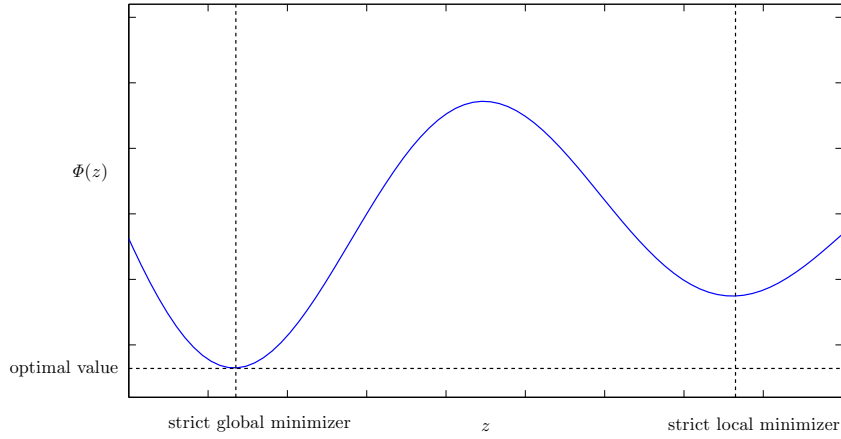
Figure 1.7: Schematic illustration of a strict local minimizer, a strict global one, and the optimal value w.r.t. (1.40) with $\mathcal{S} = \mathbb{R}$.

The immense significance of an easily formulated optimization problem as (1.40) or (1.43) is based on the fact that it can be used as a mathematical model for different real-life applications in a variety of sectors like physics, chemistry, and medicine, to name just a few. In this context, the vector $z \in Z$ can describe parameters of a model, which have not yet been determined by the modeling schemes or depict the freedom of choice and now should be chosen in an optimal way.

Next, existence of solutions to an optimization problem of the general form (1.40) is analyzed, whereby the following **WEIERSTRASS extreme value theorem** is inevitable.

Theorem 1.4.3 (WEIERSTRASS Extreme Value Theorem). *A continuous real-valued function* $\Phi : \mathcal{S} \to \mathbb{R}$ *on a non-empty compact space* $\mathcal{S} \subset Z$ *attains its infimum.*

Proof. See e.g. [Ger12]. □

This theorem guarantees the existence of at least one solution to Optimization Problem (1.40), if the aforementioned requirements of Theorem 1.4.3 are fulfilled. In the case of a **finite optimization problem** (i.e. $\mathcal{S} \subset \mathbb{R}^m$), compactness of a set $\mathcal{S} \subset \mathbb{R}^m$ is guaranteed by $\mathcal{S}$ being both closed and bounded, stated in the **HEINE–BOREL theorem**, which does noch apply to the **infinite** case ($\mathcal{S} \subset Z,\ Z \neq \mathbb{R}^m$). In this latter case, there is a modification of the WEIERSTRASS extreme value theorem making use of a **weakly compact set**, being a compact set with respect to the **weak topology**. For further details concerning this modification see [Leb12]. Thus, this theorem, formulated and proved by LEBIEDZ in [LSU11], yields statements on existence of solutions in the infinite case, if sufficient conditions are accessible guaranteeing weak compactness of the relevant set.

Theorem 1.4.4 (Existence of a Solution of Optimization Problem (1.39)). *Consider Optimization Problem (1.39). Let the constraint (1.39c) be given in the form $Az = b$ for some $(b \times m)$–matrix A of rank b and elements $a_{ij} \geq 0$, $j \in \{1, \ldots, m\}$, $b_i > 0$, $i \in \{1, \ldots, b\}$ and assume that for each index $j \in \{1, \ldots, m\}$ there is an index $i \in \{1, \ldots, b\}$ such that $a_{ij} > 0$. Let Φ be a function continuously depending on z. Then a solution of Problem (1.39) exists for all feasible choices of $z_j(t_*)$, $j \in \mathcal{I}_{\text{fixed}}$.*

Proof. See [LSU11]. $\square$

Optimization Problem (1.39), used as species reconstruction in this work (see 1.3), is a **semi-infinite optimization problem**, being an optimization problem with either a finite number of variables and an infinite number of constraints, or the other way around. Here, the dynamics in form of a system of ODEs (1.39b), whose solutions are represented by the state variable $z : I \subset \mathbb{R} \to \mathbb{R}^m$, enter the optimization problem as constraints. It turned out in application that computation of a solution of the dynamics (1.39b) within the solution algorithm for (1.39) can be very time consuming, which is why a 'local optimization problem' might be beneficial:

$$\min \quad \left. \Phi(z) \right|_{t=t_*} \tag{1.45a}$$

subject to

$$0 = g\left(z(t_*)\right) \tag{1.45b}$$

$$z_j(t_*) = z_j^{t_*}, \quad j \in \mathcal{I}_{\text{fixed}} \tag{1.45c}$$

$$0 \leq z(t_*). \tag{1.45d}$$

This local optimization problem in turn is a finite one and subordinates itself to the standard form (1.43), wherefore first order necessary and second order necessary and sufficient conditions for optimality can be stated.

Given a point z in the feasible set (1.44), an inequality constraint $g_i^{\text{in}}(z) \leq 0$ is called **active** at z if $g_i^{\text{in}}(z) = 0$. The **active set**

$$\mathcal{A}(z) := \{i \mid g_i^{\text{in}}(z) = 0, \ i = 1, \ldots, m_{\text{in}}\}. \tag{1.46}$$

at any feasible point z of (1.43) is made up of those inequality constraints $g_i^{\text{in}}(z)$ that are active at the current point and is particularly important in optimization theory as it determines which constraints will influence the final result of optimization. Additionally, a feasible point z of (1.43) with active set $\mathcal{A}(z)$ is said to fulfill the **linear independence constraint qualification (LICQ)** if the set of equality constraint gradients and active inequality constraint gradients[9]

$$\{\nabla h_j^{\text{eq}}(z), \ j = 1, \ldots, m_{\text{eq}}\} \cup \{\nabla g_i^{\text{in}}(z), \ i \in \mathcal{A}(z)\} \tag{1.47}$$

---

[9]Notation: $\nabla := \left(\frac{\partial}{\partial z_1}, \ldots, \frac{\partial}{\partial z_m} \right)^\top$

is linearly independent. First order necessary conditions for a solution to be optimal are formulated in the **KARUSH–KUHN–TUCKER (KKT) conditions**.

Theorem 1.4.5 (KARUSH–KUHN–TUCKER Conditions). *Let z^* be a local minimizer w.r.t. (1.43), Φ, h^{eq}, and g^{in} continuously differentiable, and z^* fulfill LICQ. Then there exist constants μ_i^*, $i = 1, \ldots, m_{\mathrm{in}}$ and λ_j^*, $j = 1, \ldots, m_{\mathrm{eq}}$, called **KKT multipliers**, such that*

$$\nabla \Phi(z^*) = \sum_{i=1}^{m_{\mathrm{in}}} \mu_i^* \nabla g_i^{\mathrm{in}}(z^*) + \sum_{j=1}^{m_{\mathrm{eq}}} \lambda_j^* \nabla h_j^{\mathrm{eq}}(z^*) \tag{1.48a}$$

$$g_i^{\mathrm{in}}(z^*) \leq 0, \quad \forall i = 1, \ldots, m_{\mathrm{in}} \tag{1.48b}$$

$$h_j^{\mathrm{eq}}(z^*) = 0, \quad \forall j = 1, \ldots, m_{\mathrm{eq}} \tag{1.48c}$$

$$\mu_i^*(z^*) \geq 0, \quad \forall i = 1, \ldots, m_{\mathrm{in}} \tag{1.48d}$$

$$\mu_i^* g_i^{\mathrm{in}}(z^*) = 0, \quad \forall i = 1, \ldots, m_{\mathrm{in}}. \tag{1.48e}$$

Proof. See e.g. [GK02]. □

Equation (1.48a) is known as **LAGRANGIAN stationarity**, (1.48b) and (1.48c) as **primal feasibility**, (1.48d) as **dual feasibility**, and (1.48e) is labeled **complementary slackness**. Furthermore, a point (z^*, λ^*, μ^*) that satisfies all KKT conditions (1.48) is called **KKT point**. The KKT conditions are sufficient for optimality if the following conditions are satisfied:

(i) The objective function Φ is a convex function.

(ii) The inequality constraints g_i^{in} are continuously differentiable concave functions.

(iii) The equality constraints h_j^{eq} are affine functions.

In general, however, the necessary conditions are not sufficient for optimality and additional information is necessary, such as the **second order sufficient conditions (SOSC)**. For smooth functions, SOSC involve the second derivatives, which explains its name.

Theorem 1.4.6 (Second Order Necessary and Sufficient Conditions (SONC and SOSC)). *Let Φ, g^{in}, and h^{eq} be twice continuously differentiable.*

• *(SONC) Let z^* be a local minimizer of (1.43) fulfilling LICQ and λ^*, μ^* be KKT multipliers. Then it holds[10]*

$$w^\top \left(\nabla_{zz}^2 \Phi(z^*) - \sum_{i=1}^{m_{\mathrm{in}}} \mu_i^* \nabla_{zz}^2 g_i^{\mathrm{in}}(z^*) - \sum_{j=1}^{m_{\mathrm{eq}}} \lambda_j^* \nabla_{zz}^2 h_j^{\mathrm{eq}}(z^*) \right) w \geq 0 \tag{1.49}$$

$$\forall w \in \mathcal{W}(z^*, \lambda^*, \mu^*).$$

---

[10]Notation: $\nabla_{zz}^2 := \left(\frac{\partial^2}{\partial z_i \partial z_j} \right)_{i,j=1,\ldots,m}$

1. Analytical Basics

- *(SOSC) Let (z^*, λ^*, μ^*) be a KKT point. Suppose further that*

$$w^\top \left(\nabla_{zz}^2 \Phi(z^*) - \sum_{i=1}^{m_{\mathrm{in}}} \mu_i^* \nabla_{zz}^2 g_i^{\mathrm{in}}(z^*) - \sum_{j=1}^{m_{\mathrm{eq}}} \lambda_j^* \nabla_{zz}^2 h_j^{\mathrm{eq}}(z^*) \right) w > 0 \tag{1.50}$$

$$\forall w \in \mathcal{W}(z^*, \lambda^*, \mu^*),\ w \neq 0.$$

Then z^* is a strict local minimizer for (1.43).

Proof. See e.g. [GK02]. $\qquad\qquad\qquad\qquad\qquad\qquad\qquad\qquad\qquad\qquad\qquad\qquad$ $\square$

Here,

$$\mathcal{W}(z^*, \lambda^*, \mu^*) := \{ d \in \mathcal{F}(z^*) \mid d^\top \nabla g_i^{\mathrm{in}}(z^*) \geq 0\ \forall i \in \mathcal{A}(z^*) \text{ with } \mu_i^* > 0 \} \tag{1.51}$$

is the **critical cone** with

$$\mathcal{F}(z^*) := \{ d \in \mathbb{R}^m \mid d^\top \nabla g_i^{\mathrm{in}}(z^*) \leq 0,\ i \in \mathcal{A}(z^*);\ d^\top \nabla h_j^{\mathrm{eq}}(z^*) = 0,\ j = 1, \ldots, m_{\mathrm{eq}} \}. \tag{1.52}$$

In case of $\mathcal{S} = \mathbb{R}^m$, SOSC coincide with the requirement regarding the HESSIAN $\nabla_{zz}^2 \Phi(z^*)$ to be positive definite, which is the well-known second order sufficient condition for unconstrained optimization problems.

2 Spatially Homogeneous Systems: Slow Invariant Manifold Computation

As already known from the section before, SIM computation approaches using species reconstruction aim at finding the species reconstruction function h yielding the corresponding POI on the SIM to be computed. Since the majority of those methods cannot identify the corresponding POI on the SIM exactly, there is an error of accuracy δ_{err}, defined by the difference of the species reconstruction function h representing the missing values of the POI and the approximated species reconstruction function h^{app} resulting from the respective approach and complementing the approximated POI$^{\mathrm{app}}$:

$$\delta_{\mathrm{err}} := \|h(z_j) - h^{\mathrm{app}}(z_j)\|_2, \quad j \in \mathcal{I}_{\mathrm{fixed}}. \tag{2.1}$$

If $\delta_{\mathrm{err}} \equiv 0$, the method is called named **exact** and thus, the approximated SIM, SIM$^{\mathrm{app}}$, represented by h^{app} equates with the SIM, and, as a consequence, POI$^{\mathrm{app}} \equiv$ POI as well as $h^{\mathrm{app}} \equiv h$. Figure 2.1 illustrates these notions with the help of the Linear Model (1.3a), (1.3b), where $z_2(t_*) = z_2^{t_*}$ is fixed as RPV. A hypothetical SIM computation method computes the POI$^{\mathrm{app}}$ on the SIM$^{\mathrm{app}}$ (blue line) by finding h^{app}, which has an error of accuracy of δ_{err} to the POI on the SIM (red line). Obviously, this hypothetical method is not exact.

This chapter contains one of the main results of this dissertation, namely the reduction of several different SIM computation approaches to two fundamental, basic concepts underlying, combining, and collecting those: the **derivative–of–the–state–vector–concept** and the novel **boundary–value–concept**. This is essentially presented in Section 2.6, where an improved formulation of a species reconstruction is proposed also, uniting both concepts in concentrated form in one approach. Before that, it is necessary to give a short summary of those SIM computation methods, which is realized in Section 2.1 and 2.2. After introducing two specific systems of ODEs serving as representative examples for testing and analyzing several issues (Section 2.3), two possibilities are discussed in 2.4 to quantify the POI$^{\mathrm{app}}$s resulting from a species reconstruction without knowing the position of the SIM. Section 2.5 addresses the issue, which RPVs, and accordingly, how many RPVs (i.e. $\#\mathcal{I}_{\mathrm{fixed}}$) should be chosen in a species reconstruction approach to represent at best the slow modes of the system in the reduced model formulation. In connection with Section 2.6, 2.7 shows examplarily how to obtain best possible results
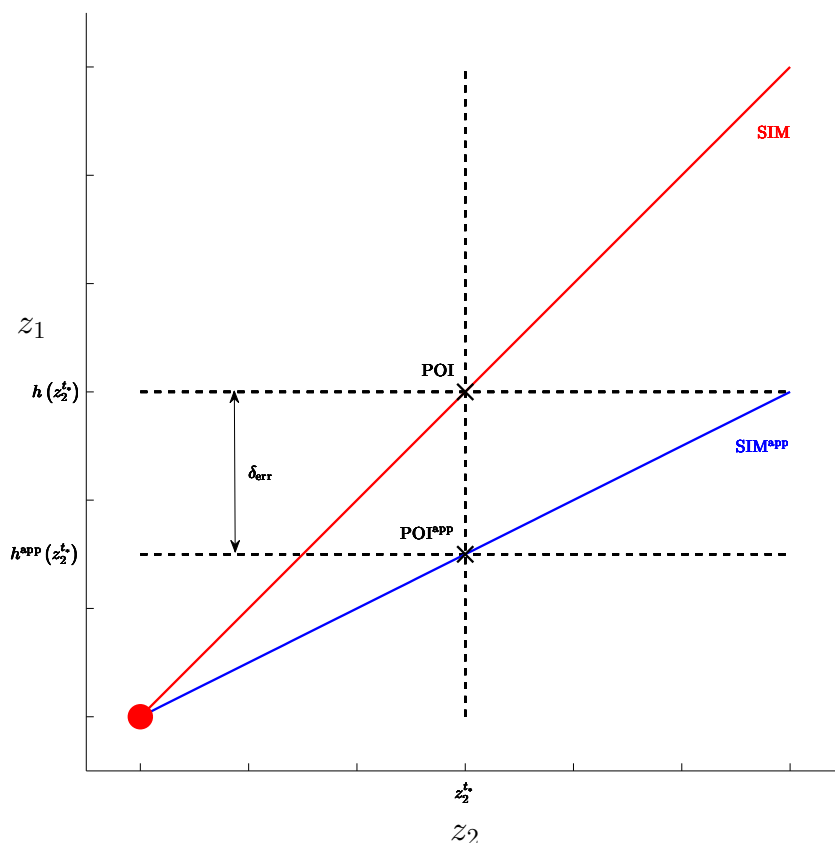
Figure 2.1: Illustration of the newly introduced notions: Error of accuracy δ_{err}, $\mathrm{POI}^{\mathrm{app}}$, $\mathrm{SIM}^{\mathrm{app}}$, h^{app}, and $\mathrm{POI}^{\mathrm{app}}$.

from the boundary–value–concept applied to realistic scenarios where the feasible phase space is restricted to a polyhedron. Section 2.8 deals with an alternative point of view of the species reconstruction method presented in 2.2. Here, $\mathrm{POI}^{\mathrm{app}}$s are computed by solving a boundary value problem resulting from interpreting the non RPVs as control, which is based on an idea of LEBIEDZ. Finally, Section 2.9 indicates a further idea concerning the search for an exact SIM identification based on HAMILTON's principle, which was also suggested by LEBIEDZ.

2.1 Methods for Slow Invariant Manifold Computation: Historical Review

Model reduction methods via SIM computation for systems of ODEs modeling chemical kinetics have been developed for about one hundred years. Some of these are exemplarily pointed out here, some clearer and in more detail than others, depending on relevance for this work. However, it is expressly advised that this listing does not claim to be exhaustive. An attempt has been made to list the approaches in chronological order, although it is not explicitly identifiable

in each case, so that the order allows no conclusion referring to the prominence of the particular method.

2.1.1 Quasi–Steady–State Assumption (QSSA)

One of the first model reduction approaches in chemical kinetics was the **quasi–steady–state assumption (QSSA)** [Bod07, Bod13, CU13] firstly published by BODENSTEIN in 1907. In this approach, certain species are assumed to be in steady state, meaning that the QSSA provides an assumption that there is no change of concentrations in time for all intermediates. In other words, the rate of formation and consumption are assumed to equalize, the consequence being that the state variables representing such species are considered as constant.

Applied to the Linear Model (1.3a), (1.3b), the QSSA yields

$$d_t z_1(t) = \left(-1 - \frac{\gamma}{2}\right) z_1(t) + \frac{\gamma}{2} z_2(t) = 0 \tag{2.2a}$$

$$d_t z_2(t) = \frac{\gamma}{2} z_1(t) + \left(-1 - \frac{\gamma}{2}\right) z_2(t). \tag{2.2b}$$

As a result, the rate of change of some species depend on the rate of change of the other species:

$$z_1 = h^{\mathrm{app}}(z_2) = \frac{\gamma}{\gamma + 2} z_2. \tag{2.3}$$

Thus, certain ODEs can be replaced by an algebraic one such that the original system of ODEs changes to a system of differential algebraic equations

$$z_1(t) = \frac{\gamma}{\gamma + 2} z_2(t) \tag{2.4a}$$

$$d_t z_2(t) = \frac{-1 - \gamma}{\frac{\gamma}{2} + 1} z_2(t) \tag{2.4b}$$

where the number of differential variables has reduced from two (z_1, z_2) to one (z_1). In this example, species reconstruction is done by using $\Phi(z) = d_t z_1$, $\mathcal{I}_{\mathrm{fixed}} = \{2\}$, and omitting constraints (1.38c) and (1.38e) in (1.38), or, alternatively, $\Phi(z) = z_1$, $\mathcal{I}_{\mathrm{fixed}} = \{2\}$, and omitting constraints (1.39c) and (1.39e) in (1.39). The error of accuracy of SIM computation (remember the analytic formula of the SIM in the linear model is given by $z_1 \equiv z_2 = h(z_2)$) results in

$$\delta_{\mathrm{err}} := h(z_2) - h^{\mathrm{app}}(z_2) = \frac{2}{\gamma + 2} z_2, \tag{2.5}$$

decreasing with increasing spectral gap parameter γ.

Provided that a singularly perturbed form of the kinetic model equation is accessible and the correct choice of the state variables is taken, the QSSA conforms with the Reduced Fast System (1.25) of the singular perturbation theory. I.e. if the dynamics are not in singularly perturbed

form, the QSSA requires detailed expert knowledge of chemical kinetics and the underlying model equations in order to decide for which species a quasi-static situation can be assumed. Due to its conceptual simplicity the QSSA is still used nowadays although more sophisticated model reduction methods have been developed. There are also implementations for an automatic application of this method, see e.g. [Nil01].

2.1.2 Partial Equilibrium Assumption (PEA)

In contrast to the QSSA where the major assumption is on species, the **partial equilibrium assumption (PEA)** [MP13] focuses on reactions in particular: fast elementary reaction steps are assumed to be relaxed to partial equilibrium immediately. In other words, forward and reverse rates of the reaction are assumed to be exactly the same, being the consequence that this reaction can be replaced by an algebraic equation.

The correlation between PEA and QSSA is analyzed in [Gou12] where it is shown that PEA and QSSA are limiting cases of leading order asymptotics. Furthermore, QSSA can be interpreted as limiting case of PEA.

2.1.3 Intrinsic Low Dimensional Manifold (ILDM)

In 1992, MAAS and POPE introduced the **intrinsic low dimensional manifold (ILDM)** method [MP92] which has become very popular and widely used in the reactive flow community, in particular in combustion applications. In this method a local time scale analysis is performed via matrix decomposition of the JACOBIAN $J_S := \left(\partial_{z_j} S_i \right)_{i,j=1,\dots,m}$ of the right-hand side $S(z)$ of the underlying system of ODEs. The eigenvalues of J_S identify those local time scales of the system, whereas the eigenvectors identify the local directions associated with the corresponding time scales in the m–dimensional phase space. For demonstration purposes, the idea of the ILDM method is demonstrated on the example of a linear system $d_t z = J_S z$ as performed in [Pet03], where J_S is a constant JACOBIAN matrix. The corresponding eigenvectors can be

obtained by the following decomposition of J_S with $\tilde{V} \equiv V^{-1}$:

$$J_S = V \Lambda \tilde{V}, \quad \text{with} \tag{2.6a}$$

$$V = \begin{pmatrix} | & & | & | & & | \\ v_1 & \cdots & v_n & v_{n+1} & \cdots & v_m \\ | & & | & | & & | \end{pmatrix} = \left(\begin{array}{c|c} V_s & V_f \end{array} \right), \tag{2.6b}$$

$$\Lambda = \left(\begin{array}{ccc|ccc} \lambda_1 & & 0 & & & \\ & \ddots & & & 0 & \\ 0 & & \lambda_n & & & \\ \hline & & & \lambda_{n+1} & & 0 \\ & 0 & & & \ddots & \\ & & & 0 & & \lambda_m \end{array} \right) = \left(\begin{array}{c|c} \Lambda_s & 0 \\ \hline 0 & \Lambda_f \end{array} \right), \tag{2.6c}$$

$$\tilde{V} = \begin{pmatrix} - & \tilde{v}_1 & - \\ & \vdots & \\ - & \tilde{v}_n & - \\ \hline - & \tilde{v}_{n+1} & - \\ & \vdots & \\ - & \tilde{v}_m & - \end{pmatrix} = \left(\begin{array}{c} \tilde{V}_s \\ \hline \tilde{V}_f \end{array} \right), \tag{2.6d}$$

where $v_1, \ldots, v_m \in \mathbb{R}^m$ represent the eigenvectors of J_S and $\lambda_1, \ldots, \lambda_m \in \mathbb{R}$ the corresponding eigenvalues contained in the diagonal matrix $\Lambda \in \mathbb{R}^{m \times m}$, for which it is assumed that they are all real, negativ, and ordered from least negative to most negative. Thus, the local time scales given by the inverse of the magnitudes of the eigenvalues $\frac{1}{|\lambda_1|}, \ldots, \frac{1}{|\lambda_m|}$ are ordered from slowest to fastest. The system of ODEs $\mathrm{d}_t z = S(z)$ can be rewritten as

$$\mathrm{d}_t z = J_S z + \mathfrak{g} \tag{2.7}$$

with $\mathfrak{g} := S - J_S z$ being the nonlinear part of S. Using $y := \tilde{V} z$ yields

$$\mathrm{d}_t y + \tilde{V} \left(\mathrm{d}_t V \right) y = \Lambda y + \tilde{V} \mathfrak{g}, \tag{2.8}$$

or, equivalently, in EINSTEIN notation[11]

$$\frac{1}{\lambda_i} \left(\mathrm{d}_t y_i + \tilde{v}_i \sum_{j=1}^{m} \left(\mathrm{d}_t v_j \right) y_j \right) = y_i + \frac{1}{\lambda_i} \tilde{v}_i \mathfrak{g}, \quad i = 1, \ldots, m, \tag{2.9}$$

---

[11]When an index variable appears twice in a single term it implies summation of that term over all the values of the index.

being in an equivalent form to that of a singularly perturbed system (see Section 1.2) with $\frac{1}{|\lambda_{n+1}|}, \ldots, \frac{1}{|\lambda_m|}$ representing the small parameter $\varepsilon \ll 1$. The assumption of equilibrated fast dynamics (i.e. equating the left hand side of Equation (2.9) for $i = n + 1, \ldots, m$ to zero) leads to

$$0 = y_i + \frac{1}{\lambda_i} \tilde{v}_i \mathfrak{g}, \quad i = n + 1, \ldots, m, \tag{2.10}$$

or, equivalently,

$$0 = \tilde{V}_{\mathrm{f}} S, \tag{2.11}$$

defining the algebraic equation for the ILDM with $\tilde{V}_{\mathrm{f}} \in \mathbb{R}^{(m-n) \times m}$. Summing up, the ILDM method reduces the kinetic model equation in form of a system of ODEs $\mathrm{d}_t z = S(z)$ to the following set of differential algebraic equations

$$\tilde{V}_{\mathrm{s}} \mathrm{d}_t z = \tilde{V}_{\mathrm{s}} S \tag{2.12a}$$

$$0 = \tilde{V}_{\mathrm{f}} S \tag{2.12b}$$

with $\tilde{V}_{\mathrm{s}} \in \mathbb{R}^{n \times m}$.

Consequently, the ILDM method is exact for linear systems (see e.g. [Pet03]) and, moreover, it is shown in [KK02], that the ILDM approach in application to singularly perturbed systems of ODEs identifies SIMs to order $\mathcal{O}(\varepsilon)$. A drawback of this method is that a solution of the ILDM Equations (2.12) does not necessarily exist and if one exists, it is not necessarily unique. Additionally, the resulting ILDM is generally not invariant.

2.1.4 Saddle Point Method (SPM)

Another SIM computation approach is the **saddle point method (SPM)** firstly described by DAVIS and SKODJE in [DS99]. In this context, one-dimensional SIMs are approximated via computation and connection of equilibria located both in physical and unphysical regions (e.g. 'fixed points at infinity') via heteroclinic orbits. This requires the use of projective geometry with coordinate transformation

$$u_i = \frac{z_i}{\sqrt{1 + |z|^2}}, \quad i = 1, \ldots, m \tag{2.13a}$$

$$u_{m+1} = \frac{1}{\sqrt{1 + |z|^2}} \tag{2.13b}$$

from EUCLIDEAN space to the hyperbolic one. Here, infinity is $u_{m+1} = 0$.

This method serves as the basis for the approach developed by AL-KHATEEB et al. [APP$^+$09] where a one-dimensional SIM is defined as heteroclinic orbit—a trajectory that connects two

equilibria—that is locally attractive along the complete trajectory. In [MP13], this concept is enhanced to the computation of one-dimensional manifolds of reactive systems including microscale diffusion effects.

2.1.5 Trajectory Based Optimization Approach (TBOA)

A detailed description of the **trajectory based optimization approach (TBOA)** originally proposed by LEBIEDZ in [Leb04] is given in Section 2.2.

2.1.6 Zero–Derivative Principle (ZDP)

Another way to use species reconstruction for SIM computation and thereby model reduction is the **zero–derivative principle (ZDP)** discussed in [GKK$^+$05, ZGK$^+$09]. The ZDP is based on a fundamental principle analyzed in [Kre85] and annulates the derivatives of the non RPVs, which can be formulated in the framework of this work (cf. (1.38)) as

$$\Phi(z) = \mathrm{d}_t^\nu z_j(t)\Big|_{t=t_*} = 0, \quad j \notin \mathcal{I}_{\mathrm{fixed}} \tag{2.14a}$$

$$\mathrm{d}_t z(t) = S\left(z(t)\right) \tag{2.14b}$$

$$0 = g\left(z(t_*)\right) \tag{2.14c}$$

$$z_j(t_*) = z_j^{t_*}, \quad j \in \mathcal{I}_{\mathrm{fixed}}. \tag{2.14d}$$

The resulting $\mathrm{POI}^{\mathrm{app}}$ $z(t_*) = \left(z_j^{t_*}, h^{\mathrm{app}}\left(z_j^{t_*}\right)\right)^\top$, $j \in \mathcal{I}_{\mathrm{fixed}}$ should lie in a small neighborhood of a SIM which is approached with increasing derivative order ν and thus, $\delta_{\mathrm{err}} \to 0$ for $\nu \to \infty$ as it is shown in [GKK$^+$05, ZGK$^+$09].

Operation of the ZDP can be illustrated by means of Linear Model (1.3a), (1.3b). As already known, elimination of the fast modes characterizes the SIM. These fast modes are represented by the second term of the sum $c_2\mathrm{e}^{(-1-\gamma)t}$ of the general analytic solution

$$z_1(t) = c_1\mathrm{e}^{-t} + c_2\mathrm{e}^{(-1-\gamma)t}, \quad c_1, c_2 \in \mathbb{R} \tag{2.15a}$$

$$z_2(t) = c_1\mathrm{e}^{-t} - c_2\mathrm{e}^{(-1-\gamma)t}, \tag{2.15b}$$

since they include the 'fast eigenvalue' $-1 - \gamma$. Besides the fixation of the RPV ($\mathcal{I}_{\mathrm{fixed}} = \{2\}$), an additional constraint $\Phi(z) = 0$ is needed to obtain a specified trajectory—ideally leading to the elimination of the fast modes ($c_2 = 0$). This is achieved via the zero point of the νth derivative of the non RPV z_1

$$\mathrm{d}_t^\nu z_1(t) = (-1)^\nu c_1\mathrm{e}^{-t} + (-1-\gamma)^\nu c_2\mathrm{e}^{(-1-\gamma)t} \tag{2.16}$$

(in the limit $\nu \to \infty$) where the corresponding eigenvalues of each mode is taken to the power of ν. Solving Equation (2.14a) for c_2 (c_1 is fixed by fixation of the RPV) yields

$$c_2 = \frac{(-1)^\nu}{(-1-\gamma)^\nu} \cdot R \tag{2.17}$$

with R being independent of ν. Since $|-1-\gamma| > |-1|$, $c_2 \to 0$ for $\nu \to \infty$, meaning a decreasing contribution of the fast mode for increasing value of ν. The resulting POI$^{\mathrm{app}}$ $z(t_*) = \left(h^{\mathrm{app}} \left(z_2^{t_*} \right), z_2^{t_*} \right)^\top$ results in (w.l.o.g. $t_* = 0$)

$$z_1 = h^{\mathrm{app}}(z_2) = z_2 \left(1 - 2\frac{(-1)^\nu}{((-1)^\nu + (-1-\gamma)^\nu)} \right) \tag{2.18}$$

showing that $\lim\limits_{\nu \to \infty} h^{\mathrm{app}}(z_2) = h(z_2)(= z_2)$ and thus, the POI on the SIM is identified by POI$^{\mathrm{app}}$ for $\nu \to \infty$.

The ZDP can be regarded as a generalization of the QSSA, the latter using $\nu = 1$ as derivative order in the 'objective function' (1.38a). This is illustrated by Figure 2.2, where δ_{err} is plotted against the derivative order ν for the ZDP (red curve) and the QSSA (blue line) applied to the Linear Model (1.3a), (1.3b) with $\gamma = 10.0$ and $z_2^0 = 6.0$. As visualized by the black dashed line the error of accuracy of SIM computation δ_{err} coincides for both methods at $\nu = 1$. Additionally, it can be seen that $\lim\limits_{\nu \to \infty} \delta_{\mathrm{err}} = 0$, which points out an increasing accuracy of the SIM computation with an increasing derivative order ν.

2.1.7 Invariant Constrained Equilibrium Edge Preimage Curves (ICE-PIC)

REN et al. introduced the **invariant constrained equilibrium edge preimage curves (ICE-PIC)** approach for SIM computation in 2006 [RPV$^+$06]. This method is based on an ICE manifold which is the union of all reaction trajectories emanating from points of a constrained equilibrium manifold. As the ICE-PIC manifold is constructed from reaction trajectories emanating from the latter, it is invariant. Based on this ICE manifold a species reconstruction can be done locally without having to generate the whole manifold in advance.

2.1.8 Functional Equation Truncation (FET)

In [RT06, Rou12], ROUSSELL and TANG were able to demonstrate the coincidence between the ILDM method and their **functional equation truncation (FET)** approach. The operation concept of FET is shown for a planar system

$$d_t z_1 = S_1(z_1, z_2) \tag{2.19a}$$

$$d_t z_2 = S_2(z_1, z_2). \tag{2.19b}$$
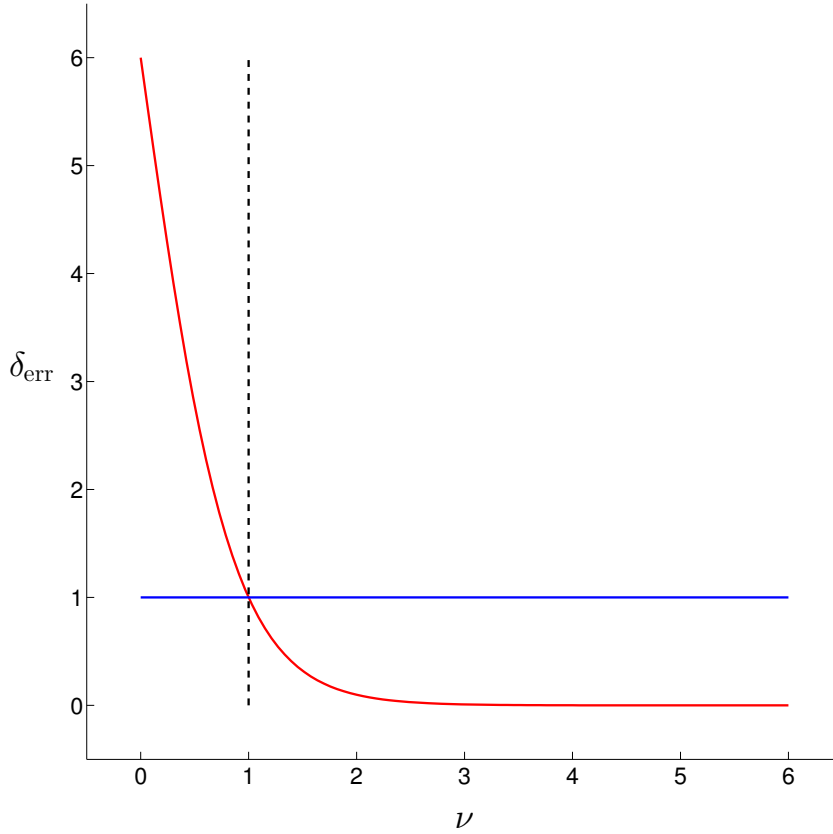
Figure 2.2: The error of accuracy δ_{err} concerning to the ZDP (red curve) and the QSSA (blue line) applied to the Linear Model (1.3a), (1.3b) with $t_{\mathrm{f}} = 0$, $\gamma = 10.0$, and $z_2^0 = 6.0$ designed as a function of ν.

The **functional equation**

$$S_2(z_1, z_2) = S_1(z_1, z_2)\mathrm{d}_{z_1} z_2 \tag{2.20}$$

is constructed by substituting $\mathrm{d}_t z_2 = S_1(z_1, z_2)\mathrm{d}_{z_1} z_2$ into (2.19b). Differentiation of the Functional Equation (2.20) with respect to z_1 yields

$$\mathrm{d}_{z_1} S_2(z_1, z_2) = S_1(z_1, z_2)\mathrm{d}_{z_1}^2 z_2 + \mathrm{d}_{z_1} S_1(z_1, z_2)\mathrm{d}_{z_1} z_2. \tag{2.21}$$

Motivated by the observation that the error in the ILDM method is directly related to the neglect of curvature [KK02], which is proportional to $\mathrm{d}_{z_1}^2 z_2$ here, Equation (2.21) becomes

$$\mathrm{d}_{z_1} z_2 \left(\partial_{z_1} S_1(z_1, z_2) + \partial_{z_2} S_1(z_1, z_2)\mathrm{d}_{z_1} z_2 \right) = \partial_{z_1} S_2(z_1, z_2) + \partial_{z_2} S_2(z_1, z_2)\mathrm{d}_{z_1} z_2 \tag{2.22}$$

denoted by **truncated equation**. Thus, two Equations ((2.20) and (2.22)) in the two unknowns $z_2, \mathrm{d}_{z_1} z_2$ for every z_1 are given allowing the computation of an approximation to the one-dimensional manifold by using an iterative method to solve (2.20). The resulting manifold is

33

called **functional equation truncation approximated (FETA) manifold** [RT06, Rou12]. Its approximation of an one-dimensional SIM is valid insofar as $\mathrm{d}^2_{z_1} z_2$ is small.

Already KAPER and KAPER [KK02] pointed out the direct relation between the ILDM method and the neglect of the curvature, which is used as a central idea in the above FET approach.

2.1.9 Stretching–Based Diagnostics (SBD)

ADROVER et al. [ACC$^+$07, ACG$^+$07] presented a method for SIM computation which is based on a geometric characterization of local tangent and normal dynamics. This description find its justification in the fact that flow along a SIM is slower than the attraction/repulsion to/from it. The method uses a ratio $r > 1$ of the local stretching (contraction) rates for vectors orthogonal to the SIM compared to those tangent to it. Then, this ratio is maximized w.r.t. z.

Again a two-dimensional system of ODEs is considered for demonstration

$$\mathrm{d}_t z = S(z) = \begin{pmatrix} S_1(z) \\ S_2(z) \end{pmatrix}, \quad z \in \mathbb{R}^2 \tag{2.23}$$

possessing an one-dimensional SIM denoted by $\mathcal{M}$. Under these circumstances, the stretching ratio r is given by

$$r(z) := \frac{\omega_\nu(z)}{\omega_\tau(z)} := \frac{\langle J_S(z(t)) \cdot \hat{n}(z), \hat{n}(z) \rangle}{\langle J_S(z) \cdot \hat{S}(z), \hat{S}(z) \rangle}, \quad z \in \mathcal{M} \tag{2.24}$$

with $\hat{S}(z) := \frac{S(z)}{\|S(z)\|_2}$, $\hat{n}(z) := \frac{n(z)}{\|n(z)\|_2}$, $n(z) := (S_2(z), -S_1(z))^\top$, $\langle \cdot, \cdot \rangle$ being the scalar product, $\|\cdot\|_2$ indicating the EUCLIDEAN norm, and $J_S(z)$ being the JACOBIAN of the right hand side $S(z)$ evaluated at z. Here, $\omega_\tau(z)$ and $\omega_\nu(z)$ denote the tangential and normal stretching rates, respectively. The SBD method can be viewed as a local embedding technique: locally projecting the dynamics onto the slowest directions. In the $m-$dimensional case ($m > 2$) the tangential stretching rate is still given by

$$\omega_\tau(z) = \langle J_S(z) \cdot \hat{S}(z), \hat{S}(z) \rangle \tag{2.25}$$

while the definition of normal stretching rates changes to

$$\omega_\nu(z) = \max_{\hat{n} \in N\mathcal{M}_z, \|\hat{n}\|_2 = 1} \langle J_S(z) \cdot \hat{n}(z), \hat{n}(z) \rangle \tag{2.26}$$

where the maximum is taken over all vectors $\hat{n}(z)$ belonging to the normal space $N\mathcal{M}_z$ at z. This value can be computed by the largest eigenvalue of a symmetric matrix (cf. [ACG$^+$07]).

2.1.10 Flow Curvature Method (FCM)

One last SIM computation approach presented here is the **flow curvature method (FCM)** proposed by GINOUX [GRC08], comprising a species reconstruction that computes a special $(m-1)$-dimensional manifold, the **flow curvature manifold**, which is defined by the location of the points at which the flow curvature vanishes. For an m-dimensional system of ODEs, the zero point of the flow curvature of a trajectory curve is defined as

$$\det\left(\mathrm{d}_t z, \mathrm{d}_t^2 z, \mathrm{d}_t^3 z, \ldots, \mathrm{d}_t^m z\right) = 0 \tag{2.27}$$

with $z \in \mathbb{R}^m$, $m \in \mathbb{N}$. Thus, Equation (2.27) performs the role of (1.38a) according to species reconstruction (1.38). Replacing the flow curvature by its successive LIE derivatives (in a two-dimensional system it is defined by the determinant of the first and third time derivatives) yields successively in higher order approximations of the SIM (see [Ros86]). For singularly perturbed systems, the analytic equation of the manifold resulting from matched asymptotic expansion in singular perturbation theory [Jon95, Kap99], which is given by a regular perturbation expansion in ε, equates with the FCM up to a suitable order in ε. The invariance property of the flow curvature manifold can be shown via the DARBOUX invariance theorem [Dar78].

2.1.11 Interim Summary

In summary, a timeline is shown in Figure 2.3, where the presented SIM computation approaches are arranged by the year of first publication. As one can see, the majority of the methods have been presented during the last twenty years. The TBOA—belonging to the previous approaches of the recent ones—is highlighted in red, since it plays an essential role in the context of this work. Furthermore, the subsequent section deals extensively with its functionality.
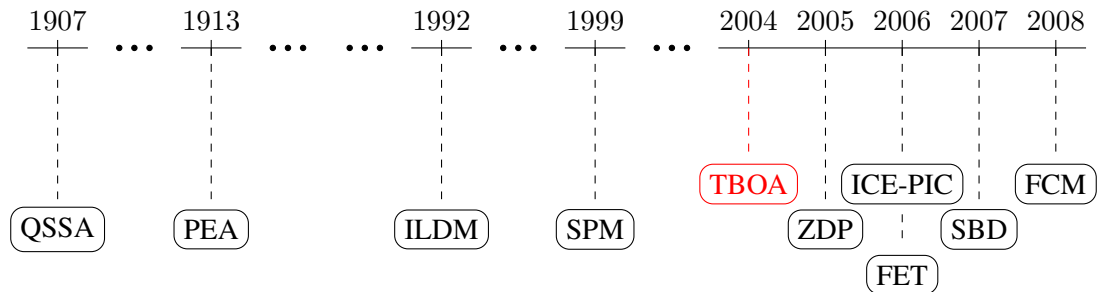

Figure 2.3: Timeline with SIM computation methods presented here arranged by year of first publication.

2.2 Trajectory Based Optimization Approach

In [Leb04], LEBIEDZ introduced the idea of a **trajectory based optimization approach (TBOA)** for SIM computation in form of species reconstruction (1.39), where—in contrast to most common approaches—reaction trajectories are involved. For this point, the use of more global information within the species reconstruction serves as fundamental motivation for the development of yet another new SIM computation approach aiming at a reduced description of the kinetic model equations. Furthermore, this approach was firstly formulated in form of an extremum principle (cf. 1.39) acting as a further incentive to examine this kind of formulation for model reduction applied to kinetic multiscale models. Thus, the TBOA was originally formulated as (1.39) with

$$\Phi(z) = \int_{t_*}^{t_f} \tilde{\Phi}(z) \, \mathrm{d}t, \tag{2.28}$$

where the integrand $\tilde{\Phi}$ should fulfill the following requirements:

- Applied to chemical combustion processes, $\tilde{\Phi}$ should describe the extent of 'chemical forces' in the evolution of reaction trajectories.

- The integrand $\tilde{\Phi}$ should be computable from easily accessible data.

- The integrand $\tilde{\Phi}$ should be (at least) twice continuously differentiable along reaction trajectories.

Furthermore, $\tilde{\Phi}$ should be at best consistent and δ_{sym} should be as small as possible (see 2.4.1 and 2.4.2) .

The way of proceeding of (1.39) together with (2.28) is demonstrated in Figure 2.4. The blue curves represent pieces of different trajectories, all starting from $z_j(t_*) = z_j^{t_*}$, $j \in \mathcal{I}_{\mathrm{fixed}}$ and integrated till $t = t_f$. The integrand $\tilde{\Phi}$ should ideally be chosen in a way that the minimal value of (2.28) identifies the blue curve lying on the red SIM.

In order to find an exact criterion $\tilde{\Phi}$, LEBIEDZ and REINHARDT developed and tested different criteria, whereof the first was related to the entropy production. In this approach, a special trajectory, the **minimal entropy production trajectory (MEPT)**, is computed by minimizing the sum of the entropy production rates of single reaction steps. The integrand $\tilde{\Phi}$ is chosen as

$$\tilde{\Phi}(z) = \sum_{r=1}^{m_{\mathrm{reac}}} \mathrm{d}_t E_r \tag{2.29}$$
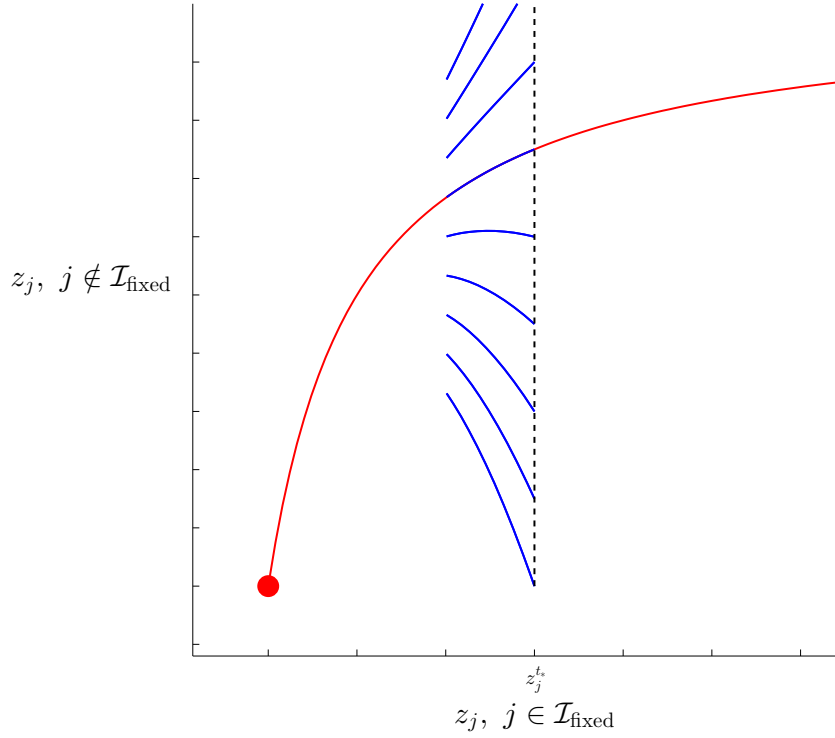
Figure 2.4: Schematic illustration of problem formulation (1.39) together with (2.28).

with

$$\mathrm{d}_t E_r = R(R_{r\rightarrow} - R_{r\leftarrow}) \ln(\tfrac{R_{r\rightarrow}}{R_{r\leftarrow}}) \tag{2.30}$$

and R being the gas constant[12]. The notations $R_{r\rightarrow}$ and $R_{r\leftarrow}$ denote the forward and backward reaction rates for an elementary reaction step r and $\mathrm{d}_t E_r$ is the entropy production rate for reaction r. The results of this formulation have been less than satisfactory since the POI$^{\mathrm{app}}$s emerged as very inconsistent (see 2.4.1) and thus, the MEPT does by far not coincide with a SIM. In [Leb10], the idea of using entropy production for SIM computation is extended and discussed with the definition of entropy in a mathematical sense.

The subsequent considerations to improve the choice of $\tilde{\Phi}$ focused on the SIM being interpreted as a minimization of relaxing 'forces' along reaction trajectories. From the opposite point of view, chemical forces are maximally relaxed along trajectories on a SIM. Regarding NEWTONIAN mechanics, forces in turn are closely related to the concept of a curvature as it is well-known from physics, especially from NEWTON's second law

$$F = m_{\mathrm{G}} \mathrm{d}_t^2 z \tag{2.31}$$

---

[12]$R = 8.314472 \frac{\mathrm{J}}{\mathrm{K \cdot mol}}$

37

where F denotes the vector sum of the external forces acting on an object, m_G the mass of the object (constant in time), and $d_t^2 z$ the second derivative of the state vector z of the object with respect to time t. This second derivative of z contains information about the curvature of z and thus, NEWTON's second law describes a relation between force and curvature. Since the kinetic model equations are given by $d_t z = S(z)$, the second time–derivative of the chemical composition z characterizing the rate of change of reaction velocity through relaxation (dissipation) of chemical forces can be indicated as

$$d_t^2 z = d_t \left(d_t z \right) = J_S(z) \cdot S. \tag{2.32}$$

This in turn is related to a directional derivative of the tangent vector of the curve $z(t)$ with respect to its own normalized direction $w := \frac{d_t z}{\|d_t z\|_2} = \frac{S}{\|S\|_2}$

$$d_\alpha S \left(z(t) + \alpha w \right) \Big|_{\alpha=0} = J_S \left(z(t) \right) \cdot \frac{S \left(z(t) \right)}{\| S \left(z(t) \right) \|_2} \tag{2.33}$$

with $\|\cdot\|_2$ denoting the EUCLIDEAN norm. Hence, the preliminary optimization criterion is chosen as

$$\tilde{\Phi}(z) = \frac{\| J_S(z) \cdot S \|_2}{\| S \|_2}. \tag{2.34}$$

The evaluation of this expression within the formulation of the objective functional (2.28) should be a path integral along the trajectory

$$\int_{\ell(t_*)}^{\ell(t_f)} \tilde{\Phi} \left(z \left(\ell(t) \right) \right) \; d\ell(t) \tag{2.35}$$

with $\ell(t)$ being the EUCLIDEAN length of the curve z at time t given by

$$\ell(t) = \int_0^t \| d_\tau z(\tau) \|_2 \; d\tau. \tag{2.36}$$

This results in the reparameterization

$$d\ell(t) = \| d_t z(t) \|_2 \; dt \tag{2.37}$$

which cancels out $\|S\|_2$ in (2.34) yielding

$$\tilde{\Phi} \left(z(t) \right) = \| J_S \left(z(t) \right) \cdot S \left(z(t) \right) \|_2 \tag{2.38}$$

as objective functional integrand. In comparison with the entropy production as objective functional, the results using the preceding formulation improved, but still emerged as inconsistent. Many other suggestions for objective functions in the TBOA (1.39) together with (2.28) have

been tested in [Leb06, LRS10, LRS$^+$11, Rei08, RWD08], which still do not provide significantly better results.

The above mentioned formulation comes with the drawback that the 'length' of the trajectory part used in Optimization Problem (1.39) together with (2.28) is limited based on the attracting equilibrium point. Based on this problem and with hope that 'longer' trajectory parts improve the SIM computation, the **reverse mode** formulation has been developed in [LSU11]. Generally, the subsequent optimization formulation comprises both, the upper formulation (called **forward mode**) and the new reverse formulation:

$$\min \quad \int_{t_0}^{t_\mathrm{f}} \| J_S(z) \cdot S(z) \|_2^2 \ \mathrm{d}t \tag{2.39a}$$

subject to

$$\mathrm{d}_t z(t) = S\left(z(t)\right) \tag{2.39b}$$

$$0 = g\left(z(t_*)\right) \tag{2.39c}$$

$$z_j(t_*) = z_j^{t_*}, \quad j \in \mathcal{I}_\mathrm{fixed}. \tag{2.39d}$$

The integrand is squared to get a simpler analysis, having no remarkable effects on the solution of the optimization problem. The forward and reverse mode arise from (2.39) by choosing $t_* = t_0$ and $t_* = t_\mathrm{f}$, respectively. Analogously to Figure 2.4, where the forward mode is schematically illustrated, Figure 2.5 demonstrates the reverse mode formulation, where—in contrast to the forward mode—the 'length' of the trajectory part used in the optimization can be chosen arbitrarily large by increasing $t_\mathrm{f} - t_0$. And in fact, it turned out that the reverse mode identifies a SIM exactly in the limit $t_0 \to -\infty$, at least applied to simple test mechanisms as it is analytically shown in [LSU11]. Numerical results applied to more realistic combustion mechanisms confirm these conclusions [LS13, LS14, Sie13]. The examination of this reverse mode formulation and elucidating why SIMs are exactly identified in the limit are important parts this work deals with.

The following local method has been used in [LS13, Sie13] and is motivated by numerical efficiency, as the accuracy of SIM computation increases marginally in comparison with the forward mode.

$$\min \quad \| J_S(z) \cdot S(z) \|_2^2 \Big|_{t=t_*} \tag{2.40a}$$

subject to

$$0 = g\left(z(t_*)\right) \tag{2.40b}$$

$$z_j(t_*) = z_j^{t_*}, \quad j \in \mathcal{I}_\mathrm{fixed}. \tag{2.40c}$$
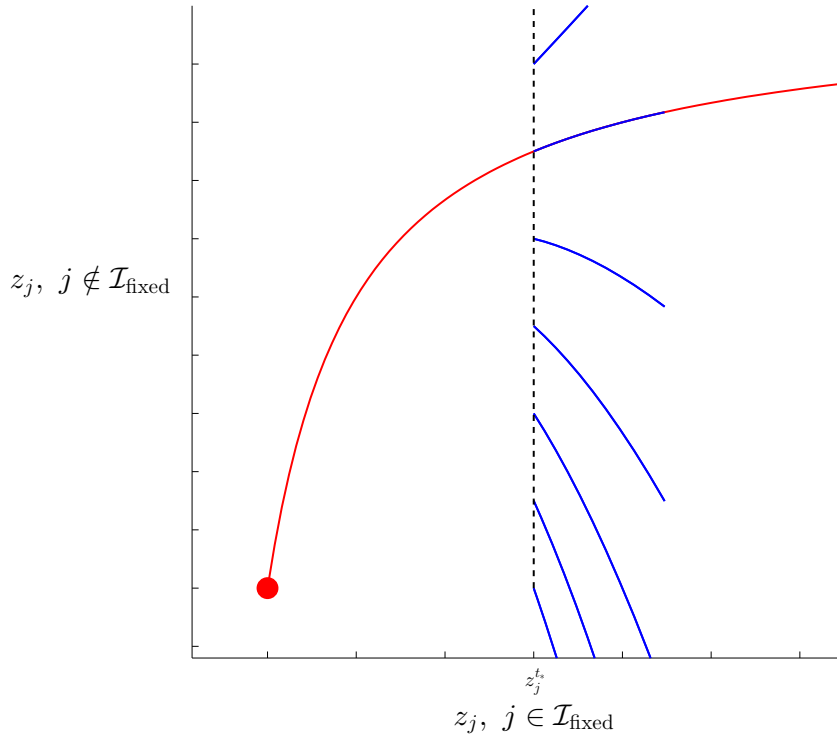
Figure 2.5: Schematic illustration of (2.39) with $t_* = t_\mathrm{f}$ (reverse mode).

Applied to (1.3a), (1.3b), the reverse mode optimization problem with $\mathcal{I}_\mathrm{fixed} = \{2\}$ reads as

$$\min \quad \int_{t_0}^{t_\mathrm{f}} \|AAz\|_2^2 \ \mathrm{d}t \tag{2.41a}$$

subject to

$$\mathrm{d}_t z(t) = Az \tag{2.41b}$$

$$z_2(t_\mathrm{f}) = z_2^{t_\mathrm{f}}, \tag{2.41c}$$

with A defined in (1.21). The corresponding $\mathrm{POI}^\mathrm{app}$ results in

$$\mathrm{POI}^\mathrm{app} = \left(z_2^{t_\mathrm{f}} \left(1 + \chi \right), z_2^{t_\mathrm{f}} \right) \tag{2.42}$$

where an error term χ quantifes the deviation from the SIM $z_1 \equiv z_2$. Out of this δ_err results in

$$\delta_\mathrm{err} = |\chi z_2^{t_\mathrm{f}}|. \tag{2.43}$$

The error term χ is computed in [LSU11] and reads as

$$\chi = \frac{2\mathrm{e}^{(-1-\gamma)2t_\mathrm{f}} - 2\mathrm{e}^{-2\gamma t_\mathrm{f}}\mathrm{e}^{-2t_0}}{\mathrm{e}^{-2\gamma t_\mathrm{f}} - \xi\mathrm{e}^{(-1-\gamma)2t_0} + (\xi - 1)\mathrm{e}^{(-1-\gamma)2t_\mathrm{f}}} \tag{2.44}$$

with $\xi = \frac{2 + 8\gamma + 12\gamma^2 + 8\gamma^3 + 2\gamma^4}{-2 - 2\gamma}$. The relation between (2.43) and t_0 is shown in Figure 2.6, where $t_\mathrm{f} = 0$, $\gamma = 10.0$, and $z_2^0 = 6.0$ is chosen equally to the situation of Figure 2.2. As can be seen, δ_err decreases exponentially with $t_0 \to -\infty$.
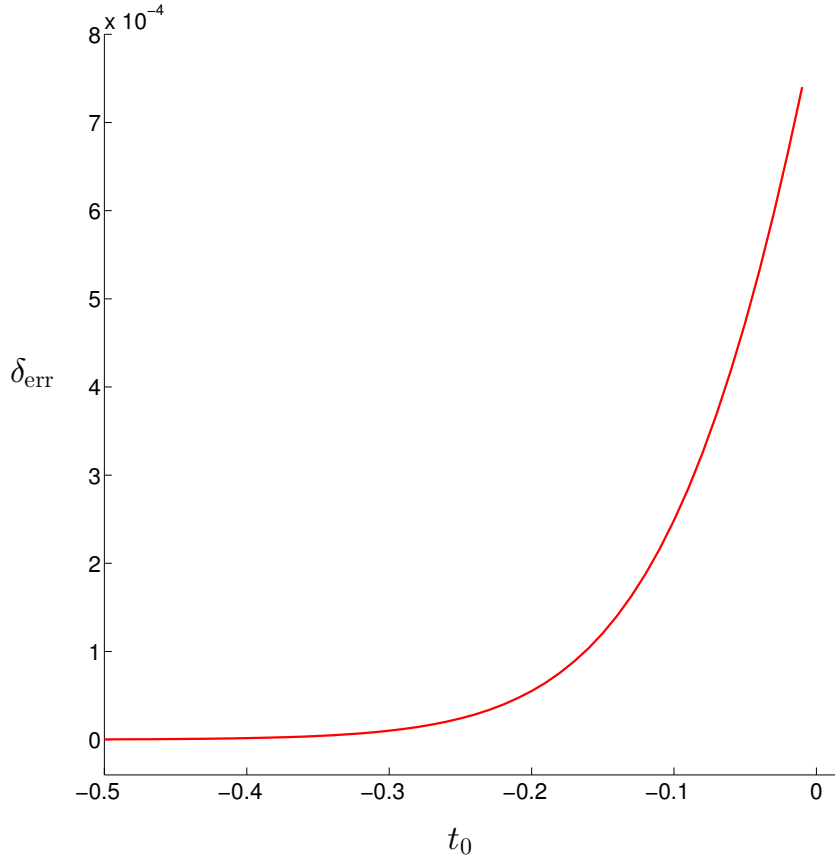
Figure 2.6: The error of accuracy δ_{err} associated with Problem (2.41) with $t_{\text{f}} = 0$, $\gamma = 10.0$, and $z_2^0 = 6.0$ as a function of t_0.

2.3 Two Simple Test Models

As could already be seen in previous sections of this work, various issues have been demonstrated for a better understanding via application to a simple example in form of a specific right-hand side $S(t)$ of the kinetic model equation. The two most important representatives are the **linear model** presented (1.3a), (1.3b) and the two-dimensional, nonlinear **DAVIS–SKODJE model** [DS99, SPP02], which has acquired a widespread publicity in the model reduction community. Briefly, and for ease of reference, the linear model is reviewed in the next part, followed by the introduction of the DAVIS–SKODJE model.

2.3.1 Linear Model

The two-dimensional linear model used in this work is given by

$$\mathrm{d}_t z = Az, \quad A = \begin{pmatrix} -1 - \frac{\gamma}{2} & \frac{\gamma}{2} \\ \frac{\gamma}{2} & -1 - \frac{\gamma}{2} \end{pmatrix} \in \mathbb{R}^{2 \times 2}, \tag{2.45}$$

where $\gamma > 0$ measures the spectral gap and consequently the stiffness of the system of ODEs (the stiffness grows with γ). As already seen in Section 1.2, the transformation into a singularly perturbed system of ODEs is known and can be realized with $\varepsilon = \frac{1}{\gamma+1}$ and $\tilde{z} = R^{-1}z$, $R = \begin{pmatrix} \cos\frac{\pi}{4} & -\sin\frac{\pi}{4} \\ \sin\frac{\pi}{4} & \cos\frac{\pi}{4} \end{pmatrix}$ yielding

$$d_t\tilde{z}_1 = -\tilde{z}_1 \tag{2.46a}$$

$$\varepsilon d_t\tilde{z}_2 = -\tilde{z}_2. \tag{2.46b}$$

As a direct consequence of FENICHEL's invariant manifold theorem (Theorem 1.2.2) the existence of a SIM is guaranteed for small ε, which in this case is given by the eigenspace Λ_s corresponding to the slowest eigenvalue $\lambda_s = -1$ of the system matrix A. Thus, the analytic formula of the SIM with reference to (2.45) is given by the first bisectrix

$$z_2 \equiv z_1, \tag{2.47}$$

which is plotted as red line in Figure 2.7, where the vector field of System (2.45) is shown for two different values of γ. As can be seen, the SIM attracts system trajectories to a greater extent in case of a larger value of γ.

(a) $\gamma = 1.0$ (b) $\gamma = 10.0$
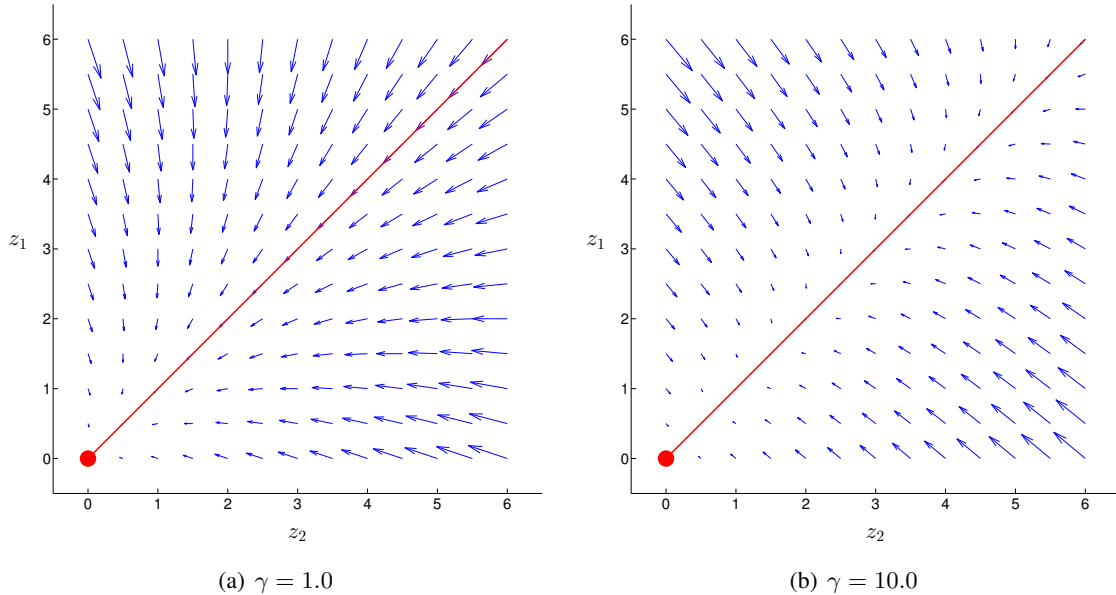
Figure 2.7: Vector fields of (2.45) for two different values of γ. The eigenspace Λ_s, that coincides with the SIM in this case, is depicted by the red line. The red dot, as is now customary, represents the equilibrium.

Considering the analytic solution of (2.45)

$$z_1 = c_1 e^{-t} + c_2 e^{(-1-\gamma)t}, \quad c_1, c_2 \in \mathbb{R} \tag{2.48a}$$

$$z_2 = c_1 e^{-t} - c_2 e^{(-1-\gamma)t}, \tag{2.48b}$$

the slow modes of the system are represented by the first term of the sum and the fast ones by the second term since including the slow and fast eigenvalues -1 and $-1 - \gamma$, respectively. As already known, an exact model reduction method eliminates the fast modes of the system, meaning $c_2 = 0$ in this case, yielding $z_1 \equiv z_2$, wherefrom the species reconstruction function h arises. A schematic illustration of what has been described above is shown in Figure 2.8, where model reduction methods aim at a direct connection between the middle box on the left and the middle one on the right. The upper and lower boxes are dashed, because neither the transformation into a singularly perturbed system nor the analytic solution is available in general. Accordingly, model reduction methods are highly inevitable. Obviously, the initial value problem
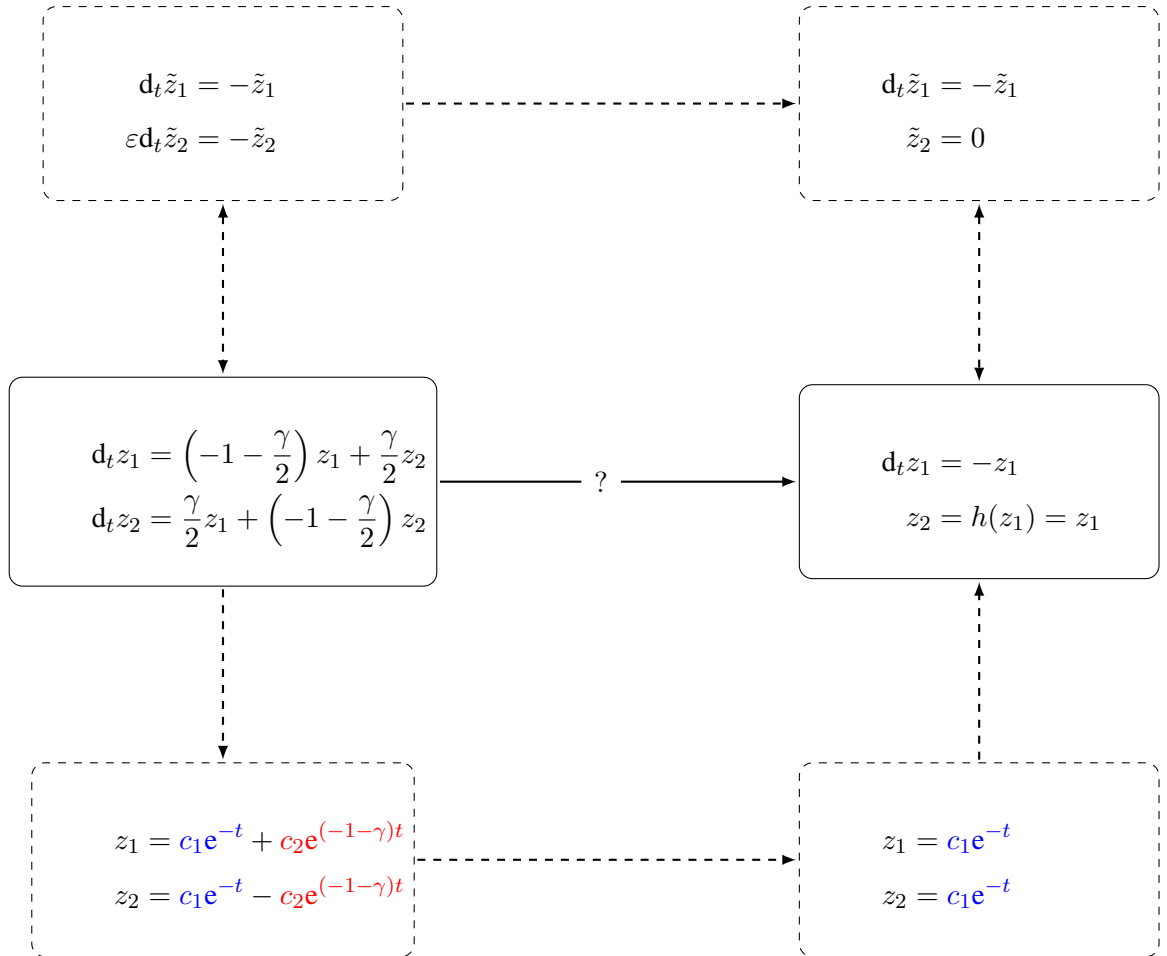
Figure 2.8: Schematic illustration of correlations between the full linear model and the reduced one.

$$\mathrm{d}_t z_1 = \left(-1 - \frac{\gamma}{2}\right) z_1 + \frac{\gamma}{2} z_2 \tag{2.49a}$$

$$\mathrm{d}_t z_2 = \frac{\gamma}{2} z_1 + \left(-1 - \frac{\gamma}{2}\right) z_2 \tag{2.49b}$$

$$z_1(t_*) = z_1^{t_*} \tag{2.49c}$$

$$z_2(t_*) = z_2^{t_*} \tag{2.49d}$$

with the analytic solution

$$z_1 = \frac{z_1^{t_*} + z_2^{t_*}}{2} \mathrm{e}^{-t} + \frac{z_1^{t_*} - z_2^{t_*}}{2} \mathrm{e}^{(-1-\gamma)t} \tag{2.50a}$$

$$z_2 = \frac{z_1^{t_*} + z_2^{t_*}}{2} \mathrm{e}^{-t} - \frac{z_1^{t_*} - z_2^{t_*}}{2} \mathrm{e}^{(-1-\gamma)t} \tag{2.50b}$$

corresponds to the reduced kinetic equations (middle box on the right side of Figure 2.8) and their solutions are equivalent, if the initial value lies on the SIM (i.e. $z_1^{t_*} = z_2^{t_*}$).

2.3.2 Davis–Skodje Model

It may happen that knowledge gained from a linear model cannot be generalized to nonlinear ones, which is the reason for using additionally the DAVIS–SKODJE model [DS99, SPP02] for different studies in this work. The ILDM method (see 2.1.3) serves as an example, as it yields exact results when computing SIMs for linear systems of ODEs, but $\delta_{\mathrm{err}} \neq 0$ in the nonlinear case. The DAVIS–SKODJE model is widely used for analysis and performance tests of model reduction techniques supposed to identify SIMs and reads

$$\mathrm{d}_t z_1 = -z_1 \tag{2.51a}$$

$$\mathrm{d}_t z_2 = -\tilde{\gamma} z_2 + \frac{(\tilde{\gamma} - 1)z_1 + \tilde{\gamma} z_1^2}{(1 + z_1)^2} \tag{2.51b}$$

with $\tilde{\gamma} > 1$ again measuring the spectral gap and consequently the stiffness of the system. Typically, model reduction algorithms show a good performance for a large time scale separation accompanied by a large value of $\tilde{\gamma}$ here, whereas small values of $\tilde{\gamma}$ impose a significantly harder challenge on the computation of a SIM. Not only for the purpose of this adjustable time scale separation but also the analytically assignable SIM

$$z_2 = h(z_1) = \frac{z_1}{z_1 + 1} \tag{2.52}$$

justify the wide use of the DAVIS–SKODJE model for testing numerical model reduction approaches. One further advantage compared with most of the other nonlinear test models is the accessibility of an analytic solution given by

$$z_1 = \tilde{c}_1 \mathrm{e}^{-t} \tag{2.53a}$$

$$z_2 = \tilde{c}_2 \mathrm{e}^{-\tilde{\gamma} t} + \frac{\tilde{c}_1}{\tilde{c}_1 + \mathrm{e}^t}, \quad \tilde{c}_1, \tilde{c}_2 \in \mathbb{R}. \tag{2.53b}$$

Once again, the vector field of Model (2.51) is plotted in Figure 2.9, where it can be recognized that the SIM represented by the red curve attracts system trajectories to a greater extent in case of a larger value of $\tilde{\gamma}$.


(a) $\tilde{\gamma} = 2.0$ (b) $\tilde{\gamma} = 11.0$
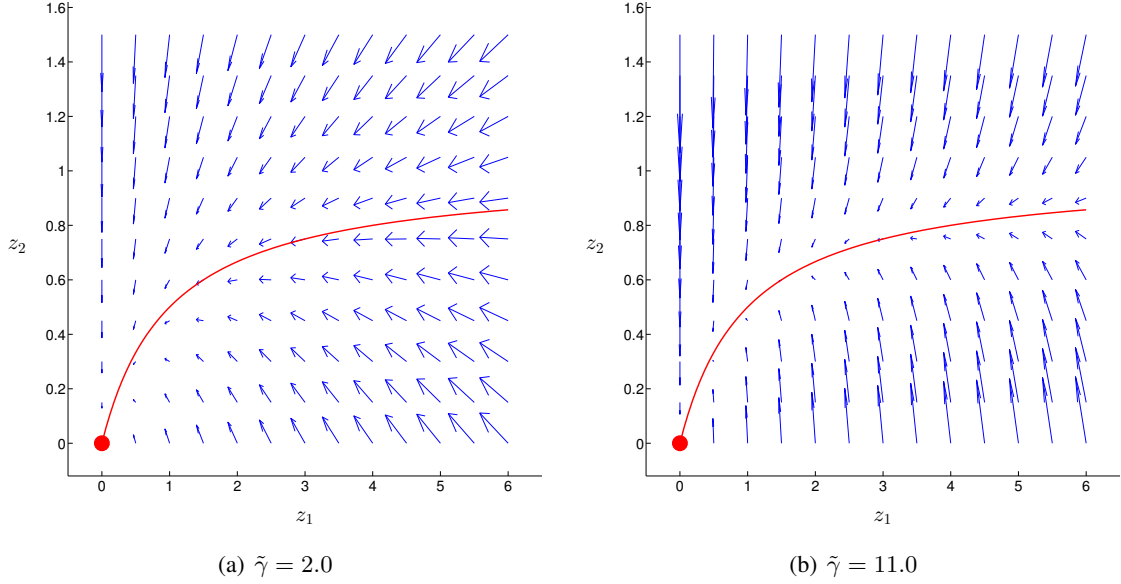
Figure 2.9: Vector fields of (2.51) for two different values of $\tilde{\gamma}$. The SIM is depicted by the red curve.

2.4 Error of Accuracy

The error of accuracy δ_{err} as defined in Chapter 2 is given by the difference of the species reconstruction function h and the approximated one h^{app} resulting from the respective model reduction method. The problem of this definition of the error is associated with the fact that δ_{err} is only computable if h and consequently the SIM is known, which generally is not the case. As a result, it is impossible to quantify the accuracy of SIM approximation of the underlying model reduction approach at first sight. Nevertheless, two approaches for making qualitative statements about the quality of SIM approximation via using a specific SIM computing method are presented and discussed in the following.

2.4.1 Consistency

In [Rei08], one of these qualitative statements is presented based on the SIM property of attracting nearby solution trajectories. Furthermore, a SIM$^{\mathrm{app}}$ should be an invariant manifold which is related to the following **consistency property** being a kind of invariance test:

Consistency property: Suppose a trajectory $z(\cdot; z^{t*})$ is identified from the solution of species reconstruction (1.38) or (1.39). Take the values of the RPVs $z_j\left(t_* + \Delta t; z^{t*}\right)$, $j \in \mathcal{I}_{\text{fixed}}$ at some time $t_* + \Delta t > t_*$ on the trajectory as new fixed parameter values $z_j\left(t_*^{\text{new}}\right)$, $j \in \mathcal{I}_{\text{fixed}}$ for the same problem (1.38) or (1.39) and solve the species reconstruction problem again. If the condition

$$z\left(t; z^{t_*^{\text{new}}}\right) = z\left(t + \Delta t; z^{t*}\right) \tag{2.54}$$

holds with the solution and its associated trajectory $z\left(\cdot; z^{t_*^{\text{new}}}\right)$ of the second species reconstruction, the species reconstruction with criterion Φ or $\tilde{\Phi}$ and its solutions—the POI$^{\text{app}}$s z^{t*} and $z^{t_*^{\text{new}}}$—are called **consistent**, otherwise **inconsistent**.

The consistency property is illustrated in Figure 2.10 with the help of a two-dimensional example: a species reconstruction is solved for a fixed value of the RPV z_1^{t*}, wherefrom the POI$^{\text{app}}$ and the associated trajectory $z\left(\cdot; \text{POI}^{\text{app}}\right)$ arises. At a later point in time, the RPV is fixed to z_1^{t*} and the same species reconstruction is solved again, resulting in either the POI$^{\text{app}}$ or the POI$^{\text{app}}$, according to whether an inconsistent or a consistent criterion is used. In contrast to the consistent case, in the inconsistent one, the trajectory $z\left(\cdot; \text{POI}^{\text{app}}\right)$ does not coincide with $z\left(\cdot; \text{POI}^{\text{app}}\right)$.

The consistency property is a helpful one in case of simple test problems consisting of a low-dimensional system of ODEs, where it can be seen via 'eye inspection' if the criterion used in the species reconstruction is consistent or inconsistent. If an inconsistent species reconstruction is identified, $\delta_{\text{err}} \neq 0$ and thus, the underlying approach is not exact. This is visualized in Figure 2.11(a), where the operation of the 'eye inspection' of the consistency property is demonstrated. The red curve is the (usually not known) SIM and the black crosses are the POI$^{\text{app}}$s computed with an inconsistent species reconstruction, wherefrom the associated trajectories (black lines) emanate. As an inconsistent criterion is used, the SIM$^{\text{app}}$ is not invariant and consequently the SIM is not identified correctly by the POI$^{\text{app}}$s. Vice versa, a consistent criterion does not necessarily imply an exact method as shown in Figure 2.11(b), where all POI$^{\text{app}}$s lie on the same invariant solution trajectory (not the SIM). In this case, the underlying species reconstruction is consistent, but the SIM is not identified at all. Certainly, this situation is more fictious than real, but not impossible. Consequently, the consistency property is necessary, but not sufficient.

2.4.2 Symmetry

A second approach to analyze the quality of SIM approximation based on ideas of LEBIEDZ and subsequent ideas of the author is presented in this work for the first time. An exact criterion for SIM point computation can be interpreted in the context of symmetry issues on an abstract level:
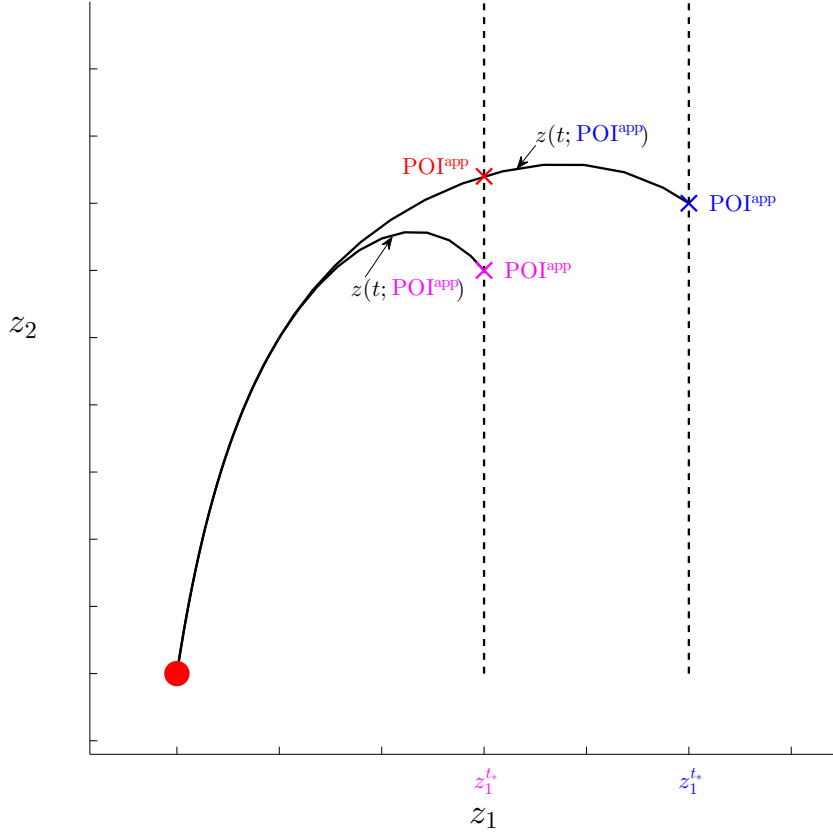
Figure 2.10: Schematic illustration of the consistency property.

as indicated previously, the result of a species reconstruction for given RPVs, parameterizing the SIM is a point in full state space—the POI^{app}. The SIM regarded as an intrinsic analytic object in state space should be coordinate independent, e.g. for any other choice (same total number) of RPVs the computed POI^{app} should coincide with the previous one. Thus, another necessary condition for an exact criterion characterizing the SIM is to yield POI^{app} results invariant under permutation of progress variables. Consequently, if a given species reconstruction within this permutation does not arise in the same SIM^{app}, it can be safely concluded that the underlying species reconstruction is not exact. Accordingly, the SIM acts as a kind of symmetry axis.

For the sake of comprehensibility and simplicity, the above mentioned symmetry aspect is demonstrated with a two-dimensional example (see Figure 2.12). First and without loss of generality, z_1 is chosen as RPV and fixed at $z_1(t_*) = z_1^{t_*}$. The result of a non-exact species reconstruction is the POI^{app} $\left(z_1^{t_*}, h^{app}\left(z_1^{t_*}\right)\right)$ (blue cross) lying not on the SIM (red curve). Subsequently, the non RPV values of this POI^{app} are chosen for the new selection of progress variables $z_2^{t_*} := h^{app}\left(z_1^{t_*}\right)$ and the same species reconstruction applied yields another POI^{app}, namely $\left(h^{app}\left(z_2^{t_*}\right), z_2^{t_*}\right)$. The difference of this two POI^{app}s is denoted by δ_{sym} and serves as a measure for the accuracy of the SIM approximation, or more specifically, if an exact species
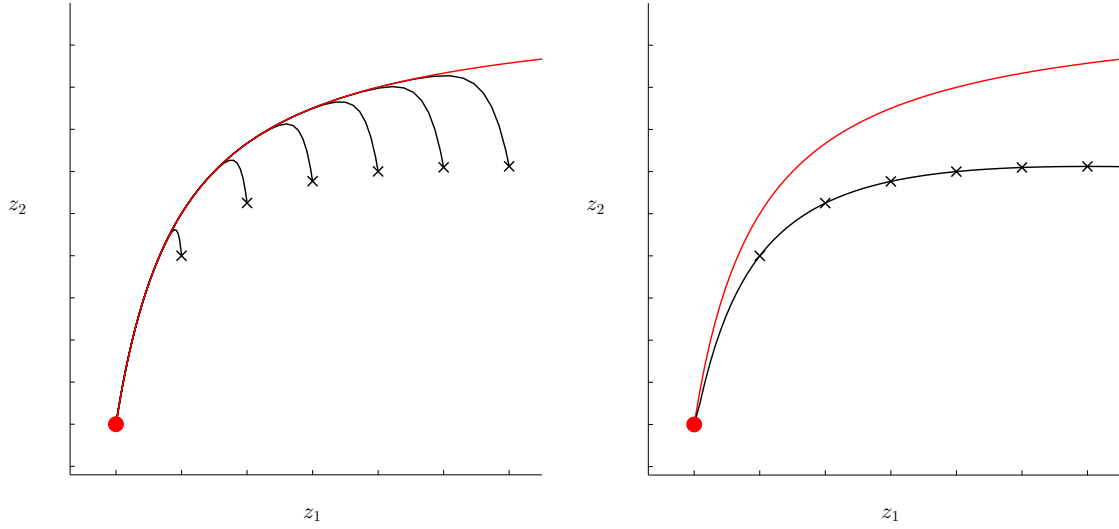
(a) The consistency property: Since the POI$^{\text{app}}$s are inconsistent ('eye inspection'), the SIM$^{\text{app}}$ is not invariant and consequently does not coincide with the SIM.

(b) A consistent criterion does not necessarily imply an exact method.

Figure 2.11: Examples of the consistency property. The red curve represents the SIM and the black crosses the POI$^{\text{app}}$s, wherefrom the associated trajectories emanate (black cruves).

reconstruction is used, it can be concluded that $\delta_{\text{sym}} \equiv 0$ for all choices of RPVs. Conversely, this condition does not provide a sufficient condition for an exact criterion in general, whereat the subsequent quotation of LEBIEDZ is very appropriate:

> "For a reasonable choice of the criterion used in the species reconstruction the symmetry aspect provides an almost sufficient condition for an exact SIM identification criterion."

This sounds highly vague, but for probably all common species reconstruction approaches it proves to be true, that $\delta_{\text{sym}} \equiv 0$ for all choices and values of RPVs provides an exact criterion.

As already announced in Subsection 2.1.6, the ZDP represents an exact species reconstruction, in the limit $m \to \infty$. Applied to the Linear Model (2.45), the POI$^{\text{app}}$ results in

$$\text{POI}^{\text{app}} = \left(z_2^0 \left(1 - 2\frac{(-1)^m}{((-1)^m + (-1-\gamma)^m)} \right), z_2^0 \right) \tag{2.55}$$

for $z_2(0) = z_2^0$ as known from (2.18). Using

$$z_1^0 := z_2^0 \left(1 - 2\frac{(-1)^m}{((-1)^m + (-1-\gamma)^m)} \right) \tag{2.56}$$
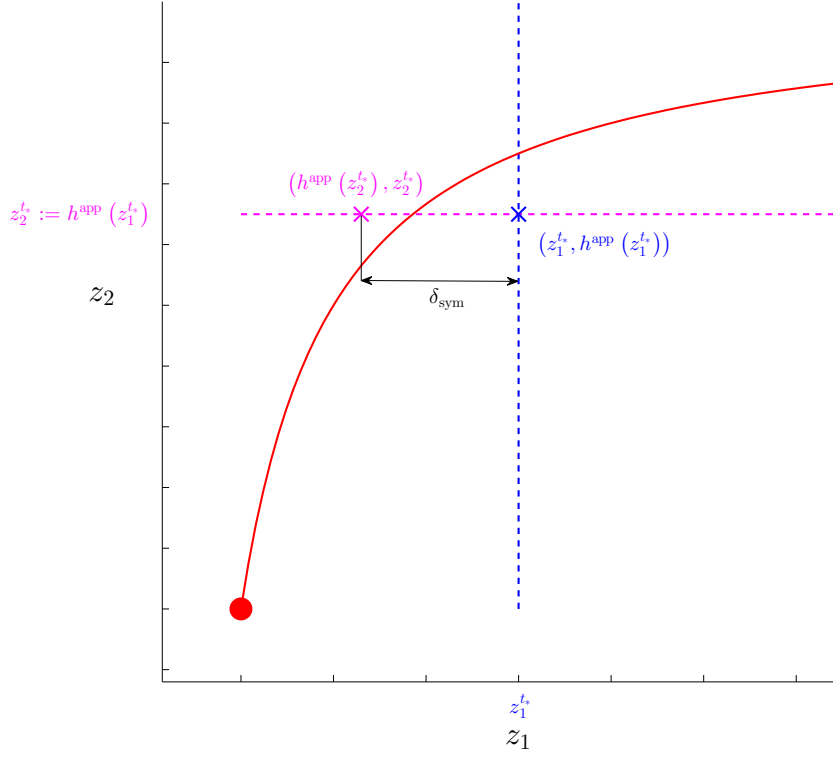
Figure 2.12: Schematic illustration of the symmetry property.

as new RPV value for the same ZDP species reconstruction yields

$$\text{POI}^{\text{app}} = \left(z_1^0, z_1^0 \left(1 - 2 \frac{(-1)^m}{((-1)^m + (-1-\gamma)^m)} \right) \right) \tag{2.57}$$

as new POI^{app}, which in turn leads to

$$\delta_{\text{sym}} = z_2^0 \left(1 - \left(1 - 2 \frac{(-1)^m}{((-1)^m + (-1-\gamma)^m)} \right)^2 \right) \tag{2.58}$$

by applying (2.56). It is not difficult to see that $\delta_{\text{sym}} \to 0$ for $m \to \infty$ comprising $\text{POI}^{\text{app}} \equiv$ $\text{POI}^{\text{app}} \equiv \text{POI}$ and thus, an exact species reconstruction criterion turned out, at least in the limit.

Normal Form

The interpretation of a SIM as symmetric manifold is emphasized by the transformation of the kinetic system equations into some kind of a normal form (cf. FENICHEL normal form [Jon95]), where the whole dynamic is projected onto the section being available after fixation of the RPVs. Generally, this transformation cannot be specified for a system of ODEs, whereas this work innovatively demonstrates the procedure with the help of the linear model (cf. 2.3.1) and the DAVIS–SKODJE one (cf. 2.3.2).

2. Spatially Homogeneous Systems: Slow Invariant Manifold Computation

Linear Model: The analytic solution of the Linear Model (2.45) is given by

$$z_1 = c_1 e^{-t} + c_2 e^{(-1-\gamma)t}, \quad c_1, c_2 \in \mathbb{R} \tag{2.59a}$$

$$z_2 = c_1 e^{-t} - c_2 e^{(-1-\gamma)t}. \tag{2.59b}$$

Via $z_2(t) = z_2^*$ yielding $c_1 = z_2^* e^t + c_2 e^{-\gamma t}$ the z_2–dynamic is projected onto the $z_2 = z_2^* = $ const. section. Substitution into (2.59a) results in

$$z_1(t) = z_2^* + 2c_2 e^{(-1-\gamma)t} \tag{2.60}$$

where it can be seen, that $\lim\limits_{t\to\infty} z_1(t) = z_2^*$ and thus, the SIM $z_1 \equiv z_2$ is identified exactly in the limit. Accordingly, the associated ODE that belongs to (2.60) is given by

$$d_t z_1 = (-1 - \gamma)z_1 + (1 + \gamma)z_2^* \tag{2.61}$$

whose solutions are depicted in Figure 2.13 for different values of z_2^*. As initial condition, $z_1(0) = 0$ is chosen (blue crosses). It is observable, that the respective solution trajectories (blue lines) converge towards the SIM (red line) along the z_2^*–axis. In order to emphasize the symmetry property of the SIM, the magenta colored lines represent the same results for exchanged z_1 and z_2.

Davis–Skodje Model: The same procedure applied to the nonlinear DAVIS–SKODJE test model (2.51) with $z_1(t) = z_1^*$ yields

$$z_2 = \tilde{c}_2 e^{-\tilde{\gamma}t} + \frac{z_1^*}{z_1^* + 1} \tag{2.62}$$

and again, $\lim\limits_{t\to\infty} z_2 = h(z_1^*)$. The associated ODE results in

$$d_t z_2 = -\tilde{\gamma} z_2 + \tilde{\gamma} \frac{z_1^*}{z_1^* + 1} \tag{2.63}$$

and the appropriate trajectories are plotted in Figure 2.14 (blue lines) as solutions of the initial value problem (2.63) together with $z_2(0) = 0$ (blue crosses) for different values of z_1^*. The SIM $h(z_1) = \frac{z_1}{z_1+1}$ is visualized as red curve, whereto the trajectories converge for $t \to \infty$. Here, the exchange of z_1 and z_2 is not feasible, since (2.51a) is decoupled from (2.51b).

As can be seen, this transformation provides an exact criterion for SIM identification or the closely related model reduction. Unfortunately, as previously mentioned, this transformation is not known for general systems of ODEs.
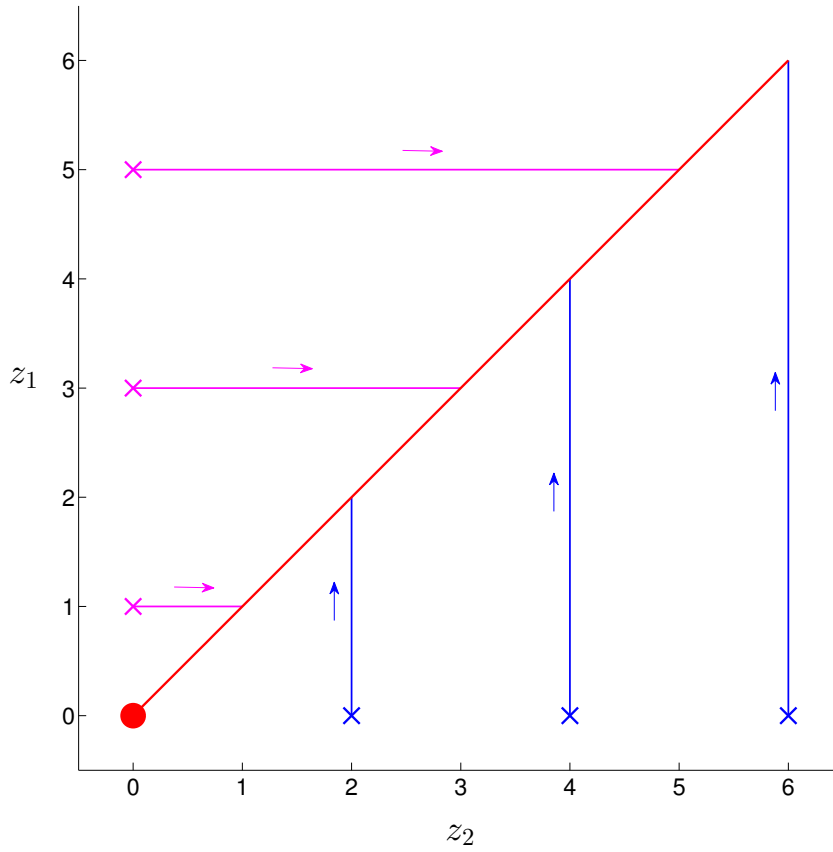
Figure 2.13: Visualization of the normal form applied to the Linear Model (2.45).

2.5 Selection of Reaction Progress Variables

As already mentioned, the choice of the RPVs in the context of species reconstruction is a still unresolved problem, although it is of major significance to SIM computation problems. Based on the symmetry aspect of a SIM presented in 2.4.2, the question which variable should be selected as RPV is less critical than the question how many variables should be chosen. Naturally, concerning the first point, there are choices performing better than others in numerical applications depending on characteristics of the SIM like monotonity and others, but an exact criterion is independent of the choice of the RPVs in the broadest sense. Several approaches that deal with this issue can be found in [Sie13]. On the other hand, the determination of the number of RPVs and the herewith associated dimension of the SIM that is computed is of greater significance, since it determines the extent of reduction of the original kinetic model equations. Since the reduced model should contain the slow modes of the system, the number of RPVs should be directly related to the time scales. These (local) time scales are

$$\tau_i = \frac{1}{|\Re(\lambda_i)|}, \quad i = 1, \ldots, m, \tag{2.64}$$
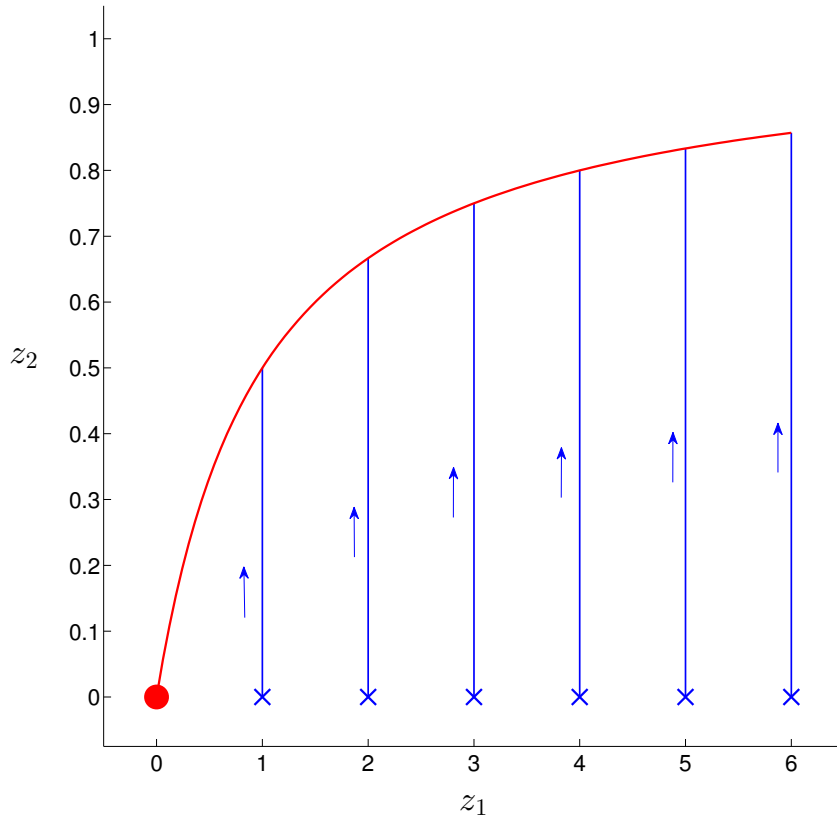
Figure 2.14: Visualization of the normal form applied to the DAVIS–SKODJE test model (2.51).

where λ_i represent the eigenvalues of the JACOBIAN J_S of the right hand side of the dynamics at point z^* in phase space and $\Re(\lambda_i)$ denotes the real part of these eigenvalues. Small and large time scales τ_i correspond to fast and slow directions in phase space, respectively. For an increasing ordering of the time scales $0 = \tau_0 \leq \tau_1 \leq \cdots \leq \tau_m$, the differences

$$\Delta\tau_i := \tau_i - \tau_{i-1}, \quad i = 1, \ldots, m \tag{2.65}$$

measure the corresponding gap. Therefore, a large spectral gap should be chosen such that $\#\mathcal{I}_{\text{fixed}} = m - \iota + 1$ with ι being the index of the largest $\Delta\tau_i$. In addition to these time scales, the singular values of the JACOBIAN of the source term (square roots of the eigenvalues of the symmetric matrix $J_S^\top J_S$) as well as the finite time LYAPUNOV exponents (see [MBI03, MTA$^+$08]) can also serve as criterion how many RPVs should be chosen.

For demonstration purposes a three-dimensional linear model is derived where the time scales and thus the spectral gaps can be modified by varying different parameters. This model is given by

$$\mathrm{d}_t z = Bz, \quad z \in \mathbb{R}^3 \tag{2.66}$$

with

$$B := R_1 R_2 \begin{pmatrix} -1 & 0 & 0 \\ 0 & -1-\gamma_1 & 0 \\ 0 & 0 & -1-\gamma_2 \end{pmatrix} R_2^{-1} R_1^{-1}$$

$$= \begin{pmatrix} -1 - \frac{\gamma_1}{4} - \frac{\gamma_2}{2} & \frac{\sqrt{2}}{4}\gamma_1 & -\frac{\gamma_1}{4} + \frac{\gamma_2}{2} \\ \frac{\sqrt{2}}{4}\gamma_1 & -1 - \frac{\gamma_1}{2} & \frac{\sqrt{2}}{4}\gamma_1 \\ -\frac{\gamma_1}{4} + \frac{\gamma_2}{2} & \frac{\sqrt{2}}{4}\gamma_1 & -1 - \frac{\gamma_1}{4} - \frac{\gamma_2}{2} \end{pmatrix}$$

(2.67)

where the rotation matrices R_1 and R_2 are defined by

$$R_1 := \begin{pmatrix} \cos\frac{\pi}{4} & 0 & -\sin\frac{\pi}{4} \\ 0 & 1 & 0 \\ \sin\frac{\pi}{4} & 0 & \cos\frac{\pi}{4} \end{pmatrix}, \quad R_2 := \begin{pmatrix} \cos\frac{\pi}{4} & -\sin\frac{\pi}{4} & 0 \\ \sin\frac{\pi}{4} & \cos\frac{\pi}{4} & 0 \\ 0 & 0 & 1 \end{pmatrix}$$

(2.68)

and $\gamma_1, \gamma_2 > 0$ represent the above mentioned parameters by which the spectral gaps can be adjusted. By assuming $\gamma_2 > \gamma_1$ the time scales are in an ordered selection such that $\lambda_1 = -1$ represents the eigenvalue belonging to the largest time scale and $\lambda_3 = -1 - \gamma_2$ the eigenvalue belonging to the slowest one. As a consequence, the spectral gaps refer to γ_1 and $\gamma_2 - \gamma_1$, respectively, meaning that for $\gamma_1 > \gamma_2 - \gamma_1$ the number of RPVs should be chosen as $\#\mathcal{I}_{\text{fixed}} = 1$, whereas $\#\mathcal{I}_{\text{fixed}} = 2$ should be chosen in case of $\gamma_1 < \gamma_2 - \gamma_1$. Incidentally, the corresponding analytic solutions read

$$z_1(t) = \hat{c}_1 \mathrm{e}^{-t} + \hat{c}_2 \mathrm{e}^{(-1-\gamma_1)t} + \hat{c}_3 \mathrm{e}^{(-1-\gamma_2)t} \tag{2.69a}$$

$$z_2(t) = \sqrt{2}\hat{c}_1 \mathrm{e}^{-t} - \sqrt{2}\hat{c}_2 \mathrm{e}^{(-1-\gamma_1)t} \tag{2.69b}$$

$$z_3(t) = \hat{c}_1 \mathrm{e}^{-t} + \hat{c}_2 \mathrm{e}^{(-1-\gamma_1)t} - \hat{c}_3 \mathrm{e}^{(-1-\gamma_2)t} \tag{2.69c}$$

with $\hat{c}_1, \hat{c}_2, \hat{c}_3 \in \mathbb{R}$.

A qualitative statement about the dimension of the SIM that should be chosen can be done if a measure for the attraction of a phase space point is accessible. A reasonable choice for this is

$$\Xi := \frac{\|J_S \cdot \hat{S}\|_2^2}{\|J_S \cdot \hat{n}\|_2^2} \in \mathbb{R}^+ \tag{2.70}$$

which is a slightly modified version of the SBD (cf. 2.1.9) and minimal, to some extent, on the SIM. The following Table 2.1 depicts values of Ξ applied to (2.66), (2.67), (2.68) for two different scenarios:

1. $\gamma_1 = 10$, $\gamma_2 = 11$: this case provides $\gamma_1 > \gamma_2 - \gamma_1$ and thus, a one-dimensional SIM should be selected as reduced model.

Table 2.1: Values of Ξ applied to Model (2.66) for different points in phase space. Points on the 1D-SIM are highlighted in red.

	$\begin{pmatrix} 1.0607 \\ 0.5000 \\ 1.0607 \end{pmatrix}$	$\begin{pmatrix} 1.0607 \\ 1.5000 \\ 1.0607 \end{pmatrix}$	$\begin{pmatrix} 1.0607 \\ 5.0000 \\ 1.0607 \end{pmatrix}$	$\begin{pmatrix} 0.3536 \\ 0.1000 \\ 0.3536 \end{pmatrix}$	$\begin{pmatrix} 0.3536 \\ 0.5000 \\ 0.3536 \end{pmatrix}$	$\begin{pmatrix} 0.3536 \\ 1.0000 \\ 0.3536 \end{pmatrix}$
$\gamma_1 = 10$ $\gamma_2 = 11$	24.2070	0.0083	27.1891	37.2405	0.0083	12.1087
$\gamma_1 = 2$ $\gamma_2 = 11$	1.8889	0.1111	2.1090	2.8460	0.1111	1.0000

2. $\gamma_1 = 2$, $\gamma_2 = 11$: this case provides $\gamma_1 < \gamma_2 - \gamma_1$ and thus, a two-dimensional SIM should be selected as reduced model.

The red colored columns represent values on the one-dimensional SIM ($z_2 = \sqrt{2}z_1$, $z_3 = z_1$) being at best at their minimal possible values, at least if an exact criterion is assumed. As can be seen, the differences between the values of Ξ (representing a reasonably working measure for the attractivity of a trajectory point) on the SIM and the values of Ξ lying elsewhere are immensely larger in the first scenario meaning that points on the SIM are much more attractive compared to points beyond. These differences serve as an indication that the one-dimensional SIM as reduced model is more appropriate in the first case conforming with the considerations above. On the basis of these values evaluated at a grid of the whole phase space it should be possible to decide where the largest spectral gap is and how many RPVs should be selected for SIM computation. On the one hand, this strategy is difficult to put into practice based on, inter alia, numerical effort, on the other hand, the idea of this strategy can be useful to develop numerically more efficient strategies for identifying the appropriate number of RPVs and therefore the associated dimension of the SIM that is computed.

2.6 A Multitude of Slow Invariant Manifold Computation Methods—No Common Denominator?

First of all, it has to be mentioned, that this section contains parts of the manuscript [LU14]. As indicated previously in Chapter 2.1, there are plenty of species reconstruction approaches all pursuing the same objective, namely the computation and, at best, identification of SIMs for using them as reduced description of the full kinetic model equations. The obvious move is therefore to find fundamental basic concepts underlying, combining, and collecting those several model reduction methods—that seem to look quite different at first glance—in order to develop a novel advanced species reconstruction making use of such basic concepts in concentrated form.

In this context, improvements should emerge in terms of accuracy of SIM approximation as well as numerical effort. Initial tendencies towards this direction are processed in this work and will be discussed in the following.

2.6.1 Derivative–of–the–State–Vector–Concept for SIM Computation

One of the species reconstruction techniques listed in 2.1, the ZDP (cf. 2.1.6), provides an exact criterion, at least in the limit $\nu \to \infty$, where ν is the derivative order of the non RPVs with respect to time t. It is precisely this time derivative of the state vector $z \in \mathbb{R}^m$ or a subset hereof that appears more or less obviously in several SIM computation approaches:

- The QSSA (cf. 2.1.1) (and consequently the direct related PEA (cf. 2.1.2)), for instance, are representatives thereof, since $d_t^{\nu=1} z_j, \ j \in \{1, \ldots, m\}$ is used as criterion for SIM approximation. Accordingly, the QSSA with general derivative order ν in turn corresponds to the ZDP approach. Obviously, the accuracy of SIM approximation increases with increasing ν such that the QSSA with $\nu = 1$ does not provide a highly accurate approximation.

- Another species reconstruction making considerably use of the time derivative of the state vector is the FCM (cf. 2.1.10) where a SIM$^{\text{app}}$ is computed by using $d_t^\alpha z, \ \alpha = 1, \ldots, m$ or, more precisely, $\det\left(d_t z, d_t^2 z, d_t^3 z, \ldots, d_t^m z\right) = 0$. Here, for singularly perturbed systems (cf. 1.2) the resulting analytic formula for the SIM$^{\text{app}}$ coincides with the asymptotic perturbation expansion (1.33) up to order $m-1$ in ε. This is not surprising taking account of the fact that the ZDP provides a coincidence up to order $\nu - 1$. Furthermore, according to personal communication with GINOUX, it holds that $\det\left(d_t z, d_t^2 z, d_t^3 z, \ldots, d_t^{m-1} z, d_t^{m+\upsilon} z\right) = 0$ identifies the exact SIM in the limit $\upsilon \to \infty$. Here again the time derivative of the state vector seems to play the central role for SIM computation.

- Additionally, the SBD (cf. 2.1.9) and the TBOA (cf. 2.2), regardless of reverse/forward mode (2.39) or local formulation (2.40), make use of $J_S \cdot S$ which corresponds to $d_t^{\nu=2} z$ (see (2.32)), the second time derivative of the state vector. Both approaches—the SBD and the TBOA—provide quite good, but no exact approximations to the SIM. Once again, δ_{err} can be decreased by increasing the derivative order of the state vector in the respective approach.

- Even in the FET approach (cf. 2.1.8) assumptions are made concerning the curvature and consequently the second derivative of the state vector. Based on the direct relation to the ILDM (cf. 2.1.3), both approaches can be categorized into those methods making use of the derivative of the state vector.

- Last but not least, this concept of using any kind of state vector derivative occurs also partially in the SPM (cf. 2.1.4), where equilibria are computed via using $\mathrm{d}_t^{\nu=1} z$ (see Section 1.1).

In summary, it is possible to state that in most instances the occurrence of $\mathrm{d}_t^\nu z$ in (1.38) or (1.39) makes a significant contribution regarding the improvement of SIM^{app}, at least for variable values of ν, since $\nu \to \infty$ provides an exact identification of the SIM. Consequently, one fundamental concept underlying serveral SIM approximation approaches has emerged, designated by **derivative–of–the–state–vector–concept**.

An example of a species reconstruction using this derivative–of–the–state–vector–concept is the following optimization problem

$$\min \quad \left. \|\mathrm{d}_t^\nu z\|_2^2 \right|_{t=t_*} \tag{2.71a}$$

subject to

$$\mathrm{d}_t z(t) = S\left(z(t)\right) \tag{2.71b}$$

$$z_j(t_*) = z_j^{t_*}, \quad j \in \mathcal{I}_{\text{fixed}}. \tag{2.71c}$$

Its application to the linear model from 2.3.1 with $\gamma = 0.5$ and $\mathcal{I}_{\text{fixed}} = \{2\}$ is demonstrated in Figure 2.15. For $z_2^{t_*} = 5.0$ the results for different values of ν are visualized by the blue crosses, which approximate the red SIM better for increasing value of ν and the POI^{app}s approach the SIM for $\nu \to \infty$.

On the one hand, although this derivative–of–the–state–vector–concept entails important theoretical results, numerical applications exhibit major problems when using $\nu > 2$, which is why other fundamental concepts would be helpful, and on the other hand, the question of why the reverse mode of the TBOA identifies the SIM for $t_0 \to -\infty$ has still not yet been answered. The latter leads to the concept of a **boundary value problem**.

2.6.2 Theory of Two-Point Boundary Value Problems

Assume a system of m ODEs to be given by

$$\mathrm{d}_t z = S(z), \quad S \colon \Omega \subset \mathbb{R}^m \to \mathbb{R}^m, \quad z \colon I \subset \mathbb{R} \to \mathbb{R}^m, \quad t \in I, \tag{2.72}$$

where the right hand side S is assumed to be smooth. In order to determine a specific solution trajectory of (2.72), the components of the state vector z have been specified at the same value of the independent variable $t = t_0 \in I$ so far. In contrast to this IVP, it is conceivable to determine
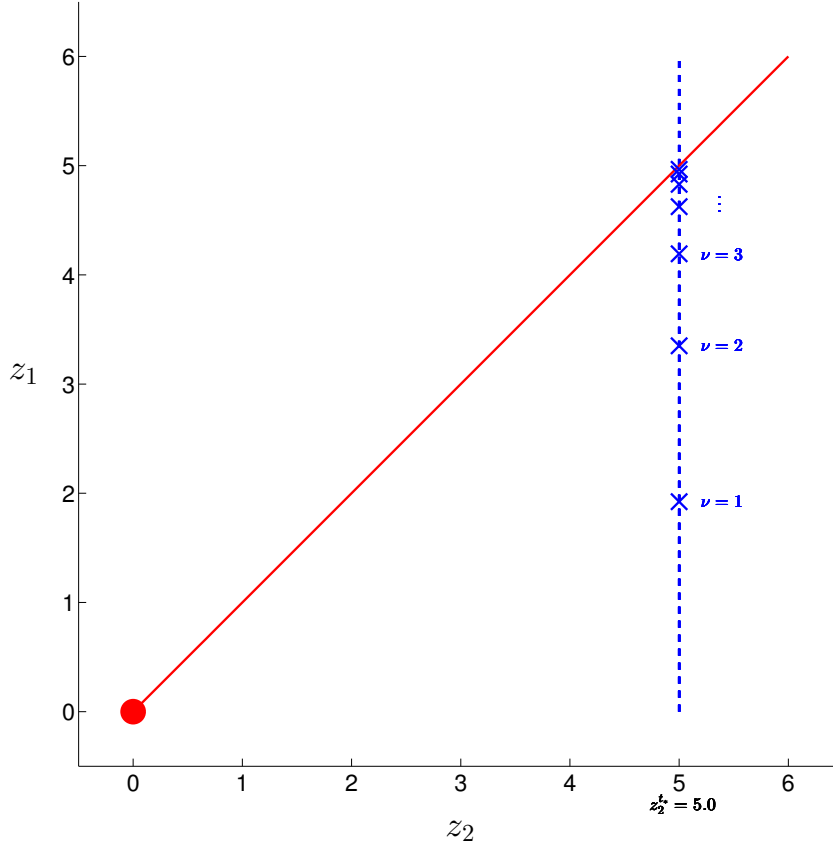
Figure 2.15: Demonstration of the derivative–of–the–state–vector–concept applied to the linear model (cf. 2.3.1) with $\gamma = 0.5$.

the state vector components at more than one value. The resulting equations are labeled **boundary conditions** and define together with (2.72) a **boundary value problem (BVP)**. Accordingly, a **two-point BVP** can be formulated as

$$\mathrm{d}_t z = S(z) \tag{2.73a}$$

$$G\left(z(t_0), z(t_*)\right) = 0 \tag{2.73b}$$

with a sufficiently smooth function $G\colon \Omega \times \Omega \to \mathbb{R}^m$. Thus, the componental description of (2.73b) reads as

$$
\begin{aligned}
G_1\left(z_1(t_0), \ldots, z_m(t_0), z_1(t_*), \ldots, z_m(t_*)\right) &= 0 \\
G_2\left(z_1(t_0), \ldots, z_m(t_0), z_1(t_*), \ldots, z_m(t_*)\right) &= 0 \\
&\vdots \\
G_m\left(z_1(t_0), \ldots, z_m(t_0), z_1(t_*), \ldots, z_m(t_*)\right) &= 0.
\end{aligned}
\tag{2.74}
$$

2. Spatially Homogeneous Systems: Slow Invariant Manifold Computation

If boundary conditions are formulated linearly, the function G can be written as

$$G\left(z(t_0), z(t_*)\right) = \underbrace{B_{t_0} z(t_0) + B_{t_*} z(t_*)}_{\equiv \mathcal{B} z(t)} - \beta \tag{2.75}$$

with constant matrices $\mathcal{B}, B_{t_0}, B_{t_*} \in \mathbb{R}^{m \times m}$ and a right hand side $\beta \in \mathbb{R}^m$. It can be assumed w.l.o.g. that $\beta = 0$, since the inhomogeneous case (i.e. $\beta \neq 0$) can be reduced to the homogeneous one (i.e. $\beta = 0$) if[13] $\mathrm{rk}\left(B_{t_0} \middle| B_{t_*}\right) = m$ by construction of $\bar{z} \in \mathcal{C}^1\left(I, \mathbb{R}^m\right)$ with $\mathcal{B}\bar{z} = \beta$ and solving the following homogeneous BVP for $\zeta := z - \bar{z}$:

$$\mathrm{d}_t \zeta = \mathrm{d}_t z - \mathrm{d}_t \bar{z} = S(z) - \mathrm{d}_t \bar{z} = S(\zeta + \bar{z}) - \mathrm{d}_t \bar{z} =: \mathcal{S}(\zeta) \tag{2.76a}$$

$$\mathcal{B}\zeta = \mathcal{B}z - \mathcal{B}\bar{z} = \beta - \beta = 0. \tag{2.76b}$$

A special case of linear boundary conditions occurs if each of the m Equations (2.75) contains only components of z evaluated at one of the two boundary points t_0 and t_*. Assumed that only t_0 occurs in p $(1 < p < m)$ equations and consequently only t_* in the other $q \equiv m - p$ ones, B_{t_0} and B_{t_*} result in (after a possible reordering of the equations)

$$B_{t_0} = \begin{pmatrix} B_{t_0}^{(1)} \\ 0 \end{pmatrix}, \quad B_{t_*} = \begin{pmatrix} 0 \\ B_{t_*}^{(2)} \end{pmatrix} \tag{2.77}$$

with $B_{t_0}^{(1)} \in \mathbb{R}^{p \times m}$ and $B_{t_*}^{(2)} \in \mathbb{R}^{q \times m}$. Boundary conditions (2.75) with B_{t_0} and B_{t_*} in form of (2.77) are referred to as **completely separated**. Especially, for $B_{t_*}^{(2)} \equiv 0$ an IVP (see 1.1) arises implying that IVPs are specific BVPs. In the further course of this work it is provided that

$$\mathrm{rk}\left(B_{t_0} \middle| B_{t_*}\right) = m \tag{2.78}$$

being a necessary condition concerning the solvability of a two-point BVP (2.73) including linear boundary conditions (2.75).

The Linear Model (2.45) together with

$$z_2(t_*) = z_2^{t_*}, \quad z_1(t_0) = z_1^{t_0}, \quad z_2^{t_*}, z_1^{t_0} \in \mathbb{R} \tag{2.79}$$

serves as representative of a two-point BVP with completely separated boundary conditions, where $p = q = 1$, $B_{t_0}^{(1)} = \begin{pmatrix} 1 & 0 \end{pmatrix}$, $B_{t_*}^{(2)} = \begin{pmatrix} 0 & 1 \end{pmatrix}$, and $\beta = \begin{pmatrix} z_1^{t_0} & z_2^{t_*} \end{pmatrix}^\top$ in (2.75) and (2.77). Furthermore, condition (2.78) holds, since

$$\left(B_{t_0} \middle| B_{t_*}\right) = \begin{pmatrix} 1 & 0 & 0 & 0 \\ 0 & 0 & 0 & 1 \end{pmatrix} \in \mathbb{R}^{2 \times 4} \tag{2.80}$$

---

[13] $\mathrm{rk}(A)$ denotes the rank of a matrix A.

has rank 2.

A solution to a BVP is a solution to the system of ODEs that also satisfies the associated bound-
ary conditions. On the other hand, verification of existence and uniqueness to solutions of a
BVP is generally much more demanding than in the IVP case. Indeed, there is no general the-
ory. BVPs can have one, none, or even infinitely many solutions. However, there is a vast
literature on individual cases (see [BL74]). Generally, it can be stated that the two-point BVP
(2.73) has as many solutions as there are zeros of

$$F(s) := G\left(s, z\left(t_*; s\right)\right) = 0, \quad s \in \mathbb{R}^m \tag{2.81}$$

where $z\left(t_*; s\right)$ is the solution of the IVP $\mathrm{d}_t z = S(z)$, $z(t_0) = s$ evaluated at $t = t_*$. Never-
theless, some requirements provided, an existence and uniqueness theorem for two-point BVPs
(2.73) with linear boundary conditions (2.75) can be stated.

Theorem 2.6.1 (Existence and Uniqueness Theorem for Two-Point BVPs with Linear Bound-
ary Conditions)**.** *Let the function $S \in \mathcal{C}\left(\Omega, \mathbb{R}^m\right)$ be* LIPSCHITZ *continuous with* LIPSCHITZ
constant L, $B_{t_0} + B_{t_*}$ being an invertible matrix, and it holds that

$$(t_* - t_0) \left\| (B_{t_0} + B_{t_*})^{-1} \right\|_\infty \max \left(\|B_{t_0}\|_\infty, \|B_{t_*}\|_\infty \right) L < 1. \tag{2.82}$$

Then a unique solution in $\mathcal{C}^1\left(I, \mathbb{R}^m\right)$ to the two-point BVP

$$\mathrm{d}_t z(t) = S\left(z(t)\right), \quad S: \Omega \subset \mathbb{R}^m \to \mathbb{R}^m, \quad z: I \subset \mathbb{R} \to \mathbb{R}^m, \quad t \in I \tag{2.83a}$$

$$\mathcal{B}z(t) = B_{t_0} z(t_0) + B_{t_*} z(t_*) = 0, \quad \mathcal{B}, B_{t_0}, B_{t_*} \in \mathbb{R}^{m \times m} \tag{2.83b}$$

exists.

Proof. See [Bey14]. □

In brief summary this means: if

- $B_{t_0} + B_{t_*}$ is invertible

- $S(\cdot)$ LIPSCHITZ continuous

- $[t_0, t_*]$ sufficiently short (see (2.82))

then the two-point BVP (2.83) can always be solved uniquely.

2.6.3 Boundary–Value–Concept for SIM Computation

The second fundamental concept different species reconstruction methods make use of in order to compute SIMs exploits the property of asymptotic stability (see 1.1) of SIMs. Provided that a SIM is globally asymptotically stable, every trajectory approaches it on an infinite time horizon. In dissipative systems of ODEs characterized by

$$\rho\left(\text{SIM}, z(t_0)\right) \left(:= \inf_{y \in \text{SIM}} \|y - z(t_0)\|\right) > \rho\left(\text{SIM}, z\left(t_*; z^0\right)\right), \quad t_0 < t_* \tag{2.84}$$

with $z\left(t_*; z^0\right)$ being the solution of the IVP $d_t z = S(z)$, $z(t_0) = z^0$ evaluated at $t = t_*$, a SIM is exactly identified for $t_* - t_0 \to \infty$ and $\rho\left(\text{SIM}, z(t_0)\right) \in \mathbb{R}$:

$$\rho\left(\text{SIM}, z\left(t_*; z^0\right)\right) = 0. \tag{2.85}$$

The stated designations are visualized in Figure 2.16 with the two-dimensional linear model from 2.3.1, where the red line represents the one-dimensional SIM and the blue curve an arbitrary trajectory.
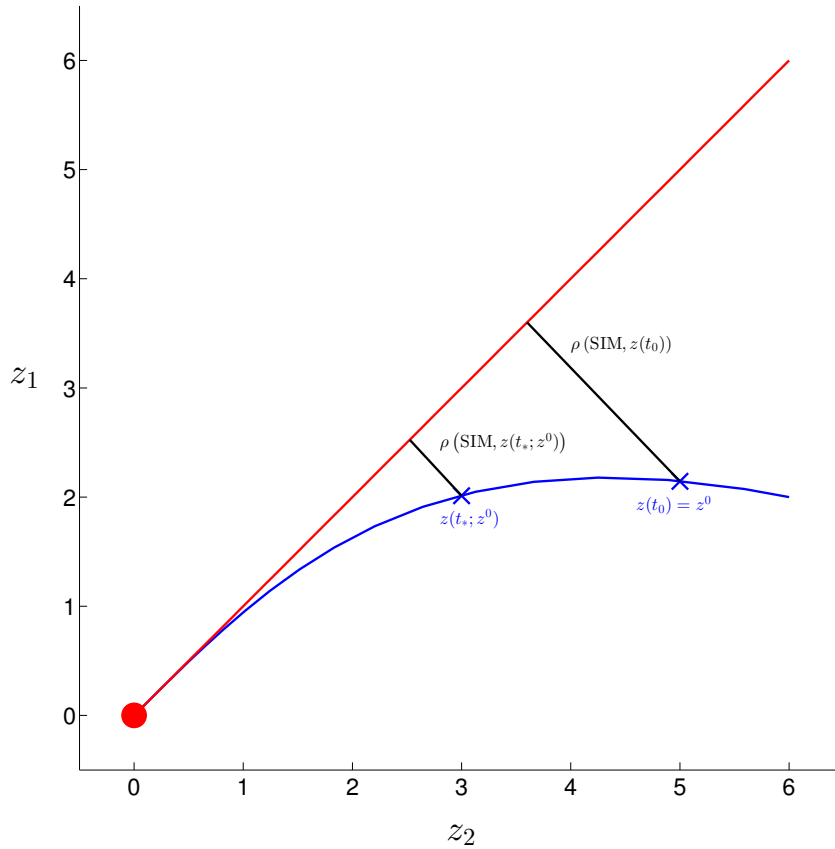
Figure 2.16: Visualization of the basic designations serving as basic idea of the boundary–value–concept.

Having this in mind, the following novel general formulation of a boundary value problem for
SIM computation is valid

$$\mathrm{d}_t z = S(z) \tag{2.86a}$$

$$z_j(t_*) = z_j^{t_*}, \quad j \in \mathcal{I}_{\text{fixed}}, \quad t_* \in I \subset \mathbb{R} \tag{2.86b}$$

$$z_j(t_0) = z_j^{t_0}, \quad j \notin \mathcal{I}_{\text{fixed}}, \quad t_0 \in I \subset \mathbb{R} \tag{2.86c}$$

where three different scenarios are conceivable:

- $t_0 < t_*$ **Reverse Mode**

- $t_0 = t_*$ **Local Mode**

- $t_0 > t_*$ **Forward Mode**

Existence and uniqueness of a solution of BVP (2.86) is guaranteed by Theorem 2.6.1 for suf-
ficiently small $t_* - t_0$. Once again, a symmetric issue of the SIM already addressed in 2.4.2
is apparent, since replacing the RPVs by the non RPVs and vice versa yields an analog BVP
with reversed roles of t_0 and t_*. Compared with the general form of a species reconstruction
problem (1.38), Φ in (1.38a) is represented by (2.86c) or rather by $z_j(t_0) - z_j^{t_0}$, $j \notin \mathcal{I}_{\text{fixed}}$ in the
boundary value formulation (2.86). Especially this $z_j^{t_0}$ has not yet been specified at all, which is,
however, the crucial issue in (2.86). For globally asymptotically stable SIMs the determination
of $z_j^{t_0}$, $j \notin \mathcal{I}_{\text{fixed}}$ is without particular significance to identify a SIM exactly, since no problem
arises by increasing $t_* - t_0$ in the reverse mode with fixed $z_j^{t_*}$, $j \in \mathcal{I}_{\text{fixed}}$. In contrast, in realis-
tic chemical combustion models, for instance, additional physical constraints restrict the domain
where the model equations in form of a system of ODEs are defined with the result that the spec-
ification of $z_j^{t_0}$, $j \notin \mathcal{I}_{\text{fixed}}$ has a significantly greater importance. It is exactly this specification
that distinguishes between several species reconstructions making use of this boundary–value–
concept. Before listing up some representatives of this concept, the functionality of BVP (2.86)
is demonstrated with application to the linear model described in 2.3.1 as well as the nonlinear
DAVIS–SKODJE model from 2.3.2.

BVP (2.86) Applied to Linear Model (2.45)...

...Analytically: The fixation of the PRVs (2.86b) applied to the Linear Model (2.45) with its
analytic solution given by (2.48) and $\mathcal{I}_{\text{fixed}} = \{2\}$ yields

$$z_2(t_*) = z_2^{t_*} = c_1 \mathrm{e}^{-t_*} - c_2 \mathrm{e}^{(-1-\gamma)t_*} \tag{2.87}$$

where $c_1(c_2)$ can be computed as

$$c_1(c_2) = z_2^{t_*} \mathrm{e}^{t_*} + c_2 \mathrm{e}^{-\gamma t_*}. \tag{2.88}$$

2. Spatially Homogeneous Systems: Slow Invariant Manifold Computation

Substituting into Equation (2.86c) with application of (2.48a) results in

$$z_1(t_0) = \left(z_2^{t_*} e^{t_*} + c_2 e^{-\gamma t_*} \right) e^{-t_0} + c_2 e^{(-1-\gamma)t_0} = z_1^{t_0} \qquad (2.89)$$

out of which an analytic formula for c_2 is obtained, namely

$$c_2 = \frac{z_1^{t_0} - z_2^{t_*} e^{t_*} e^{-t_0}}{e^{-\gamma t_*} e^{-t_0} + e^{(-1-\gamma)t_0}}. \qquad (2.90)$$

Thus, the free variable of the $\mathrm{POI}^{\mathrm{app}}$ computed by the BVP (2.86) arises as

$$z_1(t_*) \left(= c_1 e^{-t_*} + c_2 e^{(-1-\gamma)t_*} \right) = z_2^{t_*} \left(1 + \frac{2 \frac{z_1^{t_0}}{z_2^{t_*}} e^{(-2-\gamma)t_*} e^{t_0} + 2 e^{(-1-\gamma)t_*}}{e^{(-1-\gamma)t_*} + e^{-t_*} e^{-\gamma t_0}} \right), \quad (2.91)$$

where it can be seen that

$$\left(\lim_{\gamma \to \infty} z_1(t_*) = z_2^{t_*} \right) \qquad (2.92a)$$

$$\lim_{t_0 \to -\infty} z_1(t_*) = z_2^{t_*} \qquad (2.92b)$$

holds for every $z_1^{t_0} \in \mathbb{R}$ and $t_0 < t_*$, i.e. in the reverse mode. The one-dimensional SIM of the Linear Model (2.45) is known as first bisectrix ($z_1 \equiv z_2$), it is identified exactly by BVP (2.86) for $t_0 \to -\infty$, independently of the specification of $z_1^{t_0}$. This is based, as already mentioned, on the global asymptotic stability of the SIM and the omission of additional constraints that restrict the area where the model equations are defined.

...Numerically: Numerical experiments have been performed using `bvp4c`, a BVP solver for systems of ODEs used in `Matlab`® utilizing a finite difference code that implements a collocation formula. Problem (2.86) is implemented for the Linear Model (2.45) with $z_2(t_*) = z_2^{t_*} = 5.0$, $t_* = 0.0$, $z_1^{t_0} = 0.0$, and t_0 varies between -2.0 and -20.0—all of them arbitrarily chosen values. For Figure 2.17(a), $\gamma = 0.2$ is chosen—representing an almost total lack of time scale separation—and the blue rhombi show δ_{err} resulting from the numerical solution of the BVP (2.86) corresponding to the different values of t_0. With decreasing t_0, $z_1(t_* = 0.0)$ converges to $z_1(0) = z_2^0 = 5.0$ meaning that the SIM approximation improves and thus, δ_{err} decreases considerably in view of the provided spectral gap. The red dashed curve visualizes the analytic error from Equation (2.91) where it can be seen, as one might expect, that analytic error formula and numerical results coincide since the blue rhombi are located along the red dashed curve. In Figure 2.17(b) same results for $\gamma = 2.0$ are plotted, where the convergence towards $\delta_{\mathrm{err}} = 0.0$ is much more steeper based on the larger (but still relatively small) time scale separation represented by γ.

(a) $\gamma = 0.2$ (b) $\gamma = 2.0$
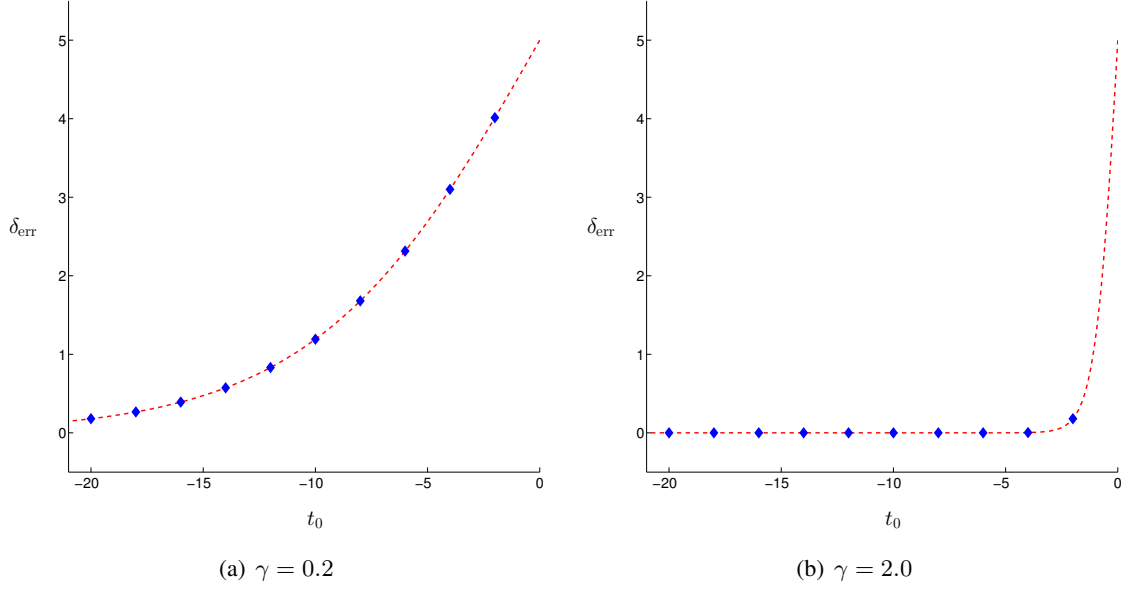
Figure 2.17: Error of accuracy δ_{err} of the POI$^{\mathrm{app}}$ $z(t_* = 0.0)$—resulting from the BVP (2.86) applied to the Linear Model (2.45) with two different values of γ—as a function of t_0. The blue rhombi represent numerical results, whereas the red dashed curve illustrates the analytic error (2.91).

BVP (2.86) Applied to Davis–Skodje model (2.51)...

...Analytically: The same procedure as done before by means of the Linear Model (2.45) is now applied to the nonlinear DAVIS–SKODJE test problem (2.51) where the analytically calculated SIM is given by (2.52) and the solution of the model equations by (2.53). With $\mathcal{I}_{\mathrm{fixed}} = \{1\}$, the boundary values

$$z_1(t_*) = z_1^{t_*} \tag{2.93a}$$

$$z_2(t_0) = z_2^{t_0} \tag{2.93b}$$

complete (2.51) to achieve the BVP that has to be solved. The expressions (2.53a) and (2.93a) result in

$$\tilde{c}_1 = z_1^{t_*} \mathrm{e}^{t_*} \tag{2.94}$$

which, substituted into (2.93b), yields (using (2.53b))

$$\tilde{c}_2 = z_2^{t_0} \mathrm{e}^{\tilde{\gamma} t_0} - \frac{z_1^{t_*} \mathrm{e}^{\tilde{\gamma} t_0}}{z_1^{t_*} + \mathrm{e}^{t_0} \mathrm{e}^{-t_*}}. \tag{2.95}$$

Herewith, the POI$^{\mathrm{app}}$ results in

$$z(t_*) = \begin{pmatrix} z_1^{t_*} \\ \frac{z_1^{t_*}}{z_1^{t_*}+1} + z_2^{t_0} \mathrm{e}^{\tilde{\gamma} t_0} \mathrm{e}^{-\tilde{\gamma} t_*} - \frac{z_1^{t_*} \mathrm{e}^{\tilde{\gamma} t_0} \mathrm{e}^{-\tilde{\gamma} t_*}}{z_1^{t_*}+\mathrm{e}^{t_0} \mathrm{e}^{-t_*}} \end{pmatrix} \tag{2.96}$$

which also implies that

$$\left(\lim_{\tilde{\gamma} \to \infty} z_2(t_*) = \frac{z_1^{t_*}}{1 + z_1^{t_*}} \right) \tag{2.97a}$$

$$\lim_{t_0 \to -\infty} z_2(t_*) = \frac{z_1^{t_*}}{1 + z_1^{t_*}} \tag{2.97b}$$

holds for every $z_2^{t_0} \in \mathbb{R}$ and $t_0 < t_*$.

...Numerically: The same numerical experiment as in the linear model case is applied to the nonlinear DAVIS–SKODJE test problem. Here, the RPV is chosen as $z_1(t_*) = z_1(0) = z_1^0 = 2.0$, $\tilde{\gamma} = 1.2$ in Figure 2.18(a), and $\tilde{\gamma} = 3.0$ in Figure 2.18(b), respectively. The constant $z_2^{t_0}$ is set to $z_2^{t_0} = 0.0$ again and t_0 varies between -1.0 and -5.0. With the analytic SIM $z_2 \equiv \frac{z_1}{1+z_1}$, the POI$^{\text{app}}$ should converge towards the POI on the SIM $\left(2 \quad \frac{2}{3} \right)^{\top}$. In Figure 2.18, it is clearly visible that δ_{err} decreases for decreasing t_0 meaning that the POI is identified for $t_0 \to -\infty$. Here again, the convergence occurs faster for a larger value of $\tilde{\gamma}$ and numerical results (blue rhombi) coincide with the analytic error formula resulting from (2.96) (red dashed curve).

(a) $\tilde{\gamma} = 1.2$ (b) $\tilde{\gamma} = 3.0$
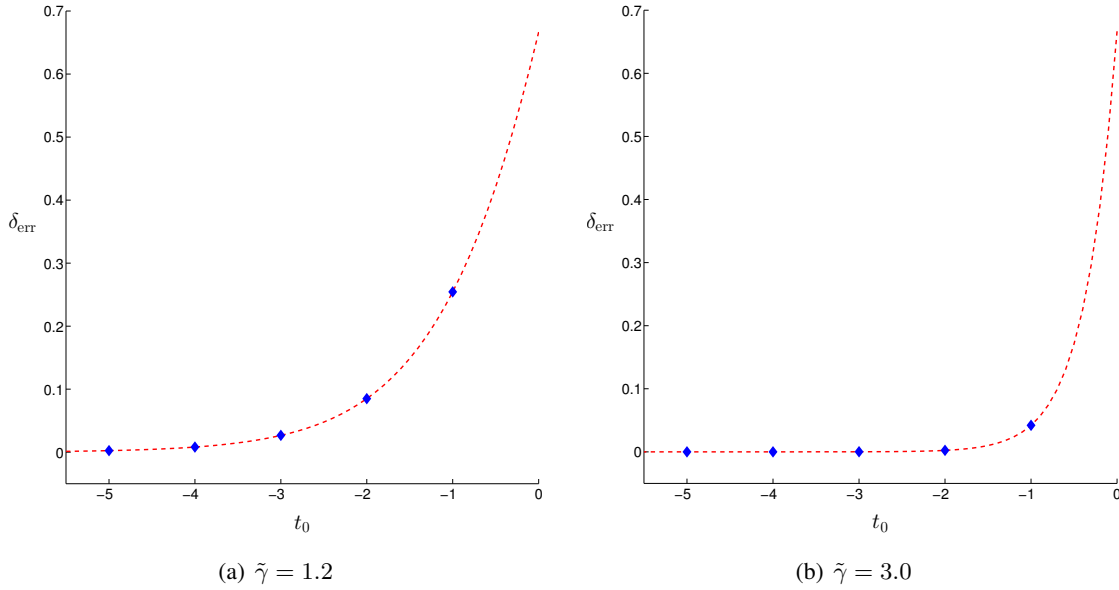
Figure 2.18: Error of accuracy δ_{err} of the POI$^{\text{app}}$ $z(t_* = 0.0)$—resulting from the BVP (2.86) applied to the DAVIS–SKODJE model (2.51) with two different values of γ—as a function of t_0. The blue rhombi represent numerical results, whereas the red dashed curve illustrates the analytic error from (2.96).

As mentioned before, there are several SIM computation approaches making use of the boundary–value–concept. Besides the SPM 2.1.4 and the ICE-PIC approach 2.1.7, where this concept

is more indirectly contained by using information of the 'foretime' (e.g. computation of fixed points at infinity), the reverse mode of the TBOA ((2.39) with $t_* = t_f$) provides the most important representative relating to this work. This formulation can be regarded as a special case of the BVP (2.86), where the objective functional to be minimized implicitly determines the specification of $z_j^{t_0}$, $j \notin \mathcal{I}_{\text{fixed}}$. Thus, the boundary–value–concept provides the fundamental idea why the reverse TBOA identifies SIM points exactly in the limit $t_0 \to -\infty$. Furthermore, this method obviously combines ideas from both previously presented concepts, the derivative– of–the–state–vector–concept as well as the boundary–value–concept.

2.6.4 Two Concepts—One Approach

Since two fundamental concepts for SIM computation are exposed in its definite form, it is obvious to develop a novel advanced species reconstruction formulation that contains both concepts in an efficient form. The advantages of this include the fact that this formulation would imply two different, independent (at least within the scope of current knowledge) ways two improve the accuracy of SIM approximation.

For this purpose it is appropriate to use the reverse TBOA with a modified objective functional, where, instead of using information of the second derivative of the state vector as formulated in (2.39), the derivative order is handled as additional parameter ν. This leads to the following species reconstruction formulation

$$\min \int_{t_0}^{t_f} \|d_t^\nu z(t)\|_2^2 \, dt, \quad \nu \in \mathbb{N}, \quad \nu \geq 1 \tag{2.98a}$$

subject to

$$d_t z(t) = S(z(t)) \tag{2.98b}$$

$$0 = g(z(t_f)) \tag{2.98c}$$

$$z_j(t_f) = z_j^{t_f}, \quad j \in \mathcal{I}_{\text{fixed}} \tag{2.98d}$$

including both concepts—the boundary–value–concept represented by the reverse mode of the TBOA and the derivative–of–the–state–vector–concept represented by using the νth derivative of z in the objective functional. Here, two parameters, t_0 and ν, are provided to improve the SIM computation as it holds

$$\lim_{t_0 \to -\infty} z(t_f) \in \text{SIM} \tag{2.99a}$$

$$\lim_{\nu \to \infty} z(t_f) \in \text{SIM}, \tag{2.99b}$$

at least applied to the Linear Model (2.45) as well as the DAVIS–SKODJE model (2.51) wherefore it is proven analytically [LSU11, Ung10]. Nevertheless, numerical experiments applied to more realistic kinetic model equations confirm the result.

Certainly, this also works the other way around meaning that a local method making use of the derivative–of–the–state–vector–concept with derivative order ν as parameter, the ZDP for instance, is modified to a method using non-local trajectory information via integration of the boundary–value–concept. The result can be formulated as

$$\mathrm{d}_t^\nu z_j(t) = 0 \Big|_{t=t_0}, \quad j \notin \mathcal{I}_{\text{fixed}} \tag{2.100a}$$

subject to

$$\mathrm{d}_t z(t) = S\left(z(t)\right) \tag{2.100b}$$

$$0 = g\left(z(t_{\text{f}})\right) \tag{2.100c}$$

$$z_j(t_{\text{f}}) = z_j^{t_{\text{f}}}, \quad j \in \mathcal{I}_{\text{fixed}}, \tag{2.100d}$$

where $t_0 < t_{\text{f}}$ has to be fulfilled in the reverse mode. As in the previous formulation, Equations (2.99) hold for the two test models (2.45) and (2.51).

Obviously, there are a multitude of possible formulations imaginable, some of these tested with the models from 2.3. Out of this, the following optimization problem has turned out as 'best working' ('best working' in the sense of indirectly specifying the best choice of $z_j^{t_0}$, $j \notin \mathcal{I}_{\text{fixed}}$ in BVP (2.86)):

$$\min \quad \|\mathrm{d}_t^\nu z(t)\|_2^2 \Big|_{t=t_0} \tag{2.101a}$$

subject to

$$\mathrm{d}_t z(t) = S\left(z(t)\right) \tag{2.101b}$$

$$0 = g\left(z(t_{\text{f}})\right) \tag{2.101c}$$

$$z_j(t_{\text{f}}) = z_j^{t_{\text{f}}}, \quad j \in \mathcal{I}_{\text{fixed}}, \quad t_0 < t_{\text{f}}. \tag{2.101d}$$

The result (applied to the Linear Model (2.45) with (w.l.o.g.) $t_{\text{f}} = 0$) is a POI$^{\text{app}}$

$$z(0) = \begin{pmatrix} z_2^0 \left(1 - \frac{2}{1+(-1-\gamma)^{2\nu}\mathrm{e}^{-2\gamma t_0}}\right) \\ z_2^{t_0} \end{pmatrix} \tag{2.102}$$

identifying the POI on the SIM exactly for $\nu \to \infty$ as well as $t_0 \to -\infty$. The error term

$$|\delta_{\text{err}}| = \left| \frac{2 z_2^0}{1 + (-1-\gamma)^{2\nu}\mathrm{e}^{-2\gamma t_0}} \right| \tag{2.103}$$
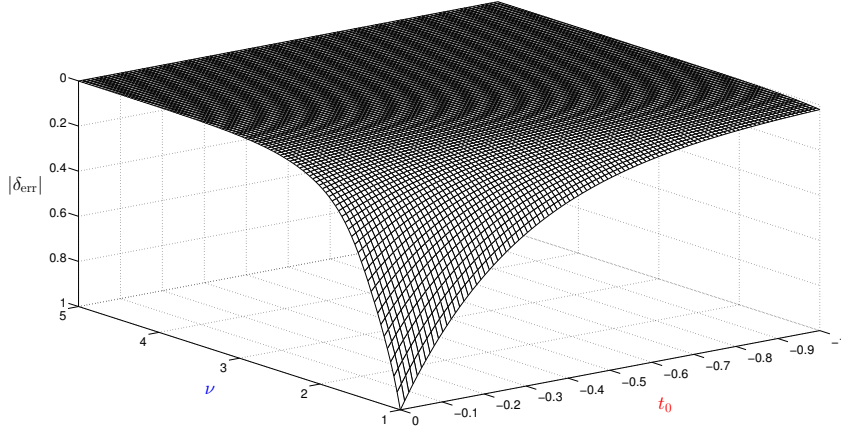
Figure 2.19: Error term (2.103) with $z_2^0 = 5.0$ and $\gamma = 2.0$ plotted against ν and t_0.

is plotted in Figure 2.19 depending on the two 'adjusting screws' ν and t_0. Here, z_2^0 is arbitrarily chosen as $z_2^0 = 5.0$ and γ is fixed to $\gamma = 2.0$. As it can easily be seen, the error $|\delta_{\mathrm{err}}|$ decreases rapidly for both increasing ν as well as decreasing t_0, even though a small spectral gap ($\gamma = 2.0$) is chosen. As stated before, it is not possible to decrease t_0 arbitrarily based on additional constraints entering the optimization problem in (2.101c) and restricting the domain where the kinetic model is defined to a polyhedron in phase space. Thus, for a good SIM approximation in realistic models the focus is on two issues to be handled:

- choosing ν as large as pratically possible (numerical computation of ν-th order derivatives required),

- choosing t_0 as small as possible (with respect to the physically feasible domain).

The latter issue is discussed in the next section.

2.6.5 Interim Summary

In this section it has been succeeded to expose two basic fundamental concepts—the derivative–of–the–state–vector–concept and the boundary–value–concept—serving as a basis for a large number of SIM computation approaches. Each of these concepts result in an exact identification of a SIM (analytically proven for test models, numerical confirmation for more realistic kinetic models) in a limiting case ($\nu \to \infty$ or $t_0 \to -\infty$). Accordingly, a novel improved species reconstruction has been developed (2.101) combining both concepts in its fundamental form yielding a SIM computation method with two adjusting screws to improve the accuracy of SIM identification. This is schematically illustrated in Figure 2.20.
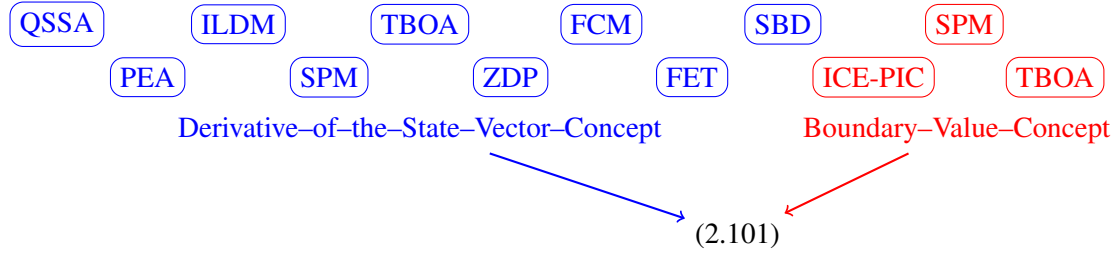
Figure 2.20: Schematic illustration of common denominators of different SIM computation approaches merged in a novel improved formulation of a species reconstruction (2.101).

2.7 Choosing t_0 as Small as Possible

As just described, the accuracy of SIM approximation in the reverse mode (representing the boundary–value–concept) improves with decreasing t_0. Unfortunately, additional constraints entering the species reconstruction and restricting the domain where the kinetic model is defined to a polyhedron in phase space ensure that t_0 cannot get arbitrarily small. In chemical combustion processes, representatives of these constraints are for instance positivity of chemical species concentrations and chemical element mass conservation relations. Thus, the aim is a feasible minimal choice of t_0, which is discussed in the following.

Figure 2.21 exemplarily visualizes a two-dimensional scenario, where the phase space polyhedron is bounded by the black lines: the z_1– and z_2–axis (i.e. $z_2 = 0$ and $z_1 = 0$) as well as two straight lines denoted by B_1 and B_2 here. The red line refers to the SIM with equilibrium visualized by the red dot, whereas the blue and magenta curves are trajectories starting from specified initial values. The vertical dashed black line represents the value $z_2^{t_f}$ where the RPV z_2 is fixed at time $t = t_f$ and the magenta cross is the result of a local species reconstruction (such as (2.101) with $t_f = t_0$). The idea why the reverse mode of a species reconstruction works significantly better than the local mode of the same one is based on the evaluation of the objective function at time $t_0(< t_f)$. Hence, the corresponding trajectory has a time period of $|t_0 - t_f|$ to converge towards the SIM before evaluating at time $t = t_f$ and obtaining the missing value(s) of the POI$^{\mathrm{app}}$. In Figure 2.21, the maximal feasible time period is represented by the blue curve between the right cross lying on B_2—the result of a reverse mode formulation with minimal t_0—and the cross lying on $z_2 = z_2^{t_f}$—the point where the corresponding trajectory is evaluated at $t = t_f$. It is obvious that the POI$^{\mathrm{app}}$ $z(t_f)$ has been significantly improved by using a reverse mode (POI$^{\mathrm{app}}$) compared to a local mode formulation with $z_2(t_f) = z_2^{t_f}$ (POI$^{\mathrm{app}}$).

It remains to be considered how to achieve the minimal value of t_0, wherefore (2.101) with (2.45)
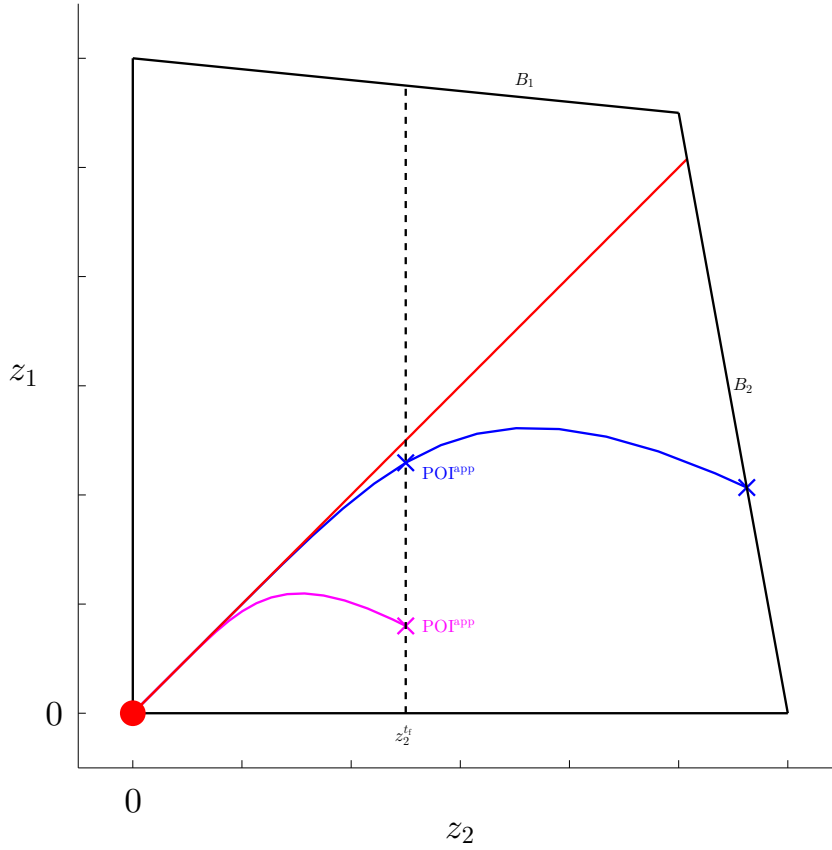
Figure 2.21: Schematic visualization of a local method in comparison with a reverse mode formulation with minimal feasible choice of t_0.

as kinetic model is regarded. Additionally, for reasons of simplicity, $t_f = 0$ is chosen which is no restriction at all. Solving this problem analytically provides formulas for the integration constants c_1, c_2 from (2.48) depending on t_0, ν, γ, and z_2^0

$$c_1 = c_1^* \left(t_0, \nu, \gamma, z_2^0 \right) \tag{2.104a}$$

$$c_2 = c_2^* \left(t_0, \nu, \gamma, z_2^0 \right) \tag{2.104b}$$

which are submitted into $z_1 = z_1 \left(c_1^*, c_2^* \right)$ and $z_2 = z_2 \left(c_1^*, c_2^* \right)$ for solving the following optimization problem yielding the minimal feasible t_0

$$\min \quad t_0 \tag{2.105a}$$

subject to

$$z_1(c_1^*, c_2^*) \geq 0 \tag{2.105b}$$

$$z_2(c_1^*, c_2^*) \geq 0 \tag{2.105c}$$

$$z_1(c_1^*, c_2^*) \leq n_1 z_2(c_1^*, c_2^*) + b_1 \tag{2.105d}$$

$$z_1(c_1^*, c_2^*) \leq n_2 z_2(c_1^*, c_2^*) + b_2. \tag{2.105e}$$

2. Spatially Homogeneous Systems: Slow Invariant Manifold Computation

Here, (2.105b) and (2.105c) are the positivity constraints of the state variables and (2.105d) and (2.105e) represent the restrictions B_1 and B_2 in Figure 2.21 where the constants $n_1, n_2, b_1, b_2 \in \mathbb{R}$ determine the position of these staight lines representing a part of the boundary of the polyhedron that restricts the domain where the kinetic model is defined. Formulas (2.105b)–(2.105e) are representatives for those additional constraints that enter the species reconstructions above as function g (e.g. in (2.101)). As an example, Problem (2.105) is solved using fmincon—a Matlab$^{\circledR}$ toolbox for solving nonlinear optimization problems via an interior point algorithm. Therefore, the following values are specified:

$$\gamma = 1.00 \quad \nu = 2.00 \quad z_2^0 = 3.00 \quad n_1 = -2.00 \quad n_2 = -0.25 \quad b_1 = 122.00 \quad b_2 = 111.00$$

As a measure for the accuracy of the resulting POI^{app}, the ratio r between the value of the free variable of the POI^{app} and the value of the free variable of the SIM ($z_1(0) = z_2^0$) is regarded. The closer this ratio r is to $r = 1$, the better is the POI^{app}. Subsequently, we compare the ratio of the local method of (2.101) (that is $t_{\text{f}} = t_0 = 0$) with the reverse mode (that is $t_0 < t_{\text{f}} = 0$) using minimal t_0. Obviously, the degree of improvement depends on the parameter values chosen above, but it holds that the smaller t_0 the larger the improvement. Analysis for the local method (2.101) yields

$$\text{POI}_{\text{loc}}^{\text{app}} := \text{POI}^{\text{app}} = \begin{pmatrix} z_1(0) \\ z_2^0 \end{pmatrix} = \begin{pmatrix} 2.6471 \\ 3.0000 \end{pmatrix} \tag{2.106}$$

which results in a ratio of $r_{\text{loc}} = \frac{2.6471}{3.0000} \approx 0.8824$. On the other hand, Solving (2.105) in the reverse mode formulation yields a minimal $t_0^{\text{min}} = -2.6056$. Using

$$c_1^{*,\text{min}} = c_1^* \left(t_0^{\text{min}}, \nu, \gamma, z_2^0 \right) \tag{2.107a}$$

$$c_2^{*,\text{min}} = c_2^* \left(t_0^{\text{min}}, \nu, \gamma, z_2^0 \right) \tag{2.107b}$$

and evaluating

$$z_1(0) = c_1^{*,\text{min}} + c_2^{*,\text{min}} \tag{2.108a}$$

$$z_2(0) = z_2^0 \tag{2.108b}$$

results in

$$\text{POI}_{t_0^{\text{min}}}^{\text{app}} := \text{POI}^{\text{app}} = \begin{pmatrix} z_1(0) \\ z_2^0 \end{pmatrix} = \begin{pmatrix} 2.9980 \\ 3.0000 \end{pmatrix} \tag{2.109}$$

giving a ratio of $r_{t_0^{\text{min}}} = 0.9993$ which is a significant improvement compared to r_{loc} by taking into consideration the small value of γ. The position of the polyhedron determines how small t_0 can become. For instance, changing b_1 from $b_1 = 122$ to $b_1 = 222$ yields a minimal t_0 of $t_0^{\text{min}} = -3.2047$ and a ratio of $r_{t_0^{\text{min}}} = 0.9998$. In contrast, choosing $b_1 = 22$ results in $t_0^{\text{min}} = -0.8957$ and $r_{t_0^{\text{min}}} = 0.9794$. Apparently, the degree of improvement $\left| r_{t_0^{\text{min}}} - r_{\text{loc}} \right|$ also depends on the specification of the other variables ν, γ, z_2^0, n_1, n_2, and b_2.

70

2.8 Reverse TBOA in the Light of Optimal Boundary Control

In the light of BVP formulation, there is a different approach to the reverse TBOA for SIM computation in its general form (based on an idea of LEBIEDZ) comprising an as yet unspecified objective functional (for reasons of simplicity additional constraints contained in function g (cf. (2.39)) are omitted)

$$\min \quad \int_{t_0}^{t_{\mathrm{f}}} \tilde{\Phi}(z) \, \mathrm{d}t, \quad t_0 < t_{\mathrm{f}} \in \mathbb{R} \tag{2.110a}$$

subject to

$$\mathrm{d}_t z(t) = S\left(z(t)\right) \tag{2.110b}$$

$$z_j(t_{\mathrm{f}}) = z_j^{t_{\mathrm{f}}}, \quad j \in \mathcal{I}_{\mathrm{fixed}}. \tag{2.110c}$$

The missing values of the POI$^{\mathrm{app}}$, $z_j(t_{\mathrm{f}})$, $j \notin \mathcal{I}_{\mathrm{fixed}}$ (supposed to be an appropriate POI approximation), are determined by the solution of Optimization Problem (2.110) and can be interpreted as a **boundary control** operating at time $t = t_{\mathrm{f}}$. Thus, the following formulation is motivated

$$\min \quad \int_{t_0}^{t_{\mathrm{f}}} \tilde{\Phi}(z) \, \mathrm{d}t, \quad t_0 < t_{\mathrm{f}} \in \mathbb{R} \tag{2.111a}$$

subject to

$$\mathrm{d}_t z(t) = S\left(z(t)\right) \tag{2.111b}$$

$$z_j(t_{\mathrm{f}}) = z_j^{t_{\mathrm{f}}}, \quad j \in \mathcal{I}_{\mathrm{fixed}} \tag{2.111c}$$

$$z_j(t) = u(t), \quad j \notin \mathcal{I}_{\mathrm{fixed}}, \tag{2.111d}$$

wherefrom the missing values of the POI$^{\mathrm{app}}$ result by evaluating the control function u at $t = t_{\mathrm{f}}$. This is why the following subsection regarding **optimal control theory** is inserted.

2.8.1 Theory of Optimal Control Problems

From an abstract point of view, an optimal control problem can be interpreted as an infinite optimization problem of the following form

$$\min \quad \Phi(z) \tag{2.112a}$$

subject to

$$H(z) = \Theta_Y \tag{2.112b}$$

$$G(z) \in \mathcal{K} \tag{2.112c}$$

$$z \in \mathcal{S} \tag{2.112d}$$

2. Spatially Homogeneous Systems: Slow Invariant Manifold Computation

with

$$\Phi\colon Z \to \mathbb{R} \qquad G\colon Z \to X \qquad H\colon Z \to Y \tag{2.113}$$

being mappings between BANACH spaces $(X, \|\cdot\|_X)$, $(Y, \|\cdot\|_Y)$, and $(Z, \|\cdot\|_Z)$, whereby Θ_X, Θ_Y, and Θ_Z represent the zero elements belonging to the respective BANACH space. In analogy to Section 1.4, $\mathcal{S} \subset Z$ is a closed and convex subset of Z and $\mathcal{K} \subset X$ is a **cone** (with its tip at Θ_Z) defined by

$$x \in \mathcal{K} \Rightarrow \alpha x \in \mathcal{K}, \quad \forall \alpha > 0 \tag{2.114}$$

being closed and convex. For infinite optimization problems as (2.112), necessary as well as sufficient conditions are well-known [Lem71, Kur76, ZK79, MZ79, Mau81]. Application of these necessary conditions to optimal control problems result in the **PONTRYAGIN'S minimum principle**, serving as a basis for indirect methods computing numerical solutions of an optimal control problem, since they induce a BVP in general.

To formulate a general form of an optimal control problem from (2.112), several specifications have to be performed:

Variable: The variables (z, u) are elements of the BANACH space

$$Z := W^{1,\infty}\left([t_0, t_{\mathrm{f}}], \mathbb{R}^{m_z}\right) \times L^{\infty}\left([t_0, t_{\mathrm{f}}], \mathbb{R}^{m_u}\right) \tag{2.115}$$

equipped with the norm

$$\|(z, u)\|_Z := \max\left\{\|z\|_{1,\infty}, \|u\|_{\infty}\right\}, \tag{2.116}$$

where $[t_0, t_{\mathrm{f}}] \subset \mathbb{R}$ is a non-empty, compact interval with $t_0 < t_{\mathrm{f}}$. Here, $L^{\infty}\left([t_0, t_{\mathrm{f}}], \mathbb{R}^{m_u}\right)$ consists of all measurable functions $u\colon [t_0, t_{\mathrm{f}}] \to \mathbb{R}^{m_u}$ which are essentially bounded, i.e.

$$\operatorname*{ess\,sup}_{t_0 \leq t \leq t_{\mathrm{f}}} |u(t)| := \inf_{\substack{N \subset [t_0, t_{\mathrm{f}}] \\ N \text{ is set of measure zero}}} \sup_{t \in [t_0, t_{\mathrm{f}}] \setminus N} |u(t)| < \infty \tag{2.117}$$

and is a BANACH space endowed with the norm $\|u\|_{\infty} := \operatorname*{ess\,sup}\limits_{t_0 \leq t \leq t_{\mathrm{f}}} |u(t)|$. Accordingly, $W^{1,\infty}\left([t_0, t_{\mathrm{f}}], \mathbb{R}^{m_z}\right)$ consists of all absolutely continuous functions $z\colon [t_0, t_{\mathrm{f}}] \to \mathbb{R}^{m_z}$ with absolutely continuous derivatives up to order 0 and $\|z\|_{1,\infty} < \infty$, where the norm is given by $\|z\|_{1,\infty} := \operatorname*{ess\,sup}\limits_{t_0 \leq t \leq t_{\mathrm{f}}} \left(|z(t)| + |\nabla z(t)|\right)$ with $\nabla z(t)$ being the weak gradient (for more information see [Ger10]). The space $W^{1,\infty}\left([t_0, t_{\mathrm{f}}], \mathbb{R}^{m_z}\right)$ endowed with the norm $\|\cdot\|_{1,\infty}$ is a BANACH space, too.

Objective function: The objective function $\Phi\colon Z \to \mathbb{R}$ is given by

$$\Phi(z, u) := \varphi\left(z(t_0), z(t_\mathrm{f})\right) + \int_{t_0}^{t_\mathrm{f}} \tilde{\Phi}\left(t, z(t), u(t)\right) \, \mathrm{d}t \tag{2.118}$$

with $\varphi\colon \mathbb{R}^{m_z} \times \mathbb{R}^{m_z} \to \mathbb{R}$ and $\tilde{\Phi}\colon [t_0, t_\mathrm{f}] \times \mathbb{R}^{m_z} \times \mathbb{R}^{m_u} \to \mathbb{R}$ sufficiently smooth.

Equality constraints: Equality constraints of an optimal control problem are given by

$$H(z, u) = \Theta_Y \tag{2.119}$$

with $H = (H_1, H_2)\colon Z \to Y$. Here, the BANACH space Y is defined by

$$Y := L^\infty\left([t_0, t_\mathrm{f}], \mathbb{R}^{m_z}\right) \times \mathbb{R}^{m_\psi} \tag{2.120}$$

together with

$$\|(y_1, y_2)\|_Y := \max\left\{\|y_1\|_\infty, \|y_2\|_2\right\} \tag{2.121}$$

and

$$H_1(z, u) = S\left(t, z(t), u(t)\right) - \mathrm{d}_t z(t), \tag{2.122a}$$
$$H_2(z, u) = -\psi\left(z(t_0), z(t_\mathrm{f})\right) \tag{2.122b}$$

with $S\colon [t_0, t_\mathrm{f}] \times \mathbb{R}^{m_z} \times \mathbb{R}^{m_u} \to \mathbb{R}^{m_z}$ and $\psi\colon \mathbb{R}^{m_z} \times \mathbb{R}^{m_z} \to \mathbb{R}^{m_\psi}$ sufficient smooth.

Inequality constraints: Accordingly, inequality constraints of an optimal control problem are given by

$$G(z, u) \in \mathcal{K} \tag{2.123}$$

with $G = (G_1, G_2)\colon Z \to X$. Here, the BANACH space X is defined by

$$X := L^\infty\left([t_0, t_\mathrm{f}], \mathbb{R}^{m_c}\right) \times \mathcal{C}\left([t_0, t_\mathrm{f}], \mathbb{R}^{m_s}\right) \tag{2.124}$$

together with

$$\|(x_1, x_2)\|_X := \max\left\{\|x_1\|_\infty, \|x_2\|_\infty\right\} \tag{2.125}$$

and

$$G_1(z, u) = -c\left(t, z(t), u(t)\right), \tag{2.126a}$$
$$G_2(z, u) = -s\left(t, z(t)\right) \tag{2.126b}$$

with $c\colon [t_0, t_\mathrm{f}] \times \mathbb{R}^{m_z} \times \mathbb{R}^{m_u} \to \mathbb{R}^{m_c}$ and $s\colon [t_0, t_\mathrm{f}] \times \mathbb{R}^{m_z} \to \mathbb{R}^{m_s}$ sufficient smooth. Additionally, the cone $\mathcal{K} := \mathcal{K}_1 \times \mathcal{K}_2 \subset X$ is defined by

$$\mathcal{K}_1 := \left\{y \in L^\infty\left([t_0, t_\mathrm{f}], \mathbb{R}^{m_c}\right) \mid y(t) \geq 0 \text{ a.e. in } [t_0, t_\mathrm{f}]\right\} \tag{2.127a}$$
$$\mathcal{K}_2 := \left\{y \in \mathcal{C}\left([t_0, t_\mathrm{f}], \mathbb{R}^{m_s}\right) \mid y(t) \geq 0 \text{ in } [t_0, t_\mathrm{f}]\right\}. \tag{2.127b}$$

2. Spatially Homogeneous Systems: Slow Invariant Manifold Computation

Set constraint: Finally, the set $\mathcal{S} \subset Z$ is given by

$$\mathcal{S} := W^{1,\infty}\left([t_0, t_{\mathrm{f}}], \mathbb{R}^{m_z}\right) \times U_{\mathrm{ad}} \tag{2.128}$$

with

$$U_{\mathrm{ad}} := \{u \in L^{\infty}\left([t_0, t_{\mathrm{f}}], \mathbb{R}^{m_u}\right) \mid u(t) \in \mathcal{U} \text{ a.e. in } [t_0, t_{\mathrm{f}}]\} \tag{2.129}$$

and $\mathcal{U} \subset \mathbb{R}^{m_u}$ being a closed set.

Based on these specifications, it can be clearly seen, that the problem

$$\min \quad \Phi(z, u) \quad (\text{w.r.t. } (z, u) \in Z) \tag{2.130a}$$

subject to

$$H(z, u) = \Theta_Y \tag{2.130b}$$

$$G(z, u) \in \mathcal{K} \tag{2.130c}$$

$$(z, u) \in \mathcal{S} \tag{2.130d}$$

is equivalent to the following form of an optimal control problem

$$\min \quad \varphi\left(z(t_0), z(t_{\mathrm{f}})\right) + \int_{t_0}^{t_{\mathrm{f}}} \tilde{\Phi}\left(t, z(t), u(t)\right) \, \mathrm{d}t \qquad \text{(Objective Function)} \tag{2.131a}$$

(w.r.t. the **state** $z \in W^{1,\infty}\left([t_0, t_{\mathrm{f}}], \mathbb{R}^{m_z}\right)$ and the **control** $u \in L^{\infty}\left([t_0, t_{\mathrm{f}}], \mathbb{R}^{m_u}\right)$)

subject to

$$\mathrm{d}_t z(t) = S\left(t, z(t), u(t)\right) \quad \text{a.e. in } [t_0, t_{\mathrm{f}}] \qquad \text{(System of ODEs)} \tag{2.131b}$$

$$\psi\left(z(t_0), z(t_{\mathrm{f}})\right) = 0 \qquad \text{(Boundary Conditions)} \tag{2.131c}$$

$$c\left(t, z(t), u(t)\right) \leq 0 \qquad \text{a.e. in } [t_0, t_{\mathrm{f}}] \quad \text{(Mixed Control–State Constraints)} \tag{2.131d}$$

$$s\left(t, z(t)\right) \leq 0 \qquad \text{in } [t_0, t_{\mathrm{f}}] \qquad \text{(Pure State Constraints)} \tag{2.131e}$$

$$u(t) \in \mathcal{U} \qquad \text{a.e. in } [t_0, t_{\mathrm{f}}]. \qquad \text{(Set Constraint)} \tag{2.131f}$$

Depending on the form of the Objective Function (2.131a), the Optimal Control Problem (2.131)

	BOLZA Problem	$(\varphi \not\equiv 0$ and $\tilde{\Phi} \not\equiv 0)$
is referred to as	**MAYER Problem**	$(\varphi \not\equiv 0$ and $\tilde{\Phi} \equiv 0)$
	LAGRANGE Problem	$(\varphi \equiv 0$ and $\tilde{\Phi} \not\equiv 0)$

being all equivalent in that each of them can be converted to any other one. It is obvious that LAGRANGE and MAYER problems are special cases of BOLZA problems. A BOLZA problem can be transformed into a MAYER problem by introducing an extra component for the state vector x which satisfies the equation

$$\mathrm{d}_t x(t) = \tilde{\Phi}\left(t, z(t), u(t)\right), \quad x(0) = 0. \tag{2.132}$$

Using this extra variable the objective function takes the MAYER form

$$\varphi\left(z(t_0), z(t_\mathrm{f})\right) + x(t_\mathrm{f}). \tag{2.133}$$

The transformation of an optimal control problem in LAGRANGE form into MAYER form can be treated in a similar way. Necessary conditions concerning a local minimizer for Problem (2.131) without mixed control–state (2.131d) and pure state constraints (2.131e) are summarized in the following form of the PONTRYAGIN'S minimum principle, wherefore the definition of the **HAMILTONIAN** is required:

$$\mathcal{H}(t, z, u, \lambda, \ell_0) := \ell_0 \tilde{\Phi}(t, z, u) + \lambda^\top S(t, z, u). \tag{2.134}$$

Theorem 2.8.1 (PONTRYAGIN'S Minimum Principle). *Let the following assumptions be fulfilled for Problem (2.131):*

(i) The functions φ, $\tilde{\Phi}$, S, ψ are continuous with respect to all arguments and continuously differentiable with respect to z and u.

(ii) $\mathcal{U} \subset \mathbb{R}^{m_u}$ is closed and convex with non-empty interior.

(iii) $(\bar{z}, \bar{u}) \in W^{1,\infty}\left([t_0, t_\mathrm{f}], \mathbb{R}^{m_z}\right) \times L^\infty\left([t_0, t_\mathrm{f}], \mathbb{R}^{m_u}\right)$ is a local minimizer of Problem (2.131).

(iv) There are no mixed control–state (2.131d) and pure state constraints (2.131e) in (2.131).

Then there exist non-trivial multipliers $\ell_0 \in \mathbb{R}$, $\sigma \in \mathbb{R}^{m_\psi}$, and $\lambda \in W^{1,\infty}\left([t_0, t_\mathrm{f}], \mathbb{R}^{m_z}\right)$ such that following conditions are fulfilled:

(a) $\ell_0 \geq 0$, $(\ell_0, \sigma, \lambda) \neq \Theta$,

(b) Adjoint Equation:

$$\mathrm{d}_t \lambda(t) = -\partial_z \mathcal{H}\left(t, \bar{z}(t), \bar{u}(t), \lambda(t), \ell_0\right)^\top \quad \textit{a.e. in } [t_0, t_\mathrm{f}], \tag{2.135}$$

(c) **Transversality Conditions:**

$$\lambda(t_0)^\top = - \left(\ell_0 D_1 \varphi \left(\bar{z}(t_0), \bar{z}(t_f) \right) + \sigma^\top D_1 \psi \left(\bar{z}(t_0), \bar{z}(t_f) \right) \right), \tag{2.136}$$

$$\lambda(t_f)^\top = \ell_0 D_2 \varphi \left(\bar{z}(t_0), \bar{z}(t_f) \right) + \sigma^\top D_2 \psi \left(\bar{z}(t_0), \bar{z}(t_f) \right), \tag{2.137}$$

$(D_i, \ i = 1, 2$ *indicates the partial derivative w.r.t. the ith argument)*

(d) **Variational Inequality of** HAMILTONIAN**:** *Almost everywhere in* $[t_0, t_f]$ *it holds*

$$\partial_u \mathcal{H} \left(t, \bar{z}(t), \bar{u}(t), \lambda(t), \ell_0 \right) (u - \bar{u}(t)) \geq 0 \tag{2.138}$$

for all $u \in \mathcal{U}$.

Proof. See e.g. [Ger10]. □

If $\ell_0 > 0$, it is convenient to fix ℓ_0 w.l.o.g. at $\ell_0 = 1$, since the statements of Theorem 2.8.1 also hold for $\frac{\lambda}{\ell_0}$. In order to assure $\ell_0 > 0$ and thus $\ell_0 = 1$, additional regularity assumptions are required.

Theorem 2.8.2. *Let the conditions of Theorem 2.8.1 be fulfilled. Furthermore, it holds that*

$$\mathrm{rk} \left(D_1 \psi \left(\bar{z}(t_0), \bar{z}(t_f) \right) \Sigma(t_0) + D_2 \psi \left(\bar{z}(t_0), \bar{z}(t_f) \right) \Sigma(t_f) \right) = m_\psi \tag{2.139}$$

with Σ *being the fundamental system of the homogeneous, linear system of ODEs*

$$d_t \Sigma(t) = \partial_z S \left(t, \bar{z}(t), \bar{u}(t) \right) \Sigma(t), \quad \Sigma(t_0) = I_{m_z}, \quad t \in [t_0, t_f]. \tag{2.140}$$

If there additionally exist $\delta z \in W^{1,\infty} \left([t_0, t_f], \mathbb{R}^{m_z} \right)$ *and* $\delta u \in \mathrm{int} \left(U_{\mathrm{ad}} - \{\bar{u}\} \right)$ *with*

$$\partial_z S \left(t, \bar{z}(t), \bar{u}(t) \right) \delta z(t) + \partial_u S \left(t, \bar{z}(t), \bar{u}(t) \right) \delta u(t) - d_t \delta z(t) = 0, \quad \textit{a.e. in } [t_0, t_f], \tag{2.141a}$$

$$D_1 \psi \left(\bar{z}(t_0), \bar{z}(t_f) \right) \delta z(t_0) + D_2 \psi \left(\bar{z}(t_0), \bar{z}(t_f) \right) \delta z(t_{rmf}) = 0 \tag{2.141b}$$

then it holds that $\ell_0 = 1$ *in Theorem 2.8.1.*

Proof. See e.g. [Ger10]. □

For a specific problem, it is often easier to show that $\ell_0 = 0$ leads to a contradiction for proving regularity. If this is successful, w.l.o.g. $\ell_0 = 1$ can be chosen.

Application of PONTRYAGIN's minimum principle 2.8.1 to the reverse TBOA (2.111) (i.e. $\varphi \equiv 0$ (LAGRANGE form), $\psi = z_j(t_f) - z_j^{t_f}, \ j \in \mathcal{I}_{\mathrm{fixed}}$) results in the following BVP for **primal** and

dual variables $z(t)$ and $\lambda(t)$, respectively:

$$\mathrm{d}_t z(t) = S\left(z(t)\right) \qquad\qquad\qquad \text{(System of ODEs)} \qquad \text{(2.142a)}$$

$$\mathrm{d}_t \lambda(t) = -\partial_z \mathcal{H}\left(z(t), \lambda(t), \ell_0\right) \qquad\qquad \text{(Adjoint Equation)} \qquad \text{(2.142b)}$$

$$z_j(t_\mathrm{f}) = z_j^{t_\mathrm{f}}, \qquad\qquad j \in \mathcal{I}_{\text{fixed}} \qquad \text{(Boundary Condition)} \qquad \text{(2.142c)}$$

$$\lambda_j(t_0) = 0, \qquad\qquad j \in \mathcal{I}_{\text{fixed}} \qquad \text{(Transversality Condition)} \qquad \text{(2.142d)}$$

$$\lambda_j(t_0) = 0, \qquad\qquad j \notin \mathcal{I}_{\text{fixed}} \qquad \text{(Transversality Condition)} \qquad \text{(2.142e)}$$

$$\lambda_j(t_\mathrm{f}) = 0, \qquad\qquad j \notin \mathcal{I}_{\text{fixed}} \qquad \text{(Transversality Condition)} \qquad \text{(2.142f)}$$

Incidentally, these BVP equations can also be obtained by analyzing the first variation of the LAGRANGIAN (see [LU14]).

For $S(z) = Az$ with A defined in (2.45) and $\tilde{\Phi} = \|\mathrm{d}_t^\nu z\|_2^2$ in (2.111), the HAMILTONIAN defined in (2.134) reads as follows:

$$\mathcal{H} = \ell_0 \|A^\nu z\|_2^2 + \lambda^\top Az. \tag{2.143}$$

As mentioned before, either $\ell_0 = 0$ or w.l.o.g. $\ell_0 = 1$, whereby the former case often can be excluded by using a contradiction argument. If $\ell_0 = 0$ is assumed in (2.143), the Adjoint Equation (2.142b) results in

$$\mathrm{d}_t \lambda_1 = -\partial_{z_1} \mathcal{H} = \left(1 + \frac{\gamma}{2}\right)\lambda_1 - \frac{\gamma}{2}\lambda_2 \tag{2.144a}$$

$$\mathrm{d}_t \lambda_2 = -\partial_{z_2} \mathcal{H} = -\frac{\gamma}{2}\lambda_1 + \left(1 + \frac{\gamma}{2}\right)\lambda_2 \tag{2.144b}$$

with analytical solution

$$\lambda_1(t) = c_3 \mathrm{e}^t + c_4 \mathrm{e}^{(1+\gamma)t} \tag{2.145a}$$

$$\lambda_2(t) = c_3 \mathrm{e}^t - c_4 \mathrm{e}^{(1+\gamma)t}. \tag{2.145b}$$

Based on the Transversality Conditions (2.142d)–(2.142f) it follows that $c_3 = c_4 = 0$ and thus, $\lambda_1 = \lambda_2 = 0$ being a contradiction to $(\ell_0, \lambda_1, \lambda_2) \neq 0$. Consequently, it is approved to set $\ell_0 = 1$ in the HAMILTONIAN (2.143) yielding

$$\begin{aligned}
\mathcal{H} = \|A^\nu z\|_2^2 + \lambda^\top Az = {}& z_1^2\left(2p_\nu^2 + 1 - 2p_\nu(-1)^\nu\right) \\
& + z_2^2\left(2p_\nu^2 + 1 - 2p_\nu(-1)^\nu\right) \\
& + z_1 z_2\left(4p_\nu\left(-p_\nu + (-1)^\nu\right)\right) \\
& + z_1\left(-\lambda_1 - \frac{\gamma}{2}\lambda_1 + \frac{\gamma}{2}\lambda_2\right) \\
& + z_2\left(\frac{\gamma}{2}\lambda_1 - \lambda_2 - \frac{\gamma}{2}\lambda_2\right)
\end{aligned} \tag{2.146}$$

2. Spatially Homogeneous Systems: Slow Invariant Manifold Computation

with

$$A^\nu = \begin{pmatrix} p_\nu & -p_\nu + (-1)^\nu \\ -p_\nu + (-1)^\nu & p_\nu \end{pmatrix} \tag{2.147}$$

and p_ν being a polynomial of the form

$$p_\nu(\gamma) := (-1)^\nu \left(1 + \frac{\nu}{2}\gamma + \cdots + \frac{\nu}{2}\gamma^{\nu-1} + \frac{1}{2}\gamma^\nu\right). \tag{2.148}$$

The Adjoint Equation (2.142b) can now be formulated as

$$d_t\lambda_1 = -\partial_{z_1}\mathcal{H}$$
$$= (1 + \frac{\gamma}{2})\lambda_1 - \frac{\gamma}{2}\lambda_2 - 2z_1\left(2p_\nu^2 + 1 - 2p_\nu(-1)^\nu\right) - z_2\left(4p_\nu\left(-p_\nu + (-1)^\nu\right)\right) \tag{2.149a}$$

$$d_t\lambda_2 = -\partial_{z_2}\mathcal{H}$$
$$= -\frac{\gamma}{2}\lambda_1 + (1 + \frac{\gamma}{2})\lambda_2 - 2z_2\left(2p_\nu^2 + 1 - 2p_\nu(-1)^\nu\right) - z_1\left(4p_\nu\left(-p_\nu + (-1)^\nu\right)\right) \tag{2.149b}$$

with analytical solution

$$\lambda_1(t) = c_3 e^t + c_4 e^{(1+\gamma)t} + c_1 e^{-t} + c_2 e^{(-1-\gamma)t}\left(\frac{(2p_\nu - (-1)^\nu)^2}{1 + \gamma}\right) \tag{2.150a}$$

$$\lambda_2(t) = c_3 e^t - c_4 e^{(1+\gamma)t} + c_1 e^{-t} - c_2 e^{(-1-\gamma)t}\left(\frac{(2p_\nu - (-1)^\nu)^2}{1 + \gamma}\right). \tag{2.150b}$$

Together with (2.15) the HAMILTONIAN can be computed as

$$\mathcal{H} = -2c_1 c_3 - 2c_2 c_4(1 + \gamma) \tag{2.151}$$

disclosing a remarkably simple structure. Finally, the BVP (2.142) can be solved analytically leading to

$$c_1 = \frac{z_2^{t_f}\xi\left(e^{t_f}e^{(-1-\gamma)2t_0} - e^{(-1-2\gamma)t_f}\right)}{\xi e^{(-1-\gamma)2t_0} - e^{(-1-\gamma)2t_f}(\xi + 1) + e^{-2\gamma t_f}e^{-2t_0}} \tag{2.152a}$$

$$c_2 = \frac{z_2^{t_f}\left(e^{(-1-\gamma)t_f} - e^{(1-\gamma)t_f}e^{-2t_0}\right)}{\xi e^{(-1-\gamma)2t_0} - e^{(-1-\gamma)2t_f}(\xi + 1) + e^{-2\gamma t_f}e^{-2t_0}} \tag{2.152b}$$

$$c_3 = \frac{z_2^{t_f}\xi\left(e^{t_f}e^{(-4-\gamma)t_0} + e^{(-1-\gamma)t_f}e^{-2t_0} - e^{(1+\gamma)t_f}e^{(-2-\gamma)2t_0} - e^{(-1-2\gamma)t_f}e^{(-2+\gamma)t_0}\right)}{\left(\xi e^{(-1-\gamma)2t_0} - (\xi + 1)e^{(-1-\gamma)2t_f} + e^{-2\gamma t_f}e^{-2t_0}\right)\left(e^{\gamma t_f} - e^{\gamma t_0}\right)} \tag{2.152c}$$

$$c_4 = \frac{z_2^{t_f}\xi\left(e^{t_f}e^{(-2-\gamma)2t_0} - e^{-t_f}e^{(-1-\gamma)2t_0} + e^{(-1-\gamma)t_f}e^{(-2-\gamma)t_0} - e^{(1-\gamma)t_f}e^{(-4-\gamma)t_0}\right)}{\left(\xi e^{(-1-\gamma)2t_0} - e^{(-1-\gamma)2t_f}(\xi + 1) + e^{-2\gamma t_f}e^{-2t_0}\right)\left(e^{\gamma t_f} - e^{\gamma t_0}\right)} \tag{2.152d}$$

with $\xi := \frac{(2p_\nu - (-1)^\nu)^2}{1+\gamma}$ and $\mathcal{I}_{\text{fixed}} = \{2\}$. The missing value of the POI$^{\text{app}}$ $z_1(t_{\text{f}})$ can now be computed as

$$z_1(t_{\text{f}}) = z_2^{t_{\text{f}}} \left(1 + \underbrace{\left(\frac{2\mathrm{e}^{(-1-\gamma)2t_{\text{f}}} - 2\mathrm{e}^{-2\gamma t_{\text{f}}}\mathrm{e}^{-2t_0}}{\mathrm{e}^{-2\gamma t_{\text{f}}}\mathrm{e}^{-2t_0} + \xi\mathrm{e}^{(-1-\gamma)2t_0} - (\xi+1)\,\mathrm{e}^{(-1-\gamma)2t_{\text{f}}}} \right)}_{= \frac{\delta_{\text{err}}}{z_2^{t_{\text{f}}}}} \right) \tag{2.153}$$

with an error of accuracy δ_{err} being equivalent to that one where the POI$^{\text{app}}$ is computed by directly solving the Optimization Problem (2.110) analytically with $\mathcal{I}_{\text{fixed}} = \{2\}$ and $\tilde{\Phi} = \|\mathrm{d}_t^\nu z\|_2^2$. Consequently, it holds

$$\lim_{\gamma \to \infty} z_1(t_{\text{f}}) = z_2^{t_{\text{f}}} \tag{2.154a}$$

$$\lim_{\nu \to \infty} z_1(t_{\text{f}}) = z_2^{t_{\text{f}}} \tag{2.154b}$$

$$\lim_{t_0 \to -\infty} z_1(t_{\text{f}}) = z_2^{t_{\text{f}}}. \tag{2.154c}$$

The optimal boundary control viewpoint could be exploited for efficient numerical implementation of trajectory–based SIM computation since the dual variable λ can be used to compute the gradient of the objective function with respect to the system state and thus yields derivative information by a single numerical integration of the adjoint equation (see [CLP$^+$03], Chapter 2.1). In particular, the HAMILTONIAN formulation has the potential to establish relations to powerful concepts from dynamical systems theory that might yield more profound insight into the model reduction concept in terms of SIM characterization and identification.

2.9 Further Ideas Concerning the Search for an Exact SIM Identification

In addition to the above-mentioned results concerning SIM computation for model reduction, several other ideas have been arisen, analyzed, and tested within the scope of this work. Some of them led nowhere, some others are presently the subject of intense ongoing research. Nevertheless, one important one—in the author's opinion—is presented here, which is based on idea of LEBIEDZ and subsequent ideas of the author.

2.9.1 Hamilton's Principle

Based on empirical work of LEBIEDZ and REINHARDT [Rei08] and their results concerning the use of an additive term in the objective function of formulation (2.39) and due to the non-

physical fact that $\lim_{t_0 \to \infty} |\mathcal{H}| = \infty$ for the 'energy–like' HAMILTONIAN $\mathcal{H}$ (2.151) with c_1–c_4 substituted from (2.152), a possible lack of some additional term in (2.39a) is conjectured in order to achieve an exact identification of SIMs via a finite–time–horizon, finite–derivative–order variational approach without using limiting arguments. This proposition is motivated by analogy reasoning with respect to HAMILTON's principle—the principle of stationary action—in classical mechanics and its conceptual generalization to dissipative systems where the 'generalized forces' cannot be derived from a potential, see e.g. [San78, San83].

Hamilton's Principle: A variational principle which states that the path of a conservative system in configuration space between two configurations is such that the integral of the **LAGRANGIAN** function over time is a minimizer (or maximizer) relative to nearby paths between the same end points and taking the same time.

The full system information is collected in the functional of the variational problem and encoded in a single function, the LAGRANGIAN $\mathcal{L}(z(t), \mathrm{d}_t z(t), t)$. In classical mechanics, this LAGRANGIAN function is characterized by the difference of kinetic and potential energy $T(\mathrm{d}_z(t), t) - V(z(t), t)$, which in our case suggests to consider the following formulation of the objective function (2.28)

$$\Phi(z) = \int_{t_0}^{t_\mathrm{f}} k_1 \|\mathrm{d}_t z(t)\|_2^2 - k_2 \|z(t)\|_2^2 \, \mathrm{d}t \tag{2.155}$$

with constants $k_1, k_2 \in \mathbb{R}$ determining the 'quality' of SIM approximation. The first integrand term corresponds to some 'generalized kinetic energy' (proportional to squared velocity) and the second to some 'generalized potential energy' (proportional to the squared state $z(t)$).

As mentioned before, exact SIM identification requires $c_2 = 0$ (or rather $\tilde{c}_2 = 0$) in (2.48)/(2.53) for the two test models analyzed in Section 2.3 which can be achieved by $k_2 = 1$ in the linear and $k_2 = \frac{\tilde{\gamma}}{z_1(t)+1}$ in the DAVIS–SKODJE test model for fixed $k_1 = 1$ in (2.155). Moreover, for the three-dimensional linear model given by (2.66), (2.67), (2.68), (2.69) a two-dimensional SIM can be computed exactly by using (2.155) with $k_1 = k_2 = 1$ as well. Here, the SIM which is spanned by the two eigenvectors corresponding to the slow eigenvalues of system (2.66) is represented by $z_2(t) = h(z_1(t), z_3(t)) = \frac{z_1(t)+z_3(t)}{\sqrt{2}}$. Last but not least, the subsequent linear model

$$\mathrm{d}_t z_1 = -z_1 \tag{2.156a}$$

$$\mathrm{d}_t z_2 = 10 z_1 + (-1 - \tilde{\gamma}) z_2 \tag{2.156b}$$

where slow and fast subspace are not perpendicular to each other yields $k_1 = 1$ and $k_2 = 1 + \check{\gamma}$ in (2.155) for an exact SIM identification

$$z_2 = h(z_1) = 10\frac{z_1}{\check{\gamma}} \tag{2.157}$$

using a finite time horizon. This can be simply verified by means of the corresponding analytic solution

$$z_1(t) = \check{c}_1 e^{-t} \tag{2.158a}$$

$$z_2(t) = 10\frac{\check{c}_1}{\check{\gamma}} + \check{c}_2 e^{(-1-\gamma)t}. \tag{2.158b}$$

To find a general characterization of k_1 and k_2 or a suitable general form of the Lagrangian (the inverse problem in the calculus of variations, see e.g. [MFV$^+$90, San78]) leading to an exact SIM identification in a variational approach without using limiting arguments would be an important issue for model reduction in chemical kinetics. We believe that a Hamiltonian variational formulation might turn out to be a promising approach towards this goal.

3 Spatially Inhomogeneous Systems: Inertial Manifold Computation

As mentioned before in the introduction, chemically reacting flows in form of combustion processes comprise an interplay between convective and diffusive species transport and chemical reaction processes. The reduction of the latter, which can be seperately modeled by a system of ODEs (1.15), is discussed in detail in the previous chapter, where the appearing time scale separation is exploited by approximation of the long time scale system dynamics via elimination of the fast relaxing modes by enslaving them to the slow ones. The outcome of this—in the ideal case a SIM—is supposed to be used as reduced reaction model within the full model equation to ensure the simulation of a combustion process which is often nearly impossible in reasonable time using the unreduced (reaction) model. Remembering the diagram from the introduction, once again illustrated in Figure 3.1, we have not yet gone beyond 1b within this thesis. For
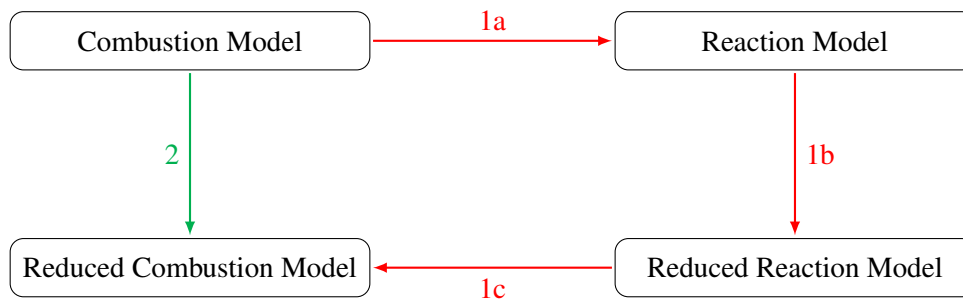
Figure 3.1: Schematic illustration of two possibilities for model reduction applied to a combustion model.

that reason, this chapter investigates the coupling between reaction and transport processes on the one hand (1c) and initial thoughts concerning the direct reduction of the combustion model, i.e. without regarding the reaction model solely (2). Accordingly, Section 3.1 deals with the modeling of reaction–comvection–diffusion processes yielding a system of PDEs, where the associated theory is analyzed in the subsequent section. This is followed by general considerations concerning reaction–convection–diffusion systems treated in Sections 3.3–3.5, before presenting solution suggestions concerning 1c (Section 3.6) and 2 (Section 3.7). Section 3.8 considers—in contrast to the previous sections where DIRICHLET boundary conditions are considered—the
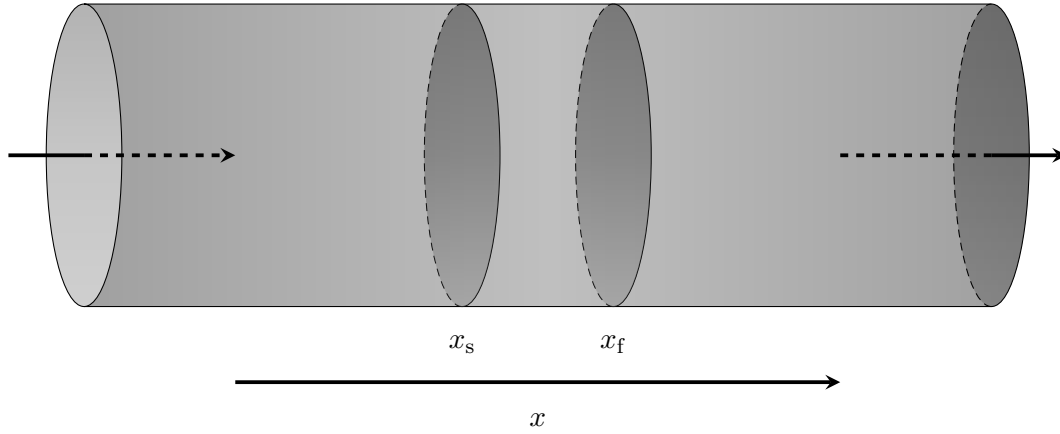
Figure 3.2: Gas flow through a pipe.

solution behavior of reaction–diffusion processes with NEUMANN boundary conditions.

3.1 Modeling of Reaction–Convection–Diffusion Processes

This section analyzes the mathematical modeling of physical transport processes in form of diffusive and convective mass transfer, or, formulated differently, where the mathematical equations in form of systems of PDEs come from. We restrict to the spatial one-dimensional case in order to simplify the presentation.

3.1.1 Modeling of Convection Processes

In order to deduce a mathematical model for (one-dimensional) convection processes, a gas flow through a pipe with small (relative to the length of the pipe) and constant cross section is considered, such that density and velocity of the gas can be assumed to be constant. In this context, $x \in \mathbb{R}$ indicates the position along the pipe and $\varrho \colon \mathbb{R} \times \mathbb{R} \to \mathbb{R}$, $(t, x) \mapsto \varrho(t, x)$ the density of the gas at time $t \in \mathbb{R}$ and position x. The latter is defined in a way, that the total mass of the gas in any particular pipe section between $x_s \in \mathbb{R}$ and $x_f \in \mathbb{R}$ can be represented by the integral of the density:

$$\text{Total mass in } [x_s, x_f] \text{ at time } t = \int_{x_s}^{x_f} \varrho(t, x) \, \mathrm{d}x. \tag{3.1}$$

A visualization of the described gas flow through a pipe is presented in Figure 3.2. Provided that the pipe wall is impermeable to gas, the total mass in pipe section $[x_s, x_f]$ can only be changed by inflow and outflow of the mass through the cross sections x_s and x_f[14]. The velocity of the

---

[14]In contrast to Section (1.2), the subscripts s and f are abbreviations for 'start' and 'final' (not to be confused with 'slow' and 'fast').

gas at time t in cross section x is described by $v \colon \mathbb{R} \times \mathbb{R} \to \mathbb{R}$, $(t, x) \mapsto v(t, x)$, wherewith the mass flow of the gas through this cross section is given by

$$\text{mass flow in } (t, x) = \varrho(t, x) v(t, x). \tag{3.2}$$

Thus, the change of the total mass in $[x_\mathrm{s}, x_\mathrm{f}]$ results in the difference of the mass flows through x_s and x_f:

$$\mathrm{d}_t \int_{x_\mathrm{s}}^{x_\mathrm{f}} \varrho(t, x) \, \mathrm{d}x = \varrho(t, x_\mathrm{s}) v(t, x_\mathrm{s}) - \varrho(t, x_\mathrm{f}) v(t, x_\mathrm{f}). \tag{3.3}$$

Integration of (3.3) over $[t_\mathrm{s}, t_\mathrm{f}]$, $t_\mathrm{f} > t_\mathrm{s}$, yields the mass conservation equation in **integral form**:

$$\int_{x_\mathrm{s}}^{x_\mathrm{f}} \varrho(t_\mathrm{f}, x) \, \mathrm{d}x = \int_{x_\mathrm{s}}^{x_\mathrm{f}} \varrho(t_\mathrm{s}, x) \, \mathrm{d}x + \int_{t_\mathrm{s}}^{t_\mathrm{f}} \varrho(t, x_\mathrm{s}) v(t, x_\mathrm{s}) \, \mathrm{d}t - \int_{t_\mathrm{s}}^{t_\mathrm{f}} \varrho(t, x_\mathrm{f}) v(t, x_\mathrm{f}) \, \mathrm{d}t. \tag{3.4}$$

Assumed that both $\varrho(t, x)$ and $v(t, x)$ are continuously differentiable with respect to x and t, Equation (3.4) can be transformed into

$$\int_{t_\mathrm{s}}^{t_\mathrm{f}} \int_{x_\mathrm{s}}^{x_\mathrm{f}} \left(\partial_t \varrho(t, x) + \partial_x \left(\varrho(t, x) v(t, x) \right) \right) \, \mathrm{d}x \, \mathrm{d}t = 0. \tag{3.5}$$

This equation holds for any pipe section $[x_\mathrm{s}, x_\mathrm{f}]$ and time interval $[t_\mathrm{s}, t_\mathrm{f}]$, the consequence being that the integrand of (3.5) must be equal to zero at any (t, x):

$$\partial_t \varrho(t, x) + \partial_x \left(\varrho(t, x) v(t, x) \right) = 0. \tag{3.6}$$

This so-called (one-dimensional) **continuity equation** is the **differential form** of the mass conservation equation. A solution to (3.6) requires the knowledge of v or $v = v\left(\varrho(t, x)\right)$. If $v(t, x) = \bar{v} = $ constant (in the course of this work w.l.o.g. $\bar{v} > 0$ is assumed), the one-dimensional linear **convection equation** model is:

$$\partial_t \varrho + \bar{v} \partial_x \varrho = 0. \tag{3.7}$$

This equation describes the passive convection of some scalar field $\varrho(t, x)$ carried along by a flow of constant speed $\bar{v}$.

3.1.2 Modeling of Diffusion Processes

The same pipe as above is considered, but this time filled with a resting liquid. Inside this liquid there is a dye diffusing from areas of large concentration to areas of lower one (cf. Figure 3.3). The diffusion proceeds along x which is why a one-dimensional process is assumed. Then, the
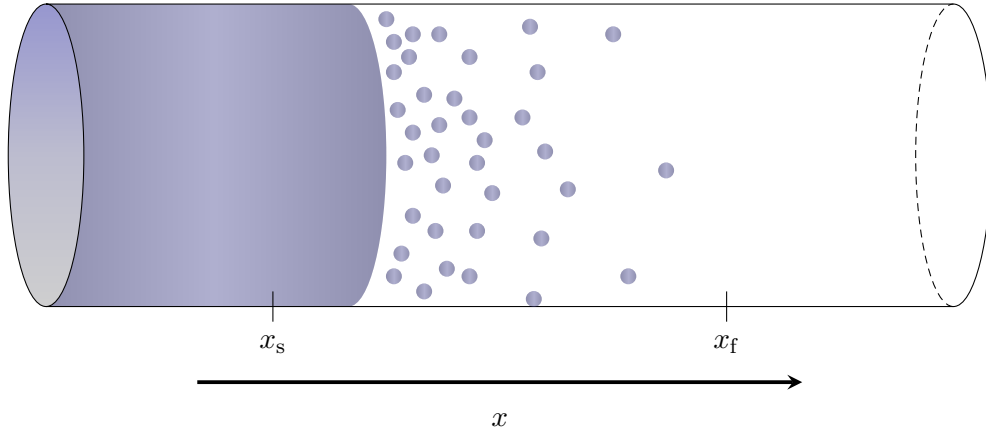
Figure 3.3: Diffusion in a pipe.

concentration of the dye at time $t \in \mathbb{R}$ and position $x \in \mathbb{R}$ is denoted by z with $z\colon \mathbb{R} \times \mathbb{R} \to \mathbb{R},\ (t, x) \mapsto z(t, x)$, so that the total mass of the dye in an interval $[x_\mathrm{s}, x_\mathrm{f}]$ results in

$$\text{total mass (of the dye) in } [x_\mathrm{s}, x_\mathrm{f}] \text{ at time } t = \int_{x_\mathrm{s}}^{x_\mathrm{f}} z(t, x)\, \mathrm{d}x. \tag{3.8}$$

The transfer of the mass per time unit is defined by the diffusion flux $q\colon \mathbb{R} \times \mathbb{R} \to \mathbb{R},\ (t, x) \mapsto q(t, x)$ yielding

$$\int_{x_\mathrm{s}}^{x_\mathrm{f}} \partial_t z(t, x)\, \mathrm{d}x = q(t, x_\mathrm{s}) - q(t, x_\mathrm{f}). \tag{3.9}$$

Furthermore, **FICK's first law of diffusion** states the existence of a (constant) **diffusion coefficient** $\mathcal{D}$ such that

$$q(t, x) = -\mathcal{D}\partial_x z(t, x). \tag{3.10}$$

Substituting into (3.9) results in

$$\int_{x_\mathrm{s}}^{x_\mathrm{f}} \partial_t z(t, x)\, \mathrm{d}x = \mathcal{D}\partial_x z(t, x_\mathrm{f}) - \mathcal{D}\partial_x z(t, x_\mathrm{s}) = \mathcal{D} \int_{x_\mathrm{s}}^{x_\mathrm{f}} \partial_{xx}^2 z(t, x)\, \mathrm{d}x \tag{3.11}$$

which in turn yields

$$\partial_t z(t, x) = \mathcal{D}\partial_{xx}^2 z(t, x) \tag{3.12}$$

since x_s and x_f are chosen arbitrarily. This equation is referred to as (one-dimensional) **heat equation** or **FICK's second law of diffusion**, describing the distribution of heat (or variation in temperature) in a given region over time.

3.1.3 Reaction / Convection / Diffusion

With this knowledge, it is possible to formulate mathematical models as part of this work so far which explain how the concentration of one or more substances distributed in space changes under the influence of three different processes: local chemical reactions in which the species are transformed into each other, convection which causes the transport of the chemical species by the bulk movement of the solvent, and diffusion within the solvent which causes the substances to spread out throughout the entire space.

$$
\begin{array}{llll}
\text{Reaction Processes:} & \partial_t z(t,x) & = & S\left((z(t,x)\right) & \text{(spatially homogeneous)} \\
\text{Convection Processes:} & \partial_t z(t,x) & = & -\bar{v}\partial_x z(t,x) & \text{(constant velocity } \bar{v}) \\
\text{Diffusion Processes:} & \partial_t z(t,x) & = & \mathcal{D}\partial_{xx}^2 z(t,x) & \text{(constant diffusion coefficient } \mathcal{D})
\end{array}
$$

with $z \in \mathbb{R}^m$, $\bar{v} = \mathrm{diag}(\hat{\bar{v}}, \dots, \hat{\bar{v}}) \in \mathbb{R}^{m \times m}$, $\hat{\bar{v}} \in \mathbb{R}$, and $\mathcal{D} = \mathrm{diag}(\mathcal{D}_1, \dots, \mathcal{D}_m)$, $\mathcal{D}_j > 0$, $j = 1, \dots, m$. However, these processes do not occur only seperately, but also in combination with others, i.e. a chemical species undergoes not only either a reaction, a convection, or a diffusion process, but also can experience two or even three simultaneously. Particularly, the following combinations are of special interest with regard to this work:

$$
\begin{array}{lllll}
\text{Reac.–Conv.:} & \partial_t z(t,x) & = & -\bar{v}\partial_x z(t,x) & & + S\left(z(t,x)\right) \\
\text{Reac.–Diff.:} & \partial_t z(t,x) & = & & +\mathcal{D}\partial_{xx}^2 z(t,x) & + S(z(t,x)) \\
\text{Reac.–Conv.–Diff.:} & \partial_t z(t,x) & = & \underbrace{-\bar{v}\partial_x z(t,x)}_{\text{Convection}} & \underbrace{+\mathcal{D}\partial_{xx}^2 z(t,x)}_{\text{Diffusion}} & \underbrace{+S\left(z(t,x)\right)}_{\text{Reaction}}
\end{array}
$$

These equations are differential equations, but this time the unknown function z does not depend on a single independent variable and its derivatives being the consequence that no system of ODEs is involved, but a system of PDEs, which is why the following section deals with the theory of systems of PDEs.

3.2 Theory of Systems of Partial Differential Equations

Systems of **Partial Differential Equations (PDEs)** are often used to construct models of the most basic theories underlying a wide variety of phenomena from physics and engineering such as sound, heat, electrostatics, electrodynamics, fluid flow, elasticity, or quantum mechanics, to name just a few. For example, the system of PDEs known as MAXWELL's equations can be written on the back of a post card, yet from these equations one can derive the entire theory of electricity and magnetism, including light. Our goal here is to state the most basic definitions from the theory of systems of PDEs which is necessary to understand the subsequent sections of this work.

3. Spatially Inhomogeneous Systems: Inertial Manifold Computation

As stated previously in Section 1.1, a PDE is a differential equation that contains unknown multivariable functions and their partial derivatives (in contrast to ODEs where the unknown function depends on a single independent variable and its derivatives). Thus, an ODE can be considered as a special case of a PDE but, as will be seen, the behavior of solutions is quite different in general. Accordingly, a system of PDEs of order n ($n \geq 1$) for the unknown function $z \colon I \to \mathbb{R}^m$, $\mathbf{x} := (t, x_1, \ldots, x_d)^\top \mapsto z(\mathbf{x})$ with I being an open subset of $\mathbb{R}^{d+1}$ and $d \geq 1$ is an equation of the form

$$F\left(\mathrm{D}^n z(\mathbf{x}), \mathrm{D}^{n-1} z(\mathbf{x}), \ldots, \mathrm{D}^2 z(\mathbf{x}), \mathrm{D}^1 z(\mathbf{x}), z(\mathbf{x}), \mathbf{x}\right) = 0 \tag{3.13}$$

with given $F \colon \Omega \subset \left(\mathbb{R}^{m(d+1)^n} \times \mathbb{R}^{m(d+1)^{n-1}} \times \cdots \times \mathbb{R}^{m(d+1)} \times \mathbb{R}^m \times I\right) \to \mathbb{R}^m$.

Notation 3.2.1. Let $\alpha \in (\mathbb{N}_0)^{d+1}$ and $|\alpha|$ being the sum of its elements $|\alpha| := \sum_{j=1}^{d+1} \alpha_j$. The expression $\mathrm{D}^\alpha z(\mathbf{x})$ refers to the partial derivative

$$\mathrm{D}^\alpha z(\mathbf{x}) := \frac{\partial^{|\alpha|}}{\partial t^{\alpha_1} \partial x_1^{\alpha_2} \cdots \partial x_d^{\alpha_{d+1}}} z(\mathbf{x}) \tag{3.14}$$

for $|\alpha| > 0$ (and $\mathrm{D}^\alpha z(\mathbf{x}) := z(\mathbf{x})$ for $|\alpha| = 0$). Here, the vector α is referred to as **multi-index**. Using this notation,

$$\mathrm{D}^n z(\mathbf{x}) = \{\mathrm{D}^\alpha z(\mathbf{x}) \mid |\alpha| = n\}, \quad n \in \mathbb{N}. \tag{3.15}$$

Equation (3.13) is labeled **linear** if it has the following form

$$\sum_{|\alpha| \leq n} a_\alpha(\mathbf{x}) \mathrm{D}^\alpha z(\mathbf{x}) = r(\mathbf{x}) \tag{3.16}$$

with $a_\alpha(\mathbf{x})$ and $r(\mathbf{x})$ being continuous functions in $\mathbf{x}$, otherwise **nonlinear** (with the exception of **quasilinear** and **semilinear** equations being irrelevant within the scope of this work). If additionally it holds that $r = 0$, the linear system of PDEs of order n (3.16) is referred to as **homogeneous**. Furthermore, a function $u \colon I \to \mathbb{R}^m$ is called **solution** of (3.13) if

- $u \in \mathcal{C}^n(I)$ and

- $F\left(\mathrm{D}^n u(\mathbf{x}), \mathrm{D}^{n-1} u(\mathbf{x}), \ldots, \mathrm{D}^2 u(\mathbf{x}), \mathrm{D}^1 u(\mathbf{x}), u(\mathbf{x}), \mathbf{x}\right) = 0.$

Although the issue of existence and uniqueness of solutions of systems of ODEs has a very satisfactory answer with the PICARD–LINDELÖF theorem (1.1.11), that is not the case for systems of PDEs. Equations (3.7) and (3.12) serve as example of a linear homogeneous system of PDEs of order $n = 1$ and $n = 2$, respectively. In the following course of this dissertation we restrict to $d = 1$ and thus, $\mathbf{x} = (t, x)^\top$.

3.2.1 Systems of Partial Differential Equations of Order One

For systems of PDEs of order one, the function F reduces to

$$F\left(\mathbf{x}, z(\mathbf{x}), \mathrm{D}^1 z(\mathbf{x})\right) = 0 \tag{3.17}$$

with $\mathbf{x} = (t, x)^\top$. A corresponding linear system has the form

$$F = \partial_t z(t, x) + a_1(t, x)\partial_x z(t, x) + a_2(t, x)z(t, x) - r(t, x) = 0 \tag{3.18}$$

with $a_1, a_2 \in \mathbb{R}^{d+1} \times \mathbb{R}^{m \times m}$. If the eigenvalues $\lambda_1, \ldots, \lambda_m$ of $a_1 = a_1(t, x)$ are real and there exists a decomposition of the form $a_1 = C^{-1}DC$ with $D = \mathrm{diag}(\lambda_1, \ldots, \lambda_m)$, then a_1 is referred to as **real–diagonalizable**. Herewith, Equation (3.18) is referred to as

> **elliptic**   if there is no real eigenvalue of $a_1(t_0, x_0)$
>
> **hyperbolic**   if $a_1(t_0, x_0)$ is real–diagonalizable

where $(t_0, x_0) \in I$ is fixed. Therefore, if a_1 is symmetric or has m different real eigenvalues, the system is hyperbolic, since these conditions are sufficient for real–diagonalizable.

Example 3.2.2. The subsequent system of PDEs of order $n = 1$ with $z = (z_1, z_2)^\top \in \mathbb{R}^2$

$$\partial_t z_1 - \partial_x z_2 = 0 \tag{3.19a}$$

$$\partial_t z_2 - \partial_x z_1 = 0 \tag{3.19b}$$

has the form (3.18) with

$$a_1 = \begin{pmatrix} 0 & -1 \\ -1 & 0 \end{pmatrix}. \tag{3.20}$$

It is hyperbolic, since

$$a_1 = \underbrace{\begin{pmatrix} 1 & 1 \\ -1 & 1 \end{pmatrix}^{-1}}_{C^{-1}} \underbrace{\begin{pmatrix} -1 & 0 \\ 0 & 1 \end{pmatrix}}_{D} \underbrace{\begin{pmatrix} 1 & 1 \\ -1 & 1 \end{pmatrix}}_{C}. \tag{3.21}$$

In contrast, the system

$$\partial_t z_1 - \partial_x z_2 = 0 \tag{3.22a}$$

$$\partial_t z_2 + \partial_x z_1 = 0 \tag{3.22b}$$

is elliptic, since it has the form (3.18) with

$$a_1 = \begin{pmatrix} 0 & -1 \\ 1 & 0 \end{pmatrix} \tag{3.23}$$

and corresponding eigenvalues $\lambda_{1,2} = \pm i$.

3.2.2 Systems of Partial Differential Equations of Order Two

For systems of PDEs of order two, the function F given by (3.13) reduces to

$$F\left(\mathbf{x}, z(\mathbf{x}), \mathrm{D}^1 z(\mathbf{x}), \mathrm{D}^2 z(\mathbf{x})\right) = 0 \tag{3.24}$$

with $\mathbf{x} = (t, x)^\top$. Furthermore, this work considers functions F of the following form

$$F = a_{11}(t, x)\partial_{tt}^2 z + 2a_{12}(t, x)\partial_{tx}^2 z + a_{22}(t, x)\partial_{xx}^2 z + \text{(lower order terms)} = 0 \tag{3.25}$$

with given functions $a_{11}, a_{12}, a_{22} \in \mathbb{R}^{d+1} \times \mathbb{R}^{m \times m}$. The problem now is to find a function $z \in \mathcal{C}^2(I)$ that solves Equation (3.25) in I. Equation (3.25) provides a further classification. Therefore, let $m = 1$, $(t_0, x_0) \in I$ be fixed, and λ_1, λ_2 the (real) eigenvalues of the symmetric matrix

$$A = \begin{pmatrix} a_{11}(t_0, x_0) & a_{12}(t_0, x_0) \\ a_{12}(t_0, x_0) & a_{22}(t_0, x_0) \end{pmatrix}. \tag{3.26}$$

Then, (3.25) in (t_0, x_0) is referred to as

elliptic	if either $\lambda_1, \lambda_2 > 0$ or $\lambda_1, \lambda_2 < 0$
hyperbolic	if either $\lambda_1 > 0$ and $\lambda_2 < 0$ or $\lambda_1 < 0$ and $\lambda_2 > 0$
parabolic	if $\lambda_1 = 0$ or $\lambda_2 = 0$.

Note that this classification depends on (t_0, x_0), meaning that a system of PDEs (3.25) can change its type within I. Accordingly, a system of PDEs with $m > 1$ is called elliptic/hyperbolic/parabolic, if each component of the system is elliptic/hyperbolic/parabolic. Generally, parabolic systems of PDEs contain a 'time variable', where the state evolution with respect to time is described by a derivation of order one, which is why they are also labeled **evolution problems**.

Example 3.2.3 (POISSON's Equation). POISSON's equation is used, for instance, to describe the potential energy field caused by a given charge or mass density distribution and reads

$$-\partial_{tt}^2 z(\mathbf{x}) - \partial_{xx}^2 z(\mathbf{x}) = r(\mathbf{x}) \tag{3.27}$$

with $z \in \mathbb{R}^{d+1} \times \mathbb{R}$. Usually, r is given and z is sought. Since $A = \begin{pmatrix} -1 & 0 \\ 0 & -1 \end{pmatrix}$ and thus, $\lambda_1, \lambda_2 = -1 < 0$, POISSON's equation is elliptic.

Example 3.2.4 (Linear Wave Equation). The linear wave equation for $z \in \mathbb{R}^{d+1} \times \mathbb{R}$

$$\partial_{tt}^2 z(\mathbf{x}) - \partial_{xx}^2 z(\mathbf{x}) = r(\mathbf{x}) \tag{3.28}$$

is hyperbolic, since $A = \begin{pmatrix} 1 & 0 \\ 0 & -1 \end{pmatrix}$ and thus, $\lambda_1 = 1 > 0$ and $\lambda_2 = -1 < 0$. As the name suggests, it is a model for the description of waves—as they occur in physics—such as sound waves, light waves, and water waves.

Example 3.2.5 (Linear Heat Equation). A prominent example of a parabolic system of PDEs is the linear heat equation for again $z \in \mathbb{R}^{d+1} \times \mathbb{R}$:

$$\partial_t z(\mathbf{x}) - \partial_{xx}^2 z(\mathbf{x}) = r(\mathbf{x}). \tag{3.29}$$

Here, $A = \begin{pmatrix} 0 & 0 \\ 0 & -1 \end{pmatrix}$ and thus, $\lambda_1 = 0$ and $\lambda_2 = -1 < 0$. It describes, for instance, the distribution of heat (or variation in temperature) in a given region over time.

Since a solution of a system of PDEs in not unique in general, additional initial and/or boundary conditions are required in order to ensure uniqueness of a solution. In this context—in contrast to systems of ODEs—different kinds of systems of PDEs call for different kinds of initial and/or boundary conditions in order to guarantee a well-posed problem. For instance, the parabolic case requires initial as well as boundary conditions (this is termed as **initial–boundary value problem (IBVP)**), whereas initial conditions can be sufficient in the hyperbolic case. In the framework of this work, boundary conditions are distinguished between

DIRICHLET **Boundary Conditions:** The boundary gives a value to the state variable
of the problem.

NEUMANN **Boundary Conditions:** The boundary gives a value to the normal
derivative of the state variable of the problem.

Example 3.2.6. For given $0 < T < \infty$ and given initial data z^0 find $z = z(t, x)$ with $z \in \mathcal{C}^0([0, T] \times [0, 1])$ and $\partial_t z, \partial_{xx}^2 z \in \mathcal{C}^0((0, T] \times (0, 1))$, such that

$$\partial_t z(t, x) = \mathcal{D}\partial_{xx}^2 z(t, x) + S(z(t, x)) \qquad \text{in } (0, T) \times (0, 1) \tag{3.30a}$$
$$z(0, x) = z^0(x) \qquad \text{in } (0, 1) \tag{3.30b}$$
$$z(t, 0) = 0 \qquad \text{in } (0, T) \tag{3.30c}$$
$$z(t, 1) = 0 \qquad \text{in } (0, T). \tag{3.30d}$$

This is a well-posed IBVP for the parabolic reaction–diffusion equation (see 3.1.3) with DIRICHLET boundary conditions.

Especially for this parabolic reaction–diffusion equation, there is a statement about solution of uniqueness for IBVPs (further results concerning existence and uniqueness of solutions for reaction–diffusion equations are listed in [Kut11]):

Theorem 3.2.7. *Let $z^1 = z^1(t,x)$ and $z^2 = z^2(t,x)$ be solutions of the reaction–diffusion equation*

$$\partial_t z(t,x) = \mathcal{D}\partial_{xx}^2 z(t,x) + S\left(z(t,x)\right) \tag{3.31}$$

with $z^1, z^2 \in \mathcal{C}^0\left([0,T] \times [0,1]\right)$, $\partial_t z^1, \partial_t z^2, \partial_{xx}^2 z^1, \partial_{xx}^2 z^2 \in \mathcal{C}^0\left((0,T] \times (0,1)\right)$, and $z^1 = z^2$ on $\{0\} \times (0,1)$ as well as on $(0,T) \times \{0,1\}$. Then it follows that

$$z^1 = z^2 \quad in\ (0,1) \times (0,T). \tag{3.32}$$

Proof. See e.g. [Kut11]. $\qquad\qquad\qquad\qquad\qquad\qquad\qquad\qquad\qquad\square$

Example 3.2.8. For given initial data $z^0 \in \mathcal{C}^0(\mathbb{R})$ with $\sup_{\mathbb{R}}|z^0| < \infty$ find $z = z(t,x)$ with $z \in \mathcal{C}^0\left([0,\infty) \times \mathbb{R}\right)$ and $\partial_t z, \partial_x z \in \mathcal{C}^0\left((0,\infty) \times \mathbb{R}\right)$, such that

$$\partial_t z(t,x) = -\bar{v}\partial_x z(t,x) + S\left(z(t,x)\right) \qquad\qquad in\ (0,\infty) \times \mathbb{R} \tag{3.33a}$$
$$z(0,x) = z^0(x) \qquad\qquad\qquad\qquad\qquad\qquad in\ \mathbb{R}. \tag{3.33b}$$

This is an IVP for the reaction–convection equation (see 3.1.3).

3.3 First Approximation

As seen in the previous chapter of this work, a transient (spatially) homogeneous[15] combustion process—i.e. in the absence of transport processes such as convection and diffusion—can be described by a system of ODEs which can be reduced by computation of a specific manifold—the SIM. It is important to note that these SIMs are identified based solely on chemical reaction, i.e. on homogeneous reactive systems without accounting for the above mentioned transport processes. However, realistic reactive flows are inhomogeneous in general and involve convection and molecular diffusion. The interesting point here is to figure out a useful reduced description of inhomogeneous combustion processes via the use of SIMs which is greatly complicated by the transport processes present and the coupling between chemistry and those transport processes.

In the spatially homogeneous case, the kinetic model equations read

$$\partial_t z(t,x) = S\left(z(t,x)\right) \tag{3.34a}$$
$$z(t_0, x) = z^{t_0}(x) \tag{3.34b}$$

---

[15]In the further course of this work '(in-)homogeneous' means 'spatially (in-)homogeneous'.

(in the remainder of this work t_0 is set w.l.o.g. to $t_0 = 0$), whereas the corresponding reduced (reaction) model is formulated as

$$\partial_t z_j(t, x) = S_j\left(z(t, x)\right), \qquad\qquad j \in \mathcal{I}_{\text{fixed}} \tag{3.35a}$$

$$z_j(0, x) = z_j^0(x), \qquad\qquad j \in \mathcal{I}_{\text{fixed}} \tag{3.35b}$$

$$z_k(t, x) = h\left(z_j(t, x)\right), \qquad\qquad j \in \mathcal{I}_{\text{fixed}},\ k \notin \mathcal{I}_{\text{fixed}} \tag{3.35c}$$

with h being the species reconstruction function representing the SIM. The reduced description of a kinetic model equation (such as (3.35)) is referred to as **suitable** (with respect to the corresponding full model (such as (3.34))) if they coincide (i.e. having the same corresponding solutions) for $z^0(x) = \left(z_j^0(x), h\left(z_j^0(x)\right)\right)^\top$, $j \in \mathcal{I}_{\text{fixed}}$, i.e. for initial values located on the SIM. As already known from the previous chapter of this work, the reduced description (3.35) is suitable with respect to (3.34) in the pure reaction case, which is demonstrated by means of an example in the following.

For the DAVIS–SKODJE model (see 2.3)

$$\partial_t z_1(t, x) = -z_1(t, x) \tag{3.36a}$$

$$\partial_t z_2(t, x) = -\tilde{\gamma} z_2(t, x) + \frac{(\tilde{\gamma} - 1)z_1(t, x) + \tilde{\gamma} z_1(t, x)^2}{\left(1 + z_1(t, x)\right)^2} \tag{3.36b}$$

$$z_1(0, x) = z_1^0(x) \tag{3.36c}$$

$$z_2(0, x) = z_2^0(x) \tag{3.36d}$$

the corresponding suitable reduced model is given by

$$\partial_t z_1(t, x) = -z_1(t, x) \tag{3.37a}$$

$$z_1(0, x) = z_1^0(x) \tag{3.37b}$$

$$z_2(t, x) = h\left(z_1(t, x)\right) = \frac{z_1(t, x)}{z_1(t, x) + 1} \tag{3.37c}$$

where $\mathcal{I}_{\text{fixed}} = \{1\}$ is chosen, since both (3.36) as well as (3.37) yield

$$z_1(t, x) = z_1^0(x)\mathrm{e}^{-t} \tag{3.38a}$$

$$z_2(t, x) = \frac{z_1^0(x)}{z_1^0(x) + \mathrm{e}^t} \tag{3.38b}$$

for $z_2^0(x) = h\left(z_1^0(x)\right) = \frac{z_1^0(x)}{z_1^0(x)+1}$ as analytic solution. This is visualized in Figure 3.4 for $z_1^0(x) = 1.0$, where z_2 is plotted against z_1 and x. As can be seen, for each x the SIM $z_2 = \frac{z_1}{z_1+1}$ is apparent.
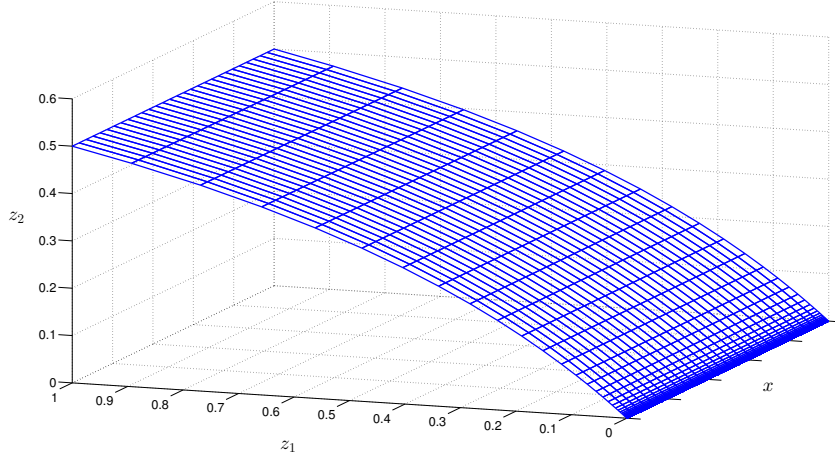
Figure 3.4: Coinciding solutions of both (3.36) and (3.37) for $z_1^0(x) = 1.0$.

The most straightforward approach in search of a suitable reduced description for inhomogeneous reactive flows involving convective and/or diffusive terms is the **first approximation (FA)**: as in the homogeneous case, the occuring non RPVs are replaced by the species reconstruction function h resulting from the SIM computation based solely on reactive terms. As a consequence, if the FA of an inhomogeneous model including diffusive and/or convective terms is suitable, there is no influence of the transport processes on the chemistry–based SIM. The following Table 3.1 depicts the different full model equations together with its appropriate FAs.

Table 3.1: List of different full model equations together with its appropriate FAs.

	Reaction	Reaction–Convection
Full	$\partial_t z = S(z)$	$\partial_t z = -\bar{v}\partial_x z + S(z)$
FA	$\partial_t z_j = S_j(z)$	$\partial_t z_j = -\hat{\bar{v}}\partial_x z_j + S_j(z)$
Suitable	✓	?

	Reaction–Diffusion	Reaction–Convection–Diffusion
Full	$\partial_t z = \mathcal{D}\partial_{xx}^2 z + S(z)$	$\partial_t z = -\bar{v}\partial_x z + \mathcal{D}\partial_{xx}^2 z + S(z)$
FA	$\partial_t z_j = \mathcal{D}_j\partial_{xx}^2 z_j + S_j(z)$	$\partial_t z_j = -\hat{\bar{v}}\partial_x z_j + \mathcal{D}_j\partial_{xx}^2 z_j + S_j(z)$
Suitable	?	?

for $j \in \mathcal{I}_{\text{fixed}}$ and $z_k = h(z_j)$, $k \notin \mathcal{I}_{\text{fixed}}$, $j \in \mathcal{I}_{\text{fixed}}$ in the FAs.

The subsequent sections are concerned with the question if the FAs stated in Table 3.1 are suitable with respect to the appropriate full model equations or not. For this purpose, the reaction–convection case is firstly regarded where it becomes apparent that there is no influence of the

convective term concerning the reduced reaction model, meaning that the FA of the reaction–convection equation is suitable. As a consequence, it shall be sufficient to focus on the reaction–diffusion case such that the reaction–convection–diffusion case can be neglected.

3.4 Coupling: Reduced Reaction and Convection

Initially, the influence of convective terms concerning the reduced reaction model is analyzed. Accordingly, diffusion effects are assumed to be nonexistent, such that the full kinetic model equation reads

$$\partial_t z(t,x) = \underbrace{-\bar{v}\partial_x z(t,x)}_{\text{Convection}} \underbrace{+S\left(z(t,x)\right)}_{\text{Reaction}} \tag{3.39}$$

with corresponding IVP given by Example 3.2.8. Here, $\bar{v}$ is allowed to be smoothly dependent on time t and space x, such that $\bar{v} = \bar{v}(t,x) = \mathrm{diag}\left(\hat{\bar{v}}(t,x), \ldots, \hat{\bar{v}}(t,x)\right) \in \mathbb{R}^{m \times m}$. The procedure to analyze the convective influence is as follows: if the solution of the full model (3.33) with initial values on the SIM equates with the solution of the respective FA (see Table 3.1), then there is no perturbation caused by convection—meaning that the FA is suitable. More precisely, we assume a partition of the state vector $z \in \mathbb{R}^m$ into RPVs and non RPVs (after a possible reordering/renaming of the components)

$$z(t,x) = \begin{pmatrix} z_{\text{rpv}}(t,x) \\ z_{\text{nrpv}}(t,x) \end{pmatrix} \tag{3.40}$$

with $z_{\text{rpv}} := (z_j)_{j \in \mathcal{I}_{\text{fixed}}} \in \mathbb{R}^{m_{\text{rpv}}}$ and $z_{\text{nrpv}} := (z_j)_{j \notin \mathcal{I}_{\text{fixed}}} \in \mathbb{R}^{m_{\text{nrpv}}}$. In 2.5, a discussion about how to choose $\mathcal{I}_{\text{fixed}}$ can be found. Thus, (3.39) can be formulated as

$$\partial_t z_{\text{rpv}}(t,x) = -\bar{v}_{\text{rpv}}(t,x)\partial_x z_{\text{rpv}}(t,x) + S_{\text{rpv}}\left(z_{\text{rpv}}(t,x), z_{\text{nrpv}}(t,x)\right) \tag{3.41a}$$

$$\partial_t z_{\text{nrpv}}(t,x) = -\bar{v}_{\text{nrpv}}(t,x)\partial_x z_{\text{rpv}}(t,x) + S_{\text{nrpv}}\left(z_{\text{rpv}}(t,x), z_{\text{nrpv}}(t,x)\right) \tag{3.41b}$$

with

$$\bar{v}_{\text{rpv}}(t,x) := \mathrm{diag}\left(\hat{\bar{v}}(t,x), \ldots, \hat{\bar{v}}(t,x)\right) \in \mathbb{R}^{m_{\text{rpv}} \times m_{\text{rpv}}}, \tag{3.42a}$$

$$\bar{v}_{\text{nrpv}}(t,x) := \mathrm{diag}\left(\hat{\bar{v}}(t,x), \ldots, \hat{\bar{v}}(t,x)\right) \in \mathbb{R}^{m_{\text{nrpv}} \times m_{\text{nrpv}}}, \tag{3.42b}$$

$S = (S_{\text{rpv}}, S_{\text{nrpv}})^\top$, and corresponding initial values

$$z_{\text{rpv}}(0,x) = z_{\text{rpv}}^0(x) \tag{3.43a}$$

$$z_{\text{nrpv}}(0,x) = z_{\text{nrpv}}^0(x). \tag{3.43b}$$

3. Spatially Inhomogeneous Systems: Inertial Manifold Computation

If $z^0_{\mathrm{nrpv}}(x) = h\left(z^0_{\mathrm{rpv}}(x)\right)$ with h being the species reconstruction function representing the SIM in the pure reaction case, the initial values are chosen on the SIM. Accordingly, the corresponding FA can be formulated as

$$\partial_t z_{\mathrm{rpv}}(t, x) = -\bar{v}_{\mathrm{rpv}} \partial_x z_{\mathrm{rpv}}(t, x) + S_{\mathrm{rpv}}\left(z_{\mathrm{rpv}}(t, x), h\left(z_{\mathrm{rpv}}(t, x)\right)\right) \tag{3.44a}$$

$$z_{\mathrm{nrpv}}(t, x) = h\left(z_{\mathrm{rpv}}(t, x)\right) \tag{3.44b}$$

together with

$$z_{\mathrm{rpv}}(0, x) = z^0_{\mathrm{rpv}}(x). \tag{3.45}$$

In case of equality of the solution regarding (3.41), (3.43) together with $z^0_{\mathrm{nrpv}}(x) = h\left(z^0_{\mathrm{rpv}}(x)\right)$ as well as (3.44), (3.45), there is no influence of the convection terms concerning the reduced reaction model and thus, the FA (3.44), (3.45) is a suitable reduced reaction–convection model. This issue is treated in the following.

By assuming $z_{\mathrm{rpv}} = \left(z_1, \ldots, z_{m_{\mathrm{rpv}}}\right)^\top$, $z_{\mathrm{nrpv}} = \left(z_{m_{\mathrm{rpv}}+1}, \ldots, z_m\right)^\top$, $S_{\mathrm{rpv}} = \left(S_1, \ldots, S_{m_{\mathrm{rpv}}}\right)^\top$, and $S_{\mathrm{nrpv}} = \left(S_{m_{\mathrm{rpv}}+1}, \ldots, S_m\right)^\top$, the full System (3.41), (3.43) can be formulated as

$$\partial_t z_j(t, x) = -\hat{v}(t, x) \partial_x z_j(t, x) + S_j\left(z_1(t, x), \ldots, z_m(t, x)\right) \tag{3.46a}$$

$$z_j(0, x) = z^0_j(x) \tag{3.46b}$$

for $j = 1, \ldots, m$. In order to solve this IVP, the following ansatz is provided

$$\mathrm{d}_t x_j(t) = \hat{v}\left(t, x_j(t)\right) \tag{3.47a}$$

$$x_j(0) = x^0_j \tag{3.47b}$$

wherefrom the follwing system of ODEs results

$$\mathrm{d}_t z_j\left(t, x_j(t)\right) = \partial_t z_j\left(t, x_j(t)\right) + \underbrace{\mathrm{d}_t x_j(t)}_{=\hat{v}(t, x_j(t))} \partial_x z_j\left(t, x_j(t)\right)$$
$$= S_j\left(z_1\left(t, x_1(t)\right), \ldots, z_m\left(t, x_m(t)\right)\right) \tag{3.48a}$$

$$z_j(0, x_j(0)) = z_j(0, x^0_j) = z^0_j(x^0_j) \tag{3.48b}$$

with $j = 1, \ldots, m$. Consequently, it is possible to solve (3.46) by solving (3.47), which is denoted by **method of characteristics**. On the other hand, the Reduced System (3.44), (3.45) can be written as

$$\partial_t z_j(t, x) = -\hat{v}(t, x) \partial_x z_j(t, x) + S_j\left(z_1(t, x), \ldots, z_{m_{\mathrm{rpv}}}(t, x), h\left(z_1(t, x), \ldots, z_{m_{\mathrm{rpv}}}(t, x)\right)\right) \tag{3.49a}$$

$$z_j(0, x) = z^0_j(x) \tag{3.49b}$$

$$z_{\mathrm{nrpv}}(t, x) = h\left(z_1, \ldots, z_{m_{\mathrm{rpv}}}\right) \tag{3.49c}$$

for $j = 1, \ldots, m_{\mathrm{rpv}}$. Accordingly, this IVP can again be solved by using (3.47) for $j = 1, \ldots, m_{\mathrm{rpv}}$ yielding

$$
\begin{aligned}
\mathrm{d}_t z_j\left(t, x_j(t)\right) &= \partial_t z_j\left(t, x_j(t)\right) + \underbrace{\mathrm{d}_t x_j(t)}_{=\hat{\bar{v}}(t, x_j(t))}\, \partial_x z_j\left(t, x_j(t)\right) \\
&= S_j\left(z_1\left(t, x_1(t)\right), \ldots, z_{m_{\mathrm{rpv}}}\left(t, x_{m_{\mathrm{rpv}}}(t)\right), h\left(z_1\left(t, x_1(t)\right), \ldots\right.\right. \\
&\qquad\qquad\qquad\qquad\qquad\qquad\left.\left.\ldots, z_{m_{\mathrm{rpv}}}\left(t, x_{m_{\mathrm{rpv}}}(t)\right)\right)\right)
\end{aligned}
\tag{3.50a}
$$

$$
z_j(0, x_j(0)) = z_j(0, x_j^0) = z_j^0(x_j^0) \tag{3.50b}
$$

with $j = 1, \ldots, m_{\mathrm{rpv}}$. Therefore, analytic solutions of the full reaction–convection equation with initial values on the SIM equate with the analytic solutions of the reduced reaction–convection equation which is why there is no influence of convection (in form of (3.39)) concerning the reduced reaction model.

The linear model $S\left(z(t, x)\right) = Az(t, x)$ with A given by (2.45) and $\bar{v}(t, x) = \begin{pmatrix} \hat{\bar{v}} & 0 \\ 0 & \hat{\bar{v}} \end{pmatrix}$ with $\hat{\bar{v}} \in \mathbb{R}$ will serve as a demonstration. The full model reads

$$
\partial_t z_1(t, x) = -\hat{\bar{v}}\partial_x z_1(t, x) + (-1 - \frac{\gamma}{2})z_1(t, x) + \frac{\gamma}{2}z_2(t, x) \tag{3.51a}
$$

$$
\partial_t z_2(t, x) = -\hat{\bar{v}}\partial_x z_2(t, x) + \frac{\gamma}{2}z_1(t, x) + (-1 - \frac{\gamma}{2})z_2(t, x) \tag{3.51b}
$$

$$
z_1(0, x) = z_1^0(x) \tag{3.51c}
$$

$$
z_2(0, x) = z_2^0(x) \tag{3.51d}
$$

with $z_1^0(x) = h\left(z_2^0(x)\right) = z_2^0(x)$ for initial values on the SIM. From (3.48) it follows that

$$
\mathrm{d}_t z_1\left(t, x_1(t)\right) = (-1 - \frac{\gamma}{2})z_1\left(t, x_1(t)\right) + \frac{\gamma}{2}z_2\left(t, x_2(t)\right) \tag{3.52a}
$$

$$
\mathrm{d}_t z_2\left(t, x_2(t)\right) = \frac{\gamma}{2}z_1\left(t, x_1(t)\right) + (-1 - \frac{\gamma}{2})z_2\left(t, x_2(t)\right) \tag{3.52b}
$$

$$
z_1\left(0, x_1(0)\right) = z_1^0(x_1^0) \tag{3.52c}
$$

$$
z_2\left(0, x_2(0)\right) = z_2^0(x_2^0) \tag{3.52d}
$$

where $x_1(t)$, $x_2(t)$, x_1^0, and x_2^0 are defined by

$$
\mathrm{d}_t x_1(t) = \hat{\bar{v}} \tag{3.53a}
$$

$$
\mathrm{d}_t x_2(t) = \hat{\bar{v}} \tag{3.53b}
$$

$$
x_1(0) = x_1^0 \tag{3.53c}
$$

$$
x_2(0) = x_2^0. \tag{3.53d}
$$

3. Spatially Inhomogeneous Systems: Inertial Manifold Computation

The latter results in

$$x_1(t) = x_1^0 + \hat{\hat{v}}t \tag{3.54a}$$

$$x_2(t) = x_2^0 + \hat{\hat{v}}t \tag{3.54b}$$

wherewith (3.52c) and (3.52d) can be rewritten into $z_1(0, x_1(0)) = z_1^0(x_1(t) - \hat{\hat{v}}t)$ and $z_2(0, x_2(0)) = z_2^0(x_2(t) - \hat{\hat{v}}t)$, respectively. Consequently, the analytic solution of (3.52) results in

$$z_1(t, x_1(t)) = \frac{z_1^0(x_1(t) - \hat{\hat{v}}t) + z_2^0(x_2(t) - \hat{\hat{v}}t)}{2} e^{-t}$$
$$+ \frac{z_1^0(x_1(t) - \hat{\hat{v}}t) - z_2^0(x_2(t) - \hat{\hat{v}}t)}{2} e^{(-1-\gamma)t} \tag{3.55a}$$

$$z_2(t, x_2(t)) = \frac{z_1^0(x_1(t) - \hat{\hat{v}}t) + z_2^0(x_2(t) - \hat{\hat{v}}t)}{2} e^{-t}$$
$$- \frac{z_1^0(x_1(t) - \hat{\hat{v}}t) - z_2^0(x_2(t) - \hat{\hat{v}}t)}{2} e^{(-1-\gamma)t} \tag{3.55b}$$

and thus, the solution of the full reaction–convection model (3.51) with $z_1^0(x) = h\left(z_2^0(x)\right) = z_2^0(x)$ is given by

$$z_1(t, x) = z_2^0(x - \hat{\hat{v}}t)e^{-t} \tag{3.56a}$$

$$z_2(t, x) = z_2^0(x - \hat{\hat{v}}t)e^{-t}. \tag{3.56b}$$

The same procedure applied to the corresponding FA

$$\partial_2(t, x) = -\hat{\hat{v}}\partial_x z_2(t, x) + \frac{\gamma}{2}\underbrace{h(z_2(t, x))}_{=z_2(t,x)} + (-1 - \frac{\gamma}{2})z_2(t, x) = -\hat{\hat{v}}\partial_x z_2(t, x) - z_2(t, x)$$

$$\tag{3.57a}$$

$$z_2(0, x) = z_2^0(x) \tag{3.57b}$$

$$z_1(t, x) = h(z_2(t, x)) = z_2(t, x) \tag{3.57c}$$

again results in (3.56) which confirms the statement described in the previous section, namely that the reduced reaction model experiences no influence caused by convective terms.

Obviously, the same conclusion is achieved by using $\bar{v}(t, x) = \begin{pmatrix} \hat{\hat{v}}(t, x) & 0 \\ 0 & \hat{\hat{v}}(t, x) \end{pmatrix}$ with exemplarily choosing $\hat{\hat{v}}(t, x) = x$. Here, the solution of the system of ODEs (3.47) results in

$$x_1(t) = x_1^0 e^t \tag{3.58a}$$

$$x_2(t) = x_2^0 e^t \tag{3.58b}$$

yielding

$$z_1(t,x) = \frac{z_1^0(xe^{-t}) + z_2^0(xe^{-t})}{2}e^{-t} + \frac{z_1^0(xe^{-t}) - z_2^0(xe^{-t})}{2}e^{(-1-\gamma)t} \tag{3.59a}$$

$$z_2(t,x) = \frac{z_1^0(xe^{-t}) + z_2^0(xe^{-t})}{2}e^{-t} - \frac{z_1^0(xe^{-t}) - z_2^0(xe^{-t})}{2}e^{(-1-\gamma)t} \tag{3.59b}$$

which coincides with the solution of the corresponding FA for $z_1^0 = z_2^0$.

To conclude, it can be stated that the FA of the reaction–convection model equation is suitable and can be used, therefore, as reduced reaction–convection model. Whether this is also the case for the reaction–diffusion case is still unclear and will be analyzed in the subsequent section.

3.5 Coupling: Reduced Reaction and Diffusion

As has just been pointed out, the FA of the reaction–convection model is suitable and thus, using a SIM of the reaction kinetics as reduced model is the appropriate choice in that case. This is why it is sufficient to analyze the reaction–diffusion equation instead of the reaction–convection–diffusion one. Accordingly, the kinetic model equations read

$$\partial_t z_{\mathrm{rpv}}(t,x) = \mathcal{D}_{\mathrm{rpv}}\partial_{xx}^2 z_{\mathrm{rpv}}(t,x) + S_{\mathrm{rpv}}\left(z_{\mathrm{rpv}}(t,x), z_{\mathrm{nrpv}}(t,x)\right) \tag{3.60a}$$

$$\partial_t z_{\mathrm{nrpv}}(t,x) = \mathcal{D}_{\mathrm{nrpv}}\partial_{xx}^2 z_{\mathrm{rpv}}(t,x) + S_{\mathrm{nrpv}}\left(z_{\mathrm{rpv}}(t,x), z_{\mathrm{nrpv}}(t,x)\right) \tag{3.60b}$$

with $\mathcal{D}_{\mathrm{rpv}} = \mathrm{diag}\left(\mathcal{D}_1, \ldots, \mathcal{D}_{m_{\mathrm{rpv}}}\right)$ and $\mathcal{D}_{\mathrm{nrpv}} = \mathrm{diag}\left(\mathcal{D}_{m_{\mathrm{rpv}}+1}, \ldots, \mathcal{D}_m\right)$. This reaction–diffusion equation is an evolution problem, i.e. a parabolic system of PDEs of order two. As seen before, this kind of problem requires both initial and boundary conditions to be well-posed, such that the resulting (one-dimensional) IBVP is given by (3.60) in $(0,T) \times (x_{\mathrm{s}}, x_{\mathrm{f}})$, $0 < T < \infty$, together with a given initial condition

$$z_{\mathrm{rpv}}(0,x) = z_{\mathrm{rpv}}^0(x) \tag{3.61a}$$

$$z_{\mathrm{nrpv}}(0,x) = z_{\mathrm{nrpv}}^0(x) \tag{3.61b}$$

in $(x_{\mathrm{s}}, x_{\mathrm{f}})$ and boundary conditions

$$\mathcal{A}_{\alpha,\mathrm{rpv}}z_{\mathrm{rpv}}(t,x_{\mathrm{s}}) + \mathcal{A}_{1-\alpha,\mathrm{rpv}}\partial_x z_{\mathrm{rpv}}(t,x_{\mathrm{s}}) = z_{\mathrm{rpv},x_{\mathrm{s}}}(t) \tag{3.62a}$$

$$\mathcal{A}_{\alpha,\mathrm{nrpv}}z_{\mathrm{nrpv}}(t,x_{\mathrm{s}}) + \mathcal{A}_{1-\alpha,\mathrm{nrpv}}\partial_x z_{\mathrm{nrpv}}(t,x_{\mathrm{s}}) = z_{\mathrm{nrpv},x_{\mathrm{s}}}(t) \tag{3.62b}$$

$$\mathcal{A}_{\alpha,\mathrm{rpv}}z_{\mathrm{rpv}}(t,x_{\mathrm{f}}) + \mathcal{A}_{1-\alpha,\mathrm{rpv}}\partial_x z_{\mathrm{rpv}}(t,x_{\mathrm{f}}) = z_{\mathrm{rpv},x_{\mathrm{f}}}(t) \tag{3.62c}$$

$$\mathcal{A}_{\alpha,\mathrm{nrpv}}z_{\mathrm{nrpv}}(t,x_{\mathrm{f}}) + \mathcal{A}_{1-\alpha,\mathrm{nrpv}}\partial_x z_{\mathrm{nrpv}}(t,x_{\mathrm{f}}) = z_{\mathrm{nrpv},x_{\mathrm{f}}}(t) \tag{3.62d}$$

in $(0,T)$. Here, $\mathcal{A}_{\alpha,\mathrm{rpv}} = \mathrm{diag}(\alpha, \ldots, \alpha) \in \mathbb{R}^{m_{\mathrm{rpv}} \times m_{\mathrm{rpv}}}$, $\mathcal{A}_{1-\alpha,\mathrm{rpv}} = \mathrm{diag}(1-\alpha, \ldots, 1-\alpha) \in \mathbb{R}^{m_{\mathrm{rpv}} \times m_{\mathrm{rpv}}}$, and $\mathcal{A}_{\alpha,\mathrm{nrpv}}$, $\mathcal{A}_{1-\alpha,\mathrm{nrpv}}$ defined accordingly. In order to select between either

3. Spatially Inhomogeneous Systems: Inertial Manifold Computation

DIRICHLET or NEUMANN boundary conditions, $\alpha \in \{0, 1\}$: the choice of $\alpha = 0$ results in NEUMANN boundary conditions, whereas $\alpha = 1$ results in DIRICHLET ones. Since there is no gerneral procedure for obtaining an analytic solution to this IBVP, a Matlab$^{\circledR}$ function called `pdepe` is used to solve this parabolic system of PDEs numerically. This `pdepe` solver converts the provided system of PDEs into a system of ODEs using a second-order accurate spatial discretisation [SB90], which is solved by time integration using `ode15s`—an IVP solver suitable for stiff systems of ODEs. In the following, numerical solutions of a reaction–diffusion equation together with several chosen values for initial and boundary conditions (solved via using `pdepe`) are plotted in order to analyze the behavior of the respective solutions.

The DAVIS–SKODJE model (see 2.3.2) extended by a diffusion term, i.e. $S_1 = -z_1(t, x)$ and $S_2 = -\tilde{\gamma} z_2(t, x) + \frac{(\tilde{\gamma}-1)z_1(t,x)+\tilde{\gamma}z_1(t,x)^2}{(1+z_1(t,x))^2}$ with $\mathcal{I}_{\text{fixed}} = \{1\}$ and $x_s = 0.0$, $x_f = 1.0$ serves as an example. Furthermore, $z_1^0(x)$ is fixed to $z_1^0(x) = 1.0$ and $\alpha = 1$ to determine DIRICHLET boundary conditions. A natural way to choose $z_{j,k}(t)$, $j \in \{1, 2\}$, $k \in \{0, 1\}$ is to choose them as solution of the corresponding homogeneous reaction equation, i.e.

$$z_{1,0}(t) = z_{1,1}(t) = z_1^0 e^{-t} = e^{-t} \tag{3.63a}$$

$$z_{2,0}(t) = z_{2,1}(t) = \left(z_2^0 - \frac{z_1^0}{z_1^0 + 1} \right) e^{-\tilde{\gamma}t} + \frac{z_1^0}{z_1^0 + e^t} = \frac{1}{1 + e^t} \tag{3.63b}$$

for $z_2^0(x) \equiv 0.5$ or $z_2^0(x) \equiv -0.1\sin(2\pi x) + 0.5$ which is chosen in Figure 3.5, where the numerical solution (computed with `pdepe`) of the above mentioned scenario is depicted for different values of $\tilde{\gamma}$, $\mathcal{D}_1$, and $\mathcal{D}_2$. As in the homogeneous case, the solution is visualized in phase space, but this time enlarged by the x-axis. Here, the red curve visualizes the initial condition (3.61), whereas the green curves represent the boundary values (3.63). Accordingly, the blue curves evolving along a specific value of $\hat{x}$ are solutions $z(t, \hat{x})$ for $t > 0$, whereas the blue curves orthogonal to them represent the solutions $z(\hat{t}, x)$ for all $x \in [0, 1]$ at a specific point in time $\hat{t}$ converging towards chemical equilibrium $z_1 = z_2 = 0.0$ for $\hat{t} \to \infty$. In Figure 3.5(a), the initial condition is chosen on the SIM, whereby the behavior of the solution is independent of $\tilde{\gamma}$, $\mathcal{D}_1$, and $\mathcal{D}_2$. Based on this special choice of initial as well as boundary conditions, there is no difference between Figure 3.5(a) and Figure 3.4. In order to analyze the influence of $\tilde{\gamma}$ as well as $\mathcal{D}_1$ and $\mathcal{D}_2$, the initial condition is changed to $z_2^0(x) = -0.1\sin(2\pi x) + 0.5$ in Figures 3.5(b), (c), and (d). As can be seen in Figure 3.5(c) in comparison with Figure 3.5(b), a larger value of $\tilde{\gamma}$ results in a faster equalization of z_1 and z_2 along x, which is not surprising when remembering the pure reaction case, where the spectral gap parameter $\tilde{\gamma}$ controls the degree of attraction of the SIM. Larger values of $\mathcal{D}_1$ and $\mathcal{D}_2$ seem to have the same effect (Figure 3.5(d)), but this influence is analyzed in more detail in the following. In this above described trivial scenario the corresponding FA is obviously suitable (on the basis of the analogy to the spatially homogeneous case).

(a) $\tilde{\gamma}, \mathcal{D}_1, \mathcal{D}_2$ arbitrarily, $z_2^0(x) = 0.5$

(b) $\tilde{\gamma} = 5.0$, $\mathcal{D}_1 = \mathcal{D}_2 = 1.0 \cdot 10^{-3}$, $z_2^0(x) = -0.1\sin(2\pi x) + 0.5$

(c) $\tilde{\gamma} = 25.0$, $\mathcal{D}_1 = \mathcal{D}_2 = 1.0 \cdot 10^{-3}$, $z_2^0(x) = -0.1\sin(2\pi x) + 0.5$

(d) $\tilde{\gamma} = 5.0$, $\mathcal{D}_1 = \mathcal{D}_2 = 1.0 \cdot 10^{2}$, $z_2^0(x) = -0.1\sin(2\pi x) + 0.5$
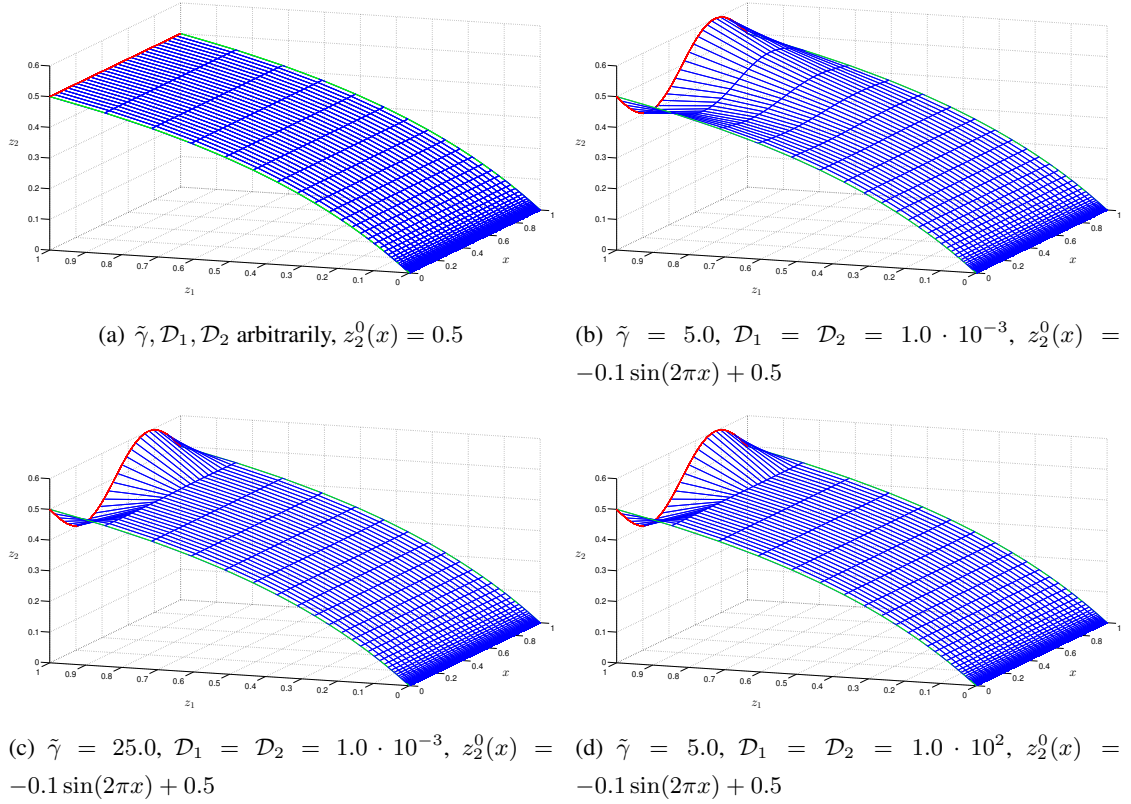
Figure 3.5: Numerical solutions of the reaction–diffusion equation for different values of $\tilde{\gamma}$, $\mathcal{D}_1$, $\mathcal{D}_2$, and $z_2^0(x)$.

In order to analyze the behavior of the solution for increasing diffusion, i.e. increasing $\mathcal{D}_1$ and $\mathcal{D}_2$, in a more general scenario, DIRICHLET boundary conditions are fixed at

$$z_{1,0}(t) = z_{1,1}(t) = 1.0 \tag{3.64a}$$

$$z_{2,0}(t) = z_{2,1}(t) = 0.5 \tag{3.64b}$$

and initial conditions again are chosen as $z_1^0(x) \equiv 1.0$ as well as $z_2^0(x) \equiv 0.5$. This is visualized for $\tilde{\gamma} = 5.0$ and four different values of $\mathcal{D}_1 = \mathcal{D}_2$ in Figure 3.6. Here, the green dots represent the boundary values at $x_\mathrm{s} = 0.0$ and $x_\mathrm{f} = 1.0$. As the figures show, for increasing diffusion, the solution approaches the line connecting both boundary conditions for $t \to \infty$ meaning that the reactive term of the model affects the solution to a decreasing degree, whereas the diffusive term experiences growing importance. This is emphasized by Figure 3.7, where different boundary and initial conditions are chosen together with large values of $\mathcal{D}_1 = \mathcal{D}_2$ to underline this be-havior. As can be seen, in each case the solution starting for $t = 0$ from the red colored initial condition curve converges again towards the line connecting the boundary values for $t \to \infty$, hereafter referred to as **diffusion line**. This scenario shows the behavior of the solution for a

(a) $\mathcal{D}_1 = \mathcal{D}_2 = 1.0 \cdot 10^{-3}$

(b) $\mathcal{D}_1 = \mathcal{D}_2 = 1.0 \cdot 10^{-2}$

(c) $\mathcal{D}_1 = \mathcal{D}_2 = 1.0 \cdot 10^{-1}$

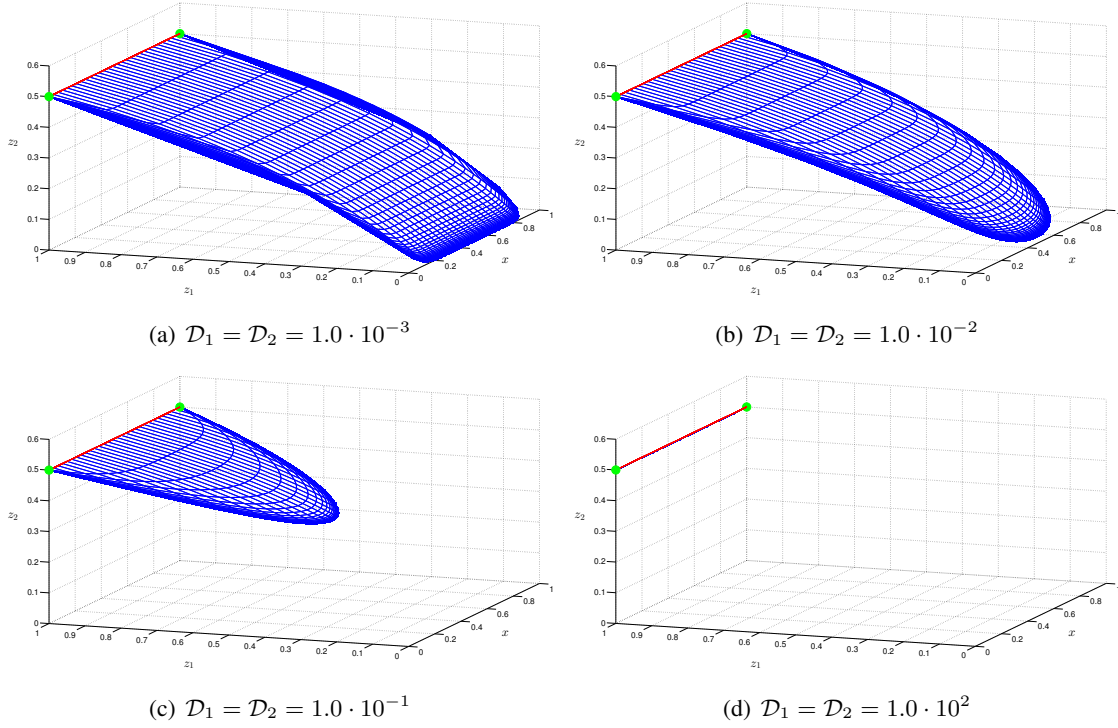(d) $\mathcal{D}_1 = \mathcal{D}_2 = 1.0 \cdot 10^{2}$

Figure 3.6: Numerical solutions of the reaction–diffusion equation for $\tilde{\gamma} = 5.0$, $z_1^0(x) \equiv 1.0$, $z_2^0(x) \equiv 0.5$, and different values of $\mathcal{D}_1$, $\mathcal{D}_2$.

diffusive term dominating strongly over the reactive one.

For the sake of completeness, the opposite scenario is visualized in Figure 3.8, where the same initial and boundary conditions are chosen as in Figure 3.7 (time scale of diffusion $\gg$ time scale of reaction), but this time the reactive term dominates the diffusive one (time scale of reaction $\gg$ time scale of diffusion) which is realized by choosing small values of $\mathcal{D}_1$ and $\mathcal{D}_2$. As one can see, the solutions show strong similarity to the pure reaction case for each value of x (in consideration of fulfillment of the given boundary conditions).

Naturally, it is possible to choose a value of $\mathcal{D}_1$ differing from $\mathcal{D}_2$ which, however, plays no essential role within the scope of this work. Nevertheless, this scenario is illustrated in Figure 3.9, where Figures 3.9(a) and (c) represent $\mathcal{D}_1 \ll \mathcal{D}_2$ and Figures 3.9(b) and (d) $\mathcal{D}_1 \gg \mathcal{D}_2$ for different initial and boundary conditions. The first case shows how $\mathcal{D}_2$ quickly forces the dynamic onto the plane of constant z_2 for each x, where the respective value of z_2 is given by the diffusion line. Based on the relatively small value of $\mathcal{D}_1$ there is no remarkable effect by diffusion regarding z_1. In contrast, the second case ($\mathcal{D}_1 \gg \mathcal{D}_2$) provides similar results for interchanged roles of z_1 and z_2 or $\mathcal{D}_1$ and $\mathcal{D}_2$, respectively.

(a) $z_1^0(x) = 1.0$, $z_2^0(x) = -0.1\sin(2\pi x) + 0.5$, $z_{1,0}(t) = z_{1,1}(t) = 1.0$, $z_{2,0}(t) = z_{2,1}(t) = 0.5$

(b) $z_1^0(x) = 1 - x^2$, $z_2^0(x) = 0.5 - \frac{x}{x+1}$, $z_{1,0}(t) = 1.0$, $z_{2,0}(t) = 0.5$, $z_{1,1}(t) = 0.0$, $z_{2,1}(t) = 0.0$

(c) $z_1^0(x) = 2(x-0.5)^2 + 0.5$, $z_2^0(x) = \frac{7}{6}x^2 - \frac{41}{30}x + 0.5$, $z_{1,0}(t) = z_{1,1}(t) = 1.0$, $z_{2,0}(t) = 0.5$, $z_{2,1}(t) = 0.3$

(d) $z_1^0(x) = -x + 1$, $z_2^0(x) = -\frac{40}{21}x^2 + \frac{20}{7}x^2 - \frac{37}{105}x$, $z_{1,0}(t) = 1.0$, $z_{2,0}(t) = z_{1,1}(t) = 0.0$, $z_{2,1}(t) = 0.6$
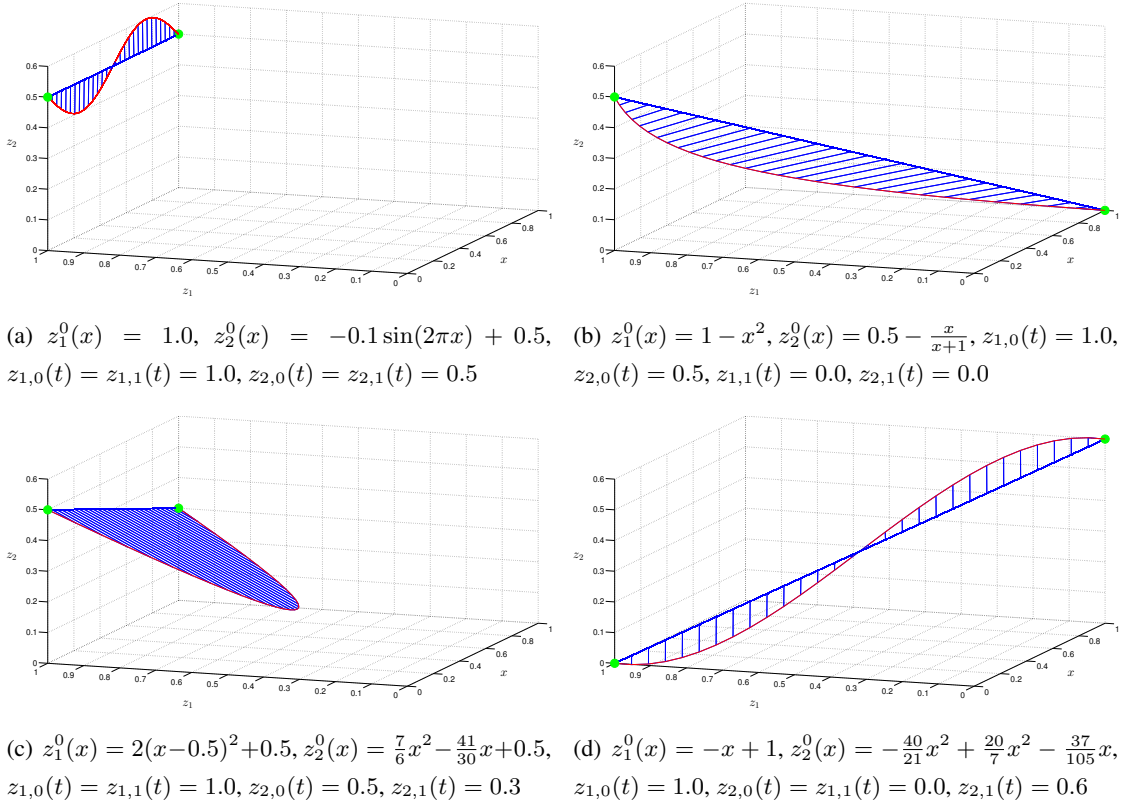
Figure 3.7: Numerical solutions of the reaction–diffusion equation for $\mathcal{D}_1 = \mathcal{D}_2 = 1.0 \cdot 10^2$ for different initial and boundary conditions. (Time Scale of Diffusion $\gg$ Time Scale of Reaction)

Thus, both extreme case scenarios for the reaction–diffusion equation (3.60) are analyzed (at least by means of the given example): on the one hand the diffusive term dominating the reactive one (large values of $\mathcal{D}$) and on the other hand the reactive term dominating the diffusive one, i.e. diffusion being almost nonexistent (small values of $\mathcal{D}$).

Time Scale of Diffusion $\gg$ Time Scale of Reaction: The solution converges directly towards the diffusion line, such that effects resulting from the reactive terms are largely imperceptible.

Time Scale of Diffusion $\ll$ Time Scale of Reaction: For each $x \in [x_\mathrm{s}, x_\mathrm{f}]$ the solution behaves as in the pure reaction case, i.e. converging towards the SIM depending on $\tilde{\gamma}$ and finally approaching the chemical equilibrium, under consideration of the given boundary values.

However, much more interesting is the case where both, reactive and diffusive processes have an effect on the behavior of the solution such as depicted in Figures 3.6(b) and (c). For discussion,

(a) $z_1^0(x) = 1.0$, $z_2^0(x) = -0.1\sin(2\pi x) + 0.5$, $z_{1,0}(t) = z_{1,1}(t) = 1.0$, $z_{2,0}(t) = z_{2,1}(t) = 0.5$

(b) $z_1^0(x) = 1 - x^2$, $z_2^0(x) = 0.5 - \frac{x}{x+1}$, $z_{1,0}(t) = 1.0$, $z_{2,0}(t) = 0.5$, $z_{1,1}(t) = 0.0$, $z_{2,1}(t) = 0.0$

(c) $z_1^0(x) = 2(x-0.5)^2 + 0.5$, $z_2^0(x) = \frac{7}{6}x^2 - \frac{41}{30}x + 0.5$, $z_{1,0}(t) = z_{1,1}(t) = 1.0$, $z_{2,0}(t) = 0.5$, $z_{2,1}(t) = 0.3$

(d) $z_1^0(x) = -x + 1$, $z_2^0(x) = -\frac{40}{21}x^2 + \frac{20}{7}x^2 - \frac{37}{105}x$, $z_{1,0}(t) = 1.0$, $z_{2,0}(t) = z_{1,1}(t) = 0.0$, $z_{2,1}(t) = 0.6$
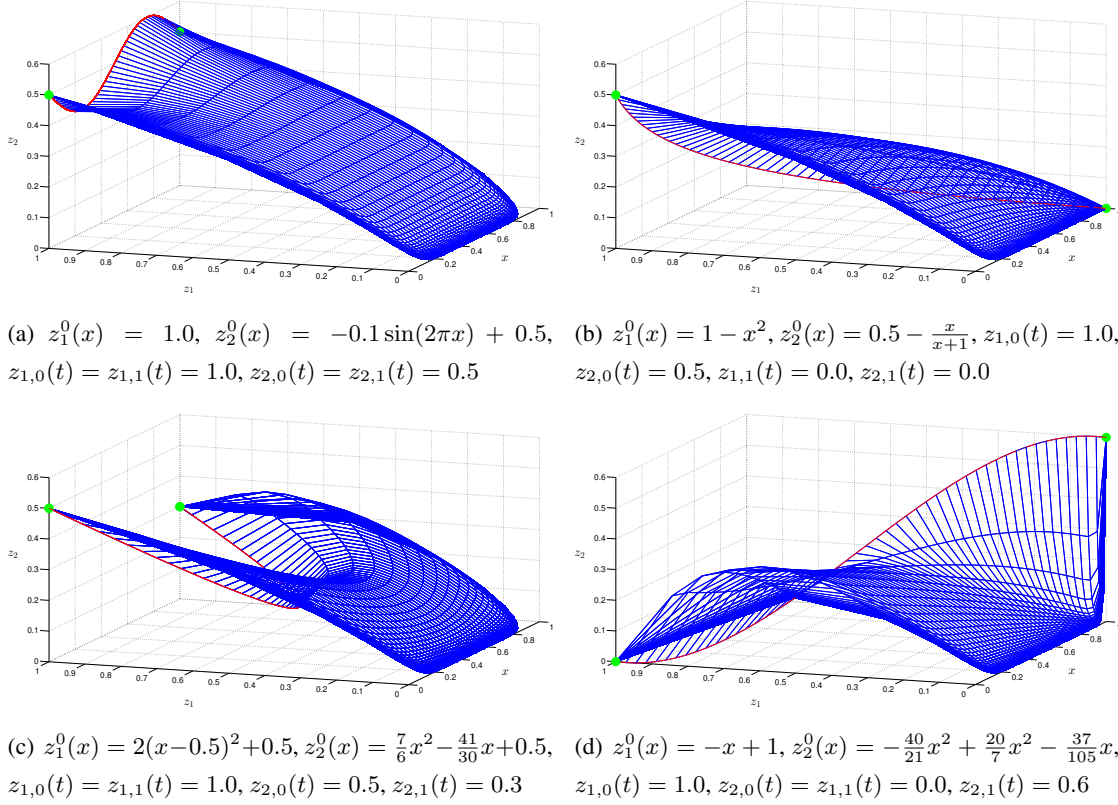
Figure 3.8: Numerical solutions of the reaction–diffusion equation for $\mathcal{D}_1 = \mathcal{D}_2 = 1.0 \cdot 10^{-3}$ for different initial and boundary conditions. (Time Scale of Reaction $\gg$ Time Scale of Diffusion)

it is helpful to know about the solution behavior in the two extreme cases mentioned above. For the sake of simplicity, we restrict to the case where the boundary conditions are given by (3.64) and corresponding initial conditions by $z_1^0(x) \equiv 1.0$ as well as $z_2^0(x) \equiv 0.5$. Then, the behavior of the solutions resulting from IBVPs with other choices of initial as well as DIRICHLET boundary conditions can be concluded from similar considerations. Qualitatively, the solution of the reaction–diffusion equation behaves as if there is a competition between reaction and diffusion which is schematically illustrated in Figure 3.10(a). Here, a vertical sectional plane of the three-dimensional z_2–z_1–x–plot is depicted for an arbitrary value of $x \in (0,1)$. The red cross represents the initial condition as well as the diffusion line evaluated at the respective x (cf. Figure 3.6(d)). On the other hand, the blue dashed curve represents the solution at x in the case where diffusion is almost nonexistent such that the dynamics is governed by the reactive term (cf. Figure 3.6(a)). Solutions of the other scenarios (Diffusion $\approx$ Reaction) schematically behave like it is demonstrated in the picture: first, the dynamics start governed by the reactive term along the blue dashed curve (1). Afterwards, the diffusion pulls the dynamic back along the direct line towards the diffusion line (2), wherefrom the reaction dynamics towards the SIM

(a) $z_1^0(x) = 1.0$, $z_2^0(x) = -0.1\sin(2\pi x) + 0.5$, $z_{1,0}(t) = z_{1,1}(t) = 1.0$, $z_{2,0}(t) = z_{2,1}(t) = 0.5$, $\mathcal{D}_1 = 1.0 \cdot 10^{-3}$, $\mathcal{D}_2 = 1.0 \cdot 10^2$

(b) $z_1^0(x) = 1.0$, $z_2^0(x) = -0.1\sin(2\pi x) + 0.5$, $z_{1,0}(t) = z_{1,1}(t) = 1.0$, $z_{2,0}(t) = z_{2,1}(t) = 0.5$, $\mathcal{D}_1 = 1.0 \cdot 10^2$, $\mathcal{D}_2 = 1.0 \cdot 10^{-3}$

(c) $z_1^0(x) = 2(x-0.5)^2+0.5$, $z_2^0(x) = \frac{7}{6}x^2 - \frac{41}{30}x+0.5$, $z_{1,0}(t) = z_{1,1}(t) = 1.0$, $z_{2,0}(t) = 0.5$, $z_{2,1}(t) = 0.3$, $\mathcal{D}_1 = 1.0 \cdot 10^{-3}$, $\mathcal{D}_2 = 1.0 \cdot 10^2$

(d) $z_1^0(x) = 2(x-0.5)^2+0.5$, $z_2^0(x) = \frac{7}{6}x^2 - \frac{41}{30}x+0.5$, $z_{1,0}(t) = z_{1,1}(t) = 1.0$, $z_{2,0}(t) = 0.5$, $z_{2,1}(t) = 0.3$, $\mathcal{D}_1 = 1.0 \cdot 10^2$, $\mathcal{D}_2 = 1.0 \cdot 10^{-3}$
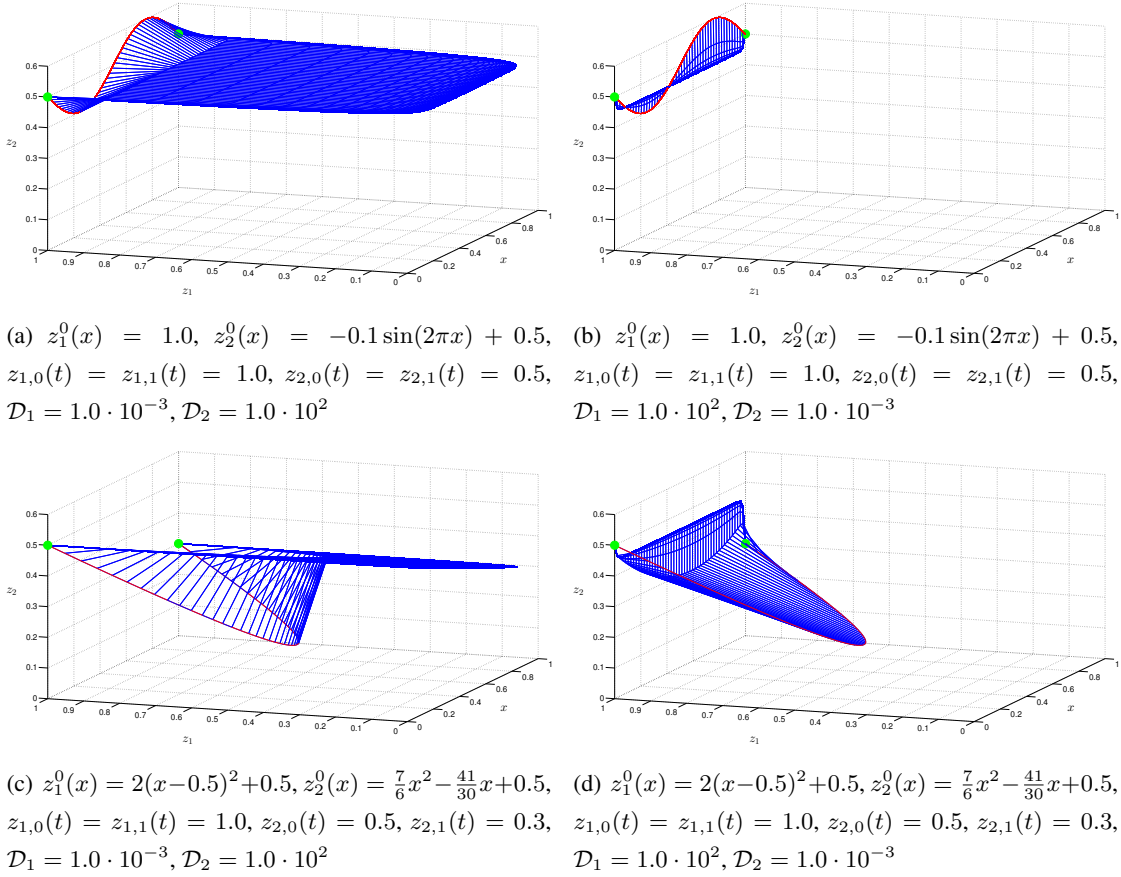
Figure 3.9: Numerical solutions of the reaction–diffusion equation for two different initial and boundary conditions. Figures (a) & (c): $\mathcal{D}_1 \ll \mathcal{D}_2$, Figures (b) & (d): $\mathcal{D}_1 \gg \mathcal{D}_2$.

starts again (3). This procedure repeats until diffusion and reaction are 'in balance', whereby it holds that the larger $\mathcal{D}_1$ and $\mathcal{D}_2$, the nearer is this balance point to the diffusion line. Incidentally, the red dot represents the chemical equilibrium. Certainly, diffusive and reactive processes do not occur sequentially as illustrated in Figure 3.10(a) but rather simultaneously, which is why it has to be interpreted as schematic illustration and not as realistic visualization. Therefore, reaction and diffusion take place in a certain proportion in each time step during time evolution. The outcome of this interplay between reactive and diffusive processes is than a curve (visualized as green curve in Figure 3.10(b)) bounded by the SIM (blue dashed) and the direct line connecting the equilibrium with the diffusion line (red dashed), which can mathematically approximated by a linear combination of SIM and diffusion line

$$z_2 = \theta\frac{z_1}{z_1 + 1} + (1 - \theta)\frac{z_1}{2} \tag{3.65}$$

with $\theta \in [0, 1]$ in the scenario considered here. For each $x \in (0, 1)$ a different θ is possible. This is clarified by regarding Figure 3.11 where Figure 3.6(c) is visualized as z_2–z_1–plot. Here, the red cross represents again the initial value function as well as the diffusion line, whereas the
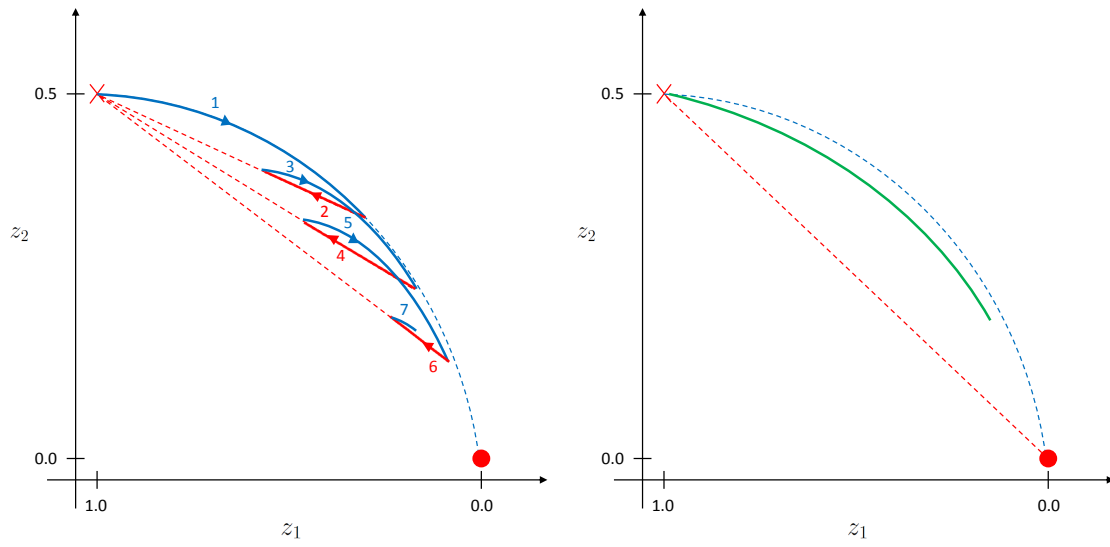
(a) Schematic illustration of the interplay between reaction and diffusion.

(b) Schematic illustration of the resulting solution.

Figure 3.10: Vertical sectional planes of the three-dimensional z_2–z_1–x–plot for an arbitrary value of $x \in (0, 1)$.
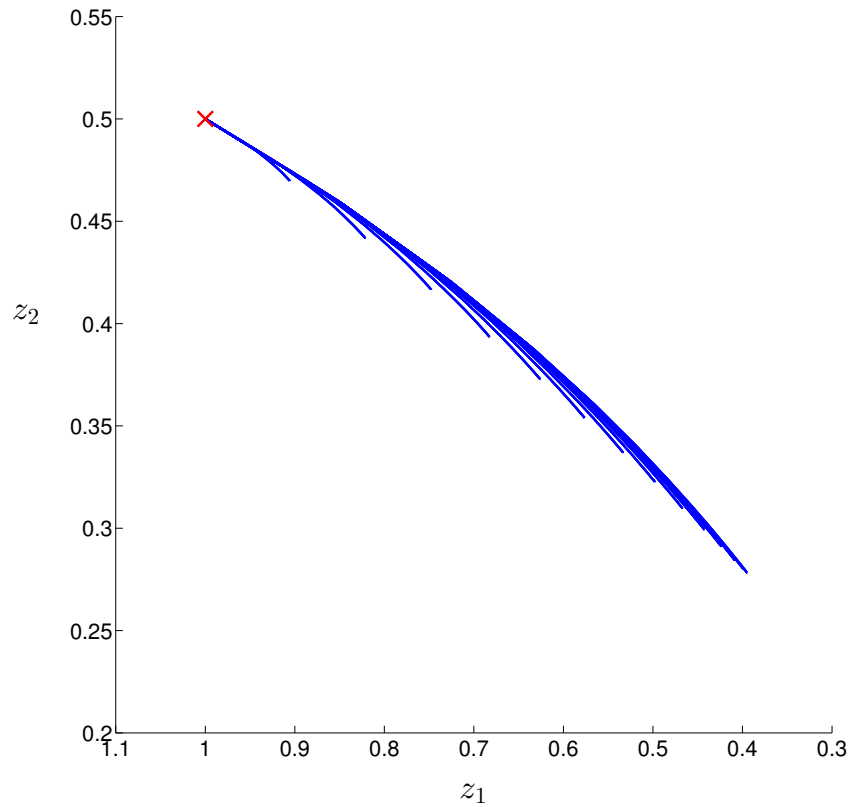

Figure 3.11: Figure 3.6(c) visualized as z_2–z_1–plot for several values of x.

blue curves are solutions of the corresponding IBVP depicted in Figure 3.6(c) for several values of x. As it can be seen, z_2 cannot be approximated by (3.65) for constant $\theta \in [0, 1]$, which is why θ has to be a function depending smoothly on x: $\theta = \theta(x)$.

With this knowledge, it is not difficult to answer the question, if the corresponding FA is suitable or not. Nevertheless, the FA corresponding to the following full reaction–diffusion IBVP

$$\partial_t z_1(t, x) = \mathcal{D}_1 \partial_{xx}^2 z_1(t, x) - z_1(t, x) \qquad \text{in } (0, T) \times (0, 1) \tag{3.66a}$$

$$\partial_t z_2(t, x) = \mathcal{D}_2 \partial_{xx}^2 z_2(t, x) - \tilde{\gamma} z_2(t, x) + \frac{(\tilde{\gamma} - 1)z_1(t, x) + \tilde{\gamma}(z_1(t, x))^2}{(1 + z_1(t, x))^2} \qquad \text{in } (0, T) \times (0, 1) \tag{3.66b}$$

$$z_1(0, x) = 1.0 \qquad \text{in } (0, 1) \tag{3.66c}$$

$$z_2(0, x) = 0.5 \qquad \text{in } (0, 1) \tag{3.66d}$$

$$z_1(t, 0) = z_1(t, 1) = 1.0 \qquad \text{in } (0, T) \tag{3.66e}$$

$$z_2(t, 0) = z_2(t, 1) = 0.5 \qquad \text{in } (0, T) \tag{3.66f}$$

is formulated as

$$\partial_t z_1(t, x) = \mathcal{D}_1 \partial_{xx}^2 z_1(t, x) - z_1(t, x) \qquad \text{in } (0, T) \times (0, 1) \tag{3.67a}$$

$$z_1(0, x) = 1.0 \qquad \text{in } (0, 1) \tag{3.67b}$$

$$z_1(t, 0) = z_1(t, 1) = 1.0 \qquad \text{in } (0, T) \tag{3.67c}$$

$$z_2(t, x) = h(z_1(t, x)) = \frac{z_1(t, x)}{z_1(t, x) + 1} \qquad \text{in } [0, T) \times [0, 1] \tag{3.67d}$$

for $\mathcal{I}_{\text{fixed}} = \{1\}$, whose solution does not coincide with the solution of (3.66) as it can obviously be seen in Figure 3.12, where Figures 3.6(c) and 3.11 are supplemented by the corresponding FA visualized in red. The consequence is that the FA of a reaction–diffusion equation is not suitable in general, which completes Table 3.1 to Table 3.2.

This further implies the question, how the FA of the reaction–diffusion equation has to be modified to achieve a suitable reduced description of the full model equation, which will be discussed in the subsequent section. But before doing so, we take a brief look at the extended linear model, i.e. a reaction–diffusion equation in form of (3.60) with S given by the right-hand side of (2.45).
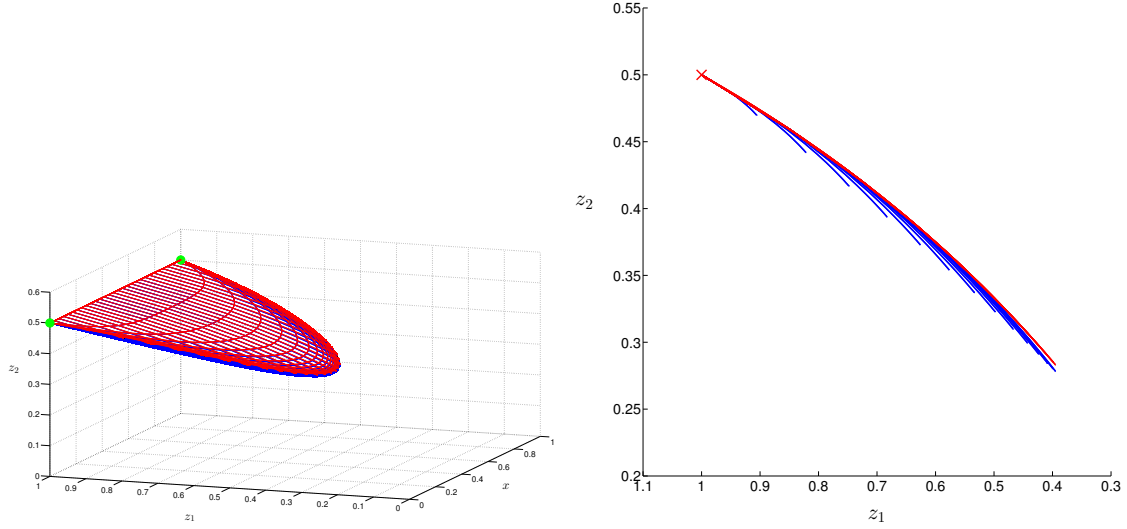
(a) Figure 3.6(c) supplemented by the corresponding FA (red).

(b) Figure 3.11 supplemented by the corresponding FA (red).

Figure 3.12: Full reaction–diffusion equation (3.66) solution (blue) compared with the corresponding FA (3.67) solution (red).

Table 3.2: List of different full model equations together with its appropriate FAs.

	Reaction	Reaction–Convection
Full	$\partial_t z = S(z)$	$\partial_t z = -\bar{v}\partial_x z + S(z)$
FA	$\partial_t z_j = S_j(z)$	$\partial_t z_j = -\hat{\bar{v}}\partial_x z_j + S_j(z)$
Suitable	✓	✓

	Reaction–Diffusion	Reaction–Convection–Diffusion
Full	$\partial_t z = \mathcal{D}\partial_{xx}^2 z + S(z)$	$\partial_t z = -\bar{v}\partial_x z + \mathcal{D}\partial_{xx}^2 z + S(z)$
FA	$\partial_t z_j = \mathcal{D}_j \partial_{xx}^2 z_j + S_j(z)$	$\partial_t z_j = -\hat{\bar{v}}\partial_x z_j + \mathcal{D}_j \partial_{xx}^2 z_j + S_j(z)$
Suitable	✗	✗

for $j \in \mathcal{I}_{\text{fixed}}$ and $z_k = h(z_j)$, $k \notin \mathcal{I}_{\text{fixed}}$, $j \in \mathcal{I}_{\text{fixed}}$ in the FAs.

Remembering the corresponding SIM in the pure reaction case, the FA is given by

$$
\begin{aligned}
\partial_t z_2(t,x) &= \mathcal{D}_1 \partial_{xx}^2 z_2(t,x) + \frac{\gamma}{2}h\left(z_2(t,x)\right) + (-1 - \frac{\gamma}{2})z_2(t,x) \\
&= \mathcal{D}_1 \partial_{xx}^2 z_2(t,x) - z_2(t,x)
\end{aligned}
\tag{3.68a}
$$

$$
z_1(t,x) = h(z_2(t,x)) = z_2(t,x)
\tag{3.68b}
$$

with $\mathcal{I}_{\text{fixed}} = \{2\}$, which is why the initial and boundary values are fixed to

$$z_1(0, x) = z_2(0, x) = 1.0 \tag{3.69a}$$

$$z_1(t, 0) = z_1(t, 1) = z_2(t, 0) = z_2(t, 1) = 1.0. \tag{3.69b}$$

For these values, the solution of the full model equation (blue) is compared to the corresponding FA solution (red) in Figure 3.13, where it can be seen that both solutions coincide, which is contrarily to the extended DAVIS–SKODJE example analyzed before, but not surprising when remembering Figure 3.10, since blue dashed curve, red dashed line, and green curve coincide in the linear case. As a consequence it can be stated, that the FA of a reaction–diffusion equation
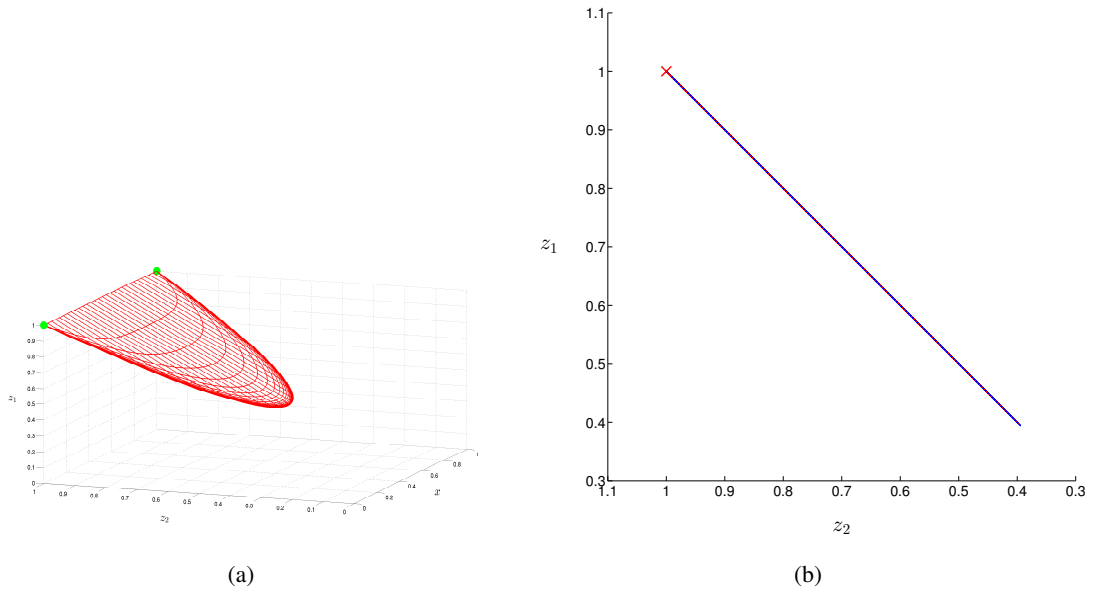

(a) (b)

Figure 3.13: Full reaction–diffusion equation solution of the extended linear model (blue) compared with the corresponding FA solution (red).

with linear reaction term S is suitable whereby it should be mentioned that realistic reactive source terms are usually highly nonlinear. Figure 3.14 shows solutions of the full extended linear model (blue) starting from several initial values all converging towards the red colored reduced model (FA).

3.6 Searching for a Suitable Reduced Reaction–Diffusion Equation

As demonstrated in the previous section, the FA of a reaction–diffusion equation is not suitable and thus not appropriate for the usage as reduced reaction–diffusion model. This is why the FA has to be modified or, more precisely, a **modified species reconstruction function** $\tilde{h} =$
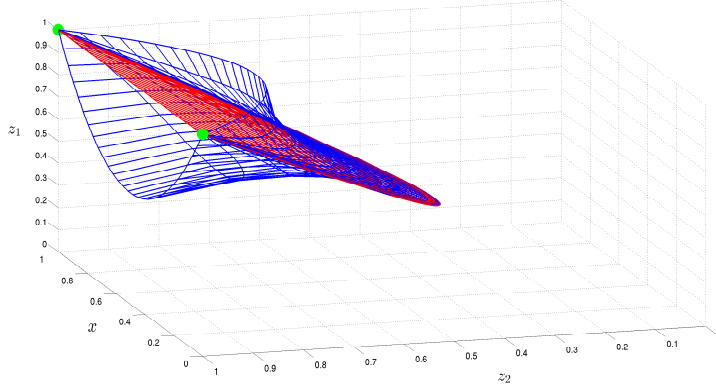
Figure 3.14: Solutions of the full extended linear model (blue) starting from several initial values all converging towards the red colored solution of the reduced model (FA). Here, $\gamma = 5.0$ and $\mathcal{D}_1 = \mathcal{D}_2 = 0.1$.

$\tilde{h}\left(h(z_{\mathrm{rpv}}), z_{\mathrm{rpv}}, x\right)$ is needed depending on the species reconstruction function resulting from the pure reaction case as well as z_{rpv} and x such that

$$z_k(t, x) = \tilde{h}\left(h(z_{\mathrm{rpv}}(t, x)), z_{\mathrm{rpv}}(t, x), x\right), \quad k \notin \mathcal{I}_{\mathrm{fixed}}, \; j \in \mathcal{I}_{\mathrm{fixed}} \tag{3.70}$$

results in a suitable reduced model with regard to the corresponding full reaction–diffusion model. As in the homogeneous case, $\tilde{h}^{\mathrm{app}}$ denotes the approximated modified species reconstruction function, since there is no method to find the exact one for the reaction–diffusion case in general so far. In the following, three approaches for a specific choice of $\tilde{h}^{\mathrm{app}}$ are listed from which the latter two have been proposed within the scope of this work.

3.6.1 Close–Parallel Assumption

The **close–parallel assumption (CPA)** was introduced in [TP02] and improved and developed by Ren et al. in [RP06, RP07, RPV$^+$07]. It states that the composition in the reduced description of an inhomogeneous combustion process, which is described in terms of the reduced composition variables z_{rpv}, is drawn onto another manifold that is close by and similar in structure to that, i.e. the compositions are assumed to lie on a low-dimensional manifold which is close to and parallel to the chemistry-based SIM. Thus, these compositions can be expressed by

$$z(t, x) = \begin{pmatrix} z_{\mathrm{rpv}}(t, x) \\ \tilde{h}\left(h\left(z_{\mathrm{rpv}}(t, x)\right), z_{\mathrm{rpv}}(t, x), x\right) \end{pmatrix} = \begin{pmatrix} z_{\mathrm{rpv}}(t, x) \\ h\left(z_{\mathrm{rpv}}(t, x)\right) + \delta z_{\mathrm{nrpv}}(t, x) \end{pmatrix} \tag{3.71}$$

where δz_{nrpv} is the departure from the SIM represented by the species reconstruction function h, i.e. $\delta z_{\mathrm{nrpv}} = z_{\mathrm{nrpv}} - h(z_{\mathrm{rpv}})$. Hence, when the reduced composition variables are used to

represent the reaction–diffusion system, the exact evolution equation for z_{rpv} (3.60a) results in

$$\partial_t z_{\mathrm{rpv}}(t,x) = \mathcal{D}_{\mathrm{rpv}} \partial_{xx}^2 z_{\mathrm{rpv}}(t,x) + S_{\mathrm{rpv}}\left(z_{\mathrm{rpv}}(t,x), h\left(z_{\mathrm{rpv}}(t,x)\right) + \delta z_{\mathrm{nrpv}}(t,x)\right) \quad (3.72)$$

when using (3.71). The assumption that $\begin{pmatrix} z_{\mathrm{rpv}} & z_{\mathrm{nrpv}} \end{pmatrix}^\top$ is close to $\begin{pmatrix} z_{\mathrm{rpv}} & h(z_{\mathrm{rpv}}) \end{pmatrix}^\top$ implies δz_{nrpv} being small and hence, the reactive term on the right-hand side of Equation (3.72) can be well approximated by the TAYLOR series of first order

$$S_{\mathrm{rpv}}\left(z_{\mathrm{rpv}}, h(z_{\mathrm{rpv}}) + \delta z_{\mathrm{nrpv}}\right) \approx S_{\mathrm{rpv}}\left(z_{\mathrm{rpv}}, h(z_{\mathrm{rpv}})\right) + \partial_{z_{\mathrm{nrpv}}} S_{\mathrm{rpv}}\Big|_{z_{\mathrm{nrpv}}=h(z_{\mathrm{rpv}})} \cdot \delta z_{\mathrm{nrpv}}$$
$$(3.73)$$

where $\partial_{z_{\mathrm{nrpv}}} S_{\mathrm{rpv}}\big|_{z_{\mathrm{nrpv}}=h(z_{\mathrm{rpv}})}$ is the $m_{\mathrm{rpv}} \times (m - m_{\mathrm{rpv}})$ matrix $\left(\partial_{z_j} S_i\right)_{i=1,\dots,m_{\mathrm{rpv}}, j=m_{\mathrm{rpv}}+1,\dots,m}$ evaluated at $z_{\mathrm{nrpv}} = h(z_{\mathrm{rpv}})$. Herewith (when assuming equality) the Evolution Equation (3.72) results in

$$\partial_t z_{\mathrm{rpv}} = \mathcal{D}_{\mathrm{rpv}} \partial_{xx}^2 z_{\mathrm{rpv}} + S_{\mathrm{rpv}}\left(z_{\mathrm{rpv}}, h(z_{\mathrm{rpv}})\right) + \partial_{z_{\mathrm{nrpv}}} S_{\mathrm{rpv}}\Big|_{z_{\mathrm{nrpv}}=h(z_{\mathrm{rpv}})} \cdot \delta z_{\mathrm{nrpv}}. \quad (3.74)$$

The unknown perturbation δz_{nrpv} can be obtained by using $N(z_{\mathrm{rpv}})$, which is an $m \times (m - m_{\mathrm{rpv}})$ orthogonal matrix spanning the normal subspace of the manifold at $\begin{pmatrix} z_{\mathrm{rpv}} & h(z_{\mathrm{rpv}}) \end{pmatrix}^\top$. Considering the reaction–diffusion system in the normal subspace, with $z = \begin{pmatrix} z_{\mathrm{rpv}} & h(z_{\mathrm{rpv}}) + \delta z_{\mathrm{nrpv}} \end{pmatrix}^\top$, we have

$$N^\top(z_{\mathrm{rpv}}) \begin{pmatrix} \partial_t z_{\mathrm{rpv}} \\ \partial_t(h(z_{\mathrm{rpv}}) + \delta z_{\mathrm{nrpv}}) \end{pmatrix} = N^\top(z_{\mathrm{rpv}}) \begin{pmatrix} \mathcal{D}_{\mathrm{rpv}} \partial_{xx}^2 z_{\mathrm{rpv}} \\ \mathcal{D}_{\mathrm{nrpv}} \partial_{xx}^2 \left(h(z_{\mathrm{rpv}}) + \delta z_{\mathrm{nrpv}}\right) \end{pmatrix}$$
$$+ N^\top(z_{\mathrm{rpv}}) \begin{pmatrix} S_{\mathrm{rpv}}\left(z_{\mathrm{rpv}}, h(z_{\mathrm{rpv}}) + \delta z_{\mathrm{nrpv}}\right) \\ S_{\mathrm{nrpv}}\left(z_{\mathrm{rpv}}, h(z_{\mathrm{rpv}}) + \delta z_{\mathrm{nrpv}}\right) \end{pmatrix}.$$
$$(3.75)$$

The CPA amounts to the approximation (based on the assumptions 'close' and 'parallel' to the chemistry-based SIM)

$$N^\top(z_{\mathrm{rpv}}) \begin{pmatrix} 0 \\ \partial_t \delta z_{\mathrm{nrpv}} \end{pmatrix} \approx 0 \quad (3.76)$$

which indicates a simplification of Equation (3.75), namely

$$0 \approx N^\top(z_{\mathrm{rpv}}) \begin{pmatrix} \mathcal{D}_{\mathrm{rpv}} \partial_{xx}^2 z_{\mathrm{rpv}} \\ \mathcal{D}_{\mathrm{nrpv}} \partial_{xx}^2 \left(h(z_{\mathrm{rpv}}) + \delta z_{\mathrm{nrpv}}\right) \end{pmatrix}$$
$$+ N^\top(z_{\mathrm{rpv}}) \begin{pmatrix} S_{\mathrm{rpv}}\left(z_{\mathrm{rpv}}, h(z_{\mathrm{rpv}}) + \delta z_{\mathrm{nrpv}}\right) \\ S_{\mathrm{nrpv}}\left(z_{\mathrm{rpv}}, h(z_{\mathrm{rpv}}) + \delta z_{\mathrm{nrpv}}\right) \end{pmatrix}$$
$$(3.77)$$

3. Spatially Inhomogeneous Systems: Inertial Manifold Computation

since $N^\top(z_{\mathrm{rpv}}) \begin{pmatrix} \partial_t z_{\mathrm{rpv}} & \partial_t h(z_{\mathrm{rpv}}) \end{pmatrix}^\top$ is exactly zero. As the terms on the right-hand side of Equation (3.77) are the components of molecular diffusion and chemical reactions in the normal subspace, respectively, there is a balance between both of them. Under the assumption that $\begin{pmatrix} z_{\mathrm{rpv}} & z_{\mathrm{nrpv}} \end{pmatrix}^\top$ is close and parallel to $\begin{pmatrix} z_{\mathrm{rpv}} & h(z_{\mathrm{rpv}}) \end{pmatrix}^\top$, a further simplification is performed by TAYLOR approximation

$$
\begin{aligned}
0 \approx & N^\top(z_{\mathrm{rpv}}) \begin{pmatrix} \mathcal{D}_{\mathrm{rpv}} \partial_{xx}^2 z_{\mathrm{rpv}} \\ \mathcal{D}_{\mathrm{nrpv}} \partial_{xx}^2 (h(z_{\mathrm{rpv}})) \end{pmatrix} + N^\top(z_{\mathrm{rpv}}) \begin{pmatrix} S_{\mathrm{rpv}}(z_{\mathrm{rpv}}, h(z_{\mathrm{rpv}})) \\ S_{\mathrm{nrpv}}(z_{\mathrm{rpv}}, h(z_{\mathrm{rpv}})) \end{pmatrix} \\
& + N^\top(z_{\mathrm{rpv}}) \begin{pmatrix} \partial_{z_{\mathrm{nrpv}}} S_{\mathrm{rpv}} \big|_{z_{\mathrm{nrpv}}=h(z_{\mathrm{rpv}})} \\ \partial_{z_{\mathrm{nrpv}}} S_{\mathrm{nrpv}} \big|_{z_{\mathrm{nrpv}}=h(z_{\mathrm{rpv}})} \end{pmatrix} \delta z_{\mathrm{nrpv}}
\end{aligned}
\tag{3.78}
$$

where $\partial_{z_{\mathrm{nrpv}}} S_{\mathrm{nrpv}} \big|_{z_{\mathrm{nrpv}}=h(z_{\mathrm{rpv}})}$ is defined in accordance to $\partial_{z_{\mathrm{nrpv}}} S_{\mathrm{rpv}}$ as $\left(\partial_{z_j} S_i\right)_{i,j=m_{\mathrm{rpv}}+1,\dots,m}$ evaluated at $z_{\mathrm{nrpv}} = h(z_{\mathrm{rpv}})$. The second term on the right-hand side of Equation (3.78) is equal to zero since the invariance property of the corresponding SIM is required. From this, an expression for the perturbation δz_{nrpv} is achieved by manipulating (3.78) yielding

$$
\delta z_{\mathrm{nrpv}} = -\left(N^\top \begin{pmatrix} \partial_{z_{\mathrm{nrpv}}} S_{\mathrm{rpv}} \big|_{z_{\mathrm{nrpv}}=h(z_{\mathrm{rpv}})} \\ \partial_{z_{\mathrm{nrpv}}} S_{\mathrm{nrpv}} \big|_{z_{\mathrm{nrpv}}=h(z_{\mathrm{rpv}})} \end{pmatrix} \right)^{-1} \cdot N^\top \begin{pmatrix} \mathcal{D}_{\mathrm{rpv}} \partial_{xx}^2 z_{\mathrm{rpv}} \\ \mathcal{D}_{\mathrm{nrpv}} \partial_{xx}^2 (h(z_{\mathrm{rpv}})) \end{pmatrix}
\tag{3.79}
$$

which in turn can be substituted into (3.74) resulting in an evolution equation for the reduced composition variable z_{rpv}

$$
\partial_t z_{\mathrm{rpv}} = \mathcal{D}_{\mathrm{rpv}} \partial_{xx}^2 z_{\mathrm{rpv}} + S_{\mathrm{rpv}}(z_{\mathrm{rpv}}, h(z_{\mathrm{rpv}})) + H^\top \mathcal{D}_{\mathrm{rpv}} \partial_{xx}^2 z_{\mathrm{rpv}}
\tag{3.80}
$$

with $H^\top \equiv -\partial_{z_{\mathrm{nrpv}}} S_{\mathrm{rpv}} \left(N^\top \begin{pmatrix} \partial_{z_{\mathrm{nrpv}}} S_{\mathrm{rpv}} \\ \partial_{z_{\mathrm{nrpv}}} S_{\mathrm{nrpv}} \end{pmatrix} \right)^{-1} N^\top$. Compared to the FA (blue), the CPA provides one extra term (red) that arises from the diffusion–chemistry coupling:

$$
\textcolor{blue}{\partial_t z_{\mathrm{rpv}} = \mathcal{D}_{\mathrm{rpv}} \partial_{xx}^2 z_{\mathrm{rpv}} + S_{\mathrm{rpv}}(z_{\mathrm{rpv}}, h(z_{\mathrm{rpv}}))} + \textcolor{red}{H^\top \mathcal{D}_{\mathrm{rpv}} \partial_{xx}^2 z_{\mathrm{rpv}}}
\tag{3.81a}
$$

$$
\textcolor{blue}{z_{\mathrm{nrpv}} = h(z_{\mathrm{rpv}})} + \textcolor{red}{\delta z_{\mathrm{nrpv}}}.
\tag{3.81b}
$$

For the purpose of illustration, the CPA of the extended DAVIS–SKODJE model is computed. For $\mathcal{I}_{\mathrm{fixed}} = \{1\}$, $S_1 = -z_1$, $S_2 = -\tilde{\gamma} z_2 + \frac{(\tilde{\gamma}-1)z_1 + \tilde{\gamma} z_1^2}{(1+z_1)^2}$, and $z_2 = h(z_1) = \frac{z_1}{z_1+1}$, the perturbation

δz_2 results in (cf. (3.79))

$$
\begin{aligned}
\delta z_2 = &-\left(\left(-\tilde{\gamma}\frac{z_1}{z_1+1} + \frac{(\tilde{\gamma}-1)z_1+\tilde{\gamma}z_1^2}{(1+z_1)^2} \quad z_1\right)\begin{pmatrix} 0 \\ -\tilde{\gamma} \end{pmatrix}\right)^{-1} \\
&\cdot \left(-\tilde{\gamma}\frac{z_1}{z_1+1} + \frac{(\tilde{\gamma}-1)z_1+\tilde{\gamma}z_1^2}{(1+z_1)^2} \quad z_1\right)\begin{pmatrix} \mathcal{D}_1\partial_{xx}^2 z_1 \\ \mathcal{D}_2\partial_{xx}^2\left(\frac{z_1}{z_1+1}\right) \end{pmatrix} \\
= &-\frac{\mathcal{D}_1\partial_{xx}^2 z_1}{\tilde{\gamma}(1+z_1)^2} + \frac{\mathcal{D}_2\partial_{xx}^2\left(\frac{z_1}{z_1+1}\right)}{\tilde{\gamma}},
\end{aligned}
\tag{3.82}
$$

wherefrom directly the CPA arises

$$\partial_t z_1 = -z_1 + \mathcal{D}_1\partial_{xx}^2 z_1 + 0 \tag{3.83a}$$

$$z_2 = \underbrace{\frac{z_1}{z_1+1} - \frac{\mathcal{D}_1\partial_{xx}^2 z_1}{\tilde{\gamma}(1+z_1)^2} + \frac{\mathcal{D}_2\partial_{xx}^2\left(\frac{z_1}{z_1+1}\right)}{\tilde{\gamma}}}_{\tilde{h}^{\mathrm{app}}}. \tag{3.83b}$$

As can easily be seen, for decreasing values of $\mathcal{D}_1$ as well as $\mathcal{D}_2$ the CPA and the FA become increasingly similar confirming the statement from [RP06] that the CPA becomes more and more suitable for decreasing diffusion. Nevertheless, based on the approximations the CPA makes use of, $\tilde{h}^{\mathrm{app}} = h + \delta z_{\mathrm{nrpv}}$ does not coincide with the exact $\tilde{h}$ which is why the CPA is no suitable reduced reaction–diffusion model.

3.6.2 Convex Combination

Another proposal for finding a suitable reduced description has already been motivated in Section 3.5. Here, the non RPVs are approximated by a convex combination of the species reconstruction function h resulting from the pure reaction case and the direct line connecting the equilibrium with the diffusion line (depending on x). Furthermore, it is conceivable that the coefficients $\theta(x)$ may also depend on time t, which results in an approximated modified species reconstruction function given by

$$\tilde{h}^{\mathrm{app}}\left(h(z_{\mathrm{rpv}}), z_{\mathrm{rpv}}, x\right) = \theta(t,x)h(z_{\mathrm{rpv}}) + (1-\theta(t,x))d(z_{\mathrm{rpv}}, x) \tag{3.84}$$

with $\theta(t,x) \in [0,1]$ and d being the direct line mentioned above (red dashed in Figure 3.10(b)). In case of the extended DAVIS–SKODJE model with boundary values given by $z_1(t,0) = z_1(t,1) = 1.0$ and $z_2(t,0) = z_2(t,1) = 0.5$, this function d is given by

$$d(z_1, x) = \frac{z_1}{2} \tag{3.85}$$

as seen before in Section 3.5. In this context, the determination of $\theta(t,x)$ is the most difficult challenge and will not be part of this work, but in the authors opinion, the correct choice of

$\theta(t, x)$ can lead to equality between $\tilde{h}^{\mathrm{app}}$ given by Equation 3.84 and the exact modified species reconstruction function $\tilde{h}$ being the consequence that a suitable reduced reaction–diffusion equation can be identified.

3.6.3 Disturbed Species Reconstruction Function

The second proposal presented novelly in this work is what we call **disturbed species reconstruction function**. This function is motivated by Figure 3.10(a) and describes the species reconstruction function h modified at each point along the SIM by a disturbance into the direction of the connection to the diffusion line. This is schematically illustrated in Figure 3.15(a), where the blue dashed curve represents the SIM and the red dashed lines the direct connection between a point on the SIM and the diffusion line (evaluated at the repective value of x) represented by the red cross. The green curve visualizes the resulting disturbed species reconstruction function which is used as approximated modified function $\tilde{h}^{\mathrm{app}}$. For reasons of clarification, the disturbed species reconstruction function is illustrated again by means of the extended DAVIS–SKODJE model with boundary values given exemplarily by $z_1(t, 0) = z_1(t, 1) = 1.0$ and $z_2(t, 0) = z_2(t, 1) = 0.5$. Afterwards, with this knowledge, this idea can be generalized to other reaction–diffusion equations and/or boundary values. The vector pointing towards the diffusion line starting from a point on the SIM $\left(z_1 \quad h(z_1) = \frac{z_1}{z_1+1} \right)^{\top}$ (blue cross in Figure 3.15(b)) is given by $\tilde{\theta}(t, x) \left(1 - z_1 \quad 0.5 - \frac{z_1}{z_1+1} \right)^{\top}$ such that the resulting point $\left(z_1^{\mathrm{new}} \quad z_2^{\mathrm{new}} \right)^{\top}$ (red thick cross) lying on the disturbed species reconstruction function is given by

$$\begin{pmatrix} z_1^{\mathrm{new}} \\ z_2^{\mathrm{new}} \end{pmatrix} := \begin{pmatrix} z_1 \\ \frac{z_1}{z_1+1} \end{pmatrix} + \tilde{\theta}(t, x) \begin{pmatrix} 1 - z_1 \\ 0.5 - \frac{z_1}{z_1+1} \end{pmatrix} \tag{3.86}$$

yielding

$$z_2^{\mathrm{new}} = \frac{z_1^{\mathrm{new}} - \tilde{\theta}}{z_1^{\mathrm{new}} - 2\tilde{\theta} + 1} + \tilde{\theta} \left(0.5 - \frac{z_1^{\mathrm{new}} - \tilde{\theta}}{z_1^{\mathrm{new}} - 2\tilde{\theta} + 1} \right). \tag{3.87}$$

As a consequence, the disturbed species reconstruction function serving as example for an approximated modified species reconstruction function results in

$$\tilde{h}^{\mathrm{app}} = \frac{z_1 - \tilde{\theta}}{z_1 - 2\tilde{\theta} + 1} + \tilde{\theta} \left(0.5 - \frac{z_1 - \tilde{\theta}}{z_1 - 2\tilde{\theta} + 1} \right). \tag{3.88}$$

Here as well, the biggest challenge is to determine $\tilde{\theta}(t, x)$ which is not discussed as part of this work. Neverthesless, it is very probable that a correct specification of $\tilde{\theta} = \tilde{\theta}(t, x)$ provides a suitable reduced reaction–diffusion equation.
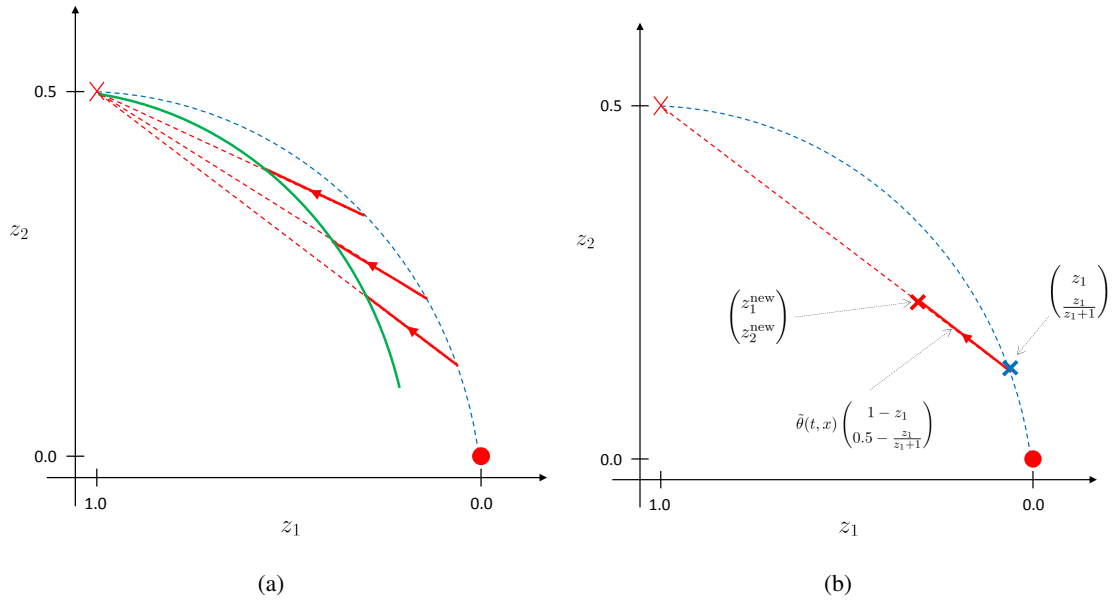
Figure 3.15: Schematic illustration of the disturbed species reconstruction function.

3.7 Inertial Manifold Computation

Just as the species reconstruction function h defines a specific manifold, the SIM, the modified species reconstruction function $\tilde{h}$, which is used as reduced description of inhomogeneous combustion processes comprising an interplay between reactive and diffusive processes, defines a specific manifold as well—the **inertial manifold (IM)**. Especially in the 1980s, IMs have been introduced and analyzed in relation to the study of the long-term behavior of solutions of dissipative evolution problems (see e.g. [FST88, MS88, Tem90]). Most of the dynamics for the system takes place on an IM, which is why a considerable simplification in the study of the dynamics can be achieved. Thus, the reduced description of the full model equation—the **inertial system**—reproduces most of the dynamical properties of the corresponding initial system. Furthermore, if an IM exists, it is a finite dimensional (even if the respective initial system is infinite dimensional), invariant, and asymptotically stable manifold [Tem90]. Statements about existence of IMs can be found in [FST88, MS88], where the most restrictive requirement for an IM to exist is the **spectral gap condition** (see e.g. [MS88]). Furthermore, this spectral gap condition applied to a reaction–diffusion system of the form

$$\partial_t z(t, x) = \mathcal{D}\partial_{xx}^2 z(t, x) + S(z(t, x)), \quad x \in \mathbb{R} \tag{3.89}$$

yields the existence of an IM for every $\mathcal{D} > 0$ with DIRICHLET or NEUMANN boundary conditions given on the interval $[0, 1]$ (cf. [FST88, MS88]). Consequently, for all reaction–diffusion systems regarded within this work the existence of an IM is ensured.

115

3. Spatially Inhomogeneous Systems: Inertial Manifold Computation

Up to now, one way towards the reduction of an inhomogeneous reaction–convection–diffusion equation model is known as part of this work so far, particularly the one where the full system (= initial system) consisting of reaction processes as well as physical transport in form of convection and diffusion is simplified to a homogeneous pure reaction model—the full reaction system comprising slow and fast modes. Afterwards, a SIM is approximated comprising the slow modes of the system yielding the reduced reaction system. This SIM approximation is discussed extensively in Chapter 2 and is already well understood. In contrast, the way to get from the reduced reaction system to the reduced system (= inertial system) remains widely unexplored, whereas this work presents novel ideas on the basis of extensive research concerning this aspect, which is demonstrated as part of Chapter 3 up to here. This procedure is visualized in Figure 3.16 by the blue lower half of the diagram. More precisely, the initial system is given
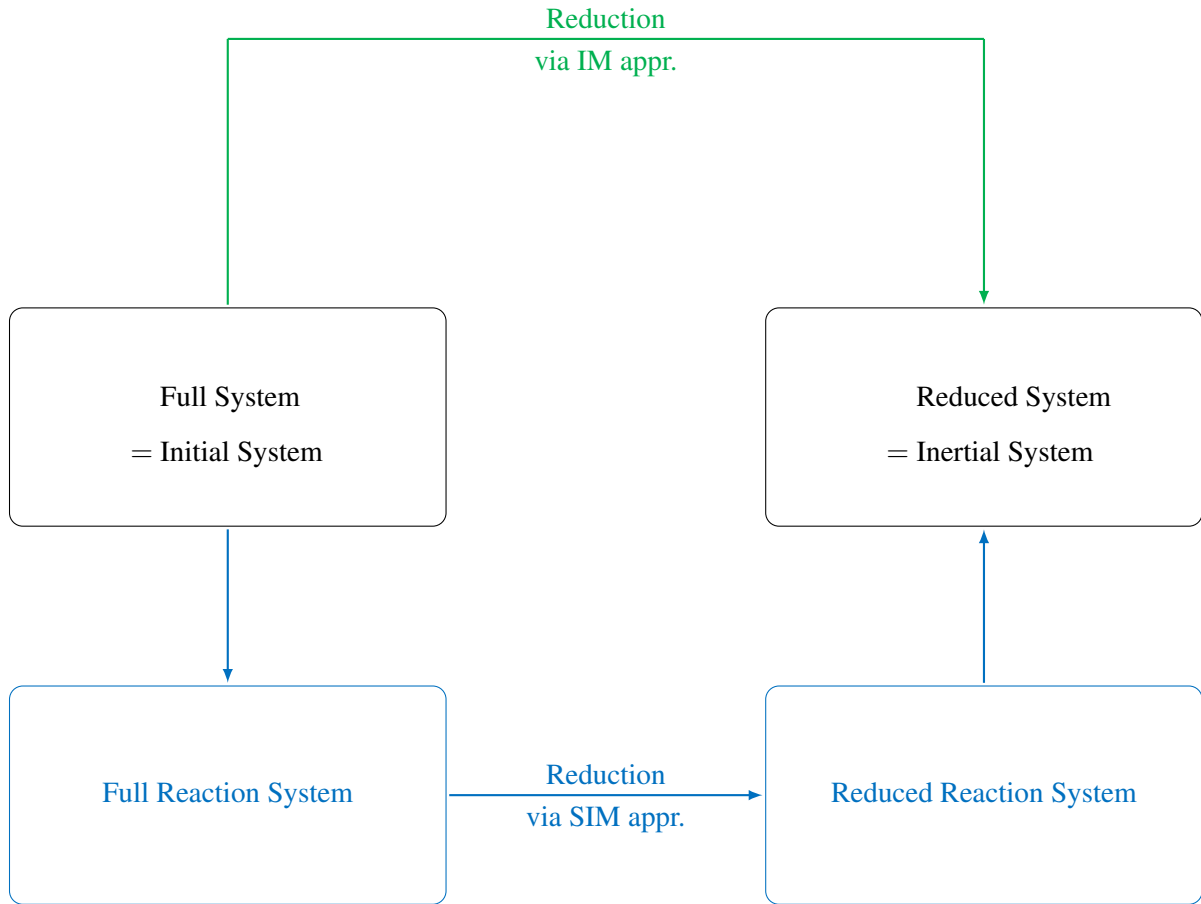

Figure 3.16: Schematic illustration of two ways of model reduction: SIM approximation and IM approximation.

by a reaction–convection–diffusion equation of the following form

$$\partial_t z(t, x) = -\bar{v} \partial_x z(t, x) + \mathcal{D} \partial_{xx}^2 z(t, x) + S(z(t, x)) \tag{3.90}$$

wherefrom the full reaction system can easily be derived by omitting both the convection as well as the diffusion term yielding the spatially homogeneous system of ODEs

$$\partial_t z(t, x) = S(z(t, x)). \tag{3.91}$$

This system in turn is reduced via computation of a SIM represented by a species reconstruction function h which results in the reduced reaction system

$$\partial_t z_{\text{rpv}}(t, x) = S(z(t, x)) \tag{3.92}$$

$$z_{\text{nrpv}}(t, x) = h(z_{\text{rpv}}(t, x)). \tag{3.93}$$

After this, the challenge is to find a function $\tilde{h} = \tilde{h}(h(z_{\text{rpv}}), z_{\text{rpv}}, x)$ that represents the IM leading finally to the inertial system

$$\partial_t z_{\text{rpv}}(t, x) = -\bar{v} \partial_x z_{\text{rpv}}(t, x) + \mathcal{D} \partial_{xx}^2 z_{\text{rpv}}(t, x) + S(z(t, x)) \tag{3.94}$$

$$z_{\text{nrpv}}(t, x) = \tilde{h}\left(h(z_{\text{rpv}}), z_{\text{rpv}}, x\right). \tag{3.95}$$

The question that arises here is:

> Is it necessary to take this indirect route (initial system → full reaction system → reduced reaction system → inertial system) or is it possible to take the direct one (initial system → inertial system) via approximation of an IM?
> (cf. Figure 3.16)

The research concerning this issue (i.e. how to approximate an IM directly) is still in its initial phase, which is why there are just a few approaches dealing with this problem. The reason for this is not only based on the more difficult complexity concerned with system of PDEs in contrast to system of ODEs, but also that there is no test model available so far (to the author's knowledge) where the IM is analytically known. As a consequence, it is hardly possible to estimate the accuracy of the result of the respective approach, i.e. of the approximated IM. Nevertheless, two approaches for IM approximation that already exist are presented in the following, whereas the third one, which is based on the boundary–value–concept presented in 2.6, is novelly presented as part of this work.

3.7.1 Reaction Diffusion Manifold (REDIM) Method

The effect, that applying the same transport operator for a reduced model as for the corresponding full one without a proper projection, while the source term is replaced by a reduced chemistry model, can lead to inaccurate results, was also recognized by MAAS et al. in 2007. This problem is exposed in [BM07b], where the **method of reaction diffusion manifolds (REDIM)** for automatic reduction of chemical kinetic models depending on transport properties is presented

3. Spatially Inhomogeneous Systems: Inertial Manifold Computation

as suggested solution approach. This method is supposed to allow to incorporate the effect of coupling of reaction and diffusion processes into the computation of a manifold-based reduced model. Based on a general reaction–diffusion equation

$$\partial_t z = \mathcal{D}\partial_{xx}^2 z + S(z) \tag{3.96}$$

the system solution is supposed to be on a manifold defined by an explicit function $z(z_{\mathrm{rpv}})$

$$M = \{z \mid z = z(z_{\mathrm{rpv}}), z \colon \mathbb{R}^{m_{\mathrm{rpv}}} \to \mathbb{R}^m\} \tag{3.97}$$

where z_{rpv} parameterizes the manifold. Here, M is defined as an invariant system manifold if at any point $z \in M$ the vector field of (3.96) defined by its right-hand side belongs to the tangent space $T_z M$ of M. Consequently, it holds that[16]

$$\left(z_{z_{\mathrm{rpv}}}^{\perp}(z_{\mathrm{rpv}})\right)^{\top} \cdot \left(\mathcal{D}\partial_{xx}^2 z + S(z)\right) \equiv 0 \tag{3.98}$$

with $z_{z_{\mathrm{rpv}}}^{\perp}$ being the normal space to the manifold: $\left(z_{z_{\mathrm{rpv}}}^{\perp}\right)^{\top} \cdot z_{z_{\mathrm{rpv}}} \equiv 0$. In terms of a projection operator onto the normal space $P_{(TM)^{\perp}} = I - z_{z_{\mathrm{rpv}}} z_{z_{\mathrm{rpv}}}^{+}$ of M this condition becomes

$$\left(I - z_{z_{\mathrm{rpv}}} z_{z_{\mathrm{rpv}}}^{+}\right) \cdot \left(\mathcal{D}\partial_{xx}^2 z + S(z)\right) = 0, \tag{3.99}$$

where $z_{z_{\mathrm{rpv}}}^{+}$ is the MOORE–PENROSE pseudo inverse of $z_{z_{\mathrm{rpv}}}$ (see [GL89]) defined for a regular matrix $z_{z_{\mathrm{rpv}}}^{\top} \cdot z_{z_{\mathrm{rpv}}}$ by

$$z_{z_{\mathrm{rpv}}}^{+} = \left(z_{z_{\mathrm{rpv}}}^{\top} \cdot z_{z_{\mathrm{rpv}}}\right)^{-1} \cdot z_{z_{\mathrm{rpv}}}^{\top}. \tag{3.100}$$

This equation system is a key relation with respect to the REDIM method and it is used as a basis to find an approximation for the reduced manifold. In order to solve this manifold equation (3.99) a reformulation in terms of a multi-dimensional parabolic system of PDEs for $z = z(z_{\mathrm{rpv}}, t)$ is suggested

$$\partial_t z(z_{\mathrm{rpv}}) = \left(I - z_{z_{\mathrm{rpv}}}(z_{\mathrm{rpv}})z_{z_{\mathrm{rpv}}}^{+}(z_{\mathrm{rpv}})\right) \cdot \left(\mathcal{D}\partial_{xx}^2 z(z_{\mathrm{rpv}}) + S(z(z_{\mathrm{rpv}}))\right) \tag{3.101}$$

such that the stationary solution $z(z_{\mathrm{rpv}}, \infty)$ defines the desired manifold. This system in turn is integrated starting from an initial guess for the invariant manifold given by the extended ILDM approach [BM07a] until convergence of the solution. As a consequence, the system dynamics is completely confined on the manifold. It is important to note that the assumption $z(t, x) = z(z_{\mathrm{rpv}}(t, x))$ is not generally valid and used as an approximation. A further problem results from the dependence of the transport part $\mathcal{D}\partial_{xx}^2 z(z_{\mathrm{rpv}})$ on the gradient of the manifold parameterizing

---

[16]The notation $z_{z_{\mathrm{rpv}}}$ represents the JACOBIAN and thus, it is defined by $z_{z_{\mathrm{rpv}}} := \left(\partial_{z_{\mathrm{rpv}j}} z_i\right)_{i=1,\ldots,m;\ j=1,\ldots,m_{\mathrm{rpv}}}$.

parameter z_{rpv} (see e.g. [BM07b]). To avoid this problem, the following modification of the evolution equation (3.101) is suggested:

$$\partial_t z(z_{\mathrm{rpv}}) = \left(I - z_{z_{\mathrm{rpv}}} z_{z_{\mathrm{rpv}}}^+\right) \cdot \left(\mathcal{D}\|z_{z_{\mathrm{rpv}}}^\top \partial_x z\|^2 \frac{1}{m_{\mathrm{rpv}}}\mathrm{Tr}(A) + S(z)\right) \tag{3.102}$$

with

$$(\mathrm{Tr}(A))_i = \sum_j z_{z_{\mathrm{rpv}_j}}^i z_{z_{\mathrm{rpv}_j}} \left(z_{z_{\mathrm{rpv}_j}}^\top z_{z_{\mathrm{rpv}_j}}\right)^{-2}, \quad z_{z_{\mathrm{rpv}_j}}^\top z_{z_{\mathrm{rpv}_j}} = \sum_k \left(\partial_{z_{\mathrm{rpv}_j}} z_k\right)^2. \tag{3.103}$$

Accordingly, this modified invariance equation (3.102) defines the REDIM and contains the impact of the diffusion through the modified diffusion term and the gradient $\partial_x z_{\mathrm{rpv}}$, which is now approximated by the norm of the original system gradient. In conclusion, it can be stated, that if the norm of the gradient is roughly known, then it is sufficient to approximate the reduced manifold with an acceptable level of accuracy. Furthermore, an application of the REDIM method to the extended DAVIS–SKODJE model can also be found in [BM07b].

3.7.2 Saddle Point Method (SPM) Extended to Reaction–Diffusion Systems

In [MP13], the SPM, already introduced in Section 2.1, is extended to reaction–diffusion equations. To briefly review the SPM applied to homogeneous systems: branches of a one-dimensional SIM are identified as heteroclinic orbits connecting equilibria. After identifying all equilibria of the system, the heteroclinic orbit that connects a (generally nonphysical) saddle equilibrium with an unstable manifold (corresponding to a positive eigenvalue of its JACOBIAN) with the (physical) sink equilibrium represents a branch of a SIM. A perturbation from the saddle along its unstable eigenspace determines the initial value for the appropriate trajectory. This technique is extended to reaction–diffusion equations by identifying steady state solutions of the full system and connecting analogous orbits in the GALERKIN–projected space. More precisely, the full system including both a reaction as well as a diffusion term is transferred into a finite system of ODEs by applying the method of weighted residuals in form of a GALERKIN method. Thus, solutions of the full system dynamics are projected onto an **approximate inertial manifold (AIM)** (see [Tem97]). The low-dimensional system of ODEs resulting from the GALERKIN projection possesses equilibria that correspond to steady state solutions of the full reaction–diffusion equation system. Subsequently, a one-dimensional manifold can be constructed by using heteroclinic orbits connecting a non-physical steady state with a physical equilibrium. For more detailed information see [Men12, MP13].

3.7.3 Boundary–Value–Concept for Approximating Inertial Manifolds

As mentioned before, an IM has the property of being invariant and asymptotically stable. As in the spatially homogeneous case, these properties can be exploited in order to approximate an

3. Spatially Inhomogeneous Systems: Inertial Manifold Computation

IM by using the boundary–value–concept (cf. 2.6.3) transferred to reaction–diffusion equation systems. For a general IBVP of the form

$$\partial_t z(t, x) = \mathcal{D}\partial_{xx}^2 z(t, x) + S(z(t, x)) \qquad \text{in } (0, T) \times (x_s, x_f),\ 0 < T < \infty \qquad (3.104a)$$

$$z(0, x) = z^0(x) \qquad \text{in } (x_s, x_f) \qquad (3.104b)$$

$$z(t, x_s) = z_{x_s}(t) \qquad \text{in } (0, T) \qquad (3.104c)$$

$$z(t, x_f) = z_{x_f}(t) \qquad \text{in } (0, T) \qquad (3.104d)$$

the IM computation approach based on this boundary–value–concept is formulated novelly as part of this work as

$$\partial_t z(t, x) = \mathcal{D}\partial_{xx}^2 z(t, x) + S(z(t, x)) \qquad \text{in } (0, T) \times (x_s, x_f),\ 0 < T < \infty \qquad (3.105a)$$

$$z_{\text{rpv}}(0, x) = z_{\text{rpv}}^0(x) \qquad \text{in } (x_s, x_f) \qquad (3.105b)$$

$$z_{\text{nrpv}}(t_0, x) = z_{\text{nrpv}}^{t_0}(x) \qquad \text{in } (x_s, x_f) \qquad (3.105c)$$

$$z(t, x_s) = z_{x_s}(t) \qquad \text{in } (0, T) \qquad (3.105d)$$

$$z(t, x_f) = z_{x_f}(t) \qquad \text{in } (0, T) \qquad (3.105e)$$

where global asymptotical stability is assumed and $t_0 < 0$ in the reverse mode formulation. Using similar arguments as in the homogeneous case, an IM should be identified exactly for $t_0 \to -\infty$ regardless of the choice of $z_{\text{nrpv}}^{t_0}(x)$. Moreover, for a specific value of x the method coincides with the boundary–value–concept applied to homogeneous systems with the difference that no SIM is computed, but a part of the IM, which is drifted away from the SIM caused by the present diffusion effect. Therefore, it is possible to approximate an IM by discretizing System (3.105) in space and afterwards applying the Matlab® BVP solver bvp4c.

Applied to the DAVIS–SKODJE model, i.e. $S = \begin{pmatrix} S_1 & S_2 \end{pmatrix}^\top = \begin{pmatrix} -z_1 & -\tilde{\gamma}z_2 + \frac{(\tilde{\gamma}-1)z_1 + \tilde{\gamma}z_1^2}{(1+z_1)^2} \end{pmatrix}^\top$ together with $z_{\text{rpv}} = z_1$ and thus, $z_{\text{nrpv}} = z_2$, $x_s = 0$, $x_f = 1$, $z_{x_s}(t) = z_{x_f}(t) = \begin{pmatrix} 1.0 & 0.5 \end{pmatrix}^\top$, $z_1^0(x) = 0.8$, and $z_2^{t_0}(x) = 0.0$, System (3.105) reads

$$\partial_t z_1(t, x) = \mathcal{D}_1 \partial_{xx}^2 z_1(t, x) - z_1(t, x) \qquad (3.106a)$$

$$\partial_t z_2(t, x) = \mathcal{D}_2 \partial_{xx}^2 z_2(t, x) - \tilde{\gamma}z_2(t, x) + \frac{(\tilde{\gamma} - 1)z_1(t, x) + \tilde{\gamma}(z_1(t, x))^2}{(1 + z_1(t, x))^2} \qquad (3.106b)$$

$$z_1(0, x) = 0.8 \qquad (3.106c)$$

$$z_2(t_0, x) = 0.0 \qquad (3.106d)$$

$$z_1(t, 0) = 1.0 \qquad (3.106e)$$

$$z_2(t, 0) = 0.5 \qquad (3.106f)$$

$$z_1(t, 1) = 1.0 \qquad (3.106g)$$

$$z_2(t, 1) = 0.5. \qquad (3.106h)$$

Using a uniform discretization grid of the space interval $[0, 1]$ as depicted in the following

with a grid width of $h = \frac{1}{n+1}$, the **finite difference method** approximates the diffusion term of (3.106a), (3.106b) by

$$\partial_{xx}^2 z_j(t, x) \approx \frac{z_j(t, x - h) - 2z_j(t, x) + z_j(t, x + h)}{h^2}, \quad j = 1, 2. \tag{3.107}$$

Thus, System (3.106) is approximated by

$$\begin{pmatrix} \partial_t z_j^1(t) \\ \partial_t z_j^2(t) \\ \vdots \\ \partial_t z_j^{n-1}(t) \\ \partial_t z_j^n(t) \end{pmatrix} = \frac{\mathcal{D}_j}{h^2} \begin{pmatrix} -2 & 1 & 0 & \dots & 0 \\ 1 & -2 & 1 & \ddots & \vdots \\ 0 & \ddots & \ddots & \ddots & 0 \\ \vdots & \ddots & \ddots & \ddots & 1 \\ 0 & \dots & 0 & 1 & -2 \end{pmatrix} \begin{pmatrix} z_j^1(t) \\ z_j^2(t) \\ \vdots \\ z_j^{n-1}(t) \\ z_j^n(t) \end{pmatrix} + \begin{pmatrix} S_j + \frac{\mathcal{D}_j}{h^2} z_j^0(t) \\ S_j \\ \vdots \\ S_j \\ S_j + \frac{\mathcal{D}_j}{h^2} z_j^{n+1}(t) \end{pmatrix} \tag{3.108a}$$

$$\begin{pmatrix} z_1^1(0) \\ \vdots \\ z_1^2(0) \end{pmatrix} = \begin{pmatrix} 0.8 \\ \vdots \\ 0.8 \end{pmatrix} \tag{3.108b}$$

$$\begin{pmatrix} z_2^1(t_0) \\ \vdots \\ z_2^n(t_0) \end{pmatrix} = \begin{pmatrix} 0.0 \\ \vdots \\ 0.0 \end{pmatrix} \tag{3.108c}$$

where $j = 1, 2$ and $z_j^i(t) := z_j(t, x_i)$, $i = 1, \dots, n$. Accordingly, this BVP can be solved using bvp4c, where the results are presented in the following for $n = 10$. For an insignificant role of diffusion, i.e. for small values of $\mathcal{D}_1$ and $\mathcal{D}_2$ such as $\mathcal{D}_1 = \mathcal{D}_2 = 1.0 \cdot 10^{-3}$, the IM should be approximated well by the FA ($z_2 = \frac{z_1}{z_1+1}$) for $t_0 \to -\infty$, which is confirmed by the computed

values

$$
\begin{pmatrix} z_2^1(0) \\ z_2^2(0) \\ \vdots \\ z_2^9(0) \\ z_2^{10}(0) \end{pmatrix} = \begin{pmatrix} 0.2741 \\ 0.2718 \\ \vdots \\ 0.2718 \\ 0.2741 \end{pmatrix}
\tag{3.109a}
$$

$$
\begin{pmatrix} z_2^1(0) \\ z_2^2(0) \\ \vdots \\ z_2^9(0) \\ z_2^{10}(0) \end{pmatrix} = \begin{pmatrix} 0.4444 \\ 0.4444 \\ \vdots \\ 0.4444 \\ 0.4444 \end{pmatrix}
\tag{3.109b}
$$

for $\tilde{\gamma} = 10.0$, where (3.109a) results from (3.108) with $t_0 = -0.1$ and (3.109b) from (3.108) with $t_0 = -1.0$. Consequently, even for a small absolute value of $t_0 = -1.0$ the IM is approximated very well. For a more significant role of diffusion, i.e. $\mathcal{D}_1 = \mathcal{D}_2 = 1.0 \cdot 10^{-2}$, the BVP (3.108) results in values

$$
\begin{pmatrix} z_2^1(0) \\ z_2^2(0) \\ \vdots \\ z_2^9(0) \\ z_2^{10}(0) \end{pmatrix} = \begin{pmatrix} 0.4440 \\ 0.4444 \\ \vdots \\ 0.4444 \\ 0.4440 \end{pmatrix}
\tag{3.110}
$$

for $t_0 = -1.0$ and $\tilde{\gamma} = 10.0$. Here, the deviation of the IM from the FA becomes apparent, which confirms the studies from Section 3.5.

Obviously, this is far from being a proof for the identification of IMs via (3.105), but based on the fundamental idea and the very simple example demonstrated above it should be considered to continue this approach. Numerical improvements as well as comparisons of the results with other IM approximation methods, inter alia, belong to future research belonging to this IM computation method (3.105) based on the boundary–value–concept.

3.8 Neumann Boundary Conditions

Finally, the behavior of solutions to IBVPs of the reaction–diffusion equation with NEUMANN boundary values is analyzed, where we restrict to zero NEUMANN boundary conditions, i.e. the

problem is formulated as

$$\partial_t z(t, x) = \mathcal{D}\partial_{xx}^2 z(t, x) + S(z(t, x)) \tag{3.111a}$$

$$z(0, x) = z^0(x) \tag{3.111b}$$

$$\partial_x z(t, x_{\mathrm{s}}) = 0 \tag{3.111c}$$

$$\partial_x z(t, x_{\mathrm{f}}) = 0. \tag{3.111d}$$

Once again, for demonstration purposes, the extended DAVIS–SKODJE model is used in the following form

$$\partial_t z_1(t, x) = \mathcal{D}_1 \partial_{xx}^2 z_1(t, x) - z_1(t, x) \tag{3.112a}$$

$$\partial_t z_2(t, x) = \mathcal{D}_2 \partial_{xx}^2 z_2(t, x) - \tilde{\gamma} z_2(t, x) + \frac{(\tilde{\gamma} - 1)z_1(t, x) + \tilde{\gamma}(z_1(t, x))^2}{(1 + z_1(t, x))^2} \tag{3.112b}$$

$$z_1(0, x) = z_1^0(x) = 1 \tag{3.112c}$$

$$z_2(0, x) = z_2^0(x) \tag{3.112d}$$

$$\partial_x z_1(t, 0) = 0 \tag{3.112e}$$

$$\partial_x z_1(t, 1) = 0 \tag{3.112f}$$

$$\partial_x z_2(t, 0) = 0 \tag{3.112g}$$

$$\partial_x z_2(t, 1) = 0 \tag{3.112h}$$

where $\tilde{\gamma}$, $\mathcal{D}_1$, $\mathcal{D}_2$, and $z_2^0(x)$ have yet to be determined. As a first choice of the initial function, $z_2^0(x) = 0.5$ is chosen, where the solution plot resulting from the Matlab$^{\circledR}$ program pdepe is depicted in Figure 3.17, where the red line visualizes the initial function. What is remarkable
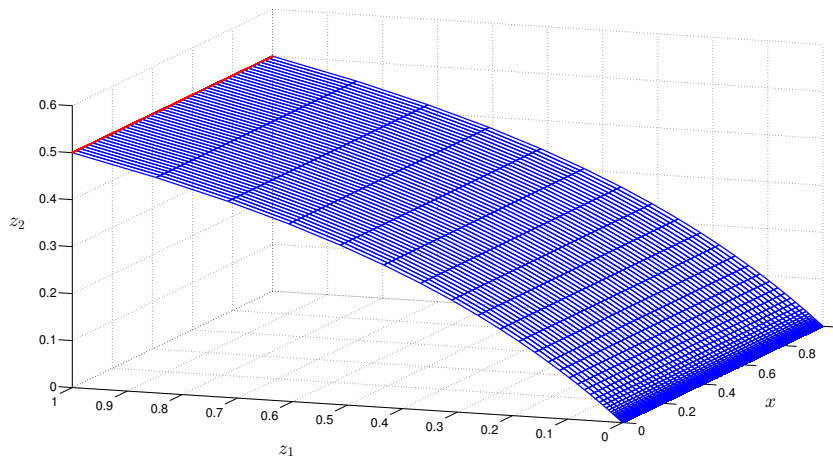

Figure 3.17: Solution of IBVP (3.112) for $z_2^0(x) = 0.5$.

here is the absolute coincidence with the corresponding FA for all admissible choices of $\tilde{\gamma}$, $\mathcal{D}_1$, and $\mathcal{D}_2$. The reason for this can be explained by analyzing other choices of $z_2^0(x)$. For this

purpose, another initial function is used in Figure 3.18(a)–(c), namely $z_2^0(x) = x^2 - 0.5x^4$. Here, $\tilde{\gamma}$ is fixed as $\tilde{\gamma} = 5.0$ and the diffusion coefficients vary between $\mathcal{D}_1 = \mathcal{D}_2 = 1.0 \cdot 10^{-3}$ and $\mathcal{D}_1 = \mathcal{D}_2 = 1.0 \cdot 10^1$, such that diffusion becomes more and more dominating over the reaction term. As can be seen, the diffusion forces the dynamics to a homogenization over space while

(a) Solution of IBVP (3.112) for $z_2^0(x) = x^2 - 0.5x^4$ together with $\tilde{\gamma} = 5.0$ and $\mathcal{D}_1 = \mathcal{D}_2 = 1.0 \cdot 10^{-3}$.

(b) Solution of IBVP (3.112) for $z_2^0(x) = x^2 - 0.5x^4$ together with $\tilde{\gamma} = 5.0$ and $\mathcal{D}_1 = \mathcal{D}_2 = 1.0 \cdot 10^{-1}$.

(c) Solution of IBVP (3.112) for $z_2^0(x) = x^2 - 0.5x^4$ together with $\tilde{\gamma} = 5.0$ and $\mathcal{D}_1 = \mathcal{D}_2 = 1.0 \cdot 10^1$.

(d) Solution of IBVP (3.112) for $z_1^0(x) = 2x^2 - x^4$ and $z_2^0(x) = x^2 - 0.5x^4$ together with $\tilde{\gamma} = 5.0$ and $\mathcal{D}_1 = \mathcal{D}_2 = 1.0 \cdot 10^1$.
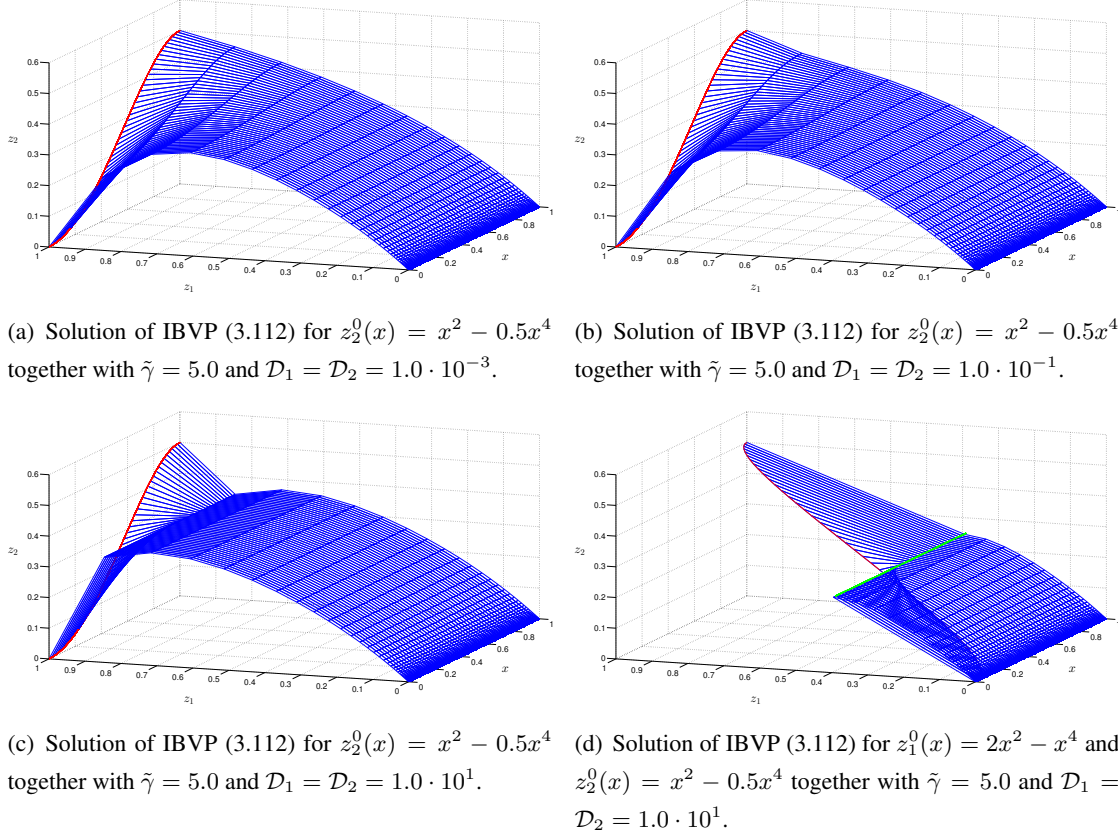
Figure 3.18: Solution of IBVP (3.112) for different values of $\mathcal{D}_1 = \mathcal{D}_2$. In Figure 3.18(d), the initial function $z_1^0(x)$ is changed from $z_1^0(x) = 1.0$ to $z_1^0(x) = 2x^2 - x^4$.

the reaction takes part. Especially in Figure 3.18(c), where the diffusion dominates significantly the reaction term, this can be observed, since the diffusion at first equalizes z_2 over x before the reaction shows effects as in the homogeneous case. This **homogenization line**, i.e. the line that describes the final state for $t \to \infty$ in absence of any reaction term, is an average value of the initial function. These statements are illustrated by Figure 3.18(d) where the initial function $z_1^0(x)$ is changed from $z_1^0(x) = 1.0$ to $z_1^0(x) = 2x^2 - x^4$. Here, the homogenization takes place not only with respect to z_2, but also with respect to z_1. Furthermore, the homogenization line is highlighted as green line.

Summarizing the above, it can be stated, that if the diffusion is slower than the fast modes of the reaction, the diffusion does not affect the behavior of the solution significantly, since the fast reaction modes have already ensured the homogenization along x. If the diffusion is faster

than the slow modes of the reactive term, the diffusion supports the homogenization which takes place anyway due to the fast reaction modes converging towards the SIM. Consequently, it can be stated, that the FA is an appropriate reduced description of a reaction–diffusion equation with zero NEUMANN boundary values, although it is not suitable by definition.

3.9 Interim Summary

In this chapter, fundamental studies concerning the reduction of reaction–convection–diffusion equations are performed. It turned out, that convection processes are without influence to the reduced chemistry-based reaction model being the consequence that it is sufficient to analyze the behavior of solutions to reaction–diffusion models. However, this case is not trivial. In this context, the fundamental behavior of solutions to reaction–diffusion models is analyzed. Furthermore, two ways of obtaining a reduced model of a combustion process are presented: on the one hand, the coupling of diffusion with the reduced reaction model and on the other hand, the direct reduction of the underlying PDE model, which is directly related to the problem of approximating inertial manifolds (IMs). For both ways, possible solution approaches are presented, whereby just fundamental ideas are proposed. Obviously, significantly more research is required for application to realistic combustion scenarios, but nevertheless, foundations for this have already been laid within this dissertation. This is particularly important since the future trend in reducing combustion processes is towards reducing the initial system directly, i.e. without regarding the chemical reaction part solely.

Summary and Conclusion

This dissertation deals with fundamental concepts concerning the reduction of multiscale combustion models. The reduction itself finds its motivation in the fact, that simulation of full model equations poses challenges due to complexity caused by an interplay between convective and diffusive species transport and chemical reaction processes and large dimension. Additionally, multiple time scales within the chemical reaction processes with time scales ranging from nanoseconds to seconds inducing high stiffness of the kinetic model equations make it even worse. Accordingly, model reduction methods aim at a lower computational complexity in the simulation of chemical combustion processes, where the reduced model should contain the most important dynamic information given by the long-term behavior and thus by the slow modes of the underlying process. Usually, there are two ways of how to obtain a reduced combustion model: on the one hand, the most common way, the reduction of the pure chemistry reaction term via approximation of **slow invariant manifolds (SIMs)** (1b). In this context, the reaction–transport coupling is considered afterwards (1c). On the other hand, quite unexplored up to now, the direct reduction of the full reaction–transport model via approximation of so-called **inertial manifolds (IM)** (2). These two ways for model reduction in chemical combustion processes are schematically illustrated in Figure 3.19.
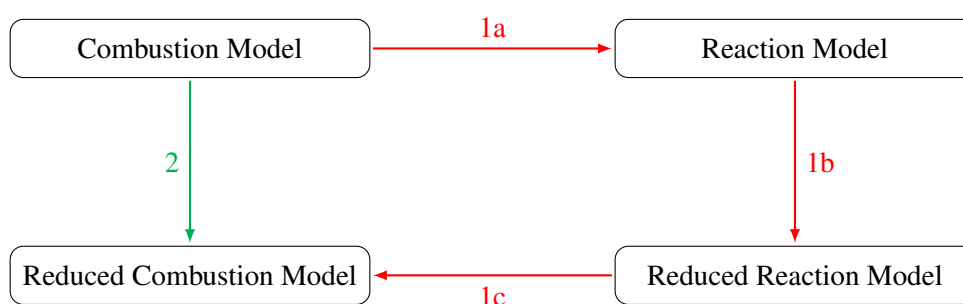

Figure 3.19: Schematic illustration of two possibilities for model reduction applied to a combustion model.

The main results of this thesis refer to the reduction of spatially homogeneous chemical reaction processes by approximating SIMs, for which there exists a large variety of approaches with little or no obvious relation to each other concerning their way of proceeding. Within this work, we identify two basic and fundamental concepts underlying, combining, and collecting a large

percentage of these approaches for model reduction via SIM computation:

- the **derivative–of–the–state–vector–concept** and

- the **boundary–value–concept**.

The former is based on the time derivative of the vector containing the concentrations of the chemical species participating in the reaction process, where it holds that an increasing derivative order increases the accuracy of the SIM computation, such that an exact identification is obtained in the limit, i.e. for an infinite derivative order. On the other hand, the boundary–value–concept is based on a two-point boundary value problem formulation where it holds that an increasing time interval between the two boundary values ensures an improvement of the SIM approximation. Once again, the error of accuracy converges to zero for an infinite time interval size. Thus, both concepts provide an exact identification of SIMs, at least by using limiting arguments. Furthermore, we succeeded to unite both concepts in condensed form in one novel approach, having the advantage over other approaches that two parameters are provided that can be used independently to improve the accuracy of the reduced reaction model—theoretically seen to any level of accuracy. However, practical applications show numerical difficulties by choosing the derivative order higher than three as well as choosing an arbitrary large interval, which is based on additional physical constraints entering the SIM computation approach for chemical reaction kinetics. For this purpose, this dissertation provides a procedure, how to obtain the maximum feasible interval size and thus, the best possible approximation of the SIM within the above framework. Furthermore, this approach is considered from a different point of view, namely in the light of optimal boundary control. This viewpoint via introduction of a HAMILTONIAN function related to conservation laws has the potential to establish relations to powerful concepts from dynamical systems theory that might yield more profound insight into the model reduction concept in terms of SIM characterization and identification.

In the second part of this dissertation, spatially inhomogeneous systems (PDE models) are analyzed, i.e. model equations that involve transport processes in form of diffusive and convective mass transfer in addition to the chemical reaction part. In this context, we confirmed, that convective processes have no remarkable influence concerning the behavior of reaction processes, being the consequence that it is sufficient to focus on systems involving just reaction and diffusion processes. The behavior of solutions to those reaction–diffusion equations is extensively investigated by means of a simple nonlinear test example. Based on these investigations, suggestions are provided how to couple a reduced reaction model with diffusive processes (1c) as well as how to reduce the underlying combustion model at once (2), i.e. without isolating the reaction processes at first. As regards the first issue, two proposals are newly presented: one based on a convex combination of the **diffusive line** and the function representing the reduced reac-

tion model, the other is denoted by **disturbed species reconstruction function** and describes the function representing the reduced reaction model modified at each point along the SIM by a disturbance into the direction of direct connection of the diffusion line. Accordingly, our suggestion for the direct reduction of the combustion model (i.e. 2 in Figure 3.19) is, roughly speaking, a generalization of the boundary–value–concept to reaction–diffusion equations providing—at least in the authors opinion—a highly promising approach for the computation of IMs and thus, model reduction of reaction–diffusion models.

Summarizing the above, it can be confidently stated that the new insights associated with this dissertation provide a significant progress in the context of the study of fundamental concepts for model reduction in multiscale combustion processes.

Bibliography

[ACC+07]   A. ADROVER, F. CRETA, S. CERBELLI, M. VALORANI, and M. GIONA. *The structure of slow invariant manifolds and their bifurcational routes in chemical kinetic models.* Comput. Chem. Eng., 31:1456–1474, 2007.

[ACG+07]   A. ADROVER, F. CRETA, M. GIONA, and M. VALORANI. *Stretching-based diagnostics and reduction of chemical kinetic models with diffusion.* J. Comput. Phys., 225:1442–1471, 2007.

[APP+09]   N.N. AL–KHATEEB, J.M. POWERS, S. PAOLUCCI, A.J. SOMMESE, J.A. DILLER, J.D. HAUENSTEIN, and J.D. MENGERS. *One-dimensional slow invariant manifolds for spatially homogeneous reactive systems.* J. Chem. Phys., 131:024118, 2009.

[BL74]   S.R. BERNFELD and V. LAKSHMIKANTHAM. *An introduction to nonlinear boundary value problems.* Academic Press, New York, 109, 1974.

[Bey14]   W.–J. BEYN. *Gewöhnliche Differentialgleichungen.* Lect. Notes, Bielefeld, Spring Term 2014.

[Bod07]   M. BODENSTEIN. *Geschwindigkeit der Bildung des Bromwasserstoffs aus seinen Elementen.* Z. Physik. Chem., 57:168–192, 1907.

[Bod13]   M. BODENSTEIN. *Eine Theorie der photochemischen Reaktionsgeschwindigkeiten.* Z. Physik. Chem., 85:329–397, 1913.

[BM07a]   V. BYKOV and U. MAAS. *Extension of the ILDM method to the domain of slow chemistry.* Proc. Comb. Inst., 31:465–472, 2007.

[BM07b]   V. BYKOV and U. MAAS. *The extension of the ILDM concept to reaction-diffusion manifolds.* Combust. Theor. Model., 11:839–862, 2007.

[Can95]   G. CANTOR. *Beiträge zur Begründung der transfiniten Mengenlehre.* Math. Ann., 46:481–512, 1895.

Bibliography

[CLP+03]   Y. CAO, S. LI, L. PETZOLD, and R. SERBAN. *Adjoint sensitivity analysis for differential–algebraic equations: the adjoint DAE system and its numerical solution.* SIAM J. Sci. Comput., 24:1076–1089, 2003.

[CU13]   D.L. CHAPMAN and L.K. UNDERHILL. *The interaction of chlorine and hydrogen. The influence of mass.* J. Chem. Soc., 103:496–508, 1913.

[Dar78]   G. DARBOUX. *Mémoire sur les équations différentielles algébriques du premier ordre et du premier degré.* Bull. Sci. Math., 2:151–200, 1878.

[DS99]   M.J. DAVIS and R.T. SKODJE. *Geometric investigation of low-dimensional manifolds in systems approaching equilibrium.* J. Chem. Phys., 111:859–874, 1999.

[Eul44]   L. EULER. *Methodus inveniendi lineas curvas maximi minimive proprietate gaudentes, sive solutio problematis isoperimetrici lattissimo sensu accepti.* Op. Om., 24, 1744.

[Fen72]   N. FENICHEL. *Persistence and smoothness of invariant manifolds for flows.* Indiana Univ. Math. J., 21:193–226, 1972.

[Fen79]   N. FENICHEL. *Geometric singular perturbation theory for ordinary differential equations.* J. Differ. Equations, 31:53–98, 1979.

[FST88]   C. FOIAS, G.R. SELL, and R TEMAM. *Inertial manifolds for nonlinear evolutionary equations.* J. Differ. Equations, 73:309–353, 1988.

[Fri06]   P. FRITZSON. *Introduction to object-oriented modeling and simulation with OpenModelica.* Tutorial, Linköping University, 2006.

[GKK+05]   C.W. GEAR, T.J. KAPER, I.G. KEVREKIDIS, and A. ZAGARIS. *Projecting to a slow manifold: singularly perturbed systems and legacy codes.* SIAM J. Appl. Dyn. Sys., 4:711–732, 2005.

[GK02]   C. GEIGER and C. KANZOW. *Theorie und Numerik restringierter Optimierungsaufgaben.* Springer, Heidelberg, 2002.

[Ger10]   M. GERDTS. *Optimale Steuerung.* Lect. Notes, Würzburg, Autumn Term 2009/2010.

[Ger12]   M. GERDTS. *Optimal control of ODEs and DAEs.* De Gruyter, Berlin, 2012.

[GL89]   G.H. GOLUB and C.F. VAN LOAN. *Matrix computation.* Johns Hopkins University Press, Baltimore, 1989.

[GRC08]   J.M. GINOUX, B. ROSSETTO, and L. CHUA. *Slow invariant manifolds as curvature of the flow of dynamical systems.* Int. J. Bifurcat. Chaos, 18:3409–3430, 2008.

[Gou12]   D.A. GOUSSIS. *Quasi steady state and partial equilibrium approximations: their relation and their validity.* Combust. Theor. Model., 16:869–926, 2012.

[Heu04]   H. HEUSER. *Lehrbuch der Analysis, Teil 2.* Teubner, Wiesbaden, 2004.

[Jon95]   C.K.R.T. JONES. *Geometric singular perturbation theory.* Lect. Notes Math., Springer, Heidelberg, 1609:44–118, 1995.

[Kap99]   T.J. KAPER. *An introduction to geometric methods and dynamical systems theory for singular perturbation problems.* Proc. Symp. Appli. Math., Am. Math. Soc., Providence, RI, 56:85–132, 1999.

[KK02]   H.G. KAPER and T.J. KAPER. *Asymptotic analysis of two reduction methods for systems of chemical reactions.* Physica D, 165:66–93, 2002.

[KM27]   W.O. KERMACK and A.G. MCKENDRICK. *A contribution to the mathematical theory of epidemics.* Proc. Roy. Soc. A, 46:700–721, 1927.

[Kre85]   H.–O. KREISS. *Problems with different time scales.* Academic Press, New York, 1985.

[Kur76]   S. KURCYUSZ. *On the existence and nonexistence of Lagrange multipliers in Banach spaces.* J. Optim. Theory Appl., 20:81–110, 1976.

[Kut11]   C. KUTTLER. *Reaction–diffusion equations with applications.* Lect. Notes, München, Spring Term 2011.

[Leb04]   D. LEBIEDZ. *Computing minimal entropy production trajectories: an approach to model reduction in chemical kinetics.* J. Chem. Phys., 120:6890–6897, 2004.

[Leb06]   D. LEBIEDZ, V. REINHARDT, and J. KAMMERER. *Novel trajectory based concepts for model and complexity reduction in (bio)chemical kinetics.* Model reduction and coarse-graining approaches for multi-scale phenomena, Springer, Berlin, 343–364, 2006.

[LRS10]   D. LEBIEDZ, V. REINHARDT, and J. SIEHR. *Minimal curvature trajectories: Riemannian geometry concepts for model reduction in chemical kinetics.* J. Comp. Phys., 229:6512–6533, 2010.

Bibliography

[Leb10]   D. LEBIEDZ. *Entropy-related extremum principles for model reduction of dynamical systems.* Entropy, 12:706–719, 2010.

[LRS$^+$11]   D. LEBIEDZ, V. REINHARDT, J. SIEHR, and J. UNGER. *Geometric criteria for model reduction in chemical kinetics via optimization of trajectories.* Coping with Complexity: Model Reduction and Data Analysis, Springer, Heidelberg, 241–252, 2011.

[LSU11]   D. LEBIEDZ, J. SIEHR, and J. UNGER. *A variational principle for computing slow invariant manifolds in dissipative dynamical systems.* SIAM J. Sci. Comput., 33:703–720, 2011.

[Leb12]   D. LEBIEDZ. *Optimierung 1.* Lect. Notes, Freiburg, Autumn Term 2011/2012.

[LS13]   D. LEBIEDZ and J. SIEHR. *A continuation method for the efficient solution of parametric optimization problems in kinetic model reduction.* SIAM J. Sci. Compu., 35:A1584–A1603, 2013.

[LS14]   D. LEBIEDZ and J. SIEHR. *An optimization approach to kinetic model reduction for combustion chemistry.* Flow Turbul. Combust., 92:885–902, 2014.

[LU14]   D. LEBIEDZ and J. UNGER. *On fundamental unifying concepts for trajectory-based slow invariant attracting manifold computation in multiscale models of chemical kinetics.* `arXiv:1405.1856v2`, 2014.

[Lem71]   F. LEMPIO. *Lineare Optimierung in unendlichdimensionalen Vektorräumen.* Computing, 8:284–290, 1971.

[Lin94]   E. LINDELÖF. *Sur l'application de la méthode des approximations successives aux équations différentielles ordinaires du premier ordre.* C. R. Hebd. Seances Acad. Sci., 116:454–457, 1894.

[MP92]   U. MAAS and S.B. POPE. *Simplifying chemical kinetics: intrinsic low-dimensional manifolds in composition space.* Combust. Flame, 88:239–264, 1992.

[MS88]   J. MALLET–PARET and G.R. SELL. *Inertial manifold for reaction diffusion equations in higher space dimensions.* J. Amer. Math. Soc., 1:805–866, 1988.

[MZ79]   H. MAURER and J. ZOWE. *First and second-order necessary and sufficient optimality conditions for infinite-dimensional programming problems.* Math. Program., 16:98–110, 1979.

[Mau81]   H. MAURER. *First and second-order sufficient optimality conditions in mathematical programming and optimal control.* Math. Program. Stud., 14:163–177, 1981.

[MBI03]   K.D. MEASE, S. BHARADWAJ, and S. IRAVANCHY. *Timescale analysis for nonlinear dynamical systems.* J. Guid. Control Dynam., 26:318–330, 2003.

[MTA$^+$08] K.D. MEASE, U. TOPCU, E. AYKUTLUĞ, and M. MAGGIA. *Characterizing two-timescale nonlinear dynamics using finite-time Lyapunov exponents and vectors.* `arXiv:0807.0239`, 2008.

[Men12]   J.D. MENGERS. *Slow invariant manifolds for reaction-diffusion systems.* Dissertation, University of Notre Dame, 2013.

[MP13]   J.D. MENGERS and J.M. POWERS. *One-dimensional slow invariant manifolds for fully coupled reaction and micro-scale diffusion.* SIAM J. Appl. Dyn. Sys., 12:560–595, 2013.

[MP13]   L. MICHAELIS and M.L. MENTEN. *Die Kinetik der Invertinwirkung.* Biochem. Z., 49:333–369, 1913.

[MM13]   J.D. MENGERS and J.M. POWERS. *One-dimensional slow invariant manifolds for fully coupled reaction and micro-scale diffusion.* SIAM J. Appl. Dyn. Sys., 12:560–595, 2013.

[MFV$^+$90] G. MORANDI, C. FERRARIO, G.L. VECCHIO, G. MARMO, and C. RUBANO. *The inverse problem in the calculus of variations and the geometry of the tangent bundle.* Phys. Rep., 188:147–284, 1990.

[Nil01]   D. NILSSON. *Automatic analysis and reduction of reaction mechanisms for complex fuel combustion.* Dissertation, Lund University, 2001.

[Pea86]   G. PEANO. *Sull'integrabilità delle equazioni differenziali del primo ordine.* R. Accad. Sci. Torino, 21:437–445, 1886.

[Pea90]   G. PEANO. *Demonstration de l'intégrabilité des équations différentielles ordinaires.* Math. Ann., 37:182–228, 1890.

[Pet03]   R.E. PETROSYAN. *Developments of the intrinsic low dimensional manifold method and application of the method to a model of the glucose regulatory system.* Master Thesis, University of Notre Dame, 2003.

[Rei08]   V. REINHARDT. *On the application of trajectory-based optimization for nonlinear kinetic model reduction.* Dissertation, Heidelberg University, 2008.

Bibliography

[RWD08]   V. REINHARDT, M. WINCKLER, and D. LEBIEDZ. *Approximation of slow attracting manifolds in chemical kinetics by trajectory-based optimization approaches.* J. Phys. Chem. A, 112:1712–1718, 2008.

[RPV$^+$06]   Z. REN, S.B. POPE, A. VLADIMIRSKY, and J.M. GUCKENHEIMER. *The invariant constrained equilibrium edge preimage curve method for the dimension reduction of chemical kinetics.* J. Chem. Phys., 124:114111, 2006.

[RP06]   Z. REN and S.B. POPE. *The use of slow manifolds in reactive flows.* Combust. Flame, 147:243–261, 2006.

[RP07]   Z. REN and S.B. POPE. *Transport-chemistry coupling in the reduced description of reactive flows.* Combust. Theor. Model., 11:715–739, 2007.

[RPV$^+$07]   Z. REN, S.B. POPE, A. VLADIMIRSKY, and J.M. GUCKENHEIMER. *Application of the ICE-PIC method for the dimension reduction of chemical kinetics coupled with transport.* P. Combust. Inst., 31:473–481, 2007.

[Ros86]   B. ROSSETTO. *Trajectoires lentes des systemes dynamiques.* Lect. Notes Contr. Inf., Springer, Heidelberg, 83:680–695, 1986.

[RT06]   M.R. ROUSSELL and T. TANG. *The functional equation truncation method for approximating slow invariant manifolds: a rapid method for computing intrinsic low-dimensional manifolds.* J. Chem. Phys., 125:214103, 2006.

[Rou12]   M.R. ROUSSELL. *Further studies of the functional equation truncation approximation.* Can. Appl. Math. Q., 20:209–227, 2012.

[RS03]   L.B. RYASHKO and E.E. SHNOL. *On exponentially attracting invariant manifolds of ODEs.* Nonlinearity, 16:147–160, 2003.

[San78]   R.M. SANTILLI. *Foundations of theoretical mechanics I: the inverse problem in Newtonian mechanics.* Springer, New York, 1978.

[San83]   R.M. SANTILLI. *Foundations of theoretical mechanics II: Birkhoffian generalization of Hamiltonian mechanics.* Springer, New York, 1983.

[SPP02]   S. SINGH, J.M. POWERS, and S. PAOLUCCI. *On slow manifolds of chemically reactive systems.* J. Chem. Phys., 117:1482–1496, 2002.

[Sie13]   J. SIEHR. *Numerical optimization methods within a continuation strategy for the reduction of chemical combustion models.* Dissertation, Heidelberg University, 2013.

[SB90]   R.D. SKEEL and M. BERZINS.   *A method for the spatial discretization of parabolic equations in one space variable.*   SIAM J. Sci. Stat. Comput., 11:1–32, 1990.

[SB02]   J. STOER and R. BULIRSCH. *Introduction to Numerical Analysis.* Springer, New York, 2002.

[TP02]   Q. TANG and S.B. POPE.   *Implementation of combustion chemistry by in situ adaptive tabulation of rate-controlled constrained equilibrium manifolds.* P. Combust. Inst., 29:1411–1417, 2002.

[Tem90]   R. TEMAM. *Inertial manifolds.* Math. Intell., 12:68–74, 1990.

[Tem97]   R. TEMAM. *Infinite-dimensional dynamical systems in mechanics and physics.* Springer, Berlin, 1997.

[Ung10]   J. UNGER. *On the analysis of an optimization approach to slow manifold computation in chemical kinetics.* Diploma Thesis, University of Freiburg, 2010.

[Vel09]   K. VELTEN. *Mathematical modeling and simulation. Introduction for Scientists and Engineers.* Wiley-VCH, Weinheim, 2009.

[Wal99]   K. WALTER. *The internal combustion engine at work.* Sci. Tech. Rev., Livermore, 4–10, 1999.

[Wal00]   W. WALTER. *Gewöhnliche Differentialgleichungen.* Springer, Berlin, 2000.

[War99]   J. WARNATZ. *Das komplexe Problem der Verbrennung.* Ruperto Carola, Heidelberg, 1, 1999.

[ZGK+09]   A. ZAGARIS, C.W. GEAR, T.J. KAPER, and I.G. KEVREKIDIS. *Analysis of the accuracy and convergence of equation-free projection to a slow manifold.* ESAIM: Math. Model. Num., 43:757–784, 2009.

[ZK79]   J. ZOWE and S. KURCYUSZ. *Regularity and stability of the mathematical programming problem in Banach space.* Appl. Math. Optim., 5:49–62, 1979.

Curriculum Vitae

Personal Data

NAME	Jonas Unger
DATE OF BIRTH	May 6, 1986
PLACE OF BIRTH	Backnang, Germany
NATIONALITY	German
E-MAIL	jonas.unger@gmx.net

Education

SINCE MAY 2012	Doctoral studies, Institute for Numerical Mathematics, University of Ulm, Germany
MAR 2011—APR 2012	Doctoral studies, Center for Biological Systems Analysis, University of Freiburg, Germany
FEB 2011	Diplom in Mathematics
OCT 2005—FEB 2011	Studies in Mathematics, University of Freiburg, Germany
2005	Abitur

Work Experience

SINCE JAN 2013	Akademischer Mitarbeiter, Institute for Numerical Mathematics, University of Ulm, Germany
MAR 2011—DEZ 2012	Akademischer Mitarbeiter, Center for Biological Systems Analysis, University of Freiburg, Germany
2007—2010	Student Teaching Assistant, University of Freiburg, Germany

Publications

Heiter, P., Lebiedz, D., and Unger, J.
On conceptual ideas concerning slow invariant manifolds in a variational problem viewpoint.
Proceedings of the 5th International Workshop on Model Reduction in Reacting Flows, Spreewald, Germany, 2015

Lebiedz, D. and Unger, J.
On fundamental unifying concepts for trajectory-based slow invariant attracting manifold computation in multiscale models of chemical kinetics.
arXiv:1405.1856v1 [math.DS], 2014

Lebiedz, D. and Unger, J.
A boundary value view on the reverse trajectory-based optimization Approach for Kinetic Model Reduction.
Proceedings of the 4th International Workshop on Model Reduction in Reacting Flows, San Francisco, USA, 2013

Lebiedz, D. and Unger, J.
Model reduction in chemical kinetics via slow manifold computation.
Proceedings of the Second International Workshop on Model Reduction for Parametrized Systems, Günzburg, Deutschland, 2012

Dedner, A., Fein, M., Klöfkorn, R., Kröner, D., Siehr, J., and Unger, J.
On the computation of slow manifolds in chemical kinetics via optimization and their use as reduced models in reactive flow systems.
Proceedings of the 13th International Conference on Numerical Combustion, Korfu, Griechenland, 2011

Lebiedz, D., Siehr, J., and Unger, J.
A variational principle for computing slow invariant manifolds in dissipative dynamical systems.
SIAM J. Sci. Comput. 33, 703, 2011

Lebiedz, D., Reinhardt, V., Siehr, J., and Unger, J.
Geometric criteria for model reduction in chemical kinetics via optimization of trajectories.
In "'Coping with complexity: Model reduction and data analysis'"
Springer Series "'Lecture Notes in Computational Science and Engineering'", 2010

Selected Talks

Invariante Mannigfaltigkeiten und Modellreduktion dynamischer Systeme in der chemischen Reaktionskinetik

Tagung des GAMM-Fachausschusses ''Dynamik und Regelungstheorie''', Hamburg, Deutschland, 2015

A Boundary Value View on the Reverse Trajectory-Based Optimization Approach for Kinetic Model Reduction

4th International Workshop on Model Reduction in Reacting Flows, San Francisco, USA, 2013

Model Reduction in Chemical Kinetics via Slow Manifold Computation

Second International Workshop on Model Reduction for Parametrized Systems, Günzburg, Deutschland, 2012

Model Reduction in Chemical Kinetics: A Variational Approach

HGS MathComp Compact Course "Multi-Scale Modeling and Simulation of Complex Chemical Reaction Networks", Heidelberg, Deutschland, 2010

Minimal Curvature Trajectories: Riemannian Geometric Concepts for Computing Slow Attracting Manifolds in Chemical Kinetics.

Oberseminar Differentialgeometrie, Freiburg, Deutschland, 2010

Erklärung

Ich, Jonas Unger, versichere hiermit, dass ich die vorliegende Arbeit selbständig angefertigt habe und keine anderen als die angegebenen Quellen und Hilfsmittel benutzt sowie die wörtlich oder inhaltlich übernommenen Stellen als solche kenntlich gemacht habe. Ich erkläre außerdem, dass die von mir vorgelegte Dissertation bisher nicht im In- oder Ausland in dieser oder ähnlicher Form in einem anderen Promotionsverfahren vorgelegt wurde. Ich versichere ferner die Richtigkeit der im Lebenslauf gemachten Angaben.

Ulm, den 07.12.2015

_____

(Unterschrift)